Silent Testing for Safety Validation of Automated Driving in Field Operation

Vom Fachbereich Maschinenbau an der
Technischen Universität Darmstadt
zur Erlangung des Grades eines
Doktor-Ingenieurs (Dr.-Ing.)
genehmigte

Dissertation

vorgelegt von

Cheng Wang, M.Eng.
aus Hubei, China

Berichterstatter:	Prof. Dr. rer. nat. Hermann Winner
Mitberichterstatter:	Prof. Dr.-Ing. Uwe Klingauf
Tag der Einreichung:	16.08.2021
Tag der mündlichen Prüfung:	26.10.2021

Darmstadt 2021
D 17

Preface

After about four years of study, the dissertation is finally finished. With excitement in my heart, I would like to review the life in Darmstadt and the research at the Institute of Automotive Engineering (FZD) at TU Darmstadt. Although the research process was arduous, it was more about happiness and sense of accomplishment under the patient guidance from my doctoral supervisor Prof. Dr. rer. nat. Hermann Winner. He gave me a lot of very constructive advice that made it possible for me to make progress step by step. With the experience and knowledge he shared, many detours were avoided in my research. He was like a lighthouse on my research road, giving me a clear direction on how to solve my doubts and confusions. With his excellent support and help, the research was no longer an insurmountable mountain for me. Moreover, I am grateful for his mentoring and coaching on my personality and the tolerance of my mistakes. At this point, I want to express great thanks to him.

Additionally, I would like to thank Prof. Dr.-Ing. Uwe Klingauf for taking over the role as the second examiner. Thanks for the valuable feedback and the precious time.

Furthermore, I want to thank all my colleagues at FZD. The exchange with them was rather informative. The seminars and workshops have broadened my knowledge greatly. Their advice in relation to my research topic provided me new thought to solve the problems raised in my research. In addition, Thanks for their help in my life, which facilitates the integration into a foreign cultural and environment.

I want to give a big thanks to all the students who I have supervised. They not only supported me in the experiments but also contributed to the necessary fundamentals.

Moreover, I would like to thank the sponsors, all the research assistants and students involved in the aDDa project. Thanks to their contribution, a test platform for implementation of the studied approach is established. Moreover, a special thank is given to the China Scholarship Council and the sponsors of the VVM project for their financial support.

Lastly, I want to thank my family and all my friends. They left a large space and options for me to do what I love. I would not be able to focus on my studies without their dedication. They were always there no matter what happened. They encouraged me whenever I failed and inspired me whenever I was frustrated. They were my emotional dependence all the way.

All in all, thanks to all the people who have been with me in my research or in my life. The dissertation is only a tiny part in the ocean of knowledge. There are many difficulties to overcome in the field of automated driving. I hope the work could be useful and a safe autonomous vehicle will arrive soon.

Darmstadt, Juni 2021

List of Contents

Abbreviations

Abbreviation	Description
ACC	Adaptive Cruise Control
ADS	Automated Driving System
AD	Automated Driving
aDDa	Automated Driving Darmstadt for Students
ADMA	Automotive Dynamic Motion Analyzer
AEB	Advanced Emergency Braking
AV	Automated Vehicle
ASIL	Automotive Safety Integrity Level
BTN	Brake Threat Number
CA	Constant Acceleration
CAS	Collision Avoidance System
CD	Cumulative Distribution
CNN	Convolution Neural Network
CTRA	Constant Turn Rate and Acceleration
CTRV	Constant Turn Rate and Velocity
CV	Constant Velocity
DDT	Dynamic Driving Task
DGNSS	Differential Global Navigation Satellite System
DiL	Driver-in-the-Loop
DNN	Deep Neural Network
DRAC	Deceleration Rate to Avoid the Crash
DSS	Difference of Space distance and Stopping distance
E/E	Electrical or Electronic
EKF	Extended Kalman Filter
ETTC	Enhanced TTC
EVT	Extreme Value Theory
FIR	Finite Impulse Response
FN	False Negative
FoV	Field of View
FP	False Positive
FSM	Finite State Machine
FuT	Function under Test
HAV	Highly Automated Vehicle
HD	High Definition Map
HiL	Hardware-in-the-Loop
IiC	Instance in Charge
IMM	Interacting Multiple Model

Abbreviation	Description
IMU	Inertial Measurement Unit
iTTC	Inverse TTC
JIPDA	Joint Integrated Probabilistic Data Association
KF	Kalman Filter
LKA	Lane Keeping Assist
LSTM	Long Short-term Memory
MCMC	Markov Chain Monte Carlo
MDP	Markov Decision Process
MI	Mixed Index
MiL	Model-in-the-Loop
MPC	Model Predictive Control
NN-UKF	Nearest Neighbor-Unscented Kalman Filter
ODD	Operation Design Domain
OSM	OpenStreetMap
PET	Post-encroachment Time
POMDP	Partially Observable MDP
RDR	Required Deceleration Rate
RMSE	Root Mean Square Error
ROC	Receiver Operation Characteristic
ROS	Robot Operation System
RoI	Region of Interest
RRT	Rapidly-exploring Random Tree
PSD	Proportion of Stopping Distance
RSS	Responsibility-Sensitive Safety
RTK	Real-time Kinematic
SciL	Scenario-in-the-Loop
SiL	Software-in-the-Loop
SOTIF	Safety of the Intended Functionality
SPI	Safety Performance Indices
STN	Steering Threat Number
SuT	System under Test
TCI	Trajectory Criticality Index
TET	Time Exposed TTC
TIDSS	Time Integrated DSS
TIT	Time Integrated TTC
TN	True Negative
TP	True Positive
TTB	Time-to-Brake
TTC	Time-to-Collision

Abbreviation	Description
TTK	Time-to-Kickdown
TTR	Time-to-React
TTS	Time-to-Steer
TTX	Time-to-X
TUDa	Technical University of Darmstadt
URTSS	Unscented Rauch-Tung-Striebel Smoother
VAAFO	Virtual Assessment of Automation in Field Operation
vAV	Virtual Automated Vehicle
ViL	Vehicle-in-the-Loop
VRU	Vulnerable Road User
WTTC	Worst Time to Collision
XiL	X-in-the-Loop

Symbols and Indices

Symbol	Unit	Description
a	m/s^2	Acceleration
c	./.	Cost
d	m	Distance
h	./.	Apothem length
it_{tc}	1/s	Inverse TTC
k_{ac}	./.	The number of acceleration constraints
l	m	Length
l_{ane}	./.	Lane number
m	kg	Vehicle mass
p	m	Position
r	m	Radial distance
s	./.	Slack vector
t	s	Time
t_{tc}	s	Time-to-Collision
u	m/s^3	Jerk in x and y directions
v	m/s	Velocity
w	m	Width
x	./.	State
C	./.	Criticality (component)
Cond	./.	Condition
C_{onvl}	./.	Convolution coefficients
C_{str}	./.	Constraint sets
D	m/s^2	Deceleration
EP	kW	Engine power
J	m/s^3	Jerk
N	./.	The total number of instances
P	./.	Covariance matrix
T_{B}	s	Birth cycle
T_{L}	s	Lifetime
Z	./.	Measurements
ξ	./.	Cost term
$\eth t$	s	Time interval of two adjacent points of a trajectory
τ	s	Duration
σ	./.	Standard deviation
ψ	rad	Yaw angle
$\dot{\psi}$	rad/s	Yaw velocity
$\ddot{\psi}$	rad/s^2	Yaw acceleration

Index	Description
a	Acceleration
adap	Adaptive cruise mode
aft	After
b	Buffer
bef	Before
chg	Lane change mode
coll	Collision
crit	Critical
cruise	Cruise mode
cs	Critical scenario
cur	Current
diff	Difference
e	Enhanced
eva	Evasion
fl	Front left
fr	Front right
l	Lower
lin	Linear
lt	Left
max	Maximum value
n	The *n*th point
obj	Object
qua	Quadratic
r	Rear
ref	Reference line
rel	Relative
req	Required
rl	Rear left
rt	Right
rr	Rear right
s	Safe
spatial	The spatial constraint
ste	Steer
stop	Stop mode
sub	The subject vehicle
u	Upper
vAV	Virtual automated vehicle
warn	Warning
x	In x-direction (corresponds to vehicle longitudinal direction)
y	In y-direction (corresponds to vehicle lateral direction)

B	Braking
D	Deceleration
E	Earth-fixed coordinate system
F	Frenet coordinate system
N	The number of total points
MAP	The maximum a posterior
IiC	Instance in charge
P	Precision
R	Reaction
RMSE	Root mean square error
S	Sensor coordinate system
V	Vehicle coordinate system
0	Initial
1	The first sensor
2	The second sensor

Figures and Tables

Kurzzusammenfassung

Die Sicherheitsvalidierung von automatisierten Fahrzeugen ist derzeit eine große Herausforderung, auch wenn bereits viele Erfolge erzielt wurden. Die Glaubwürdigkeit der Ergebnisse konventioneller Ansätze wie reale oder simulationsbasierte Tests wird trotz enormem Testaufwand in Frage gestellt. Daher werden neue Ansätze zur Absicherung mit einem hohen Maß an Glaubwürdigkeit, Anpassungsfähigkeit und Anwendbarkeit angestrebt.

Vor diesem Hintergrund ist der Ansatz „Virtual Assessment of Automation in Field Operation“ (VAAFO) zum Testen von automatisierten Fahrzeuge motiviert. Die Kernidee dieses Ansatzes ist, dass eine Instanz das Führen eines realen Fahrzeugs übernimmt, während ein virtuelles automatisiertes Fahrzeug parallel in einer virtuellen Welt fährt und reale Sensoreingaben erhält, aber von den realen Aktoren getrennt ist. Die reale Führungsinstanz kann entweder ein menschlicher Fahrer oder ein automatisiertes Vorläufer- oder Stellvertretersystem sein. So treffen das virtuelle automatisierte Fahrzeug und die Führungsinstanz Entscheidungen gleichzeitig, aber unabhängig voneinander. Auf Basis dieses Arbeitsprinzips kann die automatisierte Fahrzeugführungsfunktion unter realen Bedingungen getestet werden, ohne zusätzliche Risiken zu bringen. Ziel der Arbeit ist die Entwickelung und Implementierung dieses Ansatzes sowie die Bestimmung seines Beitrags zur Sicherheitsvalidierung von automatisierten Fahrzeugen.

Bei der Entwicklung und Umsetzung des Ansatzes werden vier Forschungsfragen untersucht. Wie eine gültige Umgebungsrepräsentation für das virtuelle Fahrzeug zu garantieren ist, ist der erste Forschungsschwerpunkt. Da die von Sensoren erfassten Objekte auf die Führungsinstanz bezogen sind, können sie bei Zustandsabweichungen zwischen Führungsinstanz und virtuellem Fahrzeug nicht direkt für das virtuelle Fahrzeug genutzt werden. Daher wird die Abbildung der Umgebungsrepräsentation in der virtuellen Welt untersucht. Zur Beantwortung dieser Forschungsfrage wird eine Koordinatentransformation durchgeführt und es werden die Lebensdauer und der Geburtszyklus der virtuellen Fahrzeuge als zwei Schlüsselparameter eingeführt. Wie die Sicherheit des virtuellen Fahrzeugs bewertet und kritische Szenarien identifiziert werden können, ist die zweite Forschungsfrage. Zur Adressierung der zweiten Forschungsfrage werden Trigger abgeleitet und durch einen entwickelten Kritikalitätsindex konkretisiert. Der dritte Forschungsschwerpunkt ist die Entwicklung eines geeigneten Ringpuffers sowie eines modularen Frameworks für diesen Ansatz. Die Bestimmung des Abdeckungsgrades des Ansatzes ist der letzte Forschungsschwerpunkt. Um den Anwendungsbereich des Ansatzes abzuleiten, werden Simulation und reale Tests durchgeführt. Schließlich wird unter Berücksichtigung des Abdeckungsgrades und der Grenzen der Anwendbarkeit die Rolle vom VAAFO-Ansatz in der gesamten Familie der Ansätze zur Sicherheitsvalidierung von automatisierten Fahrzeugen bestimmt. Abschließend wird auf weitere Studien für die Zukunft hingewiesen.

Summary

The safety validation of automated vehicles is currently a major challenge, even though substantial achievements have been made. The credibility of the results of conventional approaches such as the real-world testing or the simulation-based testing is questioned despite enormous testing effort. Therefore, new approaches for safety assurance with a high degree of credibility, adaptability and applicability are thus pursued.

Under this circumstance, the approach “Virtual Assessment of Automation in Field Operation” (VAAFO) for testing automated vehicles is motivated. The key idea of this approach is that an instance is in charge of driving a vehicle, while a virtual automated vehicle runs in parallel in a virtual world, receiving real sensor inputs but separated from the real actuators. The instance in charge in the real world can be either a human driver or an automated precursor or representative system. Thus, the virtual automated vehicle and the instance in charge make decisions simultaneously but independently. Based on this working principle, the driving function of an automated vehicle can be tested under real conditions without bringing any additional risks. The goal of the work is to develop and implement the approach and finally to determine its contribution to the safety validation of automated vehicles.

During the development and implementation of the approach, four research questions are studied. How to guarantee a valid environmental representation for the virtual vehicle is the first research focus. Since the objects detected by sensors are related to the instance in charge, they cannot be directly used for the virtual vehicle in the case of state deviations between the instance in charge and the virtual vehicle. Therefore, the mapping of the environmental representation in the virtual world is investigated. To answer this research question, a coordinate transformation is performed, and the lifetime and the birth cycle of virtual vehicles as two key parameters are introduced. How to evaluate the safety of the virtual vehicle and identify critical scenarios is the second research focus. To address the second research question, triggers are derived and substantiated by a developed criticality index. The third research focus is the development of a suitable ring buffer and a modular framework for the approach. The determination of the coverage degree of the approach is the last research focus. In order to derive the application scope of the approach, simulations and real-world tests are performed. Finally, considering the coverage degree and the limits of applicability, the role of the VAAFO approach in the whole family of approaches for the safety validation of automated vehicles is determined. Lastly, further studies for the future are pointed out.

1 Introduction

1.1 Research Background

Automated vehicles (AVs) are a very hot research topic in many different branches. Traditional car manufacturers and suppliers are currently not the only players involved in this innovation. Customer experience is regarded as the focus when shifting from internal combustion engine vehicles to AVs, since the provided services and IT platforms may become even more important to a company.[1] Therefore, many internet giants such as Waymo[2], Baidu[3], etc. have joined in this area. Through a long-term development, substantial achievements ranging from functional development to system verification have been made. Prototypes of AVs are already available and partially implemented under predefined conditions and in the field, e.g., with the Lyft[4] app, an automated driving (AD) ride can be called. However, there are still many challenges to overcome when bringing AVs to the market. The safety verification and validation of AVs is exactly one of the challenges. The existing knowledge gap in proving the safety of AVs are also highlighted by Winner et al.[5] using the Swiss cheese model.

To prove the safety of AVs, the real-world testing is a commonly used method. Since AVs are tested in a real-world environment, the test results are valid for verifying their performance. Nevertheless, hundreds of millions of kilometers and even hundreds of billions of kilometers for testing AVs would be required to achieve human-comparable safety in USA.[6] Billions of test kilometers would be necessary as well according to the traffic accidents on German motorways.[7] With such a large number of test kilometers, this method is infeasible for economic and time reasons. As a result, the statistical validation prior to the market launch is impossible. In contrast, simulation is an effective method to identify possible obvious problems at an early stage. In the verification and validation stage, a lot of different types of scenarios can be created in the simulation to test AVs. However, the simulation may result in invalid results, since every simulation technology need to be first validated. Under

[1] Jiang, H.; Lu, F.: A Story Different from Tesla Driving the Chinese Automobile Industry (2018).

[2] Waymo LLC: Waymo-Homepage (2021).

[3] Baidu: Apollo-Homepage (2021).

[4] Lyft: Lyft-Homepage (2021).

[5] Winner, H. et al.: Validation and Introduction of Automated Driving (2018).

[6] Kalra, N.; Paddock, S. M.: Driving to safety (2016).

[7] Wachenfeld, W.; Winner, H.: The new role of road testing for the safety validation, pp. 419–435.

these circumstances, the approach named virtual assessment of automation in field operation (VAAFO)[8] is proposed. In VAAFO, an instance is in charge of driving a real vehicle, while a virtual AV (vAV) runs in parallel and has no connection with the actuators of the real vehicle. The instance in charge (IiC) is the physical instance that drives a real vehicle. It can either be a human driver or a driving automation system. According to the definition from SAE[9], six levels of driving automation are introduced:

- Level 0 – *"*No driving automation. A driver performs the entire dynamic driving task*"* (DDT).
- Level 1 – "Driver assistance. An engaged driving automation system performs part of the DDT by executing either the longitudinal or the lateral vehicle motion control subtask." For example, the adaptive cruise control (ACC) or the lane keeping assist (LKA) is a level 1 system.
- Level 2 – "Partial Driving Automation. An engaged driving automation system performs part of the DDT by executing both the longitudinal and the lateral vehicle motion control subtasks." The ACC in combination with the LKA is an example of such a level 2 system. The current AVs on the market have reached this level of automation.
- Level 3 – "Conditional Driving Automation. An engaged automated driving system (ADS) performs the entire DDT within its operation design domain (ODD). The ADS determines whether ODD limits are about to be exceeded or there is a DDT performance-relevant system failure of the ADS and, if so, issues a timely request to intervene to the DDT fallback-ready user."
- Level 4 – "High Driving Automation. An engaged ADS performs the entire DDT within its ODD. The ADS performs DDT fallback and transitions automatically to a minimal risk condition when a DDT performance-relevant system failure occurs or a user requests that it achieves a minimal risk condition."
- Level 5 – "Full Driving Automation. An engaged ADS performs the entire DDT, DDT fallback and transitions automatically to a minimal risk condition when a DDT performance-relevant system failure occurs or a user requests that it achieves a minimal risk condition." An ODD is no longer necessary.

Any system or feature capable of level 1-5 driving automation is described as a driving automation system, while an ADS is defined as a driving automation system with at least level 3. The IiC could be any levels of driving automation. Currently, the IiC is mostly a driver assisted by a level 2 driving automation system. Whether there are specific requirements for the level of a vAV in the background will be studied in this dissertation. Based on the working principle of the VAAFO approach, the advantages of real-world testing and simulation are combined.

[8] Wachenfeld, W.; Winner, H.: Virtual Assessment of Automation in Field Operation (2015).

[9] SAE J3016: Taxonomy and Definitions for Terms Related to Automation Systems (2021), pp. 28-29.

1.2 Terms Definition

In this subchapter, the important terms that have been used through the dissertation are introduced and defined.

1.2.1 Online and Post-processing

The term “Online” is gradually utilized in the technical area to describe for “ at runtime” or “ during operation”.[10] In VAAFO, a vAV runs in real-time in the background during the driving of a test vehicle. This meaning matches with the definition of Wikipedia. Therefore, online is used to depict the working status of the vAV. During the online operation, some data may be recorded. There are no time requirements for data processing if the data is already recorded. The processing of the recorded data is described as post-processing.

1.2.2 Scene, Scenario, Scenery and Situation

Since one of the goals of the VAAFO approach is to identify critical scenarios, it is necessary to give a clear impression what a scenario is and how the criticality of a scenario is defined. Ulbrich et al.[11] define the scene, scenario, scenery and situation as:

> “A **scene** describes a snapshot of the environment including the scenery and dynamic elements, as well as all actors’ and observers’ self-representations, and the relationships among those entities. Only a scene representation in a simulated world can be all-encompassing (objective scene, ground truth). In the real world it is incomplete, incorrect, uncertain, and from one or several observers’ points of view (subjective scene).”
>
> “A **scenario** describes the temporal development between several scenes in a sequence of scenes. Every scenario starts with an initial scene. Actions &events as well as goals &values may be specified to characterize this temporal development in a scenario. Other than a scene, a scenario spans a certain amount of time.”
>
> “A **scenery** subsumes all geo-spatially stationary aspects of the scene. This entails metric, semantic, and topological information about roads and all their components like lanes, lane markings, road surfaces, or the roads’ domain types. Moreover, this subsumes information about conflict areas between lanes as well as information about their interconnections, e.g., at intersections. Apart from the before mentioned environment conditions, the scenery also includes stationary elements like houses, fences, curbs, trees, traffic lights, or traffic signs.”

[10] Wikipedia: Online (2021).

[11] Ulbrich, S. et al.: Defining and Substantiating the Terms Scene, Situation, and Scenario (2015), p. 983.

> "A **situation** is the entirety of circumstances, which are to be considered for the selection of an appropriate behavior pattern at a particular point of time. It entails all relevant conditions, options and determinants for behavior. A situation is derived from the scene by an information selection and augmentation process based on transient (e.g. mission-specific) as well as permanent goals and values. Hence, a situation is always subjective by representing an element's point of view."

For the definition of a critical scenario, Ponn et al.[12] use criticality metrics to quantify whether a scenario is critical or not, while the criticality is defined as the closeness to an accident. In this thesis, criticality metrics are also utilized to identify critical scenarios. Relevant scenarios are defined as any scenarios that could contribute to the approval of AVs, e.g., the speed limit is relevant for the certification, since an AV should comply with traffic regulations.[12]

1.2.3 Abstract Level of Scenarios

It is essential to define the level of detail of a scenario to describe what information should be included in a scenario when discussing the generation of scenarios. At this point, the definition from Menzel et al.[13] is applied. He introduced three different levels of detail of scenarios, which are functional scenarios, logical scenarios and concrete scenarios, respectively.

> "**Functional scenarios** include operating scenarios on a semantic level. The entities of the domain and the relations of those entities are described via a linguistic scenario notation. The scenarios are consistent. The vocabulary used for the description of functional scenarios is specific for the use case and the domain and can feature different levels of detail."

> "**Logical scenarios** include operating scenarios on a state space level. Logical scenarios represent the entities and the relations of those entities with the help of parameter ranges in the state space. The parameter ranges can optionally be specified with probability distributions. Additionally, the relations of the parameter ranges can optionally be specified with the help of correlations or numeric conditions. A logical scenario includes a formal notation of the scenario."

> "**Concrete scenarios** distinctly depict operating scenarios on a state space level. Concrete scenarios represent entities and the relations of those entities with the help of concrete values for each parameter in the state space."

The scenario is more and more specific from functional scenarios to concrete scenarios. However, only concrete scenarios can be created and executed. Therefore, the scenario should be a concrete scenario when it is performed to test AVs. Conversely, the functional

[12] Ponn, T. et al.: An Optimization-based Method to Identify Relevant Scenarios (2019), p. 3.

[13] Menzel, T. et al.: Scenarios for development, test and validation (2018), pp. 1824–1826.

scenarios are more convenient for the description of scenarios, e.g., an overtaking scenario can be simply considered as a functional scenario.

1.2.4 Perception Uncertainties

There are mainly three different types of uncertainties in the perception according to the definition of Dietmayer[14]. They are explained by

> "**Existence uncertainty** describes the uncertainty as to whether an object detected by the sensors and transferred to the representation of the surroundings actually exists at all. Errors of this kind can occur due to deficiencies in the signal processing algorithms or incorrect measurements by the sensors themselves." This concerns false positive (FP) and false negative (FN) objects. A FP object means that a nonexistent object is detected and responded to by the sensors, while a FN object means that the sensors miss to detect a relevant real existing object, thus rendering AV unable to react to it.
>
> "**State uncertainty** describes the uncertainty in the physical measured variables, such as size, position and speed, and is a direct consequence of measuring errors in the sensors and sensor signal processing that cannot always be avoided."
>
> "**Class uncertainty** refers to uncertainty with regard to the correct semantic assignment, which can be caused by deficiencies in the classification procedure or insufficiently accurate measured data."

1.3 Methodology and Architecture

The overall methodology of the VAAFO approach is illustrate in Figure 1-1. The structure of this dissertation is also organized according to this figure. An IiC perceives its surroundings and makes decisions accordingly. The perceived environment is based on the coordinate system of the IiC. Due to the probable state deviations between the IiC and the vAV, the environmental representation can be invalid for the vAV. Thus, a strategy should be introduced in order to provide a valid environmental representation for the vAV, so that it can be tested in the virtual world. The projection of the environmental representation from the IiC to the vAV is marked with dotted line in Figure 1-1, and is one of the research focusses in this dissertation. After generating a valid environmental representation for the vAV, suitable triggers should be defined to assess the safety of the vAV as well as the safety of the IiC. Chapter 3 deals with the online safety assessment of vAVs, including the creation a valid environmental representation and the definition of triggers.

[14] Dietmayer, K.: Predicting of Machine Perception for Automated Driving (2016), pp. 412–413.

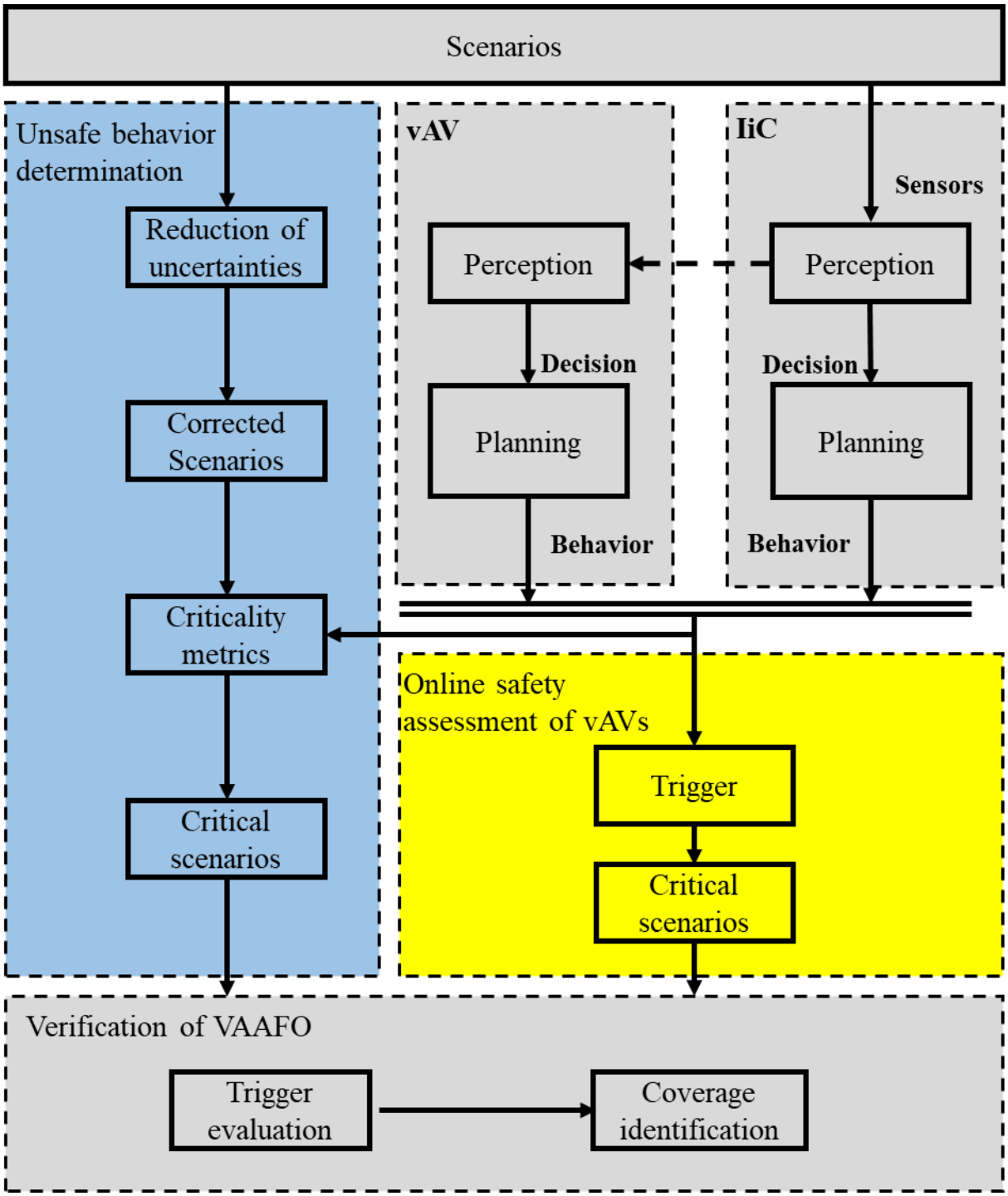

Figure 1-1: The whole architecture of the VAAFO approach.

In order to evaluate the triggers and find the reasons why the triggers are activated, the uncertainties in the environmental representation should be eliminated. Then, the behavior of the IiC and the vAV in the corrected environment is evaluated again using criticality metrics. As a result, whether the activation of the triggers caused by the uncertainties in perception or the unsafe decision in planning is clear. The possible approaches to eliminate the uncertainties and the suitable criticality metrics to assess the safety of IiC and vAV are elaborated in chapter 4. To evaluate the performance of the triggers and demonstrate the ability of the VAAFO approach, simulations and real-world tests are performed. The implementation of

the VAAFO approach in the simulations and in reality are presented in chapter 5 and 6, respectively. By analyzing the simulation results and the real test results, the triggers are evaluated, and the performance of the VAAFO approach is revealed. Based on the evaluation, the coverage and the limitations of the VAAFO approach are analyzed. Thus, the final application scope is derived and discussed in chapter 7. Chapter 8 focuses on the conclusions and the gained knowledge. The possible open researches in the future are also presented in the last chapter.

1.4 Research Focuses

As a new approach to test AVs, it is unclear which components are required for the VAAFO approach and how the approach actually works in reality. Therefore, the necessary steps to realize this concept should be first defined. As mentioned in section 1.3, the perception of the IiC cannot be used directly for the vAV due to the state deviations between them. Additionally, it is worth discussing whether multiple vAV instances are essential in the virtual world instead of just one vAV to enlarge the search area of critical scenarios. Therefore, the first research question is:

Q1: How to generate a valid environmental representation in the virtual world and whether multiple vAV instances are essential in order to test a driving automation system?

Only after having a valid environmental representation, the vAV can then make corresponding decisions. As a result, the safety evaluation of the vAV is feasible in the projected environmental representation. Additionally, the performance of the VAAFO approach to test AVs should be determined as well. However, the performance of the approach depends on the triggers to be applied. Therefore, the requirements on the triggers should be first explored. Based on the requirements, the triggers should be specified and concretized. Thus, the second question is:

Q2: What kind of metrics could be utilized to assess the safety of vAV instances and how good are the proposed triggers?

The third research question is to design an appropriate ring buffer and establish a modular framework for the approach. If the triggers are activated, the identified scenarios should be saved. A ring buffer specifically for the VAAFO approach is essential. Furthermore, the framework of the approach should be studied. It is desired that the framework utilizes the current standard interfaces to make sure its compatible with other existing approaches. Consequently, the data exchange with other approaches is seamless, and the replacement of the system under test (SuT) can be conducted without changing the framework. Thus, different algorithms can be replaced easily and tested. Additionally, the framework should be scalable so that a certain automated driving function can also be tested. Therefore, the third research question is:

Q3: How to design an appropriate ring buffer and what does the framework look like?

Finally, the application scope of the approach should be studied so that the proposed approach can be used in appropriate cases. The role of the VAAFO approach in existing approaches for safety verification and validation of AVs should be determined. The contributions of the VAAFO approach for the approval of AVs should be specified. The potential shortcomings of the approach should also be analyzed. In addition, further study aspects of the approach should be presented. This research question can thus be summarized as:

Q4: What is the application scope of the VAAFO approach and to what extent can it be used to verify and validate the safety of vAV instances?

Certainly, there are other aspects that should be addressed as well, e.g., suitable criticality metrics are required to compare the criticality metrics with the defined triggers. As a result, the performance of the defined triggers can be revealed. A driving automation system is also essential, which is regarded as the test object to demonstrate the VAAFO approach. Moreover, whether there are special requirements for the driving automation system should be determined.

2 State of the Art

In this chapter, the current state of the art is classified and summarized. In addition, pros and cons of different approaches are outlined. The differences and benefits of the VAAFO approach are highlighted. Generally, the relevant work regarding to the safety of AVs can be divided into two categories: approaches for safety by design, and approaches for safety verification and validation. These two categories will be introduced in detail in this chapter.

2.1 Approaches for Safety by Design

Waymo[15] has described five aspects of safety regarding AVs, which are behavior safety, functional safety, crash safety, operational safety and non-collision safety. The behavior safety and functional safety for level 2 AVs have been addressed in existing standards. Those standards are usually used to derive requirements, which then guide the design of AVs at their development stages. Operational safety refers to how AVs should interact with its passengers in order to create a safe and comfortable ambience. Crash safety means passive measures to mitigate injury or prevent death. A lot of reliable and robust techniques are already implemented to ensure crash safety. Other hazards from electrical systems or sensors belong to the non-collision safety. The existing standards relating to behavior safety and functional safety are discussed below, respectively.

2.1.1 ISO 26262

The standard ISO 26262[16] is applied to guide the design and development of automotive safety-related electrical or electronic (E/E) systems. Functional safety is considered and implemented during the entire development process of safety-related E/E systems. It provides guidelines for identifying and classifying hazards and risks arising from malfunctions. Subsequently, the automotive safety integrity level (ASIL) can be determined by considering the exposure, severity and controllability of each hazardous event. Safety requirements are then derived according to the ASIL to achieve an ultimately acceptable level of risk.

When the derived safety requirements are implemented, an intended function would still have residual risks that could stem from technical failures due to unexpected hardware or software problems. However, the residual risks are acceptable. Therefore, this standard is

[15] Waymo: On the Road to Fully Self-Driving: Waymo Safety Report (2017).

[16] ISO: ISO 26262: Road Vehicles—Functional Safety—Part 1: Vocabulary (2011).

widely used for functional safety. Nevertheless, the ISO 26262 is no longer applicable any more for highly AVs (HAVs), since a driver is not responsible for driving. A HAV refer to an AV with a driving automation system of at least level 3. Koopman and Wagner[17] think that the "controllability" parameter can be set to zero, but doubt that the ISO 26262 will still work for AVs, since safety requirements will increase dramatically.

2.1.2 SOTIF

Whether a driving automation system behaves safely, assuming it has no malfunctions, belongs to the behavior safety, which is outside the scope of ISO 26262. Therefore, the standard safety of the intended functionality (SOTIF)[18] is proposed as a supplement of the standard ISO 26262. It provides a guidance for addressing issues arising from the faults of sensors and algorithms, incorrectly understanding of a situation and improper operation of the intended functions. Hence, a function is robust against uncertainties from sensors and able to behave safely if the SOTIF is well implemented. The SOTIF standard is supposed to be applicable for HAVs[19], since the following three aspects are included:

- Situations, in which a driver is out of the loop.
- Non-deterministic algorithms like machine learning-based functions.
- Fail-operational systems, different from ISO 26262 which is designed for fail-safe systems.

Therefore, the SOTIF standard seems to be very proposing, but is still under development.

2.1.3 UL4600

The standard UL4600[20] is proposed for the safety of general autonomous products by defining three components: goal, argument and evidence. A goal could be intuitive like the collision avoidance with an object. Arguments are the facts to explain how the safety goal is achieved, while evidences support the arguments by using simulation, real-world tests etc. Therefore, a goal-based process is introduced in this standard. The aim of this standard is that an AV could be proved to have an acceptable level of safety by documenting the results from both arguments and evidences. By using safety performance indices (SPI), the safety of the system is evaluated during its lifecycle. The system can thus be continuously improved

[17] Koopman, P.; Wagner, M.: Challenges in Autonomous Vehicle Testing and Validation (2016), p. 17.

[18] ISO, I. S.; PAS, A. W.: 21448: Road vehicles—Safety of the intended functionality (2019).

[19] Takács, Á. et al.: Assessment and standardization of autonomous vehicles (2018).

[20] Koopman, P. et al.: A safety standard approach for fully autonomous vehicles (2019).

based on the evaluation results. However, no benchmarks for real-world tests, no criteria for evaluating safety performance or no overall design process are explicit in this standard.[21]

2.2 Safety Verification and Validation Approaches

The safety verification and validation approaches play an important role when a prototype of an AV is finished. It determines whether the predefined requirements are fulfilled and whether the AV will behave as desired. Since the proposed VAAFO approach belongs to the safety verification and validation approaches, different existing approaches are introduced. As a result, it would be possible to determine the role of the VAAFO approach in the entire family.

2.2.1 Real-World Testing

The real-world testing as a direct and valid test approach has been widely utilized for testing driving automation systems. The test results are very valuable to evaluate and improve AVs since AVs are exposed to the real-world scenarios with different complexity and diversity. Hence, the actual performance of AVs is examined. Additionally, the reality is the final place where AVs are applied to. Therefore, the real-world testing is an inseparable step. Figure 2-1 shows an example of testing perception algorithms of an AV in the real world. Object class and depth are acquired during the fusion of camera and lidar. However, hundreds of millions of kilometers and even hundreds of billions of kilometers are required to demonstrate the safety of AVs when considering the fatalities and injuries in 2015 in USA.[22] Similar statistical analysis has been conducted by Wachenfeld and Winner[23] as well according to the German fatal accidents on motorways in 2017. 6.6 billion kilometers are concluded by assuming independent occurrence and Poisson distribution of the traffic accidents. Even though Waymo[24] has tested their AVs over 32 million kilometers on public roads until 2020, it is still far behind the required statistical distance. Moreover, a safety driver must take over an AV in time in case of any kind of failures during the test, which poses additional risks to the persons on board as well as other traffic participants in the vicinity of the AV. Lastly, the hardware and software of an AV are rapidly updated, since new functions or features are added according to newly derived requirements, or the algorithms are changed to increase correctness and robustness. Consequently, an AV has to be tested again if the modular safeguarding of the AV is not yet implemented. As a result, the test effort would be multiplied

[21] Concas, F. et al.: Validation Frameworks for Self-Driving Vehicles: A Survey (2021).

[22] Kalra, N.; Paddock, S. M.: Driving to safety (2016).

[23] Wachenfeld, W.; Winner, H.: The Release of Autonomous Vehicles (2016).

[24] Waymo: Waymo Safety Report (2020).

several times. Thus, the real-world testing is unbearable at the economical level. As a result, the real-world testing is meaningful and valuable, but impractical.

Figure 2-1: The real-world testing of perception algorithms for automated vehicles[25]. (G. Ajay Kumar et al., 2020). CC-BY 4.0

2.2.2 Simulation-based Testing

Simulation as an important way to test AVs can be used not only to discover problems of algorithms in the development phase, but also to simulate critical scenarios or the scenarios that are difficult to control in reality in the verification phase. Furthermore, the scenarios in the simulation can be repeated easier than those in reality. By using a cluster of computers and tools for automatic execution, the testing process of AVs could be accelerated. Due to such great advantages of the simulation-based testing, it is regarded as an indispensable complement to the real-world testing. Many simulation platforms such as VTD[26], CarMaker[27], etc. are thus arisen. Figure 2-2 shows an example of the environment in CarMaker. Some of them such as SUMO[28] include even a traffic simulator, so that it is possible to generate more general scenarios. Co-simulation between macroscopic platforms and microscopic platforms

[25] Kumar, G. A. et al.: LiDAR and camera fusion approach for object distance estimation (2020).

[26] Neumann-Cosel, K. von: Virtual Test Drive: Simulation umfeldbasierter Fahrzeugfunktionen (2014).

[27] IPG Automotive GmbH: CarMaker (2020).

[28] Behrisch, M. et al.: SUMO - simulation of urban mobility: an overview (2011).

(e.g. VISSIM[29]) are thus performed to test and validate of AVs[30,31]. Meanwhile, scenarios in which AVs fail to operate properly can also be obtained. Among the simulation platforms, there are several open-source tools. The CARLA[32] and LGSVL[33] are the two representative ones. With respect to the application of the simulation-based approach, Hallerbach et al.[34] use it to identify critical scenarios. A similar research is conducted by Weber et al.[35] for the derivation of concrete scenarios to test AVs.

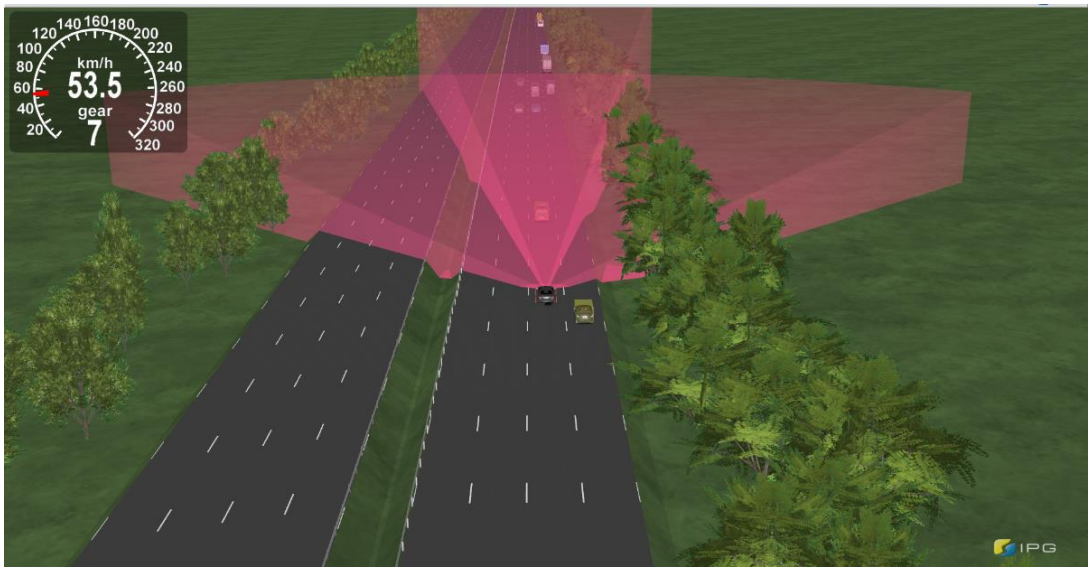

Figure 2-2: One example of the simulation environment in CarMaker.

Nevertheless, the validity of simulation models are the key challenges. The traffic objects models should be calibrated and validated by real traffic measurements to ensure their credibility. Since the calibration depends on the parameters that affect the driver behavior (assuming the traffic objects are vehicles) and is mostly case-specific[36], some kinds of assumptions have to be made. As a result, the fidelity of simulation is reduced. In addition to the models of traffic objects, vehicle models and environment should be carefully parametrized as well in the simulation. Koopman and Wagner[37] point out that the assumptions made by the various-fidelity models should be considered to build an effective simulation. Low-fidelity simulations require typically less execution time by simplifying the systems, while

[29] PTV, AG: PTV Vissim 10 user manual (2018).

[30] Nalic, D. et al.: Development of a co-simulation framework for systematic generation of scenarios (2019).

[31] Sippl, C. et al.: Distributed real-time traffic simulation for autonomous vehicle testing (2018).

[32] Dosovitskiy, A. et al.: CARLA: An open urban driving simulator (2017).

[33] Rong, G. et al.: Lgsvl simulator: A high fidelity simulator for autonomous driving (2020).

[34] Hallerbach, S. et al.: Simulation-based identification of critical scenarios for automated vehicles (2018).

[35] Weber, N. et al.: A simulation-based, statistical approach for the derivation of concrete scenarios (2020).

[36] Aparow, V. R. et al.: A Comprehensive Simulation Platform for Testing Autonomous Vehicles (2019).

[37] Koopman, P.; Wagner, M.: Toward a Framework for Highly Automated Vehicle Safety Validation (2018).

high-fidelity typically needs more time but has fewer assumptions. These two different types of models are both valuable and can be used in different applications. Furthermore, valid sensor models[38,39] as a necessary part for simulation-based testing are also obstacles. The validation of sensor models are prerequisites for testing tracking and sensor fusion algorithms of AVs. Therefore, the simulation-based approach is useful, but not powerful to test and validate AVs.

2.2.3 Function-based Testing

The function-based testing describes that a function is tested under some predefined specific procedures or scenarios. This approach has been widely used for functions like adaptive cruise control (ACC) in standard ISO 15622 and advanced emergency braking (AEB) systems in UN ECE R131. However, this approach is not applicable any more for AVs since it is difficult to define clearly what functionality an AV has. Different situations require that an AV has different abilities. Moreover, the functionalities of an AV are integrated together in one system, which could be rather difficult to test each functionality individually. However, the tests in function-based testing are usually performed separately and independently. Moreover, an AV may be designed specifically for the predefined test scenarios according to the function-based testing in order to gain e.g. a release or a license, which poses very high requirements on the representative and completeness of the test scenarios. It may even be impossible to determine these test scenarios for the release of AVs. Additionally, a lot of benchmark data is required to evaluate the performance of AVs.

2.2.4 Formal Verification

In the formal verification, a system will be designed to obey some predefined rules, which can be explicitly expressed by mathematical formulas. As a result, the safety of the system is guaranteed if the rules that the system follows are valid. One of the well-known formal verification approaches is the Responsibility-Sensitive Safety (RSS)[40]. The RSS model provides an interpretation of human judgement under comprehensive traffic situations by means of formulas, and ensures that AVs would not lead to an accident initiatively. Traffic accidents could still happen, but the responsibility of the accident is clear when analyzing the actions of those involved in the accidents. The safety validation of AVs can thus be simplified by proving the actions of the systems are in line with the predefined set of mathematical rules. In RSS, five rules are defined[41]:

[38] Holder, M. et al.: Measurements revealing challenges in radar sensor modeling for virtual validation (2018).

[39] Rosenberger, P. et al.: Benchmarking and Functional Decomposition of Lidar Sensor Models (2019).

[40] Shalev-Shwartz, S. et al.: On a formal model of safe and scalable self-driving cars (2017).

[41] Mobileye: Responsibility-Sensitive Safety (RSS) A Model for Safe Autonomous Driving (2021).

- A safe longitudinal distance is defined in order to not hit the car in front.
- A safe lateral distance is defined in order to not cut in recklessly.
- AVs should avoid a crash if other drivers violate the right of way principles.
- AVs should be cautious in areas with limited visibility.
- AVs must avoid a crash if it can do so without causing another.

These five rules can then be utilized to guide the design of a planning module. For instance, Gassmann et al.[42] integrate the RSS safety checker into the Apollo software stack. The RSS safety checker define additional constraints for the planning module of Apollo by understanding the environment data. Therefore, it is obviously that the RSS focuses solely on providing a safe planning and decision-making strategy of an AV. However, the perception as a vital part needs a safety checker as well.[43] Additionally, it is unrealistic to assume that all vehicles will follow these rules exactly at all times. The motion control is not included as well since they argue that many researches are conducted from the last decades. Thus, the feasibility and applicable of the approach should be further studied.

2.2.5 Scenario-based Testing

The scenario-based testing has been studied in several research projects, e.g. PEGASUS[44], ENABLE S3[45]. There is a growing interest in this approach. The main idea of this approach is to identify relevant scenarios and then generalize them to generate more test scenarios. These scenarios are utilized to test AVs. The test scope is reduced by abandoning irrelevant scenarios. In order to summary the process of this approach, Riedmaier et al.[46] propose a taxonomy for the scenario-based testing, which includes mainly the scenario generation, scenario selection, scenario execution and AV assessment. In this dissertation, the taxonomy is extended by considering the possible scenario sources and other newly proposed approaches. In addition, the scenario execution is not introduced in detail since the ways to execute scenarios are limited and well known. As a result, the implementation process of the scenario-based testing is shown in Figure 2-3. Each main part is introduced in the following subchapters.

---

[42] Gassmann, B. et al.: Towards standardization of av safety: a library for responsibility sensitive safety (2019).

[43] Buerkle, C. et al.: Towards Online Environment Model Verification (2020).

[44] German Aerospace Center: PEGASUS-Project (2019).

[45] Leitner, A.: ENABLE-S3: Project Introduction (2020).

[46] Riedmaier, S. et al.: Survey on Scenario-Based Safety Assessment of Automated Vehicles (2020).

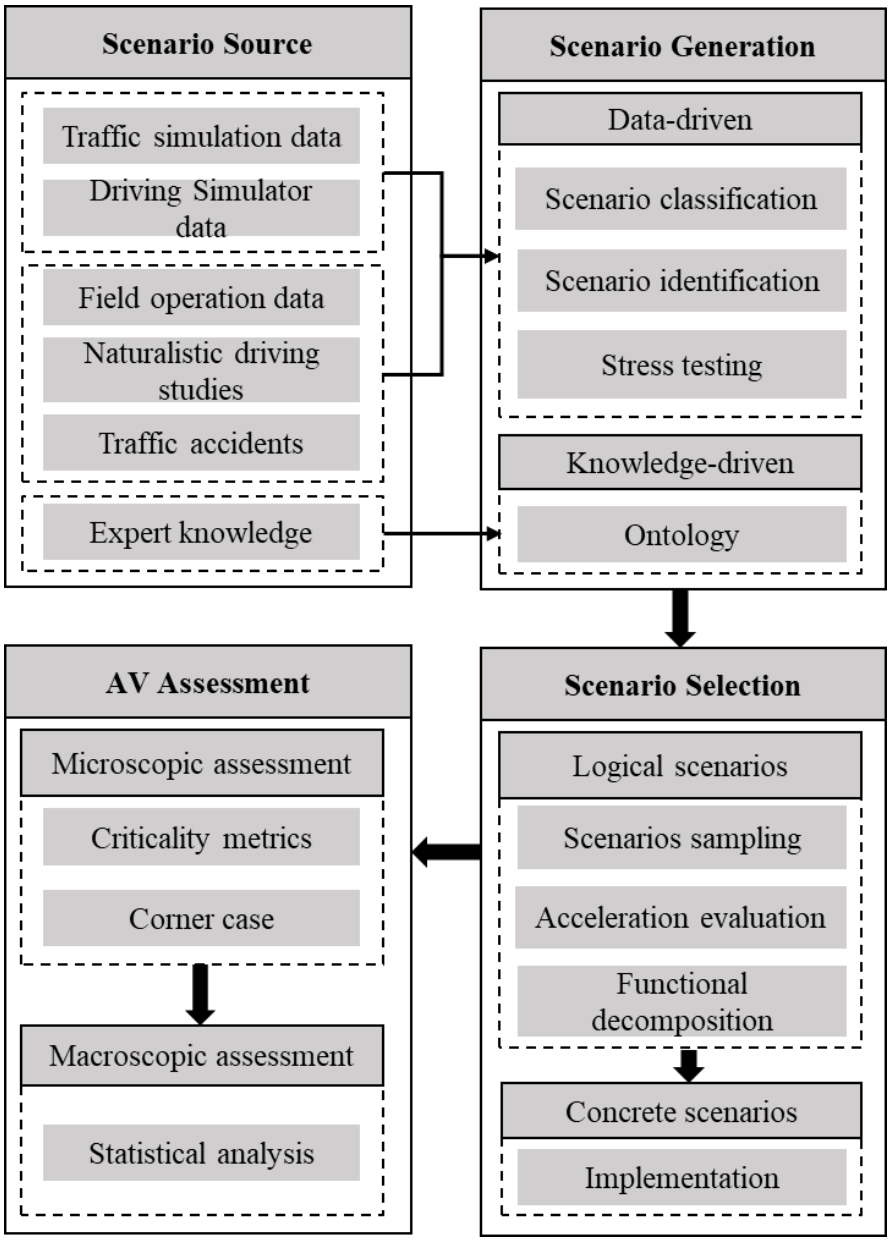

Figure 2-3: The implementation process of the scenario-based testing. Own illustration according to Riedmaier et al.[46]

2.2.5.1 Scenario Source

There are many different ways to obtain scenarios that can be used as a source for the scenario-based testing. Generally, the source of the scenario can come from the simulation data, real-world data and expert knowledge. In the simulation, both the data from a traffic simulation and a driving simulator are useful. As aforementioned, the traffic simulation can help to verify and validate AVs. Thus, critical scenarios or relevant scenarios could be gained. The risks from a human-machine interaction can be studied with a driving simulator. The field operation data is collected during the implementation of AVs on public roads. In this process, two types of data are typically recorded. Only the perception data is online recorded and the decision is performed in the post-processing phase based on the perception data. A

human driver drives the vehicle in this case. This type of test method is defined as open-loop recording. The second option is that data from the entire AV, including perception and decision data, are all recorded online. So, the test is a closed loop. With respect to the recorded data, Waymo[47] publishes its automated driving dataset that is recorded in urban scenarios with lidars and cameras. Scenarios from motorways, country roads, urban and even parking spaces are included in the dataset from Lyft[48] by using four lidars with different layers and seven cameras. The naturalistic driving data from a bird's eye perceptive rather than the view of the subject vehicle is collected by a drone in HighD[49], InD[50] and rounD[51a] datasets. HighD records the data on a motorway section, while InD focuses on an intersection. The trajectories and velocities of each object in a roundabout are available in the rounD, as shown in Figure 2-4. Kang et al.[52] summarize the currently available datasets including the KITTI dataset[53], the cityscapes dataset[54] for semantic urban scenes, etc. The traffic accidents are a useful source as well to test AVs since those scenarios pose challenges for human drivers. It is interesting to study whether the AVs would also behave unsafely in those scenarios. Lastly, an experienced engineer knows the limitations of a function or a system, it is thus possible to extract functional scenarios from the expert knowledge.

Figure 2-4: A time step of the recorded data to illustrate of the rounD dataset[51b]. ©2020 IEEE

[47] Sun, P. et al.: Scalability in perception for autonomous driving: Waymo open dataset (2020).

[48] Lyft: Data - Lyft (2019).

[49] Krajewski, R. et al.: The highd dataset (2018).

[50] Bock, J. et al.: The ind dataset: A drone dataset of road user trajectories at german intersections (2019).

[51] Krajewski, R. et al.: The round dataset: A dataset of road user trajectories at roundabouts (2020).a: -; b: p. 1.

[52] Kang, Y. et al.: Test your self-driving algorithm: An overview of publicly available driving datasets (2019).

[53] Geiger, A. et al.: Vision meets robotics (2013).

[54] Cordts, M. et al.: The cityscapes dataset for semantic urban scene understanding (2016).

2.2.5.2 Scenario Generation

With respect to the scenario generation, the knowledge-driven and data-driven are regarded as two ways. In the data-driven approach, the scenarios coming from the collected data are either classified or filtered to acquire concrete scenarios.

2.2.5.2.1 Data-driven Approach

In order to extract relevant concrete scenarios from the massive amount of data, indicators are typically essential. Althoff and Lutz[55] take the drivable area as an indicator to quantify the criticality of the subject vehicle. The drivable area infers the solution space in which the subject vehicle can drive safely without collision. Klischat and Althoff[56] optimize subsequently the indicator for more complex and diverse scenarios e.g. crossroads. Langner et al.[57] define the reproduction error as an indicator to identify anomalies in the real measurement data by applying an autoencoder neural network. A neural network is applied by Krajewski et al.[58] as well to generate many new realistic trajectories by varying the input parameters of the model. With the inverse mapping from trajectories to the parameters of the model, the parameter representation of a rare or critical maneuver is obtained. However, the definition of a rare or a critical maneuver is unclear in the paper.

In contrast to filter the collected data directly, some studies about classifying the vehicle behavior are conducted. According to the results of the classification, the exposure of each classified vehicle behavior can be acquired from the measurement data. A scenario is considered valuable if the exposure of the vehicle behavior in the scenario reaches a certain percentage of the overall collected data, since unsafe behavior in more frequently occurring scenarios is regard to be of greater risk than in infrequent scenarios.[59] Erdogan et al.[60] compare rule-based, supervised and unsupervised machine learning to classify maneuvers from the measurement data, which are used subsequently to generate logical scenarios by specifying parameter ranges or distributions.

The stress testing[61] can be categorized as identifying relevant scenarios using indicators as well, since possible failure scenarios in which an AV violates the safety requirements, can be determined by the stress testing. The indicators could be for example a proper designed reward function. The motivation of stress testing is that most of work for simulation and road

[55] Althoff, M.; Lutz, S.: Automatic generation of safety-critical test scenarios for collision avoidance (2018).

[56] Klischat, M.; Althoff, M.: Generating critical test scenarios with evolutionary algorithms (2019).

[57] Langner, J. et al.: Estimating the uniqueness of test scenarios derived from real-world-driving-data (2018).

[58] Krajewski, R. et al.: Data-driven maneuver modeling for safety validation of automated vehicles (2018).

[59] Hartjen, L. et al.: Classification of driving maneuvers in urban traffic for parametrization of scenarios (2019).

[60] Erdogan, A. et al.: Real-world maneuver extraction for validation: A comparative study (2019).

[61] Corso, A. et al.: Adaptive stress testing with reward augmentation for autonomous vehicle validatio (2019).

tests is uneventful, only those critical scenarios are useful to test AVs. Nalic et al.[62] use the same concept (stress testing), but the principle is totally different. They manipulate the traffic participants in the vicinity of an AV to provoke critical scenarios resulting from statistical accidents on motorways in Austria. As a result, the occurred frequency of critical scenarios in the simulation is increased. Finally, the critical and eventually critical scenarios increase significantly when comparing the results without using stress testing. The stress testing as an optimization-based searching approach requires constraints for the searching space. The constraints should be properly designed. Otherwise, some uninteresting scenarios would appear, e.g., an oncoming vehicle changes suddenly to the lane of the subject vehicle, this kind of scenarios could be gained during the optimization. However, they are typically uninteresting since the behavior of the traffic participant is unreasonable. Thus, the search techniques, which do not have to parameterize the search space, are applied. For example, Tuncali and Fainekos[63] utilize the rapidly-exploring random tree (RRT) to discover boundary case scenarios.

Currently, boundary case, edge case and corner case are mentioned in some researches[64,65,66]. They are potentially critical for AVs but have different definitions than the critical scenarios. The different definitions of these three terms from the literatures are summarized here.

- Edge case: unknown unsafe scenarios, which are difficult to predict using existing deterministic testing methodologies but could lead to accidents.[67]
- Corner case: a transition from a safe scenario to an unsafe one, where the individual scenario parameters are within the capability of the system, but the combination challenges the system.[68,69] However, Bolte et al.[70] define corner cases as non-predictive relevant objects/classes in the relevant locations to evaluate of the perception of an AV. Breitenstein et al.[71] consider unexpected and unknown situations that occur during the driving as corner cases, which is more general than the definition from Bolte.

[62] Nalic, D. et al.: Stress Testing Method for Scenario-Based Testing of Automated Driving Systems (2020).

[63] Tuncali, C. E.; Fainekos, G.: Rapidly-exploring random trees for testing automated vehicles (2019).

[64] Koopman, P. et al.: Autonomous vehicles meet the physical world (2019).

[65] Mullins, G. E. et al.: Adaptive generation of challenging scenarios for testing of autonomous vehicles (2018).

[66] Tuncali, C. E. et al.: Simulation-based adversarial test generation with machine learning components (2018).

[67] Karunakaran, D. et al.: Efficient statistical validation with edge cases to evaluate Automated Vehicles (2020).

[68] ISO: ISO/TR 4804: Road Vehicles – Safety and security for automated driving systems (2020).

[69] Batsch, F. et al.: Performance boundary identification using Gaussian process classification (2019).

[70] Bolte, J. A. et al.: Towards corner case detection for autonomous driving (2019).

[71] Breitenstein, J. et al.: Corner Cases for Visual Perception in Automated Driving (2021).

- Boundary case: boundaries between barely avoided collisions and collisions that could have been avoided with minor changes in the control or perception.[72]

Batsch et al.[73] summarize that the three terms describe generally a scenario, whose outcome lies on the boundary between safe and unsafe, and a small change of one parameter might result in an unsafe scenario. They agree more that the terms represent the function limit of a deployed AV. However, even though there is no standard terminology about these three items, they have the same aim. By focusing the cases toward an unsafe situation, an AV could be tested efficiently since a lot of irrelevant scenarios are abandoned.

2.2.5.2.2 Knowledge-driven Approach

Since the collected data may not include all aspects of a scenario due to the limitations of sensors, and some relevant scenarios in the data are still not included, the knowledge-driven approach is studied, and can be regarded as a complement of the data-driven approach. For example, a person who has in-depth knowledge of different components of an AV, could help to identify challenging scenarios. Ontology is typically used in the knowledge-driven approach. Guarino et al.[74] define ontology as a formal and explicit specification of a shared conceptualization. Bases on this definition, Geyer et al.[75] propose a unified and fundamental ontology for generation of test and use-cases for AVs guidance, which has been then widely adopted in the field of AVs.

The knowledge should be structured and varied on a semantic level and described linguistically in order to generate functional scenarios. Bagschik et al.[76] use ontologies as the knowledge-based approach to generate traffic scenes in natural language. These traffic scenes can then be taken as the basis for creating scenario. In order to structure the knowledge, a 5-layer model is applied by extending the 4-layer model proposed by Schuldt et al.[77] Compared to the 4-layer model, the situation-specific adaptations of the base road network are split into traffic infrastructure (including traffic signs, structural boundaries and markings), and temporary manipulation of road-level and traffic infrastructure. In PEGASUS project, Bock et al.[78] add the sixth layer namely digital information to the 5-layer model for motorway scenarios, as illustrated in Figure 2-5 (left). The 6-layer model is then refined and extended by Scholtes et al.[79a] for urban traffic and environment, as shown in Figure 2-5 (right). The differences between the 6-layer model for motorways and 6-layer

[72] Tuncali, C. E.; Fainekos, G.: Rapidly-exploring random trees for testing automated vehicles (2019).

[73] Batsch, F. et al.: A taxonomy of validation strategies to ensure safety of automated vehicles (2020).

[74] Guarino, N. et al.: What Is an Ontology? (2009).

[75] Geyer, S. et al.: Concept and development of a unified ontology for test and use-case catalogues (2013).

[76] Bagschik, G. et al.: Ontology based scene creation for the development of automated vehicles (2018).

[77] Schuldt, F. et al.: Effiziente systematische Testgenerierung in virtuellen Umgebungen (2013).

[78] Bock, J. et al.: Data basis for scenario-based validation of HAD on highways (2018).

[79] Scholtes, M. et al.: 6-Layer Model of Urban Traffic and Environment (2020).a: -; b: p. 6.

model for urban are that roadside structures, such as buildings, guardrails in urban environment, are separately considered and defined in level 2. Additionally, the level 1 (road network) and 2 (traffic infrastructure) from the 6-layer model for motorways are merged into one layer in the 6-layer model for urban. With the defined 6-layer model for urban, the environment is structurally categorized, which can be served as a foundation for the ontology.

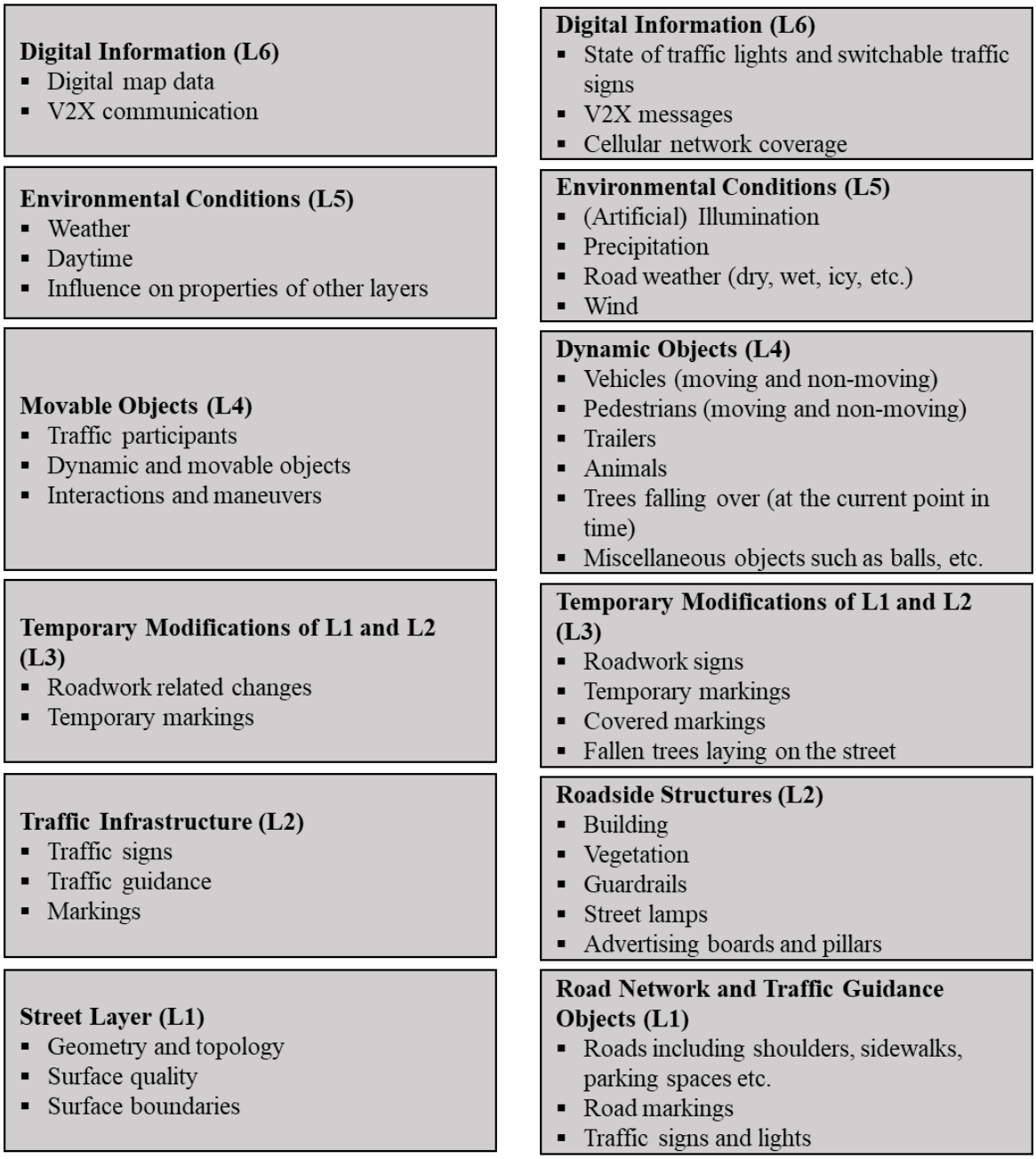

Figure 2-5: The 6-layer model for describing motorway scenarios (left) and urban scenarios (right). Own illustration according to Bock et al.[78] (left) and Scholtes et al.[79b] (right).

2.2.5.3 Scenario Selection

Once the functional scenarios are derived, logical scenarios can be created by defining parameter ranges or parameter distributions. In order to finally generate concrete scenarios,

several sampling techniques are applied. In the *N*-wise sampling, all possible combinations of all interesting values of *N* parameters are performed. If there are many parameters and each parameter is discretized with a small interval, a huge amount of combination will be available. Amersbach and Winner[80] point out that the number of possible combinations in a following scenario on motorways is $4 \cdot 10^{18}$ when using the *N*-wise sampling. Therefore, *t*-wise is a possible way to reduce the combinations, which demands every possible combination of interesting values of *t* parameters be included to form the test category.[81] The discretization of parameters and the combination of discretized values of parameters are the two key challenges in this type of sampling. Consequently, Amersbach and Winner[82] decompose the HAV into six layers, which are information access, information reception, information processing, situational understanding, behavioral decision and action, as shown in Figure 2-6. The aim of functional decomposition is that a test case can be decomposed into several particular cases to test only one or more functional layers. Consequently, the test effort is reduced, since repeated tests of the same functions and requirements are avoided.

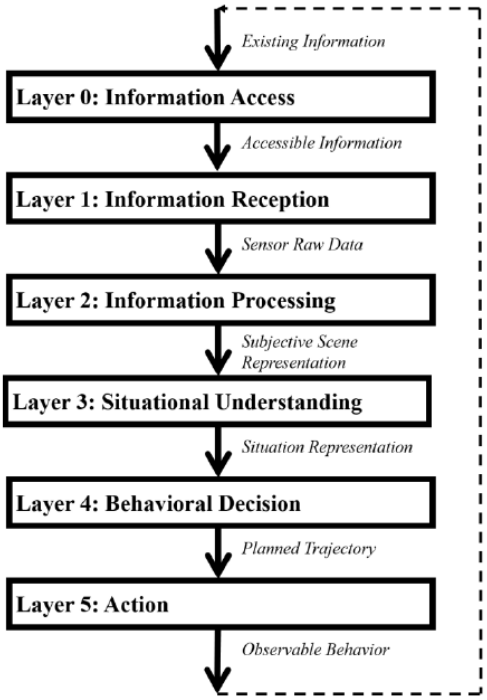

Figure 2-6: The functional decomposition of a HAV[83]. (Christian Amersbach, 2020). CC-BY-SA 4.0

Conversely, the discretization is no longer necessary in the sampling technique such as Monte Carlo. Gelder and Paardekooper[84] use Monte Carlo to generate concrete scenarios by

[80] Amersbach, C.; Winner, H.: A contribution to overcome the parameter space explosion (2019).

[81] Grindal, M. et al.: Combination testing strategies: a survey (2005).

[82] Amersbach, C.; Winner, H.: Functional Decomposition (2017).

[83] Amersbach, C. T.: Diss., Functional Decomposition Approach (2020), p. 59.

[84] Gelder, E. de; Paardekooper, J.-P.: Assessment of automated driving systems using real-life scenarios (2017).

fitting the parameter distribution with kernel density estimation. However, Monte Carlo is inefficient due to its random sampling, which then results in the occurrence of many non-safety-critical cases. Therefore, acceleration sampling is studied. Zhang et al.[85] propose the subset sampling to search the failure zone of a system iteratively. As a result, fewer testes are required to estimate the performance of a system. They compare the subset sampling with the important sampling[86], and prove that the acceleration rate of these two sampling methods are in the same level. In addition, they indicate that the subset sampling can handle black-box systems. Due to the inefficiency of Monte Carlo, Markov Chain Monte Carlo (MCMC) is proposed for sampling based on probabilistic models. Akagi et al.[87] use the MCMC method to generate scenarios predominantly having high risks by considering risk index in the probabilistic model. Thus, scenarios containing safe driving situations are less generated, and the efficiency of sampling is improved.

2.2.5.4 AV Assessment

When concrete scenarios are available, suitable test environment should be selected. Generally, X-in-the-Loop (XiL) is a typical way to perform concrete scenarios. By using a part of virtual components until pure virtual components in the whole system, XiL can be generally divided into Model-in-the-Loop (MiL), Software-in-the-Loop (SiL), Hardware-in-the-Loop (HiL), Driver-in-the-Loop (DiL) and Vehicle-in-the-Loop (ViL). Applications of various forms of XiL can be found in the field of AVs, especially in the verification and validation phase of a function or a system. Fayazi et al.[88] utilize a ViL to verify their proposed traffic management scheme for AVs in an intersection. A HiL platform is used for developing and testing automated driving functions with level 2 by Gelbal et al.[89] Scenario-in-the-Loop (SciL)[90] is thought to be the next generation of XiL validation methodology. In this framework, the boundary between reality and virtual is blurry. As a result, whether the signals are from the real world or simulated can be determined by the demand. Compared to ViL, the perception module can also be tested since the input signals required by the perception can be provided by the SciL. Consequently, it is more flexible to decide which part should be real and which part should be simulated during the test.[91]

---

[85] Zhang, S. et al.: Accelerated evaluation of autonomous vehicles in the lane change scenario (2018).

[86] Zhao, D. et al.: Accelerated evaluation of automated vehicles in car-following maneuvers (2017).

[87] Akagi, Y. et al.: A risk-index based sampling method to generate scenarios for automated vehicle (2019).

[88] Fayazi, S. A.; Vahidi, A.: Vehicle-in-the-loop verification of a smart city intersection control scheme (2017).

[89] Gelbal, Ş. Y. et al.: Hardware-in-the-loop simulator for developing automated driving algorithms (2017).

[90] Horváth, M. T. et al.: The Scenario-in-the-Loop (SciL) automotive simulation concept (2019).

[91] Szalay, Z.: Next Generation X-in-the-Loop Validation Methodology for Automated Vehicle Systems (2021).

Different XiL methodologies for testing AVs are summarized in Figure 2-7 with a V-model. From left to right, the level of abstraction of methodology decreases, while its validity increases. For instance, all components are modelled as virtual in a SiL, which strengthens the reproducible and observable of the test, but requires validated models. In contrast, SciL and ViL bring high valid results, but suffer from high economical and time cost. Hence, different methodologies should be utilized in different phases during the development of AVs. MiL and SiL could discover potential problems quickly and conveniently in the early stages of vehicle development. ViL is more suitable in the integration stage of sub-functions. The proving ground is an alternative way to execute concrete scenarios with high validity as well. However, not all components can be controlled, e.g. the surface of the road, the weather, etc. Mixed virtual and real environment[92] might be a solution as introduced in the SciL.

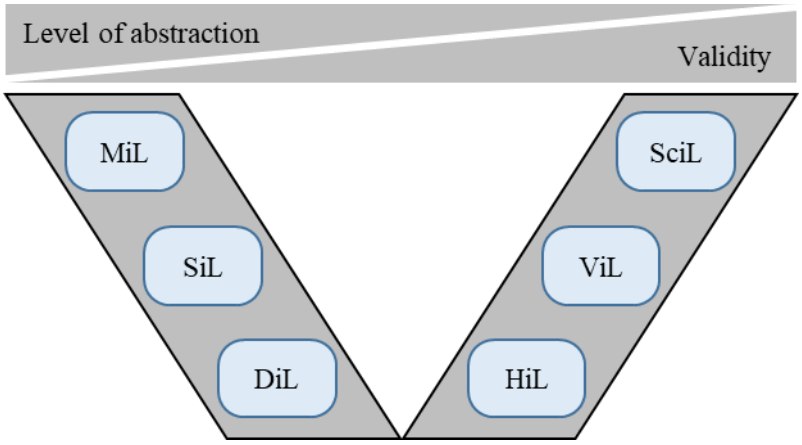

Figure 2-7: Different XiL methodologies to execute concrete scenarios. Own illustration according to Batsch et al.[93]

Generally, the assessment of AVs includes microscopic assessment and macroscopic assessment. Junietz[94] defines the macroscopic assessment in his dissertation as the average risk of a system, e.g. the occurrence rate of fatal accidents, while the risk of a system in a scene is called microscopic assessment. By using a vast amount of data or extrapolation such as the Extreme Value Theory (EVT)[95,96], the macroscopic assessment could be derived. To evaluate the safety of AVs in a scene, the indicators mentioned in the scenario generation are typically applied, i.e., the indicators can be used not only to identify relevant scenarios from the simulated data or the real-world data, but can also be considered as surrogate safety measures to evaluate the safety performance of AVs. The indicators can be generally classified as tem-

[92] Németh, H. et al.: Proving Ground Test Scenarios in Mixed Virtual and Real Environment (2019).

[93] Batsch, F. et al.: A taxonomy of validation strategies to ensure safety of automated vehicles (2020), p. 3.

[94] Junietz, P. M.: Diss., Microscopic and Macroscopic Risk Metrics (2019), p. 8.

[95] Åsljung, D. et al.: Comparing collision threat measures for verification of autonomous vehicles (2016).

[96] Åsljung, D. et al.: Using extreme value theory for vehicle level safety validation and implications (2017).

poral proximal indicators, distance proximal indicators and intensity based indicators. Intensity based indicators are used here instead of deceleration based indicators from Mahmud et al.[97] to be more general, e.g., the lateral acceleration required to evade a preceding object is also an indicator.

2.2.5.4.1 Temporal Proximal Indicators

The most commonly used temporal proximal indicator is the Time-to-X (TTX). In particular, Time-to-Collision (TTC) is well known, which describes the expected time that two vehicles with constant velocity will collide with each other. When considering extra the relative acceleration of the vehicles, TTC is extended as enhanced TTC (ETTC)[98]. A greater degree of safety could be concluded if the value of TTC is large. Nevertheless, it is not always the case, e.g., TTC is infinite when the two observed vehicles have the same speed but with a small distance gap, if the lead vehicle brakes suddenly, the situation is thus quite critical and a collision could possibly happen. Additionally, identical TTC in different situations does not mean the same level of safety if the driving speed is different. In order to quantify the severity of near-crash scenarios, minimum TTC (TTC_{min}) is often applied, which depicts the minimum value of TTC during the approach of two vehicles on the collision course. Moreover, Winner et al.[99] recommended inverse TTC instead of TTC, since the inverse TTC increases with the criticality of a situation monotonically, and infinite TTC can be avoided when the relative speed of two vehicles is zero. Time exposed TTC (TET) and Time integrated TTC (TIT) are two derivatives of TTC, which could give a more complete and comprehensive indication of the safety-level on a particular section of road during a particular period of time.[100]

Due to the limitations of TTC, other criticality metrics like Time-to-React (TTR)[101] including Time-to-Brake (TTB), Time-to-Steer (TTS) and Time-to-Kickdown (TTK) are motivated. The TTB denotes the remaining time until an emergency braking with maximum deceleration must be applied to avoid a collision. If a driver or an AV selects the steering to avoid a collision, the TTS is applied and defined as the remaining time that the vehicle's front just passes by the object's facing edge by steering along a circular arc. The principle behind TTK is that the subject vehicle could pass by an object by acceleration before a collision that occurs, when the object enters the driving lane of the subject vehicle. Compared to TTC, the TTR metrics take the driver's possible actions into account and indicate how difficulty the prevention of an accident would be.

---

[97] Mahmud, S. S. et al.: Application of proximal surrogate indicators for safety evaluation (2017).

[98] Winner, H.: Grundlagen von Frontkollisionsschutzsystemen (2015), p. 900.

[99] Winner, H. et al.: Maße für den Sicherheitsgewinn von Fahrerassistenzsystemen (2013), p. 9.

[100] Minderhoud, M. M.; Bovy, P. H.: Extended time-to-collision measures for safety assessment (2001).

[101] Hillenbrand, J. et al.: A multilevel collision mitigation approach (2006).

One popular metric for un-signalized intersection scenarios is the post-encroachment time (PET)[102], which means the time difference between the departure of a vehicle from an area of a potential collision and the entry of another vehicle into this area. PET requires less information than TTC as the relative distance and relative speed are not involved. It is possible to use solely video images to obtain the PET. However, PET may not measure the conflict severity objectively, e.g., a pedestrian in the front of or at the side of the subject vehicle may have the same PET; the situation in which the pedestrian is at the side of the subject vehicle, is definitively less critical since no lateral velocity but high longitudinal velocity of the subject vehicle exists.

Based on the above analysis, it can be found that the metrics have their own suitable application situations. The Worst-Time-to-Collision (WTTC)[103] as a metric that can be applied in different situations is thus motivated. The criticality of a situation is calculated by assuming the worst behavior of vehicles. A situation can be abandoned if it is regarded as uncritical even under the worst possible maneuvers. Based on this definition, the criticality of some situations is overestimated, e.g., the vehicles at adjacent lanes travelling at opposite direction would invade the driving lane of the subject vehicle directly under the worst case assumption. Other work focuses on the combination of several surrogate safety measures together. Nadimi et al.[104] propose a new mixed index (MI), which combines the properties of TTC and PET. The application of MI in real car-following scenarios shows that the MI would be more suitable for measuring the rear-end collision risks. In SAE J2944[105], the guidance to compute different surrogate safety measures are provided. Their distributions in naturalistic driving and safety-relevant thresholds are studied.

2.2.5.4.2 Distance Proximal Indicators

There are fewer distance proximal indicators than temporal proximal indicators. Among the distance proximal indicators, the difference of space distance and stopping distance (DSS) is well-known, which describes the difference of the space and stopping distance. The space distance is the sum of the current relative distance and the braking distance of the preceding vehicle, while the stopping distance is the sum of the brake reaction distance and the braking distance of the subject vehicle. Hence, negative DSS values mean a collision, since the subject vehicle cannot avoid the collision when the preceding vehicle stops suddenly. Nevertheless, the severity and the duration of danger is not represented by DSS. Time integrated DSS (TIDSS) is thus motivated. By comparing the traffic accidents, Okamura et al.[106] proves that TIDSS correlates strongly with traffic accidents.

---

[102] Allen, B. L. et al.: Analysis of traffic conflicts and collisions (1978).

[103] Wachenfeld, W. et al.: The worst-time-to-collision metric for situation identification (2016).

[104] Nadimi, N. et al.: Calibration and validation of a new time-based surrogate safety measure (2016).

[105] SAE J2944: Operational Definitions of Driving Performance Measures and Statistics (2015).

[106] Okamura, M. et al.: Impact evaluation of a driving support system on traffic flow (2011).

Proportion of stopping distance (PSD) is defined as the ratio between the remaining distance to the point of collision and its minimum acceptable stopping distance, whereby the minimum acceptable stopping distance is related to the maximum acceptable deceleration. Guido et al.[107] find that PSD tends to be generally more sensitive to higher risk scenarios by analyzing the traffic in a roundabout.

2.2.5.4.3 Intensity Based Indicators

In contrast to aforementioned two types of indicators, the intensity based indicators reflect how difficult it is for a driver or an AV to respond in order to avoid a collision. The severity is thus expressed intuitively. Jansson uses the required longitudinal acceleration[108a] $a_{x,\mathrm{req}}$ to quantify the acceleration required to bring the relative velocity of two objects to zero at the potential time of collision. He also applies the required lateral acceleration[108b] $a_{y,\mathrm{req}}$ to measure the severity to avoid a collision when taking an evasion action. The $a_{x,\mathrm{req}}$ and the $a_{y,\mathrm{req}}$ can be aggregated as a_{req}, which is quantified as:[108c]

$$a_{\mathrm{req}} = \min\left(a_{x,\mathrm{req}}, a_{y,\mathrm{req}}\right). \tag{2.1}$$

The $a_{x,\mathrm{req}}$ is also known as deceleration rate to avoid the crash (DRAC)[109]. Many researches prove that the DRAC correlates with the safety-level of a scenarios, since it explicitly considers relative speed of two vehicles and even the deceleration of the preceding vehicle. Nevertheless, conventional DRAC fails to represent traffic conflict accurately since the available vehicle braking capability is not considered. For instance, the same values of DRAC represent different levels of severity if the vehicle is driving on dry or wet roads. Thus, the steering threat number (STN) and the brake threat number (BTN) are studied by Brämmström et al.[110] They are expressed as:

$$\mathrm{STN} = \frac{a_{y,\mathrm{req}}}{a_{y,\max}} \tag{2.2}$$

$$\mathrm{BTN} = \frac{a_{x,\mathrm{req}}}{a_{x,\max}} \tag{2.3}$$

As is obvious in equation (2.2) and (2.3), the maximum available lateral acceleration $a_{y,\max}$ and maximum available longitudinal acceleration $a_{x,\max}$ are explicitly included in the STN and the BTN. Similarly, a deceleration-based surrogate safety measure under consideration of the vehicle performance is also studied by Tak et al.[111] The current deceleration based indicators are mainly applicable for rear-end collisions. Even though the a_{req} consider the

[107] Guido, G. et al.: Comparing safety performance measures obtained from video capture data (2011).

[108] Jansson, J.: Diss., Collision Avoidance Theory (2005).a: p. 75; b: p. 78; c: p. 80.

[109] Cunto, F.; Saccomanno, F. F.: Calibration and validation of simulated vehicle safety performance (2008).

[110] Brannstrom, M. et al.: A situation and threat assessment for a rear-end collision avoidance system (2008).

[111] Tak, S. et al.: Development of a deceleration-based surrogate safety measure for rear-end collision (2015).

braking maneuver as well as the steering maneuver, only front objects are taken into account and lateral objects are ignored.

2.2.5.4.4 Other Indicators

There are other types of surrogate safety measures that do not fall into any of the three categories listed above, e.g., Junietz et al.[112] propose a metric by optimizing the criticality of a scene based on the model predictive control (MPC) technique. They use the MPC to find the minimized cost of all possible trajectories, and the minimized value is regarded as the criticality of the situation, since the trajectory planning of an AV is typically an optimization problem. In addition to the acceleration based indicators, the jerk as the rate of change in acceleration is useful to measure the comfort of a maneuver. Broadhurst et al.[113] calculate the probability of a collision by predicting future motion of all objects using the Monte Carlo path planning. If two objects have intersection in the predicted horizon, a collision is determined. Generally, the different indicators should be combined for a more general application since different indicators are suitable for different types of collisions. Huber et al.[114] consider 11 published criticality metrics and combine them to obtain a final multidimensional criticality evaluation. Three simulated scenarios are used to prove the concept. The simulation results are in accordance with the theory. However, the calculated critical values fluctuate and underestimate the criticality of situations with many objects.

2.2.6 Operation Design Domain

Based on the above mentioned existing approaches to test AVs, it can be concluded that there is currently no satisfying method that can be applied solely to overcome the challenge of the safety validation of AVs, although the scenario-based approach is a promising one. Therefore, it is worthy to try to introduce AVs with certain but acceptable risks, which should be handled carefully. This does not mean that an AV is unsafe when being released but with an acceptable safety level required by stakeholders. Due to some unknown unknowns, a safe AV in all different kinds of scenarios cannot be guaranteed. Four generic approaches are provided in Systems Engineering[115] with respect to the risk, which are accept risk, avoid risk, transfer risk and control risk, respectively. ODD is exactly one way to avoid risk when deploying AVs on public roads. In SAE J3016[116], the ODD is defined as

---

[112] Junietz, P. et al.: Metric for the Safety Validation using Model Predictive Trajectory Optimization (2018).

[113] Broadhurst, A. et al.: Monte Carlo road safety reasoning (2005).

[114] Huber, B. et al.: Evaluation of Traffic Situations based on Multidimensional Criticality Analysis (2020).

[115] Walden, D. D. et al.: A guide for system life cycle processes and activities (2015).

[116] SAE J3016: Taxonomy and Definitions for Terms Related to Automation Systems (2021).

> "Operation conditions under which a given driving automation system or feature thereof is specifically designed to function, including, but not limited to, environmental, geographical, and time-of-day restrictions, and/or the requisite presence or absence of certain traffic or roadway characteristics."

The taxonomy of basic terms for description of an ODD is further specified by Czamecki[117]. The purpose of ODD is to guarantee the safety of AVs in a specific domain. An example of an ODD would be a certain road section, a deployment only under good weather conditions. Therefore, it is completely possible to validate the safety of AVs using existing approaches if the ODD is well-limited. Once AVs are proven to be safe within the ODD, ODD can be gradually extended by adding corresponding functionalities. For instance, an AV is safe in an ODD without traffic signals, if the ODD is prepared to include traffic signals, a detection system for traffic signals should be integrated into the AV. Therefore, the definition of ODD should be considered with the functional requirements cooperatively. In order to keep the safety of AVs always in the ODD, an ODD monitoring is essential. The aim of ODD monitoring is to determine whether the AV is still in a situation that is taken into account by the design. Colwell et al.[118] introduce a concept to restrict the runtime of ODD if subsystems degrade, which allows the AV to still keep operating within a safe domain. Gyllenhammar et al.[119] propose a framework to category the operation conditions of a use case and suggest the ODD to be described by operation conditions, which can facilitate the mapping between different use cases toward the ODD.

2.2.7 Summary of Current Common Approaches

The state-of-the-art safety verification and validation methods are summarized in this subchapter to provide a clear overview of pros and cons of different methods.

ISO 26262 provides guidelines for the functional safety of AVs under level 3, but is not applicable for HAVs. SOTIF is supposed to be useful for HAVs but should be further developed and more details should be studied. UL 4600 aims for the safety of HAVs by documentation of results from both arguments and evidences. However, no benchmarks are given for field testing or no a general design process.

Even though the real-world testing has the highest validity to test AVs, this approach is not feasible due to high economical and time costs. Simulation-based testing is a useful supplement to the real-world testing, but verified and validated simulation models are always preconditions. Function-based testing is not suitable for HAVs any more since it is very challenging to define test scenarios for the release of HAVs. The scenario-based testing is a

[117] Czarnecki, K.: Operational Design Domain for Automated Driving Systems (2018).

[118] Colwell, I. et al.: A safety concept based on runtime restriction of the operational design domain (2018).

[119] Gyllenhammar, M. et al.: Towards an operational design domain that supports safety argumentation (2020).

promising approach to reduce the test effort of AVs by identifying relevant scenarios. Nevertheless, Junietz et al.[120] emphasize that the determination of relevant scenarios, the definition of an appropriate parameter space within a scenario and the combination of parameters are great challenges. ODD as a transition solution makes the deployment of AVs possible by limiting them to a specific domain. However, the description of an ODD is unclear and a viable solution to monitor the ODD is missing.

2.3 Approaches with Silent Testing Concept

Due to the cons of current existing approaches, new approaches should be studied to complement existing approaches and find new ways to help validate the safety of AVs. The approach virtual assessment of automation in field operation (VAAFO)[121 a], the shadow model[122] approach from Tesla and the later appeared "silent testing" approach have basically the same principle. They combine real-world testing and simulation-based testing, and are considered as an innovative and useful way to test AVs. They are introduced in detail in the following subchapters. In particular, the development and implementation of the VAAFO approach is the focus of the dissertation.

2.3.1 VAAFO Approach

Winner[123] developed a device with an associated method to test a function without having to fear unexpected and unwanted function reactions that affect the vehicle dynamics with the form of a patent in 2003. Ten years later, the patent was instantiated for the first time for the safety validation of automated driving with a new name called „Trojan horse"[124], which aims to test automated driving functions in series production vehicles, but without hazardous effects. At that time, the concept was a posteriori safety assessment method as described by Wachenfeld and Winner in the paper[121a], in which the VAAFO approach was officially arisen.

Figure 2-8 illustrates the original working principle of the VAAFO approach. There is an obstacle in reality. However, it is not perceived by the sensors until the vehicle passes by in the perceived world. Hence, the driver has to take over the control in time to avoid a collision. However, the driving automation system goes through the obstacle in the parallel world and is not aware of the collision. In the retrospective world, the obstacle is there as it should

[120] Junietz, P. et al.: Evaluation of Different Approaches to Address Safety Validation (2018).

[121] Wachenfeld, W.; Winner, H.: Virtual Assessment of Automation in Field Operation (2015).a: -; b: p. 7.

[122] Templeton, B.: Tesla's "Shadow" Testing Offers A Useful Advantage (2019).

[123] Winner, H.: Device for providing signals in a motor vehicle (2006).

[124] Winner, H.; Wachenfeld, W.: Absicherung automatischen fahrens (2013).

be. As a result, a virtual collision can be observed and recognized. The driving automation system can then be assessed in the retrospective world, while the retrospective world is only available when a scenario is in the past. Therefore, a method to correct the perceived world is essential according to the original working principle of VAAFO. Junietz et al.[125] present a way to reduce the uncertainties in the perceived world. They use the human behavior as an extra information source to derive FP and FN indicators for the purpose of correcting the environmental representation.

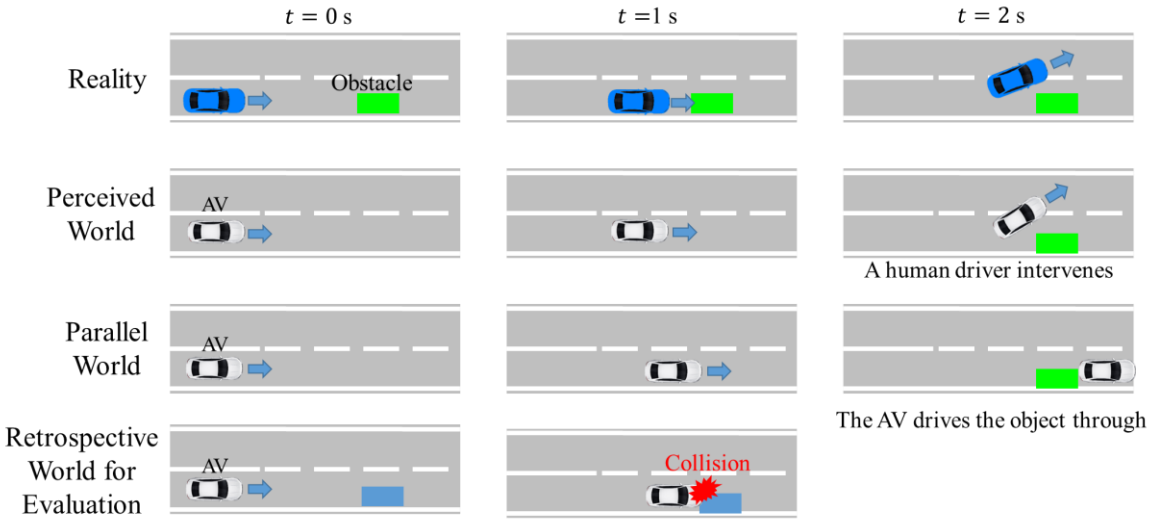

Figure 2-8: The original working principle of the VAAFO approach. Own illustration according to Wachenfeld and Winner[121b].

Since the correction of the environmental representation is a challenging or a time-consuming task such as by labeling, the working principle is updated by Wang and Winner[126]. The trajectory of a driver with or without advanced driver assistance systems (ADAS) is compared with the trajectory of a driving automation system online, while the driving automation system runs in the background and has no access to the actuators of the real vehicle. Consequently, the VAAFO approach is online feasible. Meanwhile, the correction of the environment perception is not essential, but can be utilized to verify the defined triggers in the VAAFO approach. The triggers are the metrics used to evaluate the safety of the driving automation system in the background. Finally, the approach is no longer a posteriori safety assessment method. Even though the working principle of the VAAFO approach changes, the basic idea remains unchanged and can be defined as:

> *A human driver or a driving automation system is in charge of driving a vehicle, while the System under Test (SuT) or Function under Test (FuT) receives sensor input and makes decision accordingly but does not interfere with the driving of the real vehicle.*

[125] Junietz, P. et al.: Gaining Knowledge on Automated Driving's Safety—The Risk-Free VAAFO Tool (2019).

[126] Wang, C.; Winner, H.: Validation Automated Driving and Identification of Critical Scenarios (2019).

Since a SuT does not exist in reality, and road users have no interaction with the SuT, some problems could occur with this type of open-loop simulation, e.g., a real vehicle drives through a virtual AV (vAV) instantiated by the SuT, which cannot indicate that the SuT is unsafe. With respect to the open-loop problem in the VAAFO approach, Koenig et al.[127,128a] use the Wiedemann following model and a neural network-based lane change model to simulate the surrounding vehicles, once the intended lane of a HAV differs from that of a human driver, as described in the scenario construction part in Figure 2-9. Afterwards, the HAD function is assessed by criticality metrics in the constructed scenario in the PELOPS simulation. However, the reconstructed scenario cannot be fully represented in the simulation using sensor data, and the driver behavior model may deviate from the reality as well. Due to the introduction of the simulation models, the advantages of the approach are weakened. Additionally, few details are given about the implementation of the framework.

In this dissertation, the VAAFO approach is further developed, the complete framework of VAAFO is presented, and its each essential component is introduced in detail. The defined triggers to evaluate the safety of AVs online are concretized and verified. Whether it is necessary to simulate the behavior of the surrounding road users is also discussed. A human driver or a driving automation system that controls the real vehicle is defined as instance in charge (IiC), which is used throughout this dissertation.

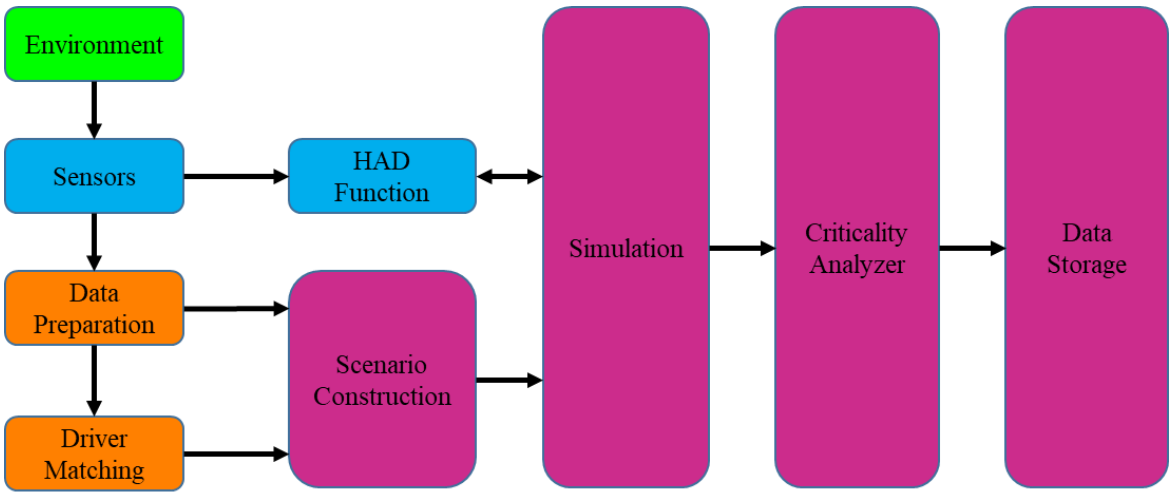

Figure 2-9: A solution to close the loop of the VAAFO approach by simulating the behavior of the surrounding vehicles. Own illustration according to Koenig et al.[128b]

2.3.2 Silent Testing

The “Silent Testing” technique is similar to the working principle of the VAAFO approach, and has been researching in OEMs and suppliers. Since the method can be used not only to

[127] Koenig, A. et al.: Bridging the gap between open loop tests and statistical validation (2017).

[128] Koenig, A. et al.: Overview of HAD validation and passive HAD as a concept (2018).a: -; b: p. 136.

test a SuT, but also to test a FuT, Tribelhorn[129a] applied the silent testing technique to assess an algorithm for lane markings recognition, as shown in Figure 2-10. The recognized features of the algorithm for lane markings are compared with the ground truth. The FuT at this point is an algorithm for recognition of the lane markings, while the ground truth is acquired by GPS. By calculation of the position deviations between them, an evaluation of the algorithm is conducted, i.e., the scenes in which the algorithm does not work well are saved during the driving.

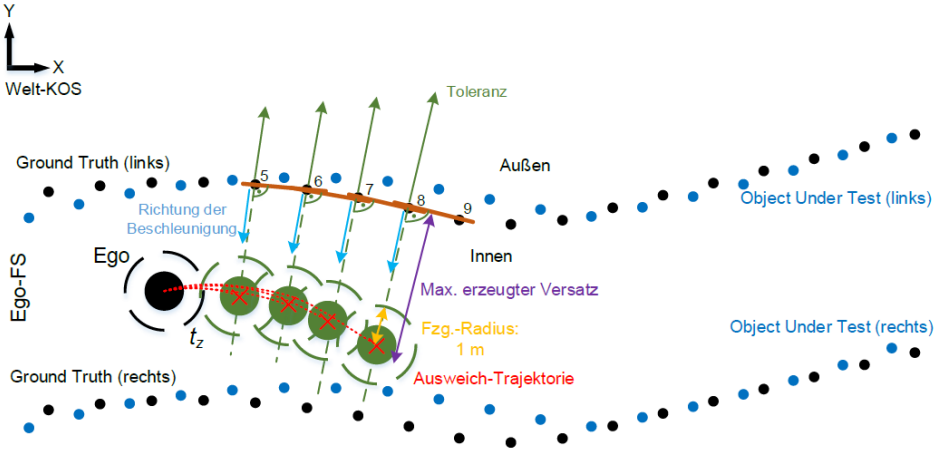

Figure 2-10: An example of using the silent testing technique to assess the algorithm for lane marking recognition[129b]. (Wadim Tribelhorn, 2018), reprinted with permission

Another example[130] is the discovery of corner cases by comparing the predicted image and the actual image. However, not each unpredictable element belongs to the relevant class. Thus, They use a semantic segmentation to differentiate relevant and irrelevant classes. Furthermore, a detection system is applied to determine whether the unpredictable relevant class is in a relevant location. Finally, an evaluation of a video-based detection system is performed.

2.3.3 Shadow Mode

The concept of shadow mode is proposed by Tesla and reported by several media[131,132]. The idea is very similar to the VAAFO approach. In shadow mode, the ADS receives data from sensors but does not take control of a vehicle. It will record how the ADS would have avoided the accident, if a real Tesla car driven by a human driver or an autopilot is in an accident. Or the other way around, a virtual accident caused by an ADS will also be recorded. Based on this technique, shortcomings in the system could be identified, and the collected data can in turn be used to improve their camera-based machine learning significantly. Due to the large

[129] Tribelhorn, W.: Konzeptionierung und Implementation einer „Silent Testing"-Methode (2018).a: -; b: p. 68.

[130] Bolte, J. A. et al.: Towards corner case detection for autonomous driving (2019).

[131] Jordan Golson: Tesla's new Autopilot will run in 'shadow mode' (2016).

[132] Tesla: What is Shadow Mode Tesla Autonomy (2019).

fleet from its customers, a huge amount of data has been collected. Fridman[133] estimates that Tesla vehicles have driven over 2.56 billion kilometers in shadow mode until the mid-year of 2018. In 2020, Tesla registers a patent[134] to obtain training data for an implemented neural network in a vehicle using trigger classifiers, while the trigger classifiers are trained beforehand to recognize images with specific image features or objects. Then, the trigger classifiers are deployed in a fleet of vehicles without influence on the core software for automated driving. As a result, the deployed neural network has an improved ability to detect the particular use cases targeted by the trigger classifiers. Those deployed trigger classifiers have shadow mode characteristics.

2.3.4 Other Similar Approaches

Other similar approaches focus mainly on online verification of AVs. For example, Pek et al.[135,136,137] propose a method to generate a fail-safe trajectory when the intended trajectory is not available or not safe. They claim that the proposed method works with any provided motion planning framework, and can verify the motion planning online. However, the transition criterion from the intended trajectory to the fail-safe trajectory is not clear formulized, i.e., the safety-critical situation is not defined. Stahl et al.[138] develop an online verification module to monitor a non-ASIL-capable system, while the online verification module can be approved by standard principles e.g. ISO 26262. As a result, the monitored system can be verified. They point out that online verification is helpful for complex driving functions, frequent updated functions, machine learning methods and online machine learning systems. Apart from the verification of motion planning, Buerkle et al.[139] utilize dynamic occupancy grid to verify the perception system of an autonomous system online. The object information will be corrected if necessary, and thus can be combined with RSS to ensure a comprehensive safety of AVs, since RSS addresses only the decision system of an AV.

2.3.5 Summary of Approaches with Silent Testing Concept

From the above analysis, it could be concluded that the VAAFO approach as a new approach has attracted a lot of interest, and is considered as a very promising approach to facilitate the

[133] Lambert, F.: Tesla's fleet has accumulated even more than 1.2 billion miles in 'shadow mode' (2018).

[134] Karpathy, A.: System and Method for obtaining training data (2020).

[135] Pek, C.; Althoff, M.: Fail-Safe Motion Planning for Online Verification of Autonomous Vehicles (2020).

[136] Pek, C. et al.: Using online verification to prevent autonomous vehicles from causing accidents (2020).

[137] Pek, C. et al.: An online verification framework for motion planning of self-driving vehicles (2019).

[138] Stahl, T. et al.: Online Verification Concept for Autonomous Vehicles (2020).

[139] Buerkle, C. et al.: Towards Online Environment Model Verification (2020).

safety validation of AVs. The role of the VAAFO approach among other existing approaches for the safety verification and validation of AVs can be seen in Table 2-1. A driving automation system can be typically divided into sense, plan and act. Based on the principle of the approach, all of them can be either virtual or real. In the real-world testing, sense, plan and act are real. Thus, it has the highest validity, but the highest test effort as well due to the necessity of safety drivers. Conversely, the simulation-based approach has the lowest validity as well as the lowest test effort, since the models are virtual in the simulation. During the open-loop recording, only the perception data is recorded, and a driver drives a test vehicle through different scenarios. Its test effort is higher than the silent testing technique, since a trained driver is still required to record and manage the data. In the VAAFO approach, since sense and plan are all real and no safety driver is essential, it has the highest validity. Meanwhile, its test effort is less than the real-world testing. Based on the table, the benefits of the VAAFO approach are apparent and its pros are clear.

With respect to the pros of the VAAFO approach, the approach does not interfere with the driving of a driver or an ADS, thus no additional risk will be involved. By implementation of the approach in a fleet, a lot of data could thus be gathered for the improvement of a driving automation system. On the other hand, the machine learning-based algorithms can be evaluated either direct online or by the acquired data, whereby the current existing methods for regulatory approval are not applicable for deep neural networks (DNNs)[140]. The new gained knowledge by the VAAFO approach can be utilized to train the machine learning-based algorithms again. Furthermore, it can be applied to test either automated driving functions or driving automation systems. Due to the commercial business, Tesla has released little studies about shadow mode. The silent testing technique is actually a derivative of the VAAFO approach. Therefore, the development and implementation of the VAAFO approach is the main research topics in this dissertation, and the necessary steps to realize this approach will be introduced in detail in order to explore more hints about the practical application of this approach.

Table 2-1: The comparison with other existing approaches. The more black dots means higher values. n.a. represents not applicable.

	Test object			**Validity**	**Test effort**
	Sense	Plan	Act		
Real-world testing	real	real	real	● ● ●	● ● ●
VAAFO	real	real	n.a	● ● ●	● ●
Open-loop recording	real	n.a	n.a	● ● ●	● ● ●
Simulation-based testing	virtual	virtual	virtual	● ●	●

[140] Utesch, F. et al.: Towards behaviour based testing to understand the black box of autonomous cars (2020).

3 Determination of VAAFO Components

In the previous chapter, the basic idea of the VAAFO approach is introduced. Since the working principle is updated during the development of the approach, it will be presented elaborately in this chapter. According to the new working principle, the necessary components are introduced and the important parameters are studied in this chapter. Figure 3-1 shows the architecture of the VAAFO approach. The IiC makes decisions based on what it perceives in the real world. Similarly, multiple virtual AV (vAV) instances use the perceived but transformed information from the real sensors in the virtual world. The perception for IiC and vAV instances can be identical if only the planning modules of the vAV instances differ from that of the IiC. So, an updated planning module can be tested in parallel. Nevertheless, the perception can also be different if, for example, the IiC is a human driver whose perception is independent of the perception sensors. Regardless of whether the perception is identical or not, the perception for vAV instances rely on the real sensors. Since those sensors are installed on the IiC, if state deviations between the IiC and a vAV instance exist, the information of the sensors cannot be directly utilized for the vAV instances. This problem is solved by applying a coordinate transformation. The tracked objects by sensors are first transformed to a local coordinate system. Importantly, the map in the real world and in the virtual world are identical. Thus, a common local coordinate system in the two worlds is ensured. After the coordinate transformation, the vAV instances know the states of the tracked objects in the virtual world. Afterwards, the behaviors of the IiC and the vAV instances flow into the defined triggers to evaluate their safety. Meanwhile, critical scenarios are identified if the triggers are activated. The number of the vAV instances depends on two key parameters, which are explained in the subchapter 3.2.

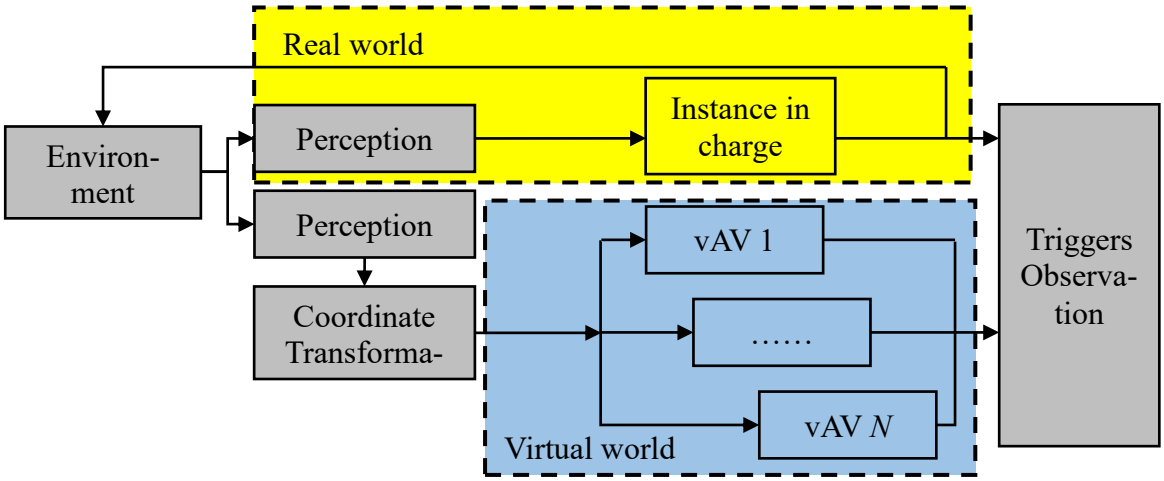

Figure 3-1: The architecture the VAAFO approach.

3.1 Coordinate Transformation

The coordinate transformation is essential for the projection of the tracked objects from the real world into the virtual world if there are state deviations between the IiC and the vAV instances. The tracked objects by a sensor are typically based on a sensor coordinate system or a vehicle coordinate system, i.e., the tracked objects are merely valid for the IiC and not directly applicable for the vAV instances. Therefore, they are transformed to a local coordinate system namely an earth-fixed coordinate system. The information of the tracked objects is now available in the virtual world, since the same map is loaded in the virtual and real world. Additionally, the state of each vAV instance in the virtual world is also known, using the information about the desired planned trajectory as well as the interpolation technique. As a result, the vAV instances know the relative information to the real tracked objects in the virtual world and can make decisions accordingly.

3.1.1 Theoretical Analysis

Before the theory of the transformation is introduced, the notations of three coordinate systems are given.

- E denotes the values in an earth fixed coordinate system.
- V denotes the values in a vehicle coordinate system.
- S denotes the values in a sensor coordinate system.

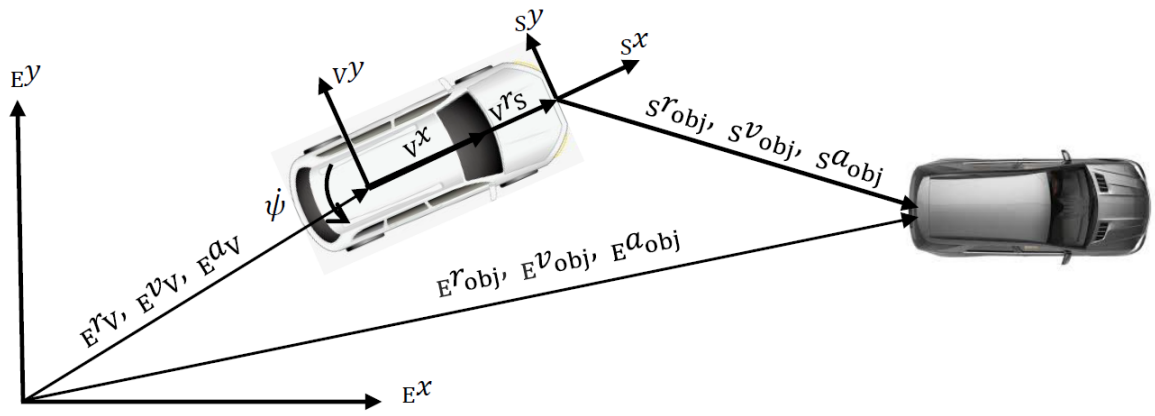

Figure 3-2: The coordinate transformation of a tracked object to an earth-fixed coordinate system.

A sensor at the bumper of a vehicle is taken as an example to depict the process of the coordinate transformation as illustrated in Figure 3-2. A similar process can be conducted for sensors at other positions as well. Basically, all the state variables of an object should be transformed to an earth-fixed coordinate system. The variables to be transformed could be determined in a targeted manner by analyzing the planner's requirements and the input of the triggers. In the studied case, the transformation of position, velocity, orientation and acceleration of an object are essential.

The variables in Figure 3-2 are used to describe the equations for the transformation. Using the equations (3.1) - (3.4), the state of a tracked object in the earth-fixed coordinate system is generally available. The estimated dimension of a tracked object can be directly utilized, since it is not changed during the coordinate transformation.

- Position

$$ {}_{\mathrm{E}}\boldsymbol{r}_{\mathrm{obj}} = {}_{\mathrm{E}}\boldsymbol{r}_{\mathrm{V}} + {}_{\mathrm{V}}\boldsymbol{r}_{\mathrm{S}} + {}_{\mathrm{S}}\boldsymbol{r}_{\mathrm{obj}} \tag{3.1} $$

- Velocity

$$ {}_{\mathrm{E}}\boldsymbol{v}_{\mathrm{obj}} = {}_{\mathrm{E}}\boldsymbol{v}_{\mathrm{V}} + \dot{\boldsymbol{\psi}} \times ({}_{\mathrm{S}}\boldsymbol{r}_{\mathrm{obj}} + {}_{\mathrm{V}}\boldsymbol{r}_{\mathrm{S}}) + {}_{\mathrm{S}}\boldsymbol{v}_{\mathrm{obj}} \tag{3.2} $$

- Yaw angle

$$ {}_{\mathrm{E}}\boldsymbol{\psi}_{\mathrm{obj}} = {}_{\mathrm{E}}\boldsymbol{\psi}_{\mathrm{V}} + {}_{\mathrm{V}}\boldsymbol{\psi}_{\mathrm{S}} + {}_{\mathrm{S}}\boldsymbol{\psi}_{\mathrm{obj}} \tag{3.3} $$

- Acceleration

$$ \begin{aligned} {}_{\mathrm{E}}\boldsymbol{a}_{\mathrm{obj}} = {}_{\mathrm{E}}\boldsymbol{a}_{\mathrm{V}} + {}_{\mathrm{S}}\boldsymbol{a}_{\mathrm{obj}} + 2\left(\dot{\boldsymbol{\psi}} \times {}_{\mathrm{S}}\boldsymbol{v}_{\mathrm{obj}}\right) \\ + \ddot{\boldsymbol{\psi}} \times {}_{\mathrm{S}}\boldsymbol{r}_{\mathrm{obj}} + \dot{\boldsymbol{\psi}} \times \left(\dot{\boldsymbol{\psi}} \times {}_{\mathrm{S}}\boldsymbol{r}_{\mathrm{obj}}\right) \end{aligned} \tag{3.4} $$

The $\boldsymbol{r}$, $\boldsymbol{v}$, $\boldsymbol{a}$, $\boldsymbol{\psi}$ in the equations represent position, velocity, acceleration and yaw angle, respectively. The right subscript obj denotes a tracked object. For instance, ${}_{\mathrm{S}}\boldsymbol{a}_{\mathrm{obj}}$ describes the acceleration of a tracked object in the sensor coordinate system. $\dot{\boldsymbol{\psi}}, \ddot{\boldsymbol{\psi}}$ are the yaw rate and yaw acceleration of the subject vehicle, respectively.

3.1.2 Yaw Acceleration Estimation

The position, velocity and the yaw angle could be transformed to the earth-fixed coordinate system without problems, since the required variables for the transformation can be measured or obtained directly. Nevertheless, the yaw acceleration is needed for the transformation of the acceleration and cannot be acquired directly. If a large ${}_{\mathrm{S}}\boldsymbol{r}_{\mathrm{obj}}$ and a large $\ddot{\boldsymbol{\psi}}$ exist simultaneously, the term $\ddot{\boldsymbol{\psi}} \times {}_{\mathrm{S}}\boldsymbol{r}_{\mathrm{obj}}$ could not be ignored. To estimate the yaw acceleration, the algorithm for differentiating noisy functions from Chartrand[141] is helpful. However, the method is only suitable for post-processing, which does not meet the real-time requirement.

A further research about estimating the yaw acceleration online, Kim et al.[142] derive the transfer function between the yaw rate and the steer wheel angle. A Kalman filter (KF) is then designed using the transfer function to estimate the yaw acceleration in real-time. However, the estimated yaw acceleration deviates from the offline derived yaw acceleration when

[141] Chartrand, R.: Numerical differentiation of noisy, nonsmooth data (2011).

[142] Kim, W. et al.: Vehicle Path Prediction Using Yaw Acceleration for Adaptive Cruise Control (2018).

the yaw rate rises and falls. Therefore, other methods are studied. The Savitzky-Golay filter[143] fits successive adjacent data points in a window length by polynomial least squares regression, so that the features of the distribution, such as relative maxima, are well preserved. Furthermore, it is suitable for calculating derivative of noisy signals. Thus, the Savitzky-Golay filter is applied to acquire the yaw acceleration in real-time. However, the standard Savitzky-Golay filter belongs to the linear phase finite impulse response (FIR) filters, which has principally a delay of half a window length. In order to avoid the delay, two strategies are introduced:

- Method 1 - The derived yaw acceleration at the latest time step rather than the value in the middle of window is regarded as the estimated yaw acceleration.
- Method 2 - Data points are predicted for a half window length based on the polynomial from the Savitzky-Golay filter so that the middle value of the window locates exactly at the latest time step.

In method 1, a certain accuracy is sacrificed, since the value at the latest value is used instead of the value in the middle of the window of the filter. In method 2, a prediction is performed, which may bring certain uncertainties. The detailed implementation of these two methods is described in A.1. As a result, the comparison of these two methods should be performed to find the method with less delay and higher accuracy.

3.1.3 Validation of the Coordinate Transformation

To validate the coordinate transformation especially the transformed acceleration, a suitable scenario should be designed. Figure 3-3 shows the scenario that is carried out on a proving ground. Due to the continuous large change in the yaw rate, the designed scenario is quite appropriate to validate the transformation of acceleration. In this scenario, the target object accelerates from still to 30 km/h and then maintains this speed, while the subject vehicle equipped with sensors drives from 0~30 km/h and performs a slalom driving. Both vehicles are equipped with an automotive dynamic motion analyzer (ADMA).

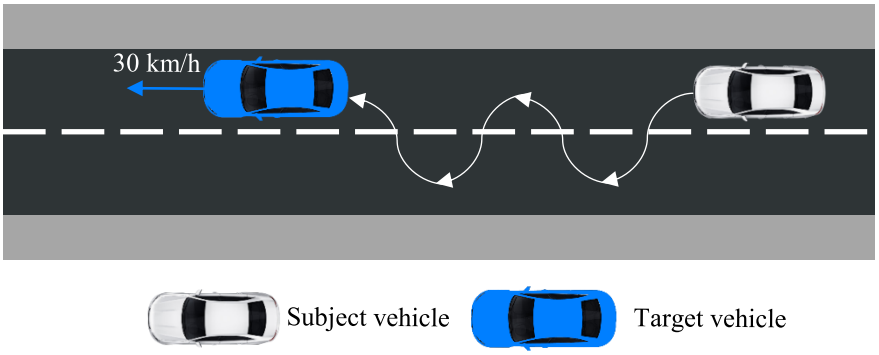

Figure 3-3: The scenario description for validation of the coordinate transformation.

[143] Schafer, R. W.: What is a Savitzky-Golay filter?[lecture notes] (2011).

The ADMA includes a highly precise inertial measurement unit (IMU) corrected by a differential global navigation satellite system (DGNSS), and can measure the position, speed and acceleration etc. in all three directions of a vehicle. Through a WiFi-Kit, the two ADMAs can communicate with each other. As a result, the relative information between the subject vehicle and target vehicle is available, which is regarded as the ground truth to validate the transformed results. Additionally, the subject vehicle has a long range radar in the front bumper. The state of a tracked object by the radar ${}_{S}x = ({}_{S}p_x, {}_{S}p_y, {}_{S}v_x, {}_{S}v_y, {}_{S}a_x)$ is known. Using the equations (3.1), (3.2) and (3.4), the transformed position, velocity and acceleration of the target vehicle on the earth-fixed coordinate system are obtained. In particular, the yaw accelerations estimated by the two different online methods are compared with the yaw acceleration obtained by an offline method, i.e. a Savitzky-Golay filter. Due to all available data in the offline phase, the delay does not exist in the offline method. The results of the comparison are presented in Figure 3-4. As is obvious in this figure, both the method one and the method two have little delay when compared to the offline method. Additionally, the online method two matches better to the offline method especially at peaks than the online method one. Therefore, the online method two is suggested to estimate the yaw acceleration.

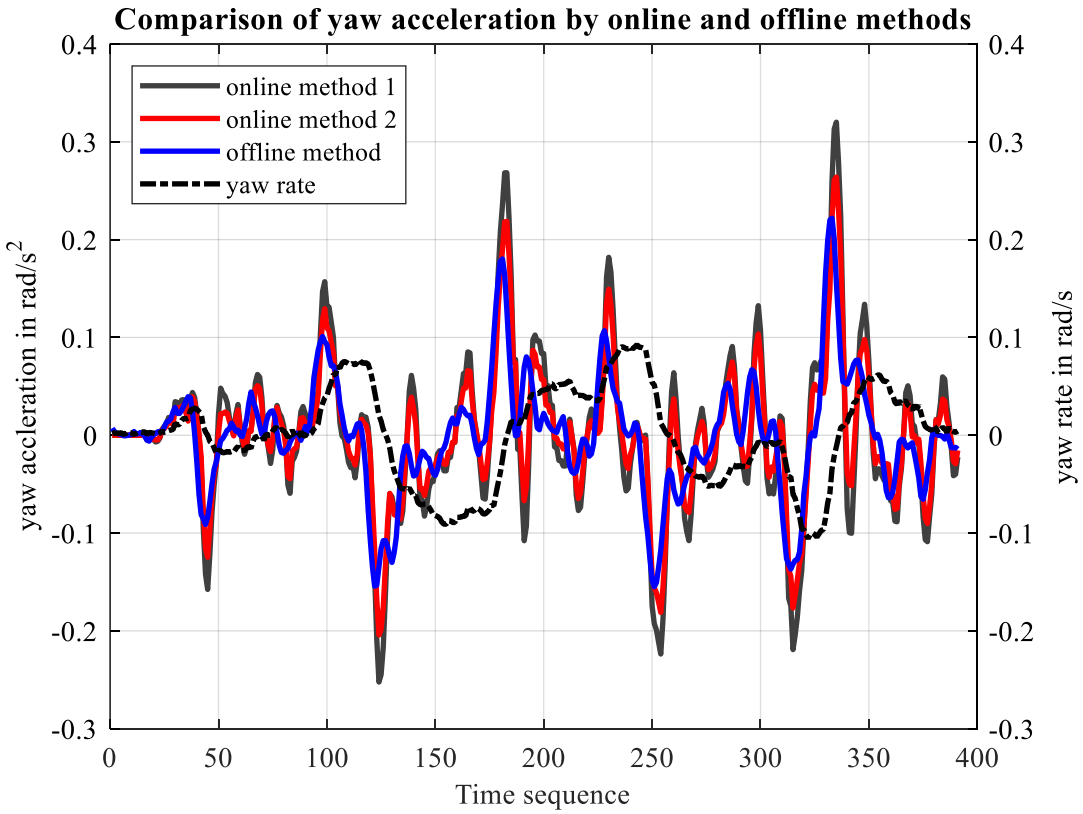

Figure 3-4: The yaw acceleration comparison between the offline and online methods.

Subsequently, the transformed position, velocity and acceleration are compared with the ground truth. The root mean square error (RMSE) is utilized to quantify how large the error is. The RMSE values of the transformed positions in *x* direction and *y* direction on the earth-

fixed coordinate system are about 0.21 m and 0.67 m, respectively. Due to the unclear tracking point of the radar and the uncertainties of the tracking algorithm, small position deviations are observed. Apart from the position, the velocity and the acceleration are important state variables as well. Figure 3-5 shows the results of the comparison. Generally, the transformed velocity and acceleration are very accurate compared to the ground truth. The RMSE of the transformed velocity is 0.16 $\mathrm{m/s}$, and the transformed acceleration is approximately 0.45 $\mathrm{m/s^2}$ when using the online method two to estimate the yaw acceleration.

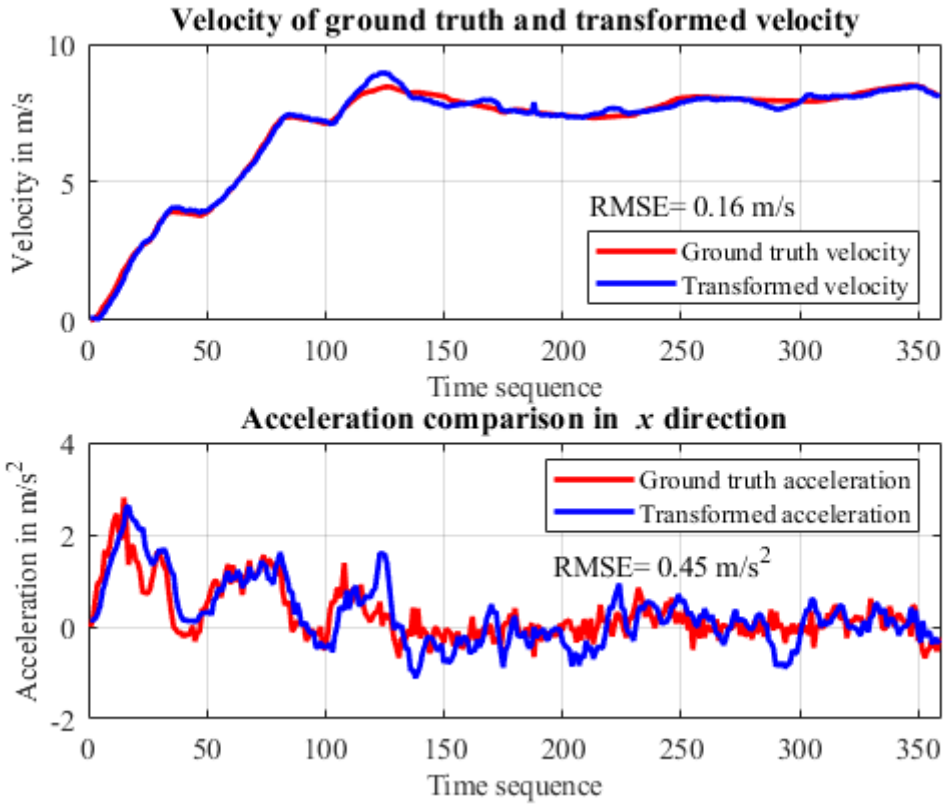

Figure 3-5: The comparison of the transformed velocity and acceleration with the ground truth.

Through this experiment, the process of the coordinate transformation is demonstrated. Its results prove that the transformed values are highly accurate. Since the yaw angle cannot be obtained by the tracking algorithm of the built-in radar, the transformation of the yaw angle is not illustrated. Nevertheless, the equation for transforming the yaw angle is identical to the transformation of position, since the yaw angle can be regarded as a scalar quantity as well. Using the aforementioned introduced theory, the state of a tracked object can thus be transformed to the earth-fixed coordinate system. The tracked objects after coordinate transformation are then projected into the virtual world, which creates an environmental representation for the vAV instances.

3.2 Parameter Study

In order to build a valid environmental representation in the virtual world, the coordinate transformation is necessary but not sufficient. It can be imaged that all projected objects could be irrelevant for the vAV if large state deviations between the IiC and the vAV emerge, i.e., the decision module of the vAV knows the states of the objects but will not respond to them due to the large distance. As a result, the vAV cannot be tested. This situation would happen frequently if no strategy is introduced, since it is highly likely that the IiC and a vAV would have different decisions even under the same scenario. The generated state deviations between them could get increasingly larger with time passing by. Consequently, the projected environmental representation would be meaningless for the decision module of a vAV. Therefore, a lifetime parameter T_{L} is introduced. The definition of the lifetime parameter is:

> *The state of a vAV instance is reset to the state of an IiC after a certain period of time. The time interval between two temporally adjacent resets is defined as the lifetime.*

With the lifetime parameter, large state deviations between the vAV instance and the IiC are avoided. By defining a suitable value for the lifetime parameter, a valid environmental representation is guaranteed after the coordinate transformation. As a result, the vAV can be tested in the virtual world. However, a critical situation would be missed when it could happen in the time steps after a reset when the reset were not performed, i.e., if the vAV instance would not be reset, a critical situation could appear. The critical situation provides useful evidence for the safety of a vAV and should not be overlooked. Therefore, the second parameter is introduced to solve this problem, and defined as the birth cycle parameter:

> *A new instance is born after the birth of the previous one. The time interval between the births of two temporally adjacent instances is defined as birth cycle.*

With the T_{B}, the coverage of critical situations is enlarged. If one instance is reset, and a critical situation is missed, the other instances still have the chance to meet this critical situation. Consequently, there is hardly any gap in the situation regarding the vAV testing. The two key parameters are illustrated in Figure 3-6. The solid line represents the entire life of a vAV instance. There would be multiple vAV instances in parallel depending on the ratio of T_{L} and T_{B}. These two parameters affect the performance of the VAAFO approach significantly, and are one of the research questions in this dissertation.

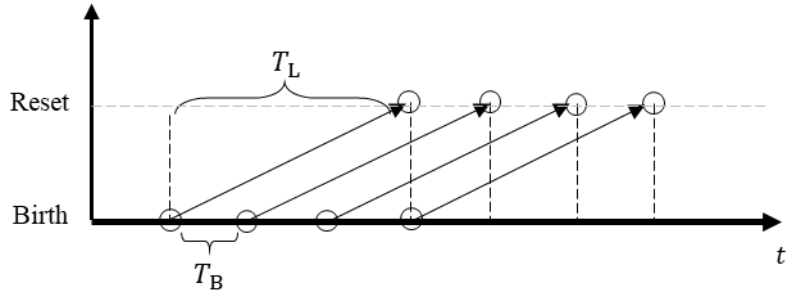

Figure 3-6: The description of the lifetime parameter and the birth cycle parameter.

3.2.1 Parameter Analysis

In the aforementioned chapter, the two parameters are explained. Further studies are essential to finally determine the parameters. Since both parameters can be either constant or dynamic, there are a total of four combinations. These four combinations are discussed and compared in order to derive the best combination.

Combination one: the lifetime is constant and the birth cycle is constant.

In the combination one, a vAV instance is reset, and a new vAV instance is born after constant time. Therefore, the number of vAV instances that are running in parallel is predetermined. The shorter the birth cycle T_B is, the more instances exist, and consequently the higher the probability to cover critical scenarios. However, the corresponding computational cost is also increasing due to the numerous parallel running instances. Furthermore, the vAV instances behave similarly if T_B is too short, so that some of them are useless. Considering the computational cost and the ability to cover critical scenarios, suitable constant lifetime and birth cycle should be determined for ensuring a large search area of critical scenarios, while keeping the computational cost acceptable.

Combination two: the lifetime is constant and the birth cycle is dynamic.

This combination is shown in Figure 3-7. The birth cycle is changed with the time. Constant T_L and dynamic T_B have the potential to lower the computational cost. A new vAV instance will be initialized at the right moment when possible critical scenarios will occur. For instance, a new vAV instance is initialized when the state deviation emerges because the vAV has an increased probability to have an unsafe trajectory in the next few time steps. A threshold for the state deviation that decides when a new vAV instance should be initialized is essential in this case. Compared to the constant lifetime and birth cycle, this combination could have a smaller number of vAV instances, resulting in a lower computational burden as a vAV instance is born on demand. However, the worst case should be considered. In the worst case, even more vAV instances are born since the state deviation exceeds the threshold for several times. As a result, the potential benefit of this combination could become a drawback due to the undeterminable threshold. Since this combination is subject to large uncertainties, the combination two is abandoned.

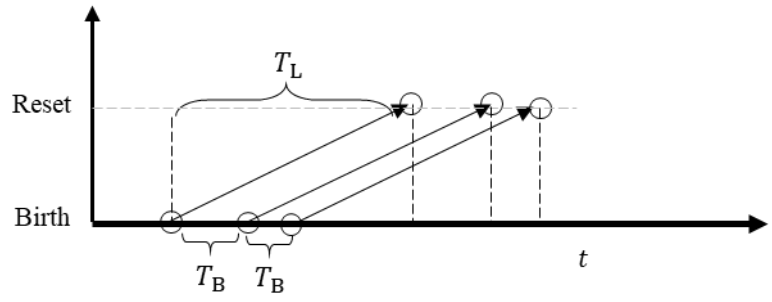

Figure 3-7: The description of the constant lifetime parameter and the dynamic birth cycle.

Combination three and four: the lifetime is dynamic.

If lifetime T_L is dynamic, the birth cycle T_B is no longer necessary. A vAV instance will not be reset until the environmental representation in the virtual world is invalid or a critical scenario is discovered before reaching the invalidity of the environmental representation. Figure 3-8 illustrates this process. In the case of no critical scenarios, lifetime T_L should have an upper limit. Otherwise, the state deviations between a vAV and the IiC will probably continuously increase as time goes on, which will result in an invalid environmental representation in the virtual world. If the upper limit of the lifetime is too short, the vAV instance may not have enough time to make its own decisions before a reset. As a result, a critical scenario cannot be covered, i.e., it is hardly to test the vAV in the virtual world. In this case, determining a suitable upper limit for the lifetime in different situations is the main problem. In addition, some critical scenarios, which occur when a vAV is reset upon reaching the upper limit, are neglected. Consequently, the birth cycle parameter is needed again, which violates the prerequisite of this combination. Therefore, these two combinations are not further studied.

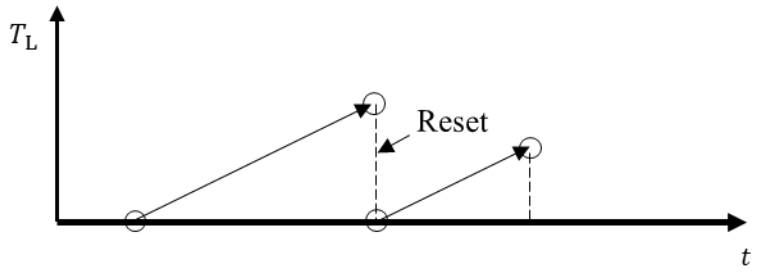

Figure 3-8: The description of the dynamic lifetime parameter.

Table 3-1: A summary of the comparison of different combinations.

		Lifetime T_L	
		Constant	Dynamic
Birth cycle T_B	Constant	+ Intuitive, the number of instances is predetermined - Values should be designed carefully	+ T_B is not necessary - An upper limit of T_B is required, critical situations can be neglected falsely
	Dynamic	+ Unnecessary instances could be avoided - The determination of a threshold to start a new instance is challenging	+ T_B is not necessary - An upper limit of T_B is required, critical situations can be neglected falsely

The summary of the four combinations is shown in Table 3-1. The combination one is intuitive. The suitable lifetime and birth cycle should be studied. Regarding the combination two, unnecessary instances could be potentially avoided. Nevertheless, the determination of a threshold to start a new instance is challenging. For dynamic lifetime, birth cycle is no

longer necessary. However, an upper limit of the lifetime should be defined to avoid large state deviations between the IiC and a vAV instance in the cased of no critical situations occur. Due to the introduction of the upper limit of the lifetime, critical situations can be neglected falsely. Considering the pros and cons of all four combinations, the combination one is finally chosen.

3.2.2 Parameter Determination

The determination of suitable constant lifetime and birth cycle are studied in this subchapter. In order to define the lifetime parameter, its maximum and minimum values are first analyzed. As the aim of the lifetime parameter is to cover any possible critical scenarios online, so that a vAV can be tested in those scenarios before its reset, i.e., the lifetime should be at least as long as the maximum duration τ_{cs} from the beginning of critical scenarios until their discovery. However, if T_{L} equals to τ_{cs}, a critical scenario will probably missed by one vAV instance, since it is unknown when a critical scenario will occur, i.e., if a critical scenario occurs during the life of a vAV instance, the vAV instance cannot live through the entire critical scenario. The other AV instances would also miss this critical scenario due to the different decisions made in different states. Therefore, the minimum lifetime is defined as

$$T_{\mathrm{L}} \geq T_{\mathrm{B}} + \tau_{\mathrm{cs}} \tag{3.5}$$

By using the condition, whenever a critical scenario occurs, its entire duration can always be covered by one vAV instance. The total number of instances N is decided by

$$N = \left\lceil \frac{T_{\mathrm{L}}}{T_{\mathrm{B}}} \right\rceil \tag{3.6}$$

N is the round up result of T_{L} divided by T_{B}. Thus, the equation (3.5) can be reformulated as

$$\frac{N}{N-1}\tau_{\mathrm{cs}} \leq T_{\mathrm{L}} \tag{3.7}$$

The equation (3.7) describes the minimum value of the lifetime parameter. N and τ_{cs} are two factors that affect the minimum lifetime, and are studied, respectively. In order to determine the τ_{cs}, critical scenarios should be firstly acquired. Junietz[144a] proposes a trajectory criticality index (TCI) in his dissertation to evaluate the criticality of the scenarios in the highD[145] dataset. The evaluated results can be taken as the basis for estimating τ_{cs}. The overall computation process of the TCI is illustrated in Figure 3-9. The basic idea is to consider the cost of the optimal trajectory as the TCI value, while the optimal trajectory is obtained using a model

[144] Junietz, P. M.: Diss., Microscopic and Macroscopic Risk Metrics (2019).a: pp. 76-93; b: p. 78.

[145] Krajewski, R. et al.: The highd dataset (2018).

predictive approach by considering the criticality of reaction C_{R}, precision C_{P} and acceleration C_{a}. a_x and a_y are the control variables that are passed to a vehicle model to update the state of the subject vehicle.

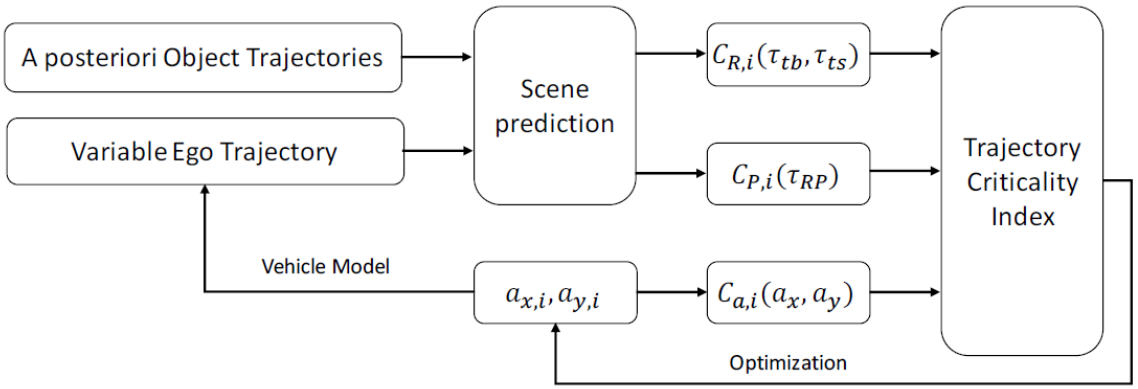

Figure 3-9: The overview of the TCI computation process[144b]. (Philipp Junietz, 2019). CC-BY-SA 4.0

By setting a relatively low threshold for TCI, all possible critical scenarios are preserved. The identified possible critical scenarios are summarized in his dissertation, and depicted in Figure 3-10. The hollow points represent those identified scenarios, in which their minimum TTC values and the corresponding relative velocities are shown. In addition, a warning TTC line is drawn. The warning distance $d_{\mathrm{warn}}(v_{\mathrm{diff}})$ for two non-accelerated objects is expressed by

$$d_{\mathrm{warn}}\left(v_{\mathrm{diff},x}\right) = v_{\mathrm{diff},x} \cdot (\tau_{\mathrm{B}} + \tau_{\mathrm{R}}) + \frac{v_{\mathrm{diff},x}^2}{2D_{\mathrm{max}}} \tag{3.8}$$

The $v_{\mathrm{diff},x}$ is the relative velocity, τ_{B} is the brake loss time and τ_{R} denotes the reaction time of a driver. D_{max} is the maximum available deceleration. Considering the formula of TTC in equation (3.9) with relative clearance between two objects d_x.

$$t_{\mathrm{tc}} = \frac{d_x}{v_{\mathrm{diff},x}} \tag{3.9}$$

The equation (3.8) can thus be reformulated as

$$t_{\mathrm{warn}} = \tau_{\mathrm{R}} + \tau_{\mathrm{B}} + \frac{v_{\mathrm{diff},x}}{2D_{\mathrm{max}}} \tag{3.10}$$

Using the equation (3.10), the relationship between the warning TTC and relative velocity is obtained, and illustrated as a solid black line in Figure 3-10. τ_{R} and τ_{B} in equation (3.10) are defined as 1 s and 0.1 s, respectively. D_{max} is 10 m/s^2. t_{warn} is proportional to the relative velocity, i.e., a warning moment comes earlier with a larger relative velocity. As is obvious in Figure 3-10, some scenarios are probably critical, since the minimum TTC values

are even lower than 1 s, which is almost the limit for drivers to avoid a collision.[146] Meanwhile, some scenarios identified by TCI may not critical, since their minimum TTC values are relative large.

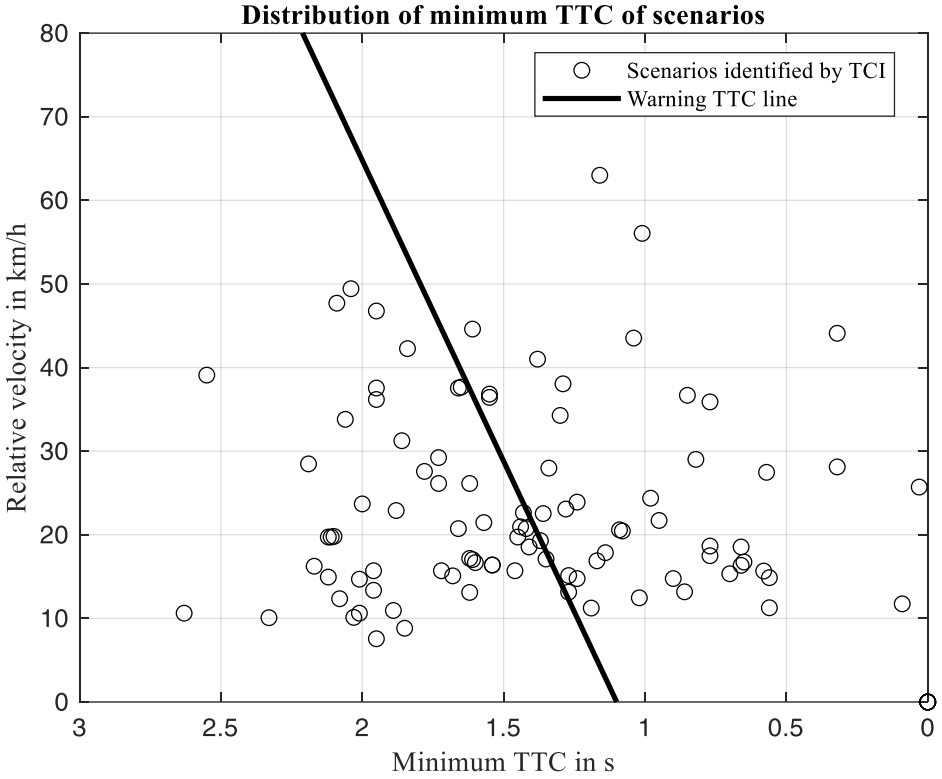

Figure 3-10: The distribution (hollow points) of the possible critical scenarios identified by TCI in the HighD dataset, and the illustration of the warning TTC line.

The scenarios, in which the minimum TTC values exceed the warning TTC, are further analyzed since the duration of those scenarios is of interest. Because almost all possible critical scenarios occur during the lane changing maneuvers, the start time to calculate the duration is the time step when the lane changing begins. It is determined by whether the lateral distance of a vehicle on an earth-fixed coordinate system is continuously increasing or decreasing over several time steps compared to the lateral distance at current time step. Similarly, if the lateral distance of the vehicle stops changing after continuous increasing or decreasing, the time step is regarded as the end of the lane changing maneuver. Figure 3-11 shows the cumulative distribution (CD) function of the duration of the studied scenarios. The solid line represents the CD of the duration of a whole lane changing process, while the dotted line describes the CD of the duration from the beginning of a lane changing maneuver until the warning TTC threshold is reached. It can be seen from this figure that the duration to reach the warning TTC threshold is less than 4 s, while the duration of the entire lane changing processes in all critical scenarios lasts less than 7 s. As it is not necessary to cover the entire lane changing process since a critical scenario is already found earlier, the duration of a

[146] Winner, H.: Grundlagen von Frontkollisionsschutzsystemen (2015), p. 905.

critical scenario τ_{cs} until its discovery is therefore defined as 4 s. Thus, the number of instances N is the only remaining factor to be determined according to equation (3.7).

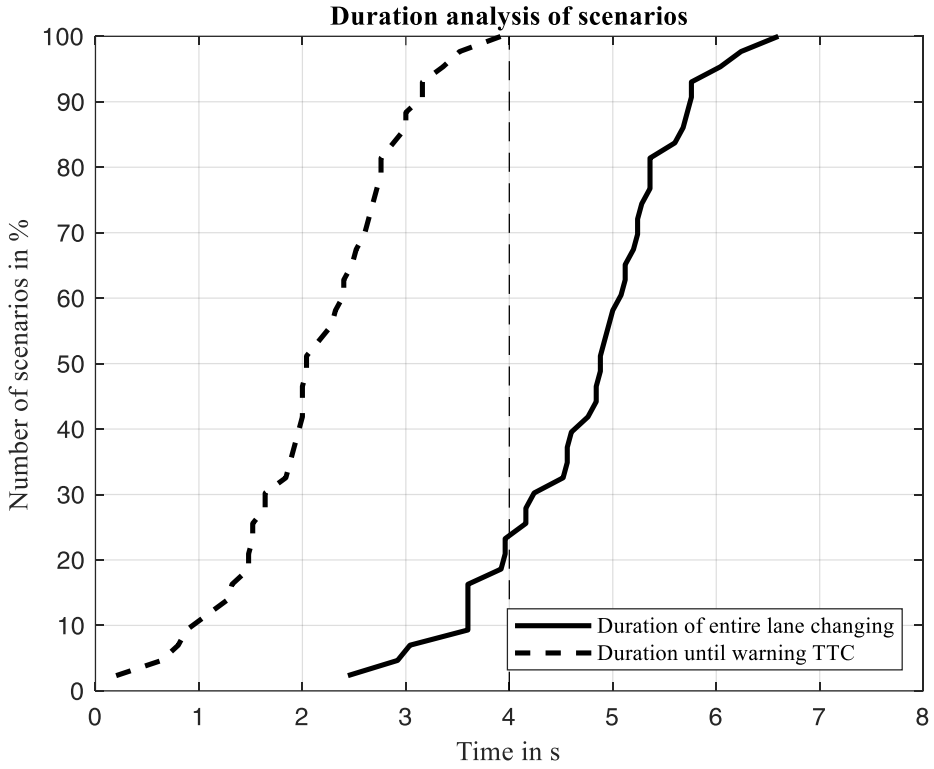

Figure 3-11: The cumulative distribution function of the duration of the entire lane changing (solid line) process and the cumulative distribution function of the duration from beginning of the lane changing until warning TTC line is reached (dotted line) in the potential critical scenarios.

If N is too large, a new instance will be born frequently as required. It will thus burden the on-board computation unit. Furthermore, some of the vAV instances are useless due to a small time interval between two adjacent vAV instances. As is obvious in Figure 3-11, there are little scenarios whose duration is less than 1 s. Therefore, the number of instances N should not be too large. Conversely, small N will lead to large T_{L}, which will likely result in large position deviations between the vAV instance and the IiC in one lifetime.

According to the above analysis, the minimum value of the lifetime parameter is determined. To define the maximum value of the lifetime parameter, the projected environmental representation in the virtual world is discussed. If there is a large deviation between the IiC and the vAV instance, the projected environmental representation could be invalid for the vAV. Invalid in this context means that there is a blind area in front of the vAV, i.e., the vAV is outside the perception range of real sensors. As a result, the vAV cannot be tested. Therefore, the lifetime T_{L} can be maximum so long that the projected environmental representation covers exactly the front view of the vAV. For simulating this situation, the worst case is conducted. In the worst case, the IiC accelerates, while the vAV keeps speed. Due to the large relative acceleration a_{rel} and the short rear perception range d_{r} compared to the front perception range, a large deviation will appear soon, and thus the above mentioned situation

will occur soon. The vAV has no motivation to decelerate if the IiC accelerates in the case of no perception errors. Thus, the upper limit of the lifetime parameter is expressed by

$$T_{\mathrm{L}} \leq \sqrt{\frac{2d_{\mathrm{r}}}{a_{\mathrm{rel}}}} \tag{3.11}$$

The relationship between the rear detection range of sensors after fusion, the acceleration of the IiC and the remaining time of the vAV out of the rear detection range of sensors can be found in Figure 3-12. It is apparent that the rear detection range has a positive influence on the lifetime parameter. Conversely, the lifetime T_{L} has an inverse relation to the acceleration a_{rel} of the IiC. Short range radars or cameras are usually used for the rear side of an AV, which have about 100 m range[147], i.e., d_{r} is consider to be 100 m. The time to reach this range is 6.32 s with an acceleration of 5 m/s^2. With an acceleration less than 5 m/s^2, the corresponding time is thus even longer. However, less lifetime is better for the validity of the environmental presentation for a vAV. With a larger acceleration, the lifetime will be lower. Nevertheless, such large acceleration would be rather rare on public roads. An acceleration with 5 m/s^2 could be already a rare case. This value is thus used in the worst case. Therefore, the upper limit of lifetime is defined as 6.32 s considering the equation (3.11).

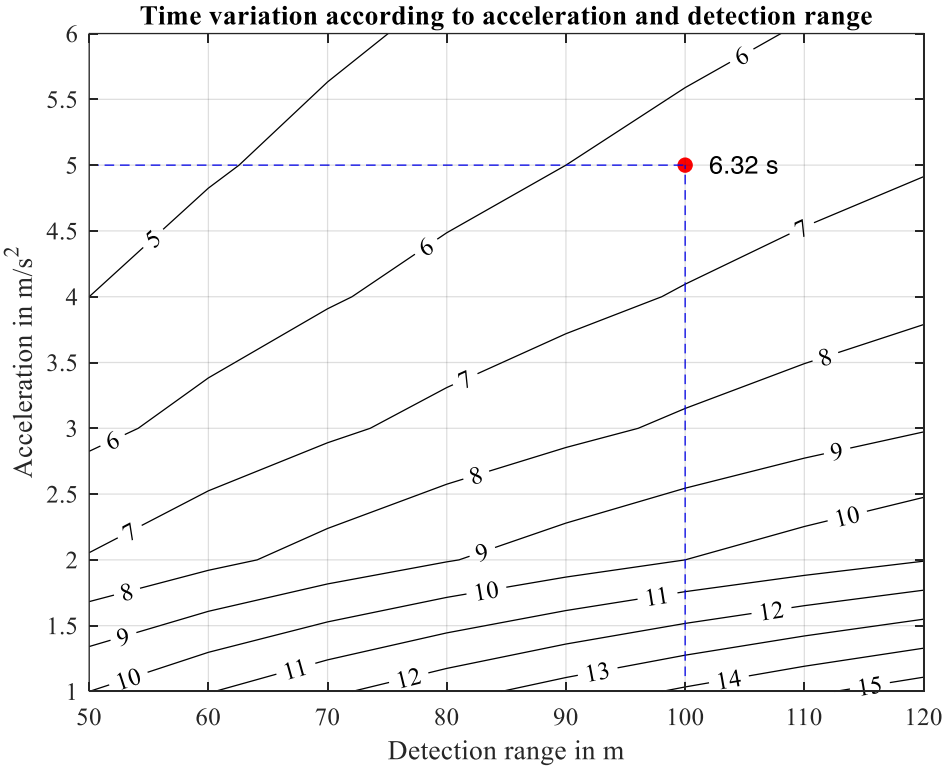

Figure 3-12: The remaining time of a vAV outside the rear detection range of sensors is denoted by contour lines at different detection ranges and accelerations. The remaining time is highlighted when the rear detection range is 100 m and the acceleration is 5 m/s^2.

[147] Ponn, T. et al.: Systematic Analysis of the Sensor Coverage of Automated Vehicles (2019).

Combining the derived upper limit and the τ_{cs}, the limitation of the lifetime parameter is summarized as:

$$\frac{N}{N-1} \cdot 4\ \text{s} \leq T_{\text{L}} \leq 6.32\ \text{s} \tag{3.12}$$

Since the number of the vAV instance must be an integer and a small number of instances reduces the computational load, N is defined as the minimum number that satisfies the equation (3.12). As a result, the number of instances N is 3. Subsequently, the lifetime T_{L} is 6 s when considering the lower limit in equation (3.12), since a lower T_{L} is better for the validity of the projected environmental representation. Then, the birth cycle T_{B} is 2 s. Finally, three vAV instances exist in the virtual world. After every 2 s a new vAV instance is born, and after every 6 s the vAV instance is reset. However, every vAV instance shares the same perception from the on-board sensors regardless of whether it is reset or not, i.e., sensor measurements will not be reset and are always continuously performed during the driving. Each vAV instance is independent of the others. Additionally, the increased load from multiple planners, including the behavior planner and trajectory planner for on-board computer, is nearly none, since the perception, such as convolution neural networks (CNNs), requires the most computation power according to the research from Liu[148].

3.3 Triggers Definition

Using lifetime and birth cycle parameters, a valid environmental representation is ensured in the virtual world, and there are a total of three vAV instances. Each vAV instance makes its own decision based on the projected environmental representation. In order to evaluate the safety of vAV instances, triggers should be defined. When the trigger is activated, the scenario is saved both before activation and after activation. On the one hand, the identified scenarios can be served as the basis for the scenario-based testing method. With the help of a large fleet, previous unknown scenarios could be discovered. On the other hand, those identified scenarios indicate that the tested driving automation system is unsafe in certain situations. Once the driving automation system is updated or improved, it can be tested again in the identified scenarios to determine if the previous unsafe behavior no longer exists.

3.3.1 Requirements for Triggers

Before defining the triggers, the necessary requirements for them should be investigated. The aim is to discover critical scenarios with the defined triggers. To describe the requirements clearly, several terms are defined. An actual critical scenario that is neglected falsely is a false negative (FN) scenario. In contrast, an uncritical scenario that is saved by mistake

[148] Liu, S. et al.: Computer Architectures for Autonomous Driving (2017).

is a false positive (FP) scenario. A true positive (TP) scenario means that an actual critical scenario is assessed as critical as well. A true negative (TN) scenario is an actual uncritical scenario, and is classified as uncritical equally based on the defined triggers. Using the defined terms, the requirements on the triggers are described as:

- FN scenarios shall not emerge.
- FP scenarios shall be as few as possible.

The first requirement defines that critical scenarios should not be missed. Ideally, all critical scenarios should be found, since they are meaningful for the safety validation of AVs. In order to only save necessary data, identification of non-critical scenarios through triggers should be avoided. However, saving critical scenarios and discarding uncritical scenarios are often rather difficult to meet simultaneously. As a result, a compromise is usually essential. Therefore, the saved uncritical scenarios shall be as few as possible.

3.3.2 Triggers Definition

Thus, the following four triggers are designed according to the aforementioned derived two requirements. It is worth to mention that the defined triggers are based on a criticality metric rather than the position deviations between the IiC and a vAV instance, since the position deviations between them cannot indicate that a vAV is unsafe. Both the IiC and vAV instances can have different decisions even under a same scenario.

- Criticality change

$$|\Delta C_{\mathrm{vAV}}(t)| > \Delta C_{\mathrm{crit}} \tag{3.13}$$

$$|\Delta C_{\mathrm{IiC}}(t)| > \Delta C_{\mathrm{crit}} \tag{3.14}$$

- Maximum criticality

$$\left(\underset{t=t_0 \ldots t_0+T_{\mathrm{L}}}{\mathrm{Max}} C_{\mathrm{vAV}}(t)\right) > C_{\mathrm{crit}} \tag{3.15}$$

$$\left(\underset{t=t_0 \ldots t_0+T_{\mathrm{L}}}{\mathrm{Max}} C_{\mathrm{IiC}}(t)\right) > C_{\mathrm{crit}} \tag{3.16}$$

$C_{\mathrm{vAV}}(t)$ is the criticality of a vAV instance, while $C_{\mathrm{IiC}}(t)$ is the criticality of the IiC at time t. $\Delta C_{\mathrm{IiC}}(t)$ and $\Delta C_{\mathrm{vAV}}(t)$ denote the change in the criticality with respect to the previous time step. $\mathrm{C_{crit}}$ and $\Delta \mathrm{C_{crit}}$ define the thresholds of maximum criticality and maximum criticality change.

Table 3-2 describes the triggers in detail and explains the reason why they are defined. Trigger (3.13) and trigger (3.14) are derived from perception errors. The objects discussed here are in front of a vAV instance or an IiC. When an IiC approaches an object, the acquired information by on-board sensors about the object becomes more accurate with decreasing distance and increasing perception time. Therefore, the calculated criticality changes strongly when an object suddenly appears or disappears. Trigger (3.13) will be activated by

FN objects, since the vAV instances do not react to the FN objects, their criticality changes suddenly when the FN objects become TP objects. Similarly, trigger (3.14) is designed for FP objects. An IiC keeps driving without considering the FP objects if the IiC is a human driver. When the IiC comes closer to the FP objects, FP objects turn into TN objects. As a result, the criticality of the IiC has large change. Behavior errors will be covered in trigger (3.15) and (3.16), which quantify whether the behavior of a vAV instance or even an IiC is appropriate. It is worthy to mention that trigger (3.15) and (3.16) may be activated by perception errors as well, since perception errors may result in an unsafe behavior of a vAV instance. Trigger (3.13) - (3.16) are thus error-based. If several triggers are activated almost simultaneously, a special ring buffer should be designed for saving the same critical scenarios only once.

Table 3-2: The explanations of the triggers.

Triggers	Designed for	Comments
(3.13)	FN objects	The criticality of a vAV instance changes strongly in the case of a FN object
(3.14)	FP objects	The criticality of an IiC changes strongly in the case of a FP object
(3.15)	Behavior errors	The behavior of an IiC is assessed by a criticality metric
(3.16)	Behavior errors	The behavior of a vAV is assessed by a criticality metric

Finally, perception errors and behavior errors are observed by the defined triggers, so that the first requirement on the triggers is fulfilled. Since the criticality is utilized in the triggers, it cannot reflect all different types of errors. Some error classes, such as map errors or classification errors of objects, may not be discovered. Therefore, it depends on what kind of error that is to be discovered in an AV, i.e., which part of an AV is the focus to be tested. The triggers could be adapted accordingly within the framework. In principle, any other type of trigger, such as a machine-learning based trigger, can also be applied in the VAAFO approach. For instance, the provided framework can be utilized to collect required data from the perception, such as an image with specific features, if the level of perception is of interest. In order to meet the second requirement, the thresholds in triggers (3.13) - (3.16) should be calibrated to avoid saving uncritical scenarios as many as possible and meanwhile identifying critical scenarios. Further determination and verification of the thresholds could be realized by analyzing the receiver operation characteristic (ROC) curve if datasets of critical scenarios are available.

3.3.3 Triggers Specification

Since criticality metrics are mentioned in the defined triggers, it is essential to concrete the criticality metrics for the application of the VAAFO approach in both simulations and real

world. As discussed in the chapter 2.2.5.4, there are mainly three types of indicators. Among the temporal proximal indicators, the TTC, THW and PET criticality metrics are frequently applied. However, their usability is limited to certain situations. For example, PET is quite suitable for the criticality analysis in an intersection, but not appropriate for a straight section. In addition, not all of them are applicable online. Minimum TTC can be utilized to assess the safety of an AV in the longitudinal direction. However, it becomes zero when two vehicles are travelling in opposite directions in different lanes, and this situation is actually non-critical. Therefore, a new criticality metric is proposed in this context. It belongs to the category of intensity-based indicators. Consequently, the severity of a scenario is directly reflected by the possible driving maneuvers. Compared to the minimum TTC, a critical scenario could be recognized earlier, since the relative acceleration is applied rather than the relative velocity. This point is further proved by analyzing the data from the tests of the VAAFO approach in reality.

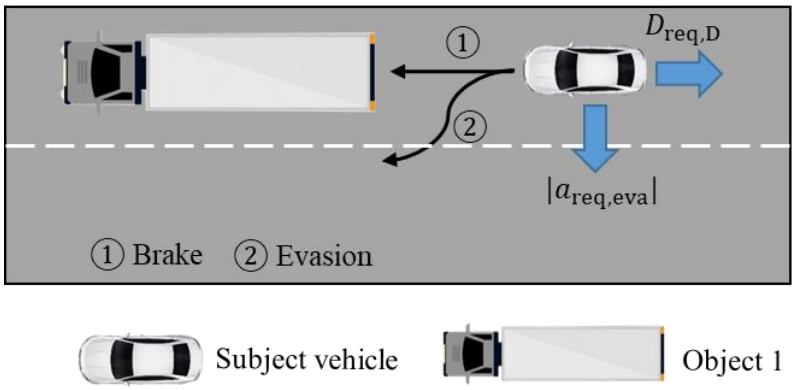

Figure 3-13: An illustration to explain the required longitudinal deceleration and the required lateral acceleration.

The proposed criticality index C_{a} consists of the required longitudinal deceleration $D_{\mathrm{req,D}}$, the required lateral acceleration $a_{\mathrm{req,eva}}$ for evasion, and the required lateral acceleration for steering $a_{\mathrm{req,ste}}$. Longitudinal deceleration rather than acceleration is used in order to be consistent with the meaning of required, since the deceleration is a positive value. So, required means in any case as greater than or equal to. For an object with deceleration D_{obj} in front, the required longitudinal deceleration $D_{\mathrm{req,D}}$ is expressed by

$$D_{\mathrm{req,D}}(t) = D_{\mathrm{obj}}(t) + \frac{v_{\mathrm{diff},x}^2(t)}{2d_x(t)} \tag{3.17}$$

The $v_{\mathrm{diff},x}$ is the differential speed and d_x is the clearance in the longitudinal direction between the subject vehicle and the preceding object. However, a vAV instance can not only brake and then keep current lane, but also take evasive action, as illustrated in Figure 3-13.

If an evasive maneuver is possible, the lateral required acceleration $a_{\mathrm{req,eva}}$ for evasion can be described by

$$a_{\mathrm{req,eva}}(t) = 2(y_{\mathrm{eva}}(t) - v_{\mathrm{y}}(t)t_{\mathrm{tc,e}}(t))t_{\mathrm{tc,e}}^{-2}(t) \tag{3.18}$$

$v_y(t)$ is the lateral velocity toward the evasion direction. $y_{eva}(t)$ is the necessary offset for evasive action and defined as

$$y_{eva}(t) = \frac{w_{sub} + w_{obj}}{2} - \Delta\ {}_F d(t) \tag{3.19}$$

$\Delta\ {}_F d(t)$ ($\Delta\ {}_F d(t) =\ {}_F d_{obj}(t) -\ {}_F d_{sub}(t)$) is the lateral relative distance between the center of the subject vehicle and the preceding object in a Frenet coordinate system (F). ${}_F d_{obj}(t)$ and ${}_F d_{sub}(t)$ are the lateral displacement with respect to the reference path. w_{sub} and w_{obj} are the width of the subject vehicle and the preceding object, respectively. Notably, only the evasion to the left is taken into account, analog to the overtaking maneuver. $t_{tc,e}(t)$ is the enhanced TTC value in the longitudinal direction by considering the relative deceleration $D_{rel}(t)$ ($D_{rel}(t) = D_{obj}(t) - D_{sub}(t)$). $D_{obj}(t)$ is the deceleration of the preceding object, while $D_{sub}(t)$ denotes the deceleration of the subject vehicle.

$$t_{tc,e}(t) = \frac{\sqrt{v_{diff,x}^2(t) + 2D_{rel}(t)d_x(t)} - v_{diff,x}(t)}{D_{rel}(t)} \tag{3.20}$$

$$\text{With } v_{diff,x}^2(t) + 2D_{rel}(t)d_x(t) > 0$$

If the evasion maneuver is feasible, the maneuver with minimum risk with respect to the preceding object is defined as the final critical index C_a ($C_a = \min(D_{req,D}, |a_{req,eva}|)$). As a result, the safety of a vAV instance in the longitudinal direction can be assessed. The criticality of such situation can be assessed by many other criticality metrics as well. In order to transfer the proposed criticality index to other situations, such as a lane-changing maneuver considering the rear left vehicle, the extension of the proposed criticality index should be conducted.

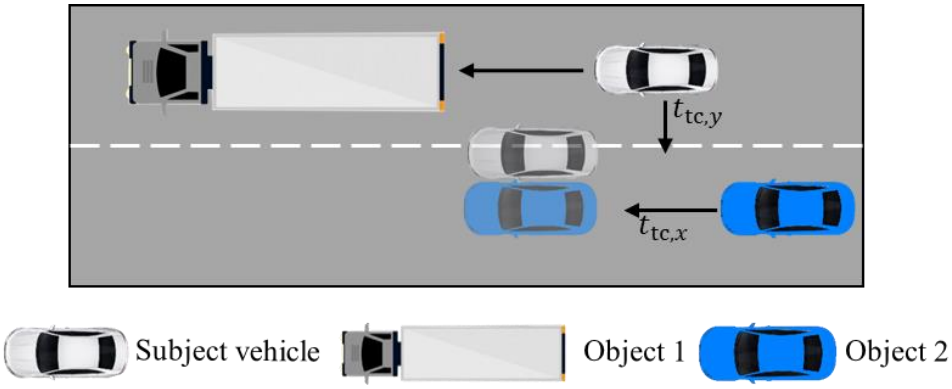

Figure 3-14: An extension of the proposed criticality index by considering the objects in an adjacent lane.

Figure 3-14 shows the process to consider an extra object in an adjacent lane. In this case, there is another object in the left lane of the subject vehicle. Due to the preceding slow object 1, the subject vehicle is motivated to change the lane. Meanwhile, the object 2 goes forward in the lane where the ego vehicle wants to change. If the remaining time that the subject

vehicle needs to change the lane $t_{\mathrm{tc},y}$ is approximate to the remaining time that the object 2 catches the subject vehicle $t_{\mathrm{tc},x}$, it will be rather critical if the subject vehicle keeps changing the lane. As a result, the subject vehicle should steer and brake simultaneously.

$$\Delta t_{\mathrm{tc}}(t) = \left| t_{\mathrm{tc},y}(t) - t_{\mathrm{tc},x}(t) \right| \tag{3.21}$$

$t_{\mathrm{tc},x}(t) = d_x(t)/v_{\mathrm{diff},x}(t)$ and $t_{\mathrm{tc},y}(t) = d_y(t)/v_{\mathrm{diff},y}(t)$. $d_y(t)$ is the clearance and $v_{\mathrm{diff},y}(t)$ is the differential speed in the lateral direction between the subject vehicle and the adjacent object, respectively. If $\Delta t_{\mathrm{tc}}(t)$ is too low, then the subject vehicle will collide with object 2. Considering the length of vehicle and a safe gap, a threshold Δt_{crit} for $\Delta t_{\mathrm{tc}}(t)$ is defined. In other words, if $\Delta t_{\mathrm{tc}}(t)$ is lower than the threshold Δt_{crit}, the subject vehicle should stop changing lane and steer back to the previous lane. The required lateral acceleration for steering $a_{\mathrm{ste,req}}$ to the previous lane is expressed by

$$a_{\mathrm{req,ste}}(t) = 2(d_y(t) + \left| v_{\mathrm{diff},y}(t) \right| t_{\mathrm{tc},y}(t))/t_{\mathrm{tc},y}^2(t) \tag{3.22}$$

$a_{\mathrm{req,ste}}(t)$ is the required lateral acceleration to move back to the previous lane with $t_{\mathrm{tc},y}(t) > 0$. Finally, the criticality index C_{a} of a situation is thus summarized as

$$C_{\mathrm{a}} = \begin{cases} \min\left(D_{\mathrm{req,D}}, \left| a_{\mathrm{req,eva}} \right|\right), \text{if } \Delta t_{\mathrm{tc}}(t) \geq \Delta t_{\mathrm{crit}} \text{ or no approaching objects} \\ \sqrt{D_{\mathrm{req,D}}^2 + a_{\mathrm{req,ste}}^2}, \text{if } \Delta t_{\mathrm{tc}}(t) < \Delta t_{\mathrm{crit}} \end{cases} \tag{3.23}$$

The equation (3.23) summarizes the calculation process of the proposed criticality index. If there is only a risk posed by an object in front of a vAV instance, the criticality of the vAV instance is the smaller of the required longitudinal deceleration and the required lateral acceleration for evasion. If, in addition to the longitudinal risk, there is an additional risk from the lateral direction, the vector of required lateral acceleration for steering $a_{\mathrm{req,ste}}$ to avoid a collision with objects in adjacent lanes is added with the vector of required longitudinal deceleration $D_{\mathrm{req,D}}$ to determine the final criticality index. The proposed criticality index C_{a} is then utilized in the triggers. As a result, the defined triggers are concretized. The proposed criticality index is more general. It can be not only utilized to assess the safety in the longitudinal direction as most other criticality metrics do, but also applicable in the lateral direction. Moreover, it can be utilized online, which is a very important factor when performing the VAAFO approach in real vehicles.

$D_{\mathrm{req,D}}$ is positive according to its definition. To be able to determine the maneuver with minimal risks from the sign of the criticality index, a sign function is added to C_{a}, i.e., if a braking maneuver has lower risks, C_a^* is negative. However, if C_a^* is positive, it can either be the required lateral acceleration for evasion $a_{\mathrm{req,eva}}$ or the vector result of $a_{\mathrm{req,ste}}$ and $D_{\mathrm{req,D}}$.

$$C_a^* = \begin{cases} \min\left(D_{\mathrm{req,D}}, \left| a_{\mathrm{req,eva}} \right|\right) \cdot \mathrm{sgn}, \text{if } \Delta t_{\mathrm{tc}}(t) \geq \Delta t_{\mathrm{crit}} \text{ or no approaching objects} \\ \sqrt{D_{\mathrm{req,D}}^2 + a_{\mathrm{req,ste}}^2}, \text{if } \Delta t_{\mathrm{tc}}(t) < \Delta t_{\mathrm{crit}} \end{cases} \tag{3.24}$$

3.4 Ring Buffer Design

When a trigger is activated, the identified scenario should be saved. Therefore, a ring buffer is essential to save both the data before and after the activation of the trigger. Typically, there are two different architectures for the ring buffer when considering the multiple vAV instances, as shown in Figure 3-15. In the distributed ring buffer, each vAV instance is assigned with a ring buffer. If one trigger of one vAV instance is activated, the data including but not limited to the environmental representation and the states of the vAV instances are saved. The process is repeated if a trigger is activated by the second vAV instance. As a result, when several triggers are activated simultaneously or in close proximity in time, the identified same scenario is saved for multiple times, which poses a high requirement on the on-board storage capacity. Meanwhile, the real-time ability of the ring buffer can be violated if multiple writing processes for saving the data are running simultaneously. As a result, the working principle of the ring buffer should be designed carefully. The possible problems that come from the ring buffer can be avoided by using a central ring buffer. The triggers of all three vAV instances are observed centrally, and the data is managed centrally as well. If a trigger is activated by one vAV instance, its activation will be ignored for a while in the next time steps. As a result, the data will not be saved if the trigger is activated again by other vAV instances during the period of ignoring. However, the data keeps flowing into the ring buffer during the ignoring period. Consequently, the same critical scenario is saved only once. The real-time requirement on the ring buffer is also fulfilled. In addition to the architecture design of the ring buffer, a suitable time length of the ring buffer should be studied as well. The ring buffer should be long enough, so that the saved scenario can be utilized to test AVs in the post-processing phase. Additionally, a suitable format to save a scenario should be chosen. Thus, the scenario can be further visualized and analyzed conveniently by most of the simulation platforms in the field of AD.

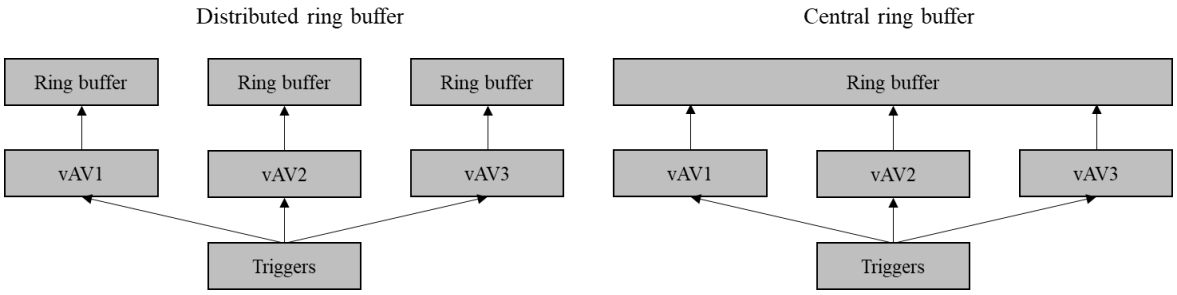

Figure 3-15: The two different architectures for the design of the ring buffer.

3.4.1 Length Study of the Ring Buffer

With respect to the length of the ring buffer, one important requirement is that the length should cover an entire critical scenario. As can be seen from Figure 3-11, the entire lane-changing maneuvers in all critical scenarios last less than 7 s. Therefore, the total time length of the ring buffer τ_{b} should be longer than this value in order to record the entire maneuver

completely. To determine the time length more accurate, two sub-time lengths are defined: the time before triggering $\tau_{\mathrm{b,bef}}$ and the time after triggering $\tau_{\mathrm{b,aft}}$. The lower limit of $\tau_{\mathrm{b,bef}}$ can be defined as

$$\tau_{\mathrm{b,bef}} \geq T_{\mathrm{L}} + 2 \cdot T_{\mathrm{B}} \tag{3.25}$$

With this equation, the full lifetimes of the three vAV instances are all buffered. Thus, the different decisions of the three vAV instances are obvious, and the reason for the triggering is clear. With respect to the lower limit of $\tau_{\mathrm{b,aft}}$, the data from triggering to collision should be recorded in the period of $\tau_{\mathrm{b,aft}}$ if the vAV instance does not take any action or the action is not strong enough. Taking the warning TTC as an example, with a rather high relative velocity 135 km/h the remaining time until a collision is approximate 3 s according to equation (3.10). With a lower relative velocity, the remaining time will be less. However, the longer remaining time should be considered when defining the length of the $\tau_{\mathrm{b,aft}}$ in order to cover more situations. In this case, the $\tau_{\mathrm{b,aft}}$ should be longer than 3 s.

The data size from all sensors on-board determines the upper limit of the total time length. It is not difficult to image that the data size to be saved increases with the time length of the ring buffer. As we know, there are many sensors on an AV. They generate a lot of data per second. In particular, the cameras and lidars occupy the largest proportion. According to the estimation of Heinrich[149], the total sensor bandwidth could be at least 3 Gbit/s. The large amount of data poses a huge challenge to the storage capacity on-board. Therefore, the upper limit should be as low as possible. In conclusion, the time length of the ring buffer is defined as 15 s by considering some margin. Generally, the time length of the ring buffer is designed to be adjustable. In the real tests, the time length could be further optimized.

3.4.2 Working Modes

In the subchapter 3.3, the triggers are defined. Since more than one triggers could be activated almost simultaneously, and even the same trigger could be activated by more than one vAV instance, a special ring buffer is required to record the same identified scenario for only once. Based on this requirement, a ring buffer with three working modes is designed, as illustrated in Figure 3-16.

- Idle mode; if none triggers are activated, the ring buffer is in an idle mode. The data flows into the ring buffer and too old data is deleted.
- Trigger mode; if one trigger is activated by one of the vAV instances, the activations of other triggers caused by any other vAV instances are ignored for a certain period of time, so that the same scenario will not be saved for multiple times.

[149] Heinrich, S.: Flash memory in the emerging age of autonomy (2017).

- Save mode; if the $\tau_{b,aft}$ is reached, the data in the ring buffer will be saved. A new process in the on-board computer is responsible for the writing process to ensure that the real-time requirement is met. In parallel, the ring buffer turns into the idle mode again and prepare for the next activation of the triggers.

As aforementioned, the other triggers should be ignored for a while once one trigger has been activated. As a result, the triggers will not be activated any more by other vAV instances, and the same environmental representation is avoided being recorded for multiple times. If the ignored time is too long, a new critical situation would be lost because the activation of triggers are still ignored since the last activation. Conversely, the same environmental representation would be probably recorded for multiple times with a too short time of ignoring. Meanwhile, multiple simultaneously writing processes violate probably the real-time requirement of the ring buffer. Since a critical situation is likely to end by resetting the vAV instance if the behavior of the IiC is safe, the ignored time is identical to the lifetime and defined as 6 s.

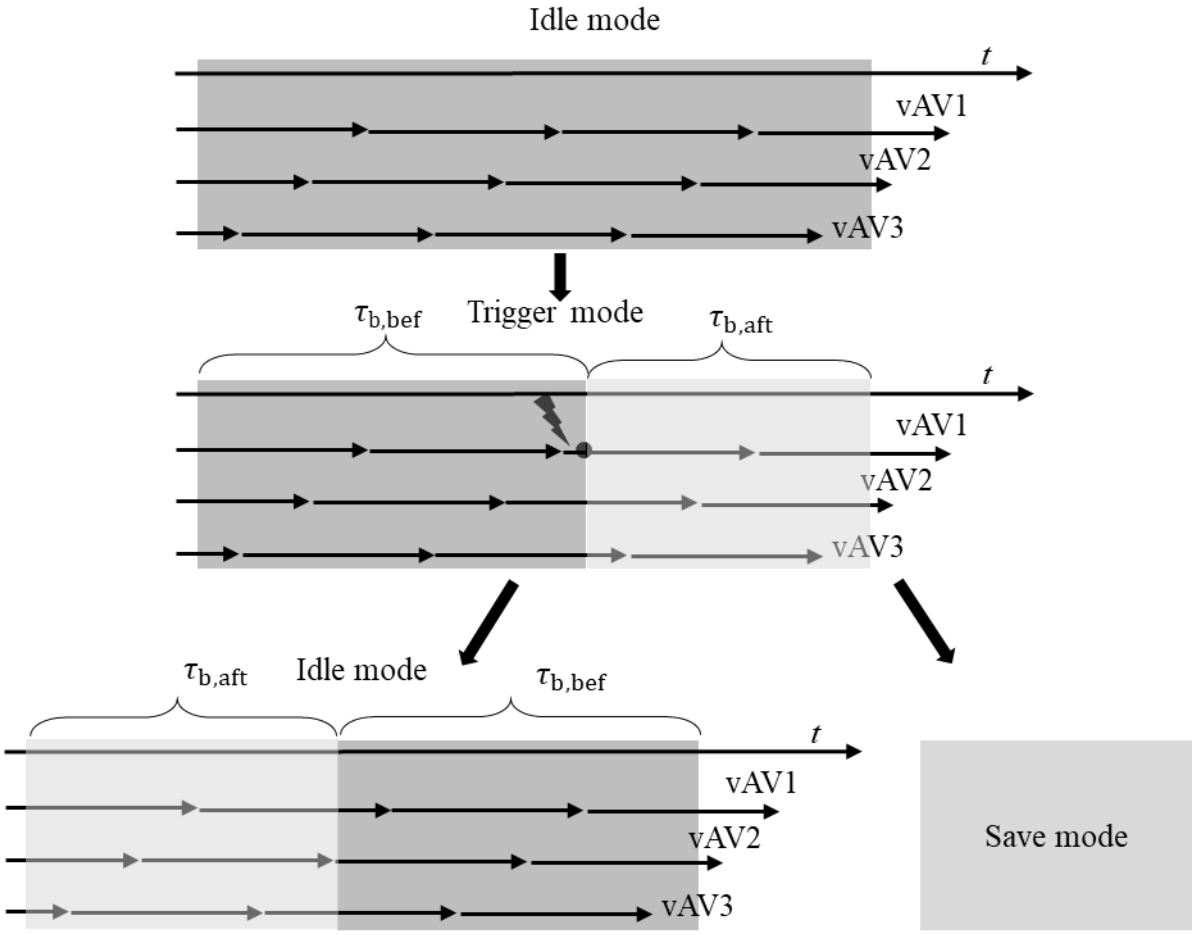

Figure 3-16: The ring buffer changes from idle mode to trigger mode if one trigger is activated. The data keeps flowing into the trigger to save a scenario before and after the activation. The ring buffer switches back to idle mode when the defined time length after triggering is reached.

3.4.3 Data Format Specification

When the data in the ring buffer is ready to be saved, a suitable format should be selected. The aim of recording the identified scenarios is that the scenarios can be further utilized to test AVs. Therefore, the format is desired to be universal, and can be supported by many simulation platforms. Furthermore, the language used to describe scenarios should be machine readable so that the parameters of a scenario can be changed and new scenarios can be created. Therefore, the OpenX format is utilized to save the data in the ring buffer. Since it is more convenient to record the data online by using the rosbag format, a converter is developed to converter the rosbag format to the OpenSCENARIO[150] format. With respect to the OpenSCENARIO, it is a publicly developed standard format, which allows the interchangeability and usage of scenarios in various applications such as esmini [151] and OpenPASS[152]. The attributes of a scenario and their relations are constructed with a hierarchical schema. Unlike OpenSCENARIO that describes the dynamic content of a scenario, OpenDRIVE[153] focuses on the description of a static environment, including road networks and traffic signs, using the XML-based syntax (Extensible Markup Language). Many applications such as CarMaker[154], VTD[155], CARLA[156] etc. can support the OpenDRIVE format. As a result, the identified scenarios by the VAAFO approach can be further utilized for the scenario-based testing. With respect to the data that should be saved, different abstract levels can be selected. For example, the point clouds of a lidar are of interest when testing perception algorithms, while the tracked objects are more crucial for testing the decision module of an AV. For each abstract level, the variables to be saved can be determined according to the requirements.

3.5 Framework Introduction

Since the necessary components to realize the VAAFO approach are already introduced, how to connect them together to establish the framework of the approach is the next step. Figure 3-17 illustrates the entire framework of the VAAFO approach and the connection between the necessary components.

---

[150] ASAM: OpenSCENARIO (2021).

[151] Knabe, E.: Environment Simulator Minimalistic (esmini) (2021).

[152] Dobberstein, J. et al.: The openPASS-an approach to safety impact assessment via simulation (2017).

[153] ASAM: OpenDRIVE (2021).

[154] IPG Automotive GmbH: CarMaker (2020).

[155] Neumann-Cosel, K. von: Virtual Test Drive: Simulation umfeldbasierter Fahrzeugfunktionen (2014).

[156] Dosovitskiy, A. et al.: CARLA: An open urban driving simulator (2017).

As aforementioned, a System under Test (SuT), including sense and plan, receives sensor data from the perception sensors on a vehicle, while the vehicle can be driven by either a human driver or an engaged driving automation system. The sensor data is processed by the sense module of the SuT. The perceived environment by the sense module is then transformed and given to the plan module. Due to the lifetime and birth cycle parameter, the plan module are duplicated for three times. Thus, three vAV instances exist in the virtual world that share the same perceived environment and have the same plan module. The safety of their decisions are evaluated by the trigger system in real-time. Meanwhile, the three vAV instances also receive the vehicle data, so that they can be reset to the state of the real vehicle after every lifetime. Once one trigger is activated, the trigger system sends a trigger signal to the ring buffer. As a result, the data both before and after the activation in the ring buffer is recorded. The VAAFO user or organization can configure which variables to save, and can adjust the time length of the ring buffer as needed through a data recording interface. The recorded data is temporarily stored in the vehicle with a suitable format such as the rosbag format if robot operation system (ROS) for the SuT is used.

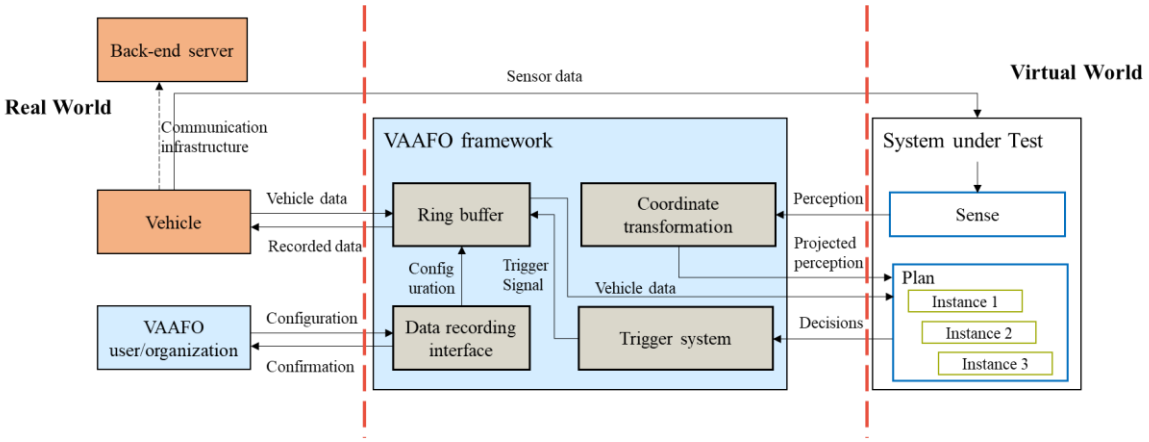

Figure 3-17: The elaborated working process of the VAAFO approach.

The data recorded on-board can be transmitted to a database via communication infrastructures such as WiFi or 5G, depending on how far and how fast the data should be transmitted. The communication infrastructures are not a focus in this dissertation, and will not be further discussed. Consequently, a lot of identified scenarios are saved during the driving. Finally, the collected data infers how safe the SuT is, and can be in turn used to improve the SuT if the SuT is not safe enough. By applying the illustrated framework, the VAAFO approach is online capable. Additionally, the sense and plan module of the SuT can be replaced easily to test different perception and planning algorithms. The VAAFO user or organization can apply this framework to their existing vehicles to collect relevant data. The application is easy to perform, since the framework is modular designed and only a few changes to their systems are required. They can also change the triggers in the trigger system according to their demands.

3.6 Summary

In this chapter, all the essential components of the VAAFO approach have been introduced. The aim and the process of the coordinate transformation are presented. In particular, two methods to estimate the yaw acceleration are compared. The transformed results are demonstrated and validated. Importantly, the map, where the IiC controls a vehicle, is also imported into the virtual world. The map bridges the gap to between the real world and the virtual world, and paves the way for the coordinate transformation. The coordinate transformation is responsible for projecting the tracked objects into the virtual world in order to generate the environment. The two key parameters are studied and determined. As a result, a valid environmental representation in the virtual world is guaranteed. Due to the ratio between the lifetime and the birth cycle parameters, three vAV instances are determined. The triggers are defined and concreted by a new proposed criticality index. Thus, the safety of the vAVs can be evaluated online. A special ring buffer for the VAAFO approach is designed. Finally, the framework of the VAAFO approach is established to introduce the entire working process. The interface between different components are also defined.

Due to the silent testing concept of the VAAFO approach, the objects have no interaction with a vAV instance, but a vAV instance can react to the objects. Because of the short lifetime parameter, this kind of open-loop problem is mitigated, since an IiC builds a closed loop with its surroundings. Additionally, this problem only matters for the objects behind a vAV instance, and it becomes worse only if a vAV instance and an IiC have very obvious position deviations, e.g., they are running in different lanes. However, if this situation happens, the vAV instance will be reset soon, since a lane changing maneuver has been executed since the last reset. Therefore, the open-loop problem exists, but is mitigated and is not a major problem. Therefore, a simulation of the behavior of objects behind a vAV instance to close the loop is not necessary in the approach.

4 Verification Procedures

In order to verify the VAAFO approach, either simulations or tests under real conditions can be performed. No matter which method is utilized, the goal is the same, i.e., the performance of the defined triggers should be identified, and the verification of the framework should be performed. In order to realize this goal, a database with critical scenarios is desired, since one of the aim of the VAAFO approach is to identify critical scenarios. Thus, another existing criticality metric is applied to evaluate the safety of the IiC and the vAV instances again. By comparing the identified scenarios using a different criticality metric, the pros and cons of the proposed C_a can be determined. The verification procedures are illustrated in Figure 4-1. The uncertainties in the scenarios are reduced to obtain an environmental representation with few uncertainties. The behavior of the IiC and vAV instances is then evaluated again by another existing criticality metric in the environmental representation with few uncertainties. By comparing the scenarios identified online with those identified in the post-processing phase, the performance of the defined triggers is inferred. Meanwhile, it is clear whether the errors come from the perception or the planning. Consequently, the application scope of the VAAFO approach can be determined.

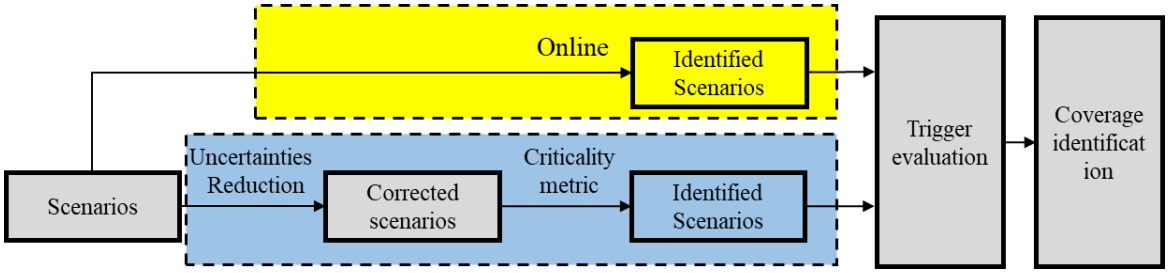

Figure 4-1: The aim of the uncertainties reduction.

4.1 Uncertainties Analysis

There are three types of uncertainties in the environmental representation. They are existence uncertainties, state uncertainties and class uncertainties. According to the summary of Dietmayer[157], the existence uncertainties result from the detection uncertainties of individual sensors, such as cameras or radars. The state uncertainties come from the stochastic, bias and scale measurement errors of the used sensors, as well as model errors, such as the large dispersion of the focus in the modeling of point clouds. The limitations of the sensors or the class uncertainties of the algorithms are the reason for the class uncertainties. Taking the lidar sensor for example, reflections of non-relevant objects could result in FP objects, and

[157] Dietmayer, K.: Prädiktion von maschineller Wahrnehmungsleistung (2015), p. 432.

objects with planar surfaces that do not reflect the light rays back to the sensor lead to FN objects. In addition to the sensor level, the fusion level can also occur existence uncertainties. The existence of an object is estimated either by the heuristic quality criterion of the object hypothesis or by the existence probability.[158] In the first estimation method, the object is considered to be existent if the quality criterion of an object exceeds its threshold. For example, the object is successfully associated for several time steps since its initialization. In the probabilistic approach, the existence of an object is represented by the likelihood. The likelihood is a decision factor in this method. If the likelihood is high enough, an object is added to the object list. From the above analysis, it can be inferred that an environmental representation without any uncertainties is rather difficult to obtain. The uncertainties occur even very often during the tracking. Figure 4-2 shows an example with existence and class uncertainties. The object 1 in Figure 4-2 has two ghost objects. Moreover, no class is assigned to the object 2 and 3. UB denotes unknown big and US means unknown small. Due to the uncertainties, unsafe decisions could be made by the planning module of an AV.

Figure 4-2: An example with existence uncertainties[159]. (Kai Domhardt, 2016), reprinted with permission

4.2 Uncertainties Reduction

As aforementioned, the reduction of the uncertainties is a necessary step in the post-processing analysis. Since the proposed criticality index evaluates the safety of AVs at the decision level, it is unclear where an error comes from when a critical scenario is identified. However, the derivation of the coverage degree of the VAAFO approach depends on the type of errors it can discover. Therefore, possible approaches should be studied to reduce the uncertainties in the environmental representation in the post-processing phase.

4.2.1 Possible Approaches

In order to eliminate uncertainties in the environmental representation, possible methods are discussed and compared. Generally, the uncertainties can be reduced online, for example, by providing additional available information, adapting more advanced algorithms or labeling.

[158] Dietmayer, K. et al.: Repräsentation fusionierter Umfelddaten (2015), p. 457.

[159] Domhardt, K.: Retrospektive Korrektur von Objektexistenzfehlern (2016), pp. 26–27.

The C2X-Communication is considered as a sensor with an extended field of view (FoV) beyond the range of conventional sensors such as lidars and radars. As a result, the uncertainties can be reduced, e.g., the information of an occluded object can be acquired by this technology. Rauch et al.[160] use the C2X-Communication as an extra sensor for a high-level sensor data fusion. The experiment results prove the accuracy and consistency of this method. The behavior prediction of vulnerable road users (VRUs) is a particular challenging problem, which could be mitigated by the C2X-Communication. Engel et al.[161] demonstrate that the positions of pedestrians can be significantly improved by using C2X-Communication, especially in the scenarios with turning or sudden changes in motion. However, the C2X-Communication is currently limited to small applications because of the insufficient infrastructures and the unrefined technique. The second option is to use reference sensors. In this case, reference sensors such as GNSSs with real-time kinematic (RTK) are installed on the traffic participants, so that their states can be acquired accurately. Thus, this approach is only suitable for the tests on a proving ground, since it is impracticable to implement reference sensors on all traffic participants on public roads. The idea from Krajewski et al.[162a] is a new way to reduce uncertainties by using a drone above a road, as illustrated in Figure 4-3. Thus, the occlusion is avoided and the FoV is extended. After image processing, the accuracy of the positions of the recorded traffic participants are thought to be smaller than 10 cm.

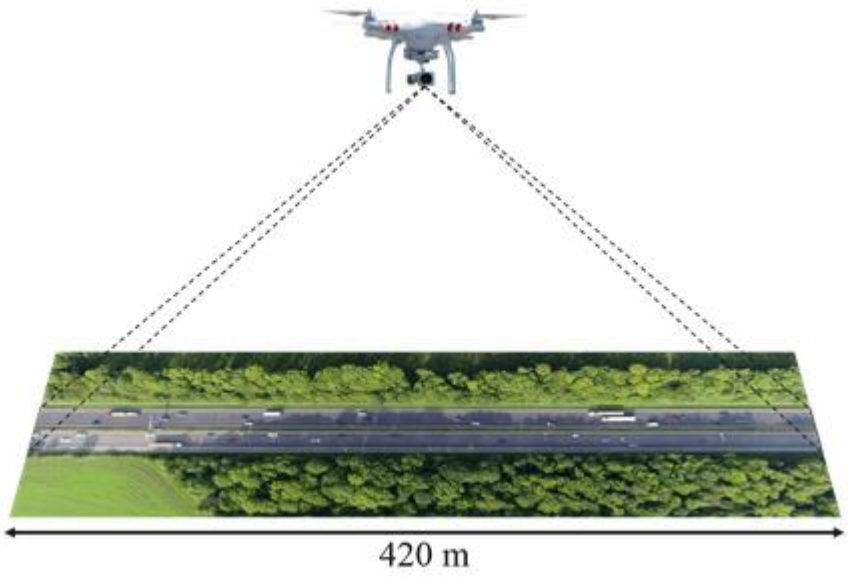

Figure 4-3: Uncertainties reduction by using a drone above the road[162b]. © 2018 IEEE

[160] Rauch, A. et al.: Car2x-based perception in a high-level fusion architecture for perception systems (2012).

[161] Engel, S. et al.: Car2pedestrian positioning: Methods for improving gps positioning (2013).

[162] Krajewski, R. et al.: The highd dataset (2018).a: -; b: p. 2119.

Nuss et al.[163] utilize grid maps to differentiate dynamic and static objects. Then, a joint integrated probabilistic data association (JIPDA) filter is applied to reduce the number of FP objects. The FP objects are greatly reduced compared to the ground truth. It demonstrates that the approach is capable of reducing existence uncertainties. Notably, this method brings high computational cost if the JIPDA filter is utilized to track all detected objects, since a soft data association is applied in this filter.

Due to the high computational cost of the original JIPDA filter, a new method[164a] is proposed, which combines the retrospective post-processing[165] and the JIPDA filter to reduce existence uncertainties. The working process of this method is illustrated in Figure 4-4. The retrospective post-processing means that the present information can be used to supplement or correct the information in the past. Thus, it is particularly useful for static variables of an object such as the dimension. With respect to the dynamic variables of the object, such as velocity, the missing information could be supplemented by interpolation in the retrospective post-processing. In the method described in Figure 4-4, not only the tracked objects but also the detected objects of a NN-UKF tracker (Nearest Neighbor-Unscented Kalman Filter) are saved. Each detected object is assigned an ID that comes from the tracked results. Subsequently, the tracked objects are retrospectively analyzed to obtain only dynamic objects by defining a speed threshold. Afterwards, the detected objects, which have identical IDs with the dynamic objects, are given to the JIPDA-UKF tracker. Finally, the tracking performance of the JIPDA-UKF tracker is fully utilized, while the tracking effort is reduced below an acceptable level. Detailed information on this approach can be found in the published paper listed at the end of this dissertation.

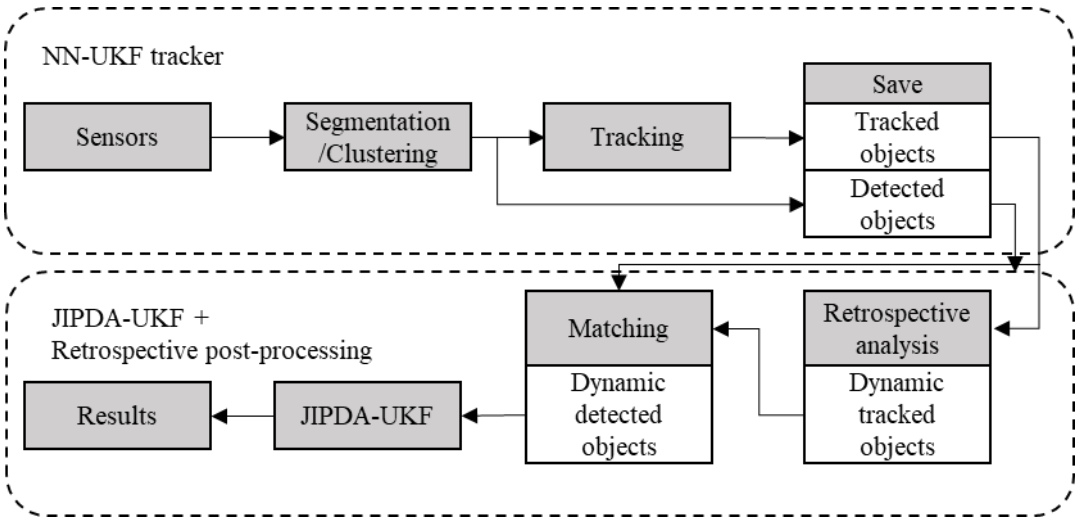

Figure 4-4: The working flow of the retrospective post-processing combined with JIPDA-UKF[164b]. © 2020 IEEE

[163] Nuss, D. et al.: Using grid maps to reduce the number of false positive measurements (2012).

[164] Wang, C. et al.: Reduction of Uncertainties for Safety Assessment of Automation (2020).a: -; b: p. 155.

[165] Wachenfeld, W.; Winner, H.: Virtual Assessment of Automation in Field Operation (2015).

With respect to the state uncertainties, the Unscented Rauch-Tung-Striebel smoother[166] (URTSS) can provide a satisfying result. It filters the posteriori states and covariance in the backward pass. The forward pass is identical to the UKF. Nevertheless, it is not measurements but the filtered values from UKF are applied to update state and covariance in the past in the backward pass. This process has exactly the same principle as the retrospective post-processing. Basically, the environmental representation is more accurate if an AV has more time to interact with the objects. When the AV approaches the near vicinity of the objects, the information about them becomes even better. Based on these sensing characteristics, the URTSS would be a solution to reduce state uncertainties.

Lastly, the labeling as an intuitive method to achieve an environmental representation with fewest uncertainties is the most commonly used method. The annotation of the image and point clouds are the two research focuses if typical automotive sensors for perception are used. Several tools such as LabelMe[167] for image annotation, SAnE[168] and LATTE[169] for point clouds are developed and even open-source. Despite of the relative huge effort, this approach provides the most accurate environmental representation, which is called “ground truth”. In addition, some tools have intergraded the annotation of image and point clouds together, such as the Ground Truth Labeler toolbox from MATLAB. Even if the other methods can indeed reduce the uncertainties, some uncertainties still remain. Furthermore, they are usually limited to reduce certain type of uncertainties. However, it is desired that all the three types of uncertainties can be reduced at the same time. The labeling provides exactly the possibility to achieve this goal. Meanwhile, the labeled results are usually very accurate. Therefore, the labeling is chosen to correct the environmental representation for verifying the defined triggers in the VAAFO approach.

4.2.2 Trigger Evaluation

After the perceived environmental representation is labeled, the behavior of the IiC and the vAV instances can be evaluated again in the corrected environment. In order to evaluate the performance of the proposed criticality index C_a, it is necessary to compare it with another criticality metric. If a labeled scenario that is rated critical by another criticality metric is also classified as critical by the C_a, the performance of the proposed criticality index can thus be evaluated. Moreover, the threshold of C_a can be optimized according to the actual critical scenarios. In the chapter 2.2.5.4, different criticality metrics are discussed. Even if some of them can represent the severity level, and can be utilized in more complex situations, few of them have a clear definition of the threshold. TTC has been studied for a long time

[166] Särkkä, S.: Unscented Rauch ‐ Tung ‐ Striebel Smoother (2008).

[167] Russell, B. C. et al.: LabelMe: a database and web-based tool for image annotation (2008).

[168] Arief, H. A. et al.: SAnE: Smart Annotation and Evaluation Tools for Point Cloud Data (2020).

[169] Wang, B. et al.: LATTE: point cloud annotation via sensor fusion, one-click annotation and tracking (2019).

and defined as[170] "the time required for two vehicles to collide if they continue at their present speed and on the same path." A great deal of data and experience about TTC has been gained in triggering collision avoidance systems (CASs). It is recommended to take a soft brake engagement when the TTC value is between 1.5 and 2.0 s, while 1.0 s is suggested for a strong brake intervention.[171] Since the goal at this point is to distinguish critical and uncritical scenarios, TTC is not applicable any more. Instead, the minimum TTC ($t_{\mathrm{tc,min}}$) is the appropriate metric. Archer[172] considers the $t_{\mathrm{tc,min}}$ as a critical measurement in estimating conflict severity. A similar definition is drawn by Van der Horst and Hogema[173]. Furthermore, they state that the $t_{\mathrm{tc,min}}$ indicates how imminent an actual collision has been. Therefore, the criticality of a scenario can be quantified by the $t_{\mathrm{tc,min}}$. However, the $t_{\mathrm{tc,min}}$ is only obtained after all TTC values are available, i.e., the $t_{\mathrm{tc,min}}$ is hardly obtained online, but is suitable for the criticality analysis of a scenario in the post-processing phase. TTC reaches its minimum value if

$$f'(t) = \left(\frac{d_x(t)}{v_{\mathrm{diff},x}(t)}\right)' = 0, \text{ i.e., } v_{\mathrm{diff,x}}^2(t) = d_x(t) D_{\mathrm{rel}}(t) \tag{4.1}$$

Thus, the current relative deceleration $D_{\mathrm{rel}}(t)$ is twice the relative deceleration required to avoid a collision if a linear motion with constant deceleration is assumed.

With respect to the threshold of $t_{\mathrm{tc,min}}$, Mahmud et al.[174] have summarized the thresholds from different literatures, and 1 s is recommended by some of them. Hence, if the $t_{\mathrm{tc,min}}$ is large than 1 s, the scenario is considered as uncritical, since an AV still has an enough large time gap before a collision. However, it is difficult to distinguish critical and uncritical scenarios by a single threshold, since different drivers have different feelings and evaluations in different situations. The same conclusion is also drawn by Das and Maurya[175]. They suggest to use different $t_{\mathrm{tc,min}}$ thresholds for different situations. Moreover, there is little agreement on which threshold should be applied, and many publications including $t_{\mathrm{tc,min}}$ discuss the interactions in the analysis instead of using a predefined threshold.[176] As a result, when classifying a scenario as critical, the threshold should be low enough so that the covered situations are actual critical. Based on equation (4.1), $t_{\mathrm{tc,min}}$ can be expressed as

$$\frac{d_x(t)}{v_{\mathrm{diff},x}(t)} \Big|_{v_{\mathrm{diff,x}}^2(t) = d_x(t) D_{\mathrm{rel}}(t)} = t_{\mathrm{tc,min}} \tag{4.2}$$

[170] Hayward, J. C.: Near miss determination through use of a scale of danger (1972).

[171] Winner, H.: Grundlagen von Frontkollisionsschutzsystemen (2015), pp. 907–908.

[172] Archer, J.: Traffic conflict technique: Historical to current state-of-the-art (2001).

[173] van der Horst, R.; Hogema, J.: Time-to-collision and collision avoidance systems (1993).

[174] Mahmud, S. S. et al.: Application of proximal surrogate indicators for safety evaluation (2017).

[175] Das, S.; Maurya, A. K.: Defining Time-to-Collision Thresholds in Non-Lane-Based Environments (2019).

[176] Olszewski, P. et al.: Review of current study methods for VRU safety. Part 1 - Main report (2016), p. 75.

Therefore, $d_x(t) = t_{\mathrm{tc,min}}^2 D_{\mathrm{rel}}(t)$, i.e., when $t_{\mathrm{tc,min}}$ decreases, $d_x(t)$ decreases even more due to the square relationship if $D_{\mathrm{rel}}(t)$ does not change.

If $t_{\mathrm{tc,min}} = 0.2$ s and $D_{\mathrm{rel}}(t) = 10\ \mathrm{m/s^2}$, $d_x(t)$ is 0.4 m. This means that even if the relative deceleration is so large, the remaining relative distance is rather small if $t_{\mathrm{tc,min}} = 0.2$ s. Similarly, if $t_{\mathrm{tc,min}} = 0.4$ s and $D_{\mathrm{rel}}(t) = 10\ \mathrm{m/s^2}$, $d_x(t)$ is 1.6 m. With the same large relative deceleration, the remaining relative distance is 1.6 m when $t_{\mathrm{tc,min}}$ doubles. Therefore, a scenario is regarded as critical in this dissertation if the $t_{\mathrm{tc,min}}$ is lower than 0.2 s since an AV is so close to a collision. In the area between 0.2 and 1 s, the criticality of a scenario is unknown. Through these criteria, the recorded scenarios can be classified by $t_{\mathrm{tc,min}}$. The classified results can then be compared with the online identified scenarios in order to evaluate the C_a. Since the $t_{\mathrm{tc,min}}$ is only applicable in the longitudinal direction, the performance of the C_a cannot be verified completely. According to equation (3.22), the C_a can also be used to assess the safety of AVs in the lateral direction. Therefore, some extra effort must be made when a scenario is assessed as critical by C_a but not by $t_{\mathrm{tc,min}}$.

4.2.3 Coverage Identification

Another reason why $t_{\mathrm{tc,min}}$ is calculated in the corrected environment is to determine the sources of error. The determination of the sources of error is a key element for the derivation of the coverage of critical scenarios of the VAAFO approach. If a scenario is classified as critical by $t_{\mathrm{tc,min}}$ in the corrected environment, there are then decision errors in vAV instances, since few perception errors exist after labeling. Additionally, if the IiC and one of the vAV instances have a large C_a simultaneously, this large C_a is caused probably by a perception error, since the same environmental representation is utilized for the calculation of C_a of IiC and vAV instances. A critical situation caused by other objects can also lead to this result. Thus, further observation should be performed to determine whether it is the fault of other objects or the perception module. With respect to large C_a values in other cases, the scenarios should be analyzed in detail in order to explore the reasons. By analyzing what type of errors in an AV can be discovered by the triggers, and what the limitations of the VAAFO framework have, the application scope of the VAAFO approach can be finally derived. As a result, the role of the VAAFO approach for the safety verification and validation of AVs is determined.

4.3 Summary

The aim of this chapter is to introduce the procedures to verify the defined triggers and the VAAFO framework. The existence uncertainties, state uncertainties and class uncertainties are analyzed. Possible approaches to reduce the uncertainties are compared. In particular, the JIPDA filter combined with the retrospective post-processing to reduce the existence

uncertainties is described. URTSS as an option to reduce state uncertainties is presented. The labeling approach is finally chosen due to its high accuracy. Finally, the process to verify the triggers is introduced. The above described process can be also applied to the open-loop recording. However, all the sensor data has to be recorded and saved on-board in the open-loop recording. In contrast, only relevant scenarios are saved online by the VAAFO approach. Furthermore, the process described in this chapter is used to verify the VAAFO approach, and is not essential when the approach is already verified. The performance of the C_a is determined by comparing it with $t_{\mathrm{tc,min}}$. In the scenarios in which the C_a cannot be evaluated by the $t_{\mathrm{tc,min}}$, extra effort should be paid. The coverage degree of the VAAFO approach is derived by analyzing the sources of error, which can be determined by implementation of $t_{\mathrm{tc,min}}$ in the corrected environment and by the detailed analysis of the scenarios. The detail implementation of the procedures described in this chapter will be introduced through the real-world testing of the VAAFO approach in chapter 6.

5 Verification in the Simulation

Before the VAAFO approach is applied in reality, simulations are first performed to quickly identify potential problems of the approach. The simulation platforms should be first determined. The interface between different simulation platforms should be developed. Additionally, an automated driving system (ADS) is essential for the vAV instances. Test scenarios for evaluating the approach should also be designed. Based on the simulation results, the performance and characteristics of the VAAFO approach could be preliminarily derived. Finally, its working flow is also demonstrated.

5.1 Simulation Components

In order to perform the simulation, two platforms are selected. The IPG Driver in CarMaker is utilized to simulate the behavior of an IiC. Notably, only an independent instance in charge of driving a vehicle is required. The vAV instances can thus be reset to the state of the IiC at the beginning of every lifetime. Therefore, there is no special requirement for the accuracy of the driver model, and the driver model form CarMaker is sufficient for demonstrating the approach. Additionally, CarMaker provides also different sensor models. They are ideal sensor models, high fidelity sensor models and raw signal interface sensor models, respectively.

- Ideal sensor models: physical effects are not considered and ground truth information is provided.
- High fidelity sensor models: several basic and prominent physical effects are taken into account, e.g. object occlusion.
- Raw signal interface sensor models: little processed sensor data is provided. The data should be handled and interpreted to acquire the object list.

In the simulation, ideal sensor model is chosen, since the different sensor effects are not important if the aim is to evaluate the VAAFO approach rather than an ADS. Besides, traffic participants can be configured and predefined in CarMaker. Different types of roads can be created. Finally, it is able to simulate numerous concrete scenarios in the simulation. The second platform is ROS in which the three vAV instances will run. Due to the independent and interchangeable modules, ROS is a practical middleware to design algorithms for AVs.

5.1.1 Simulation Architecture

The simulation architecture for verifying the VAAFO approach is illustrated in Figure 5-1. Several sensors are installed on a vehicle, and the IiC drives the vehicle to perceive the en-

vironment. Since the tracked objects from different sensors can be directly read from CarMaker, a tracking algorithm is not essential. Then, the tracked objects are transmitted to the ROS platform through a bridge between the CarMaker and ROS platforms. Subsequently, the tracked objects are fused in the ROS platform. The fused results are given to the behavior module. Based on the desired behavior and the information provided by the map, a desired trajectory is generated. Since the act module is not considered, the desired trajectory is used directly to update the state of a vAV instance. However, the update frequency of the state is higher than the trajectory planning, an interpolation is thus necessary to update the state of a vAV instance at each time step using the available desired trajectory. Then, the current state of the vAV instance is fed back to the behavior planner and the trajectory planner for the next cycle. Based on the current state of the vAV instance and the surrounding objects, the criticality index of the vAV instance can be calculated. Since the behavior planner and the trajectory planner are essential for the simulation, they are introduced in this chapter as well.

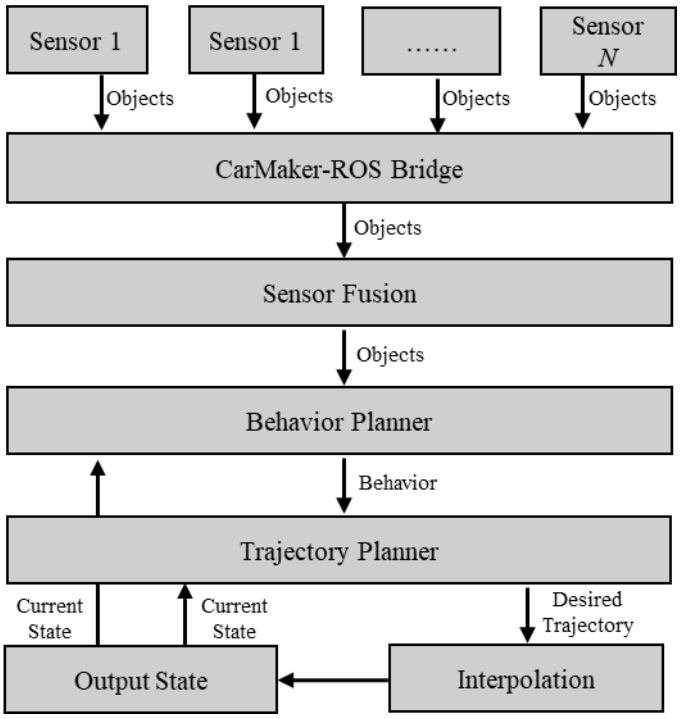

Figure 5-1: The simulation architecture of a vAV instance.

5.1.2 Sensor Configuration

As aforementioned, several sensors from CarMaker are utilized. Since each sensor provide the ground truth of the environment in its field of view (FoV), the fusion strategy in the simulation is intuitive. If one object is detected by different sensors simultaneously, the tracked results of this object from one sensor are taken, since the results from different sensors are identical. If two sensors have totally different object lists, the object lists are added directly together. Afterwards, the fused objects are transformed to the earth-fixed coordinate system. Due to the same map in CarMaker and in ROS, the transformed results can be pro-

jected into the virtual world in which the three vAV instances run. As a result, the environmental representation in the virtual world is established. Figure 5-2 shows an example of three tracked objects in CarMaker. The FoV of the sensors at the rear of the IiC are not shown in the left image for a better visualization. The fused and projected results in the ROS are illustrated in the right image.

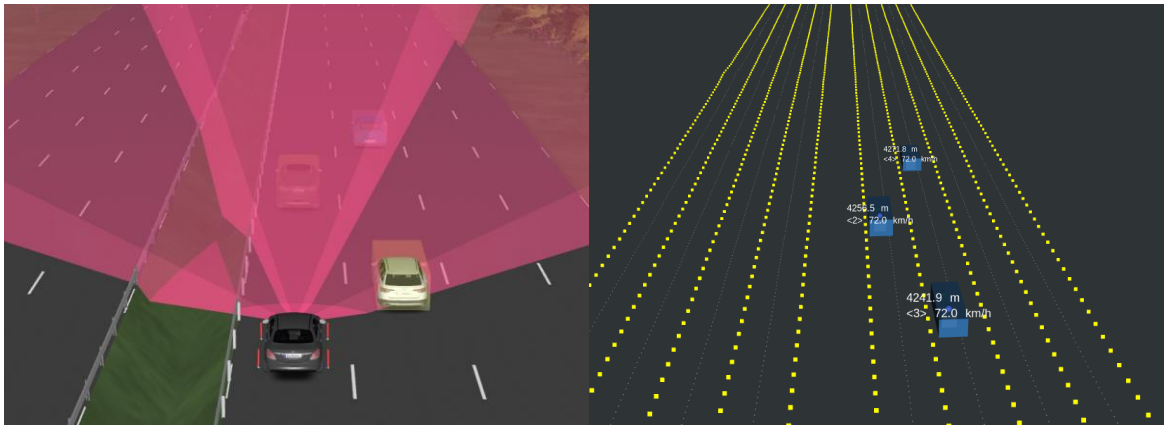

Figure 5-2: The description of the sensor set-up and the detected objects in CarMaker (left); the fused and transformed objects in the ROS platform (right).

5.1.3 Behavior Planner

As mentioned in the last subchapter, a behavior planner is essential for the vAV instances. The developing of an excellent behavior planner is not the focus in this dissertation. Therefore, a behavior planner limited for motorway scenarios is sufficient for demonstrating the VAAFO approach. With respect to the behavior planner, the rule-based approaches are frequently applied. For example, Zhang et al.[177] propose a finite state machine-based controller for AD on multi-lane motorways by considering adaptive cruise control mode, cruise control mode, lane change mode and lane change pause mode. Since the rule-based approach cannot handle unknown situations and uncertainties, some other approaches are studied. For example, Brechtel et al.[178] utilize a Markov decision process (MDP) to infer optimal behavior decisions by describing the evolution of traffic situations in a sophistical and probabilistic way. In order to deal with uncertain and incomplete perception, partially observable MDP (POMDP) is motivated. However, the solution of the POMDP problems is challenging. As a result, Brechtel et al.[179] propose an approach that learns a suited representation of the specific situation instead of discretizing the state space. In addition, other new decision making

[177] Zhang, M. et al.: A finite state machine based controller and its stochastic optimization (2017).

[178] Brechtel, S. et al.: Probabilistic MDP-behavior planning for cars (2011).

[179] Brechtel, S. et al.: Probabilistic decision-making under uncertainty using continuous POMDPs (2014).

approaches such as machine learning-based methods[180,181] have shown promising results in various domains.

Even if the rule-based approach does not take the uncertainties into account, it can be clear structured. Due to the finite number of parameters, the calibration and optimization are relative simple compared to the MDP-based approach. Therefore, the rule-based approach is utilized for the behavior planner. Basically, lane change left, lane change right, adaptive cruise mode, cruise mode and stop are defined for the motorway scenarios. Table 5-1 describes the definition of each behavior. The connection and the transition conditions between different behaviors are given in appendix A.2.

Table 5-1: The definition and description of each state.

State	Description
Lane change left	The subject vehicle changes to the left lane
Lane change right	The subject vehicle changes to the right lane
Cruise mode	No vehicle is ahead or the preceding vehicle is faster than the reference speed, and the subject vehicle maintains the reference speed
Adaptive cruise mode	The subject vehicle decelerates or accelerates to keep a same speed as the preceding vehicle if the preceding vehicle is slower than the reference speed
Stop	The subject vehicle stops when reaching the destination or encountering an emergency situation

The basic principle of the designed behavior planner is that each behavior first has an initial cost according to the traffic rules, efficiency and driving comfort, e.g., stop has the highest cost due to low efficiency and comfort, while cruise mode has the lowest cost to reduce maneuvers that need to be performed. Lane change left is more preferred than lane change right if both maneuvers are feasible. During the driving, the initial cost of each behavior is updated online by considering the safety. If one behavior is critical, the cost of that behavior is increased to a collision cost, which is the highest among the other costs. Whether a behavior has the collision cost is determined by the predefined criteria such as relative distance, TTC, etc. Similarly, when the subject vehicle is quite close to a static object, the cost of stop is decreased to make sure the stop maneuver is the optimal one. Finally, each enumerated behavior has an up-to-date cost at each cycle of the behavior planner. Subsequently, the total cost of each behavior, which has a transition with the current behavior, is compared. The behavior with minimum cost is handed over to the trajectory planer module. It should be

[180] Shi, T. et al.: Driving Decision for Lane Change Behavior based on Deep Reinforcement Learning (2019).

[181] Hoel, C.-J. et al.: Combining Planning and Deep Reinforcement Learning in Decision Making (2020).

noted that the thresholds in the criteria should be further calibrated. More data would be helpful to improve the designed behavior planner.

5.1.4 Trajectory Planner

The trajectory planner as a sublevel of the behavior planner receives the desired behavior and generates a corresponding trajectory. The trajectory planner is one of core components in an AV. Different approaches are studied to solve this problem. Basically, there are mainly four categories for the trajectory planning: graph search-based, sampling-based, curve interpolation-based and optimization-based trajectory planning. A*[182] and Dijkstra[183] are well-known approaches to generate shortest paths on a graph by discretization of the environment. Since the resolution of the graph has a strong impact on the planned path and it is difficult to take into account the constraints of vehicle dynamics, they are not appropriate for AVs. Rapidly-exploring Random Trees (RRTs)[184], which belongs the sampling-based category, has being studied in recent years. Compared to the search-based method, discretization of the environment is no longer necessary. Instead, feasible trajectories can be generated over high-dimensional spaces. By increasing the number of samples, the asymptotic optimality can even be achieved by the RRT*[185]. However, the high computational complexity brought by the increased sampling is a tough problem that hinders its practical application. Figure 5-3 illustrates the process of generating a path through the graph search-based and the sampling-based approach. As is obvious in the figure, fewer states are explored in A* than in Dijkstra.

The interpolation-based approaches, including polynomial curves[186], clothoid curves[187], spline curves[188] and Bezier curves[189], gain much interest as well. By setting several key points or parameters, a trajectory with continuity of curvature can be generated. Therefore, the computational cost is low. Nevertheless, the optimality of the generated trajectory cannot be guaranteed. Additionally, some vehicle dynamic constraints are not considered. As a result, the generated trajectories must be compared with each other in order to find the one that meets all constraints. A well-known example is the trajectory generation method proposed

[182] Hart, P. E. et al.: A formal basis for the heuristic determination of minimum cost paths (1968).

[183] Dijkstra, E. W.; others: A note on two problems in connexion with graphs (1959).

[184] LaValle, S. M.: Rapidly-exploring random trees: A new tool for path planning (1998).

[185] Karaman, S.; Frazzoli, E.: Optimal motion planning using incremental sampling-based methods (2010).

[186] Petrov, P.; Nashashibi, F.: Modeling and nonlinear adaptive control for overtaking (2014).

[187] Brezak, M.; Petrović, I.: Real-time approximation of clothoids with bounded error for path planning (2013).

[188] Piazzi, A. et al.: Quintic G/sup 2/-splines for iterative steering of vision-based autonomous vehicles (2002).

[189] Rastelli, J. P. et al.: Dynamic trajectory generation using continuous-curvature algorithms (2014).

by Werling et al.[190] By using the Frenet frame, a trajectory is decoupled by a longitudinal and a lateral trajectory, each represented by a quintic polynomial. Afterwards, the movements in two directions are combined to determine the points in the final trajectory.

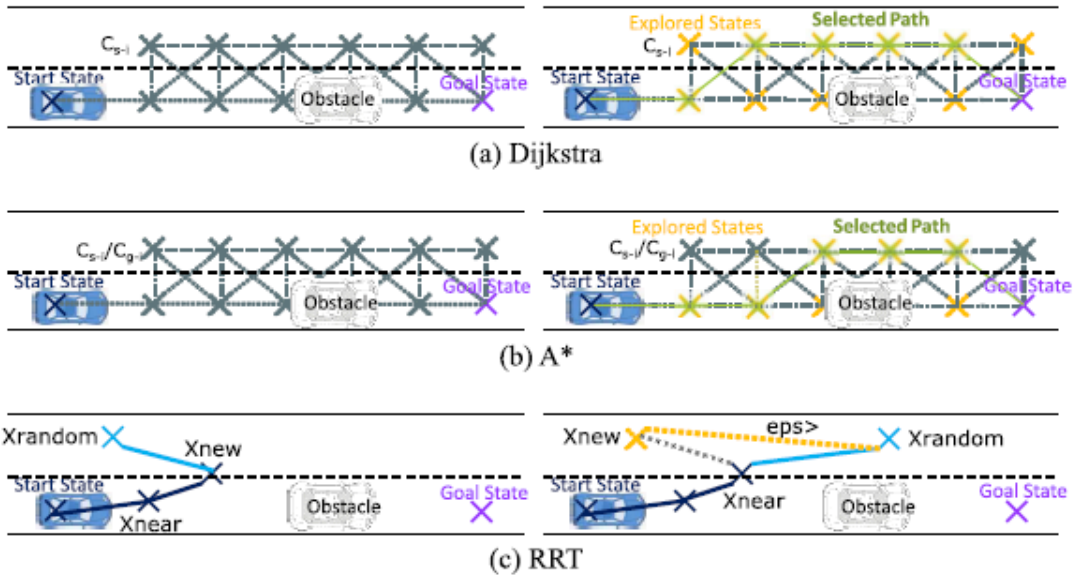

Figure 5-3: Description of the process of (a) Dijkstra, (b)A*, and (c) RRT.[191] © 2020 IEEE

The last category is the optimization-based approach. The basic idea is to formulize the trajectory planning as an optimization problem, taking into account obstacle constrains, vehicle dynamic constraints, etc. The advantages of this approach are that different kinds of requirements can be implemented flexibly and easily. Moreover, several solvers such as Ipot[192] and Hpipm[193] are able to solve non-linear optimization problems online. The model predictive control (MPC) approach is exactly an optimization-based approach, and has been widely used in the trajectory planning for AVs. The MPC solves the optimal trajectory in a recursive manner, and takes the dynamic and stochastic of the environment into account. Therefore, the MPC approach is utilized for the trajectory planning.

5.1.4.1 MPC Trajectory Planner

In the MPC trajectory planner, the generation of the trajectory is regarded as an optimization problem by considering some constraints. The problem can be formulized as[194]

[190] Werling, M. et al.: Optimal trajectory generation for dynamic street scenarios in a Frenét Frame (2010).

[191] Claussmann, L. et al.: A Review of Motion Planning for Highway Autonomous Driving (2020), p. 1833.

[192] Wächter, A.; Biegler, L. T.: An interior-point filter line-search algorithm for nonlinear programming (2006).

[193] Frison, G.; Diehl, M.: HPIPM: a quadratic programming framework for model predictive control (2020).

[194] Alrifaee, B.; Maczijewski, J.: Real-time Trajectory optimization using Sequential Linearization (2018).

$$\text{minimize} - x_N + \sum_{n=0}^{N} (\xi_{\text{lin},x} x_n + x_n^{\text{T}} \xi_{\text{qua},x} x_n + \xi_{\text{lin},u} u_n + u_n^{\text{T}} \xi_{\text{qua},u} u_n) \tag{5.1}$$

$$\text{Subject to} \quad x_{n+1} = A_n x_n + B_n u_n \tag{5.2}$$

$$x_{\text{l},n} \leq C_{\text{str},n} x_n + s_n x_n \leq x_{\text{u},n} \tag{5.3}$$

$$n \in [0, N] \tag{5.4}$$

$\xi_{\text{lin,x}}$ and $\xi_{\text{qua,x}}$ are linear and quadratic cost terms for the state x_n, which is the state of a point on the planned trajectory.

$$x_n = \{ {}_{\text{E}}p_{x,n},\ {}_{\text{E}}p_{y,n},\ {}_{\text{E}}v_{x,n},\ {}_{\text{E}}v_{y,n},\ {}_{\text{E}}a_{x,n},\ {}_{\text{E}}a_{y,n} \} \tag{5.5}$$

$u_n = [\ {}_{\text{E}}J_{x,n},\ {}_{\text{E}}J_{y,n}]^T$ denotes the control variable (jerk) on an earth-fixed coordinate system. Thus, $\xi_{\text{lin},u}$ and $\xi_{\text{qua},u}$ are the linear and quadratic cost terms of the jerk. N is the total prediction steps, while n is one step of N. x_N is selected as the goal to make the vehicle always go forward since no global planner is designed. The constraints are described by the equation (5.3). $x_{\text{l},n}$ is the lower limit of the state at step n. $x_{\text{u},n}$ denotes the upper limit of the state at step n. $C_{\text{str},n}$ represents the constraints including reference line, speed, acceleration and jerk. Slack vector s_n is defined to determine the priority of the constraints. The vehicle model is simplified as a point mass model as shown in equation (5.2). The reference point of the mode locates in the middle of a vehicle. The model parameters A and B are expressed by

$$A = \begin{bmatrix} 1 & 0 & \eth t & 0 & \frac{1}{2}\eth t^2 & 0 \\ 0 & 1 & 0 & \eth t & 0 & \frac{1}{2}\eth t^2 \\ 0 & 0 & 1 & 0 & \eth t & 0 \\ 0 & 0 & 0 & 1 & 0 & \eth t \\ 0 & 0 & 0 & 0 & 1 & 0 \\ 0 & 0 & 0 & 0 & 0 & 1 \end{bmatrix} \tag{5.6}$$

$$B = \begin{bmatrix} 0 & 0 \\ 0 & 0 \\ 0 & 0 \\ 0 & 0 \\ \eth t & 0 \\ 0 & \eth t \end{bmatrix} \tag{5.7}$$

$\eth t$ is the time interval between two adjacent points on the trajectory. The different constraints are summarized in appendix A.3. By solving such problem, the desired state at every time step of a planned trajectory is finally available.

In the designed MPC trajectory planner, spatial constraint, speed constraint and acceleration constraint are considered. With respect to the spatial constraint, the middle line of a lane is regarded as the reference line. Thus, if the subject vehicle deviates from the reference line,

this action is penalized. A reference line is switched to that of an intended lane if lane changing is motivated from the behavior planner. The optimization process is illustrated in Figure 5-4. k denotes the current time step and N is the total number of predicted points.

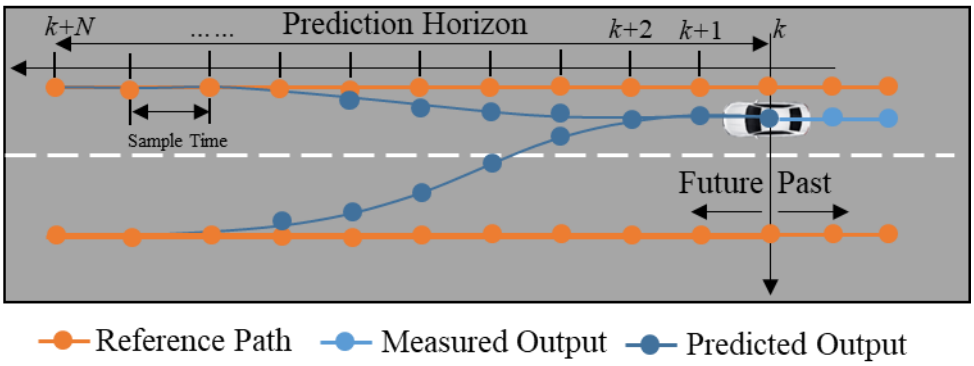

Figure 5-4: The optimization process of a MPC planner toward the reference line. Own illustration according to Wikipedia[195].

If a lane changing maneuver is motivated, the reference path is changed to the middle line of the intended lane decided by the behavior planer. Otherwise, the middle line of current lane is regarded as the reference line. By adjusting the control output, the current position approaches gradually to the reference path. Additionally, the intended velocity from behavior planer is also regarded as a constraint to realize cruise and adaptive cruise modes. As a result, the subject vehicle keeps a constant speed if there is no object in front. The speed will be adapted accordingly in case of a slow preceding obstacle. The last constraint is the acceleration constraint to ensure the output acceleration is physically realizable. Typically, the acceleration constraint can be modelled as two ellipses. In order to linearize the ellipse of friction, an inscribed polygon is utilized. The more constraints are used, the more sides the inscribed polygon will have and the closer the planner can achieve the border of the ellipse. The detailed descriptions about the constraints can be found in appendix A.3. The Hpipm solver[196] is utilized to optimize the goal function in equation (5.1) due to its efficiency and reliability.

5.2 Simulation Scenarios

The above subchapters has introduced the simulation platforms and the ADS for the vAV instances. The test scenarios are the last task that should be determined in order to start the simulation. With respect to the scenarios, Menzel et al.[197] propose three different types of

[195] Wikipedia: Model predictive control - Wikipedia (2021).

[196] Frison, G.; Diehl, M.: HPIPM: a quadratic programming framework for model predictive control (2020).

[197] Menzel, T. et al.: Scenarios for development, test and validation (2018).

scenarios based on the abstract level of a scenario. They are functional scenario, logical scenario and concrete scenario, respectively. The functional scenario describes a scenario at the most abstract level, e.g. a cut-in scenario. All parameters are specified in a concrete scenario. In logical scenario, the parameter distribution or parameter range is given. Therefore, only concrete scenarios can be utilized directly to test the proposed approach. However, there are many parameters in one scenario, such as object parameters, road parameters and even weather parameters, it is thus rather difficult to enumerate all scenarios. Hence, certain methods should be applied to derive specific test scenarios for testing the VAAFO approach.

5.2.1 Scenarios Derivation

Generally, the top-down and bottom-up methods are useful to derive test scenarios. In the top-down method, an overview of the system is formulated. Any first-level subsystems are specified but not elaborated. Then, each subsystem is refined in yet greater detail, sometimes in many additional subsystem levels, until the entire specification is reduced to base elements.[198] Typical application of the top-down method is the functional decomposition of an ADS proposed by Amersbach and Winner[199]. They define six functional layers to describe an ADS. They are information access, information reception, information processing, situational understanding, behavioral decision, and action layers, respectively. The aim of functional decomposition is that if only one layer is changed, the other layers are not necessary to test again. As a result, the test effort is reduced. Instead of deriving test scenarios from the entire ADS, the six functional layers can be separately studied.

In the bottom-up method, the individual base elements of a system are first specified elaborately. These elements are then linked together to form larger subsystems, which in turn are connected again. Such connection can be repeated for several times sometimes. Finally, a complete top-level system is formed after the linking. Based on this method, the individual base elements should be first defined. Therefore, the derived scenarios from the top-down method are theoretically complete but difficult to be specified. Conversely, the bottom-up method provides an intuitive way to derive test scenarios starting from a specific situation but the completeness is hardly guaranteed.

Additionally, the test scenarios could come from other sources including but not limited to[200]:

- Challenging scenarios during the operation of an ADS in the real world
- Scenarios result from the human traffic accidents in the real world
- Systematic variation of generic human scenarios known to result in accidents
- Systematic variation of the parameters in the ODD

[198] Wikipedia: Top-down and bottom-up design - Wikipedia (2021).

[199] Amersbach, C.; Winner, H.: Defining Required and Feasible Test Coverage for Validation of HAV (2019).

[200] ISO: ISO/TR 4804: Road Vehicles – Safety and security for automated driving systems (2020), p. 61.

- Scenarios from brainstorming of experts
- Currently unknown scenarios explored by artificial intelligent or other optimization algorithms

Table 5-2: The possible errors from three different methods to derive test scenarios.

Method	**Scenario description**		**error**
	Functional layer	**Layer description**	
Top-down	Information access	Whether the information is generally accessible	Map errors Localization errors Existence uncertainties State uncertainties Class uncertainties
	Information reception	Whether the accessible information is receivable	
	Information processing	Whether objects are detected/classified/tracked successfully	
	Situational understanding	Goal and value-specific information, selection and augmentation	Motion prediction errors
	Behavior decision	A decision is made based on the situation model	Behavior- and Trajectory planner errors
Crash scenarios from human drivers	The crash scenarios of human drivers occur in the real world		Improper operation of human drivers
Challenging scenarios of an ADS	The challenging scenarios that an ADS encounters during the real-world testing		Errors of an ADS

After analyzing possible methods to derive the test scenarios, the top-down method, a crash scenario from human accidents and a challenging scenario previously encountered by an ADS are selected to demonstrate the VAAFO approach. Since the aim of the VAAFO approach is to evaluate the safety of AD and identify critical scenarios during the driving, the scenarios that are utilized to verify the VAAFO approach are previously known critical or challenging scenarios. If the scenarios can be covered and identified successfully by the VAAFO approach, the performance of the VAAFO approach could be proved. The possible errors from the functional layers, the crash scenarios from human drivers and the challenging scenarios from an ADS are summarized in Table 5-2. From the information access, information reception and information processing, map errors, localization errors and perception errors can be derived. In the situational understanding layer, motion prediction errors can be a cause for a misunderstanding of the situation. Behavior- and trajectory planner errors could

occur in the behavior decision layer. From each type of error, corresponding functional scenarios can be derived. For instance, a scenario with a relevant FP object can be simulated to generate existence uncertainties.

5.2.2 Simulation Cases

Based on the Table 5-2, only functional scenarios can be derived, which are not concrete enough to build them in the simulations. In order to obtain concrete scenarios, the parameters in functional scenarios should be first specified either by a distribution or a range. The parameters are further determined in the concrete scenarios. As a result, numerous concrete scenarios can be derived. For this reason, some representative scenarios to show the results of the approach have to be chosen.

With respect to the crash scenarios of human drivers, cut-in, following scenarios are the most common critical scenarios on motorways. In particular, cut-in and following scenarios account for 27.1 % and 43.6 % of all critical scenarios caused by human drivers, respectively, according to the researches by Zhou et al.[201]. Feng et al.[202] consider the cut-in, highway exit and car-following scenarios as basic scenarios as well when generating the scenario library. Even if the critical scenarios occur more frequently in following scenarios than in cut-in scenarios, cut-in scenarios are more challenging for AVs. Therefore, the first study case is a cut-in scenario.

Case 1: A cut-in scenario from statistical traffic accident analysis of human drivers

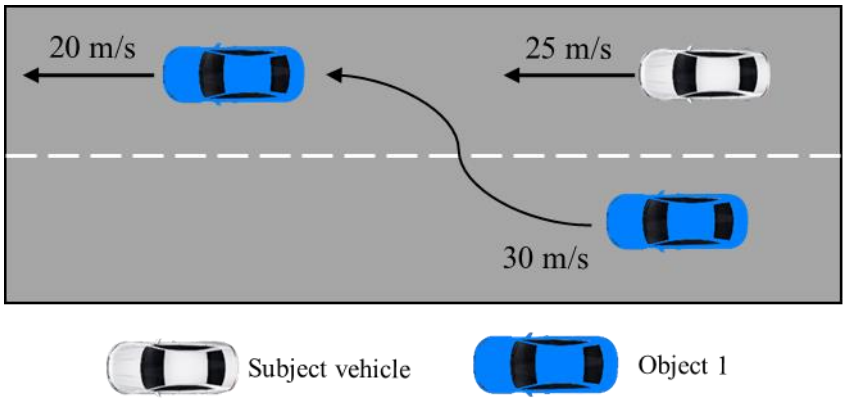

Figure 5-5: A cut-in scenario to test the VAAFO approach.

Case 1 describes a cut-in scenario as illustrated in Figure 5-5. Object 1 has a high initial velocity with 30 m/s, and is in the adjacent lane of the subject vehicle. Due to the high speed, it is approaching the subject vehicle. In order to simulate a critical scenario, object 1 even brakes for a short time to reach a lower velocity with 20 m/s after cutting in. As a result, this

[201] Zhou, J.; Re, L. d.: Reduced Complexity Safety Testing for ADAS & ADF (2017).

[202] Feng, S. et al.: Testing scenario library generation for connected and automated vehicles (2020).

scenario would be rather critical. It is interesting to see whether the safety of the vAVs can be evaluated by the designed criticality index C_a and whether this critical scenario can be successfully discovered.

After defining the scenario, the scenario is built in CarMaker, and the designed ADS runs in ROS. Figure 5-6 illustrates three important variables $v_{\mathrm{diff},x}$, d_x and y_{eva} for the calculation of $a_{\mathrm{req,eva}}$ and $D_{\mathrm{req,D}}$ in the cut-in scenario.

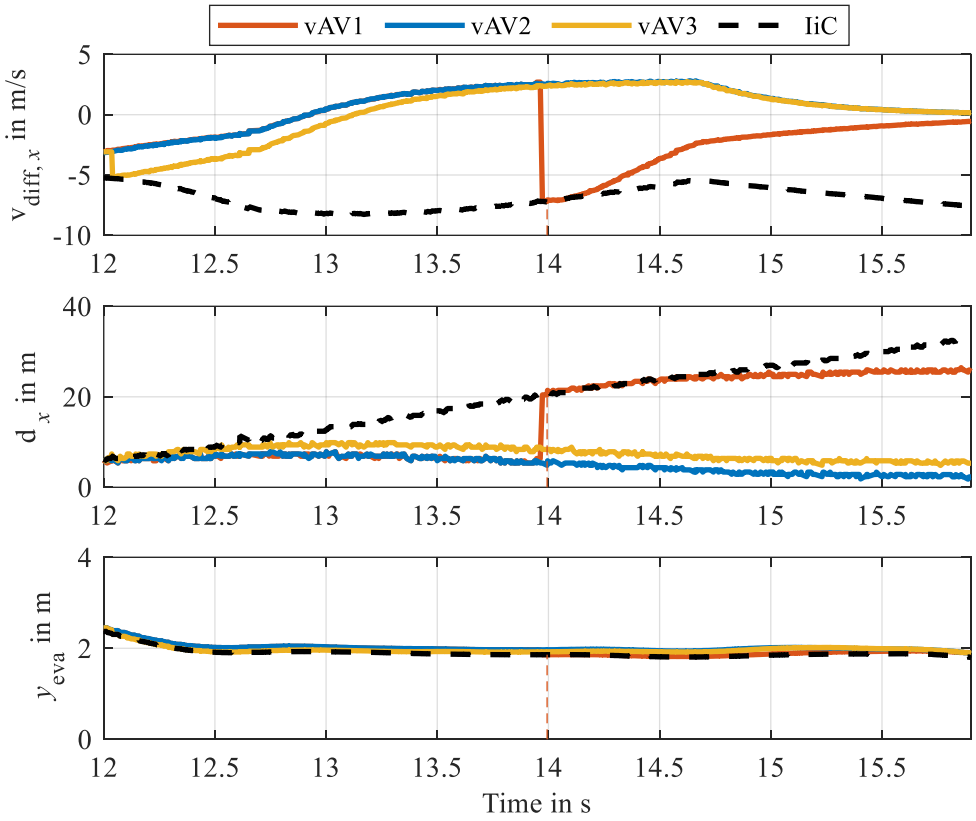

Figure 5-6: The three important variables are displayed in the cut-in scenario. The reset time steps are represented by vertical dotted lines.

As can be seen in Figure 5-6, the longitudinal relative velocity $v_{\mathrm{diff},x}$ of the three vAV instances increase, while the IiC has already reduced its velocity. The vAV1 is reset at 14 s and then accelerates to finally achieve the same velocity as the preceding object. The IiC is conservative since its velocity is always lower than the preceding object. As a result, its longitudinal clearance d_x increases continuously. In contrast, vAV2 and vAV3 have a smaller distance gap to the preceding object. The evasion offset y_{eva} stays approximately at 2 m after object 1 cuts in, since the preceding objects and the vAV instances are in the same lane.

Based on the available values of the above variables, the criticality index C_a of the three vAV instances in this scenario can be obtained over time, as shown in Figure 5-7. Negative values of the required lateral acceleration for evasion $a_{\mathrm{req,eva}}$ are ignored, since they represent that a situation is uncritical. In order to differentiate $a_{\mathrm{req,eva}}$ and $D_{\mathrm{req,D}}$ clearly in the figure, the $-D_{\mathrm{req,D}}$ is drawn, i.e., negative values of the required longitudinal deceleration for braking

$D_{\mathrm{req,D}}$ are not considered, since $D_{\mathrm{req,D}}$ itself is positive if the subject vehicle should brake. Therefore, the curves above zero show the $a_{\mathrm{req,eva}}$ of three vAV instances. The $-D_{\mathrm{req,D}}$ is shown below the zero line. The $a_{\mathrm{req,eva}}$ and $-D_{\mathrm{req,D}}$ of the three vAV instances are marked with different colors. In addition, their respective reset time steps are marked by vertical dotted lines with corresponding colors.

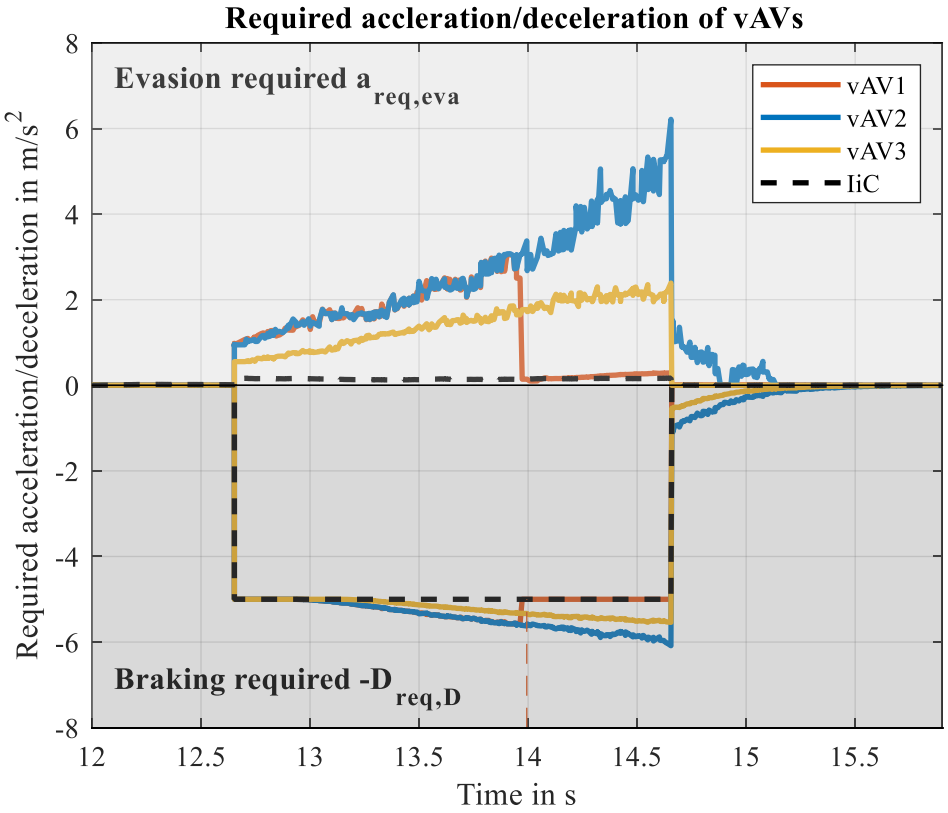

Figure 5-7: The required longitudinal decelerations below the zero line and the required lateral acceleration for evasion above the zero line of the three vAV instances in the cut-in scenario.

In this scenario, $a_{\mathrm{req,eva}}$ and $D_{\mathrm{req,D}}$ are first zero, since there is no object in front of vAV instances. They do not have to take any actions. Nevertheless, when object 1 finishes cutting in, all vAV instances brake hard to avoid collision with object 1. The IPG driver also brakes in the current lane. As can be seen from Figure 5-7, the $D_{\mathrm{req,D}}$ values of all vAV instances increase abruptly to 5 m/s^2 and then rise slowly. Meanwhile, the $a_{\mathrm{req,eva}}$ values of vAV instances grow as well but are much lower than the corresponding $D_{\mathrm{req,D}}$, since the relative deceleration is considered in equation (3.20) instead of the absolute deceleration of object 1 in equation (3.17). Additionally, the necessary evasion offset y_{eva} is at the beginning lower than d_x. Nevertheless, if the vAV instance is too close to the object 1, the evasion maneuver is rather difficult, and $a_{\mathrm{req,eva}}$ is thus too large. This phenomenon can be found at time step 14.6 s. At this time step, the deceleration is a better choice for vAV2, since the $D_{\mathrm{req,D}}$ is lower than the $a_{\mathrm{req,eva}}$. Before this time step, the evasion maneuvers for all vAV instances are superior, since the $a_{\mathrm{req,eva}}$ values are lower than $D_{\mathrm{req,D}}$.

The vAV2 does not decelerate until it changes from the cruise mode to the adaptive cruise mode, i.e., it will keep its cruise speed until the transition condition between these two modes is fulfilled. This transition condition is applied for other vAV instances as well. However, the other two vAV instances are either reset or have different states, their C_a values are smaller than that of vAV2. The maximum C_a of the vAV1 during this period is 3.02 m/s^2. Then, it is reset at 14 s to the state of the IiC and has afterwards a very low $a_{\mathrm{req,eva}}$, since the IiC takes braking action earlier than the vAV instances. The maximum C_a of the vAV3 is even lower, i.e., the critical situation cannot be discovered by vAV3. By means of the C_{a} of vAV2 is this critical situation identified, since both its maximum $a_{\mathrm{req,eva}}$ and maximum $D_{\mathrm{req,D}}$ are rather large. In this case, the maximum C_{a} of vAV2 is the required longitudinal deceleration $D_{\mathrm{req,D}}$ at time step 14.6 s when considering the equation (3.23), and its value is 6.21 m/s^2 in the studied scenario. That required deceleration would be rather critical if the suggested value of 3.35 m/s^2 from Archer[203] is taken as the reference value. The American Association of State Highway and Transportation Officials[204] suggests a threshold of a little higher than 3.40 m/s^2 for most drivers. Guido et al.[205] utilized the recommended value by Archer as well to evaluate vehicle interactions with high risks. In other words, the designed behavior planner should take the acceleration of the detected objects into account to make less aggressive decisions. A well designed motion prediction could also be helpful to take corresponding actions earlier.

From this scenario, it can be concluded that a critical situation can be discovered by the multiple vAV instances. Even if one or two vAV instances miss the opportunity to discover their defects due to the different states caused by the birth cycle parameter, the other instances still have chance to encounter the critical situations in which their actions are critical. Thus, the action space is enlarged by using three vAV instances. Additionally, every action is tested so that the test scope is large. In addition, the $a_{\mathrm{req,eva}}$ and the $D_{\mathrm{req,D}}$ are able to quantify the criticality of a scenario. However, only objects which are located in the same lane as the subject vehicle can be assessed when using solely $a_{\mathrm{req,eva}}$ and $D_{\mathrm{req,D}}$. Therefore, other scenarios are essential to demonstrate the criticality index completely.

Case 2: A scenario with a motion prediction error derived from the top-down method

The case 2 describes a scenario with a motion prediction error, and is derived from the top-down method based on the Table 5-2. In contrast to the case 1, another object exists in the left lane of the subject vehicle at a speed of 30 m/s. The initial velocity of the IiC and vAV instances are 25 m/s, which are higher than the velocity of the preceding object (20 m/s) but lower than the speed of the adjacent object. Hence, vAV instances are motivated to change the lane if the adjacent object is not predicted correctly. Meanwhile, the adjacent object is

[203] Archer, J.: Methods for the assessment and prediction of traffic safety at urban intersections (2004).

[204] Bars, C.-R. C.: American Association of State Highway and Transportation Officials (2000).

[205] Guido, G. et al.: Comparing safety performance measures obtained from video capture data (2011).

approaching the vAV instances. The scenarios is illustrated in Figure 5-8. Since, a motion prediction error is simulated, the vAV instances make lane changing decisions. After certain time steps, the adjacent object is predicted well again. Thus, the vAV instances would stop the lane changing maneuver and steer back to the previous lane. Whether the proposed criticality index C_a is also appropriate for assessing the criticality in the lateral direction can be proved by this scenario.

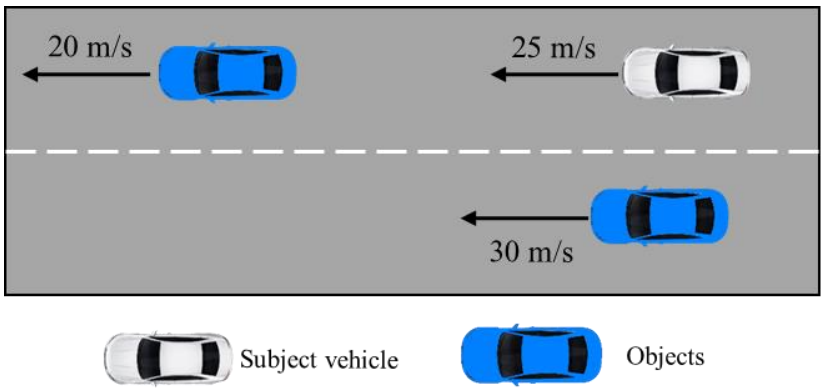

Figure 5-8: A scenario derived from the top-down method to show the performance of the triggers.

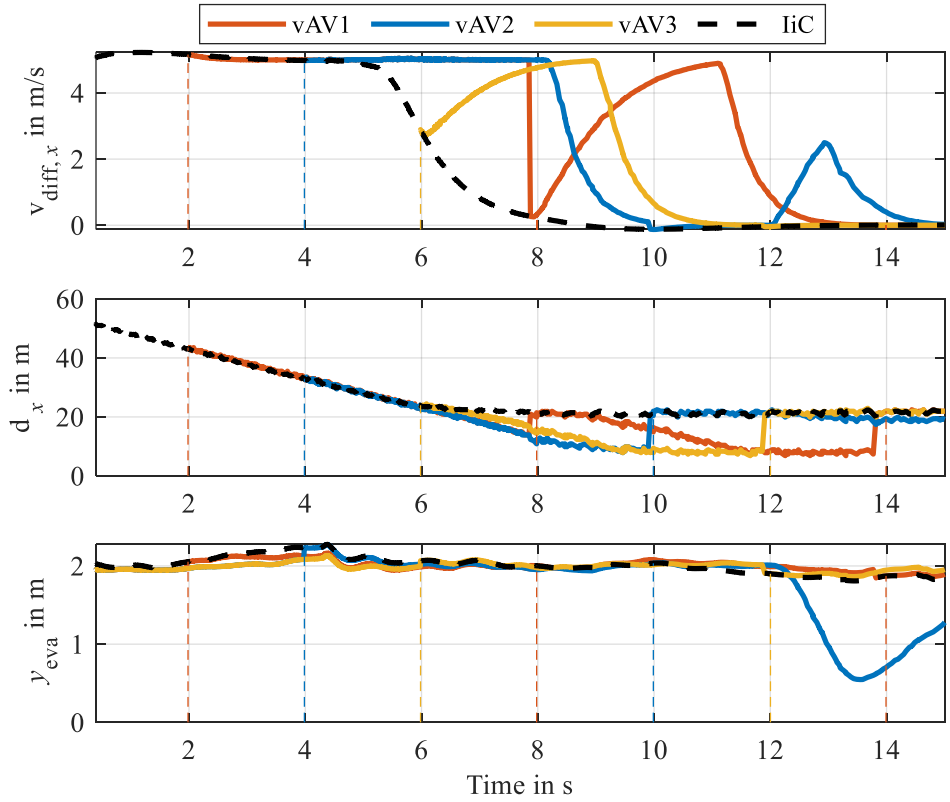

Figure 5-9: The change in the three important variables in case 2. The reset time steps are represented by vertical dotted lines with the corresponding colors of the vAV instances.

In this scenario, the important variables relative to the preceding object are shown in Figure 5-9. At the beginning, higher velocity of vAV instances than the preceding object can be found. vAV3 and vAV1 are reset at 6 s and 8 s, respectively. Afterwards, they accelerate until

they enter the adaptive cruise mode and then decelerate. The longitudinal clearance d_x decreases due to the positive $v_{\mathrm{diff},x}$, and stays almost at a constant value at the end. Obviously, a large variation of y_{eva} of vAV2 is shown. It indicates that vAV2 changes the lane, and then interrupts the lane changing since y_{eva} decreases and increases again. As a result, the $a_{\mathrm{req,eva}}$ and $D_{\mathrm{req,D}}$ regarding the preceding object are obtained, as illustrated in Figure 5-10.

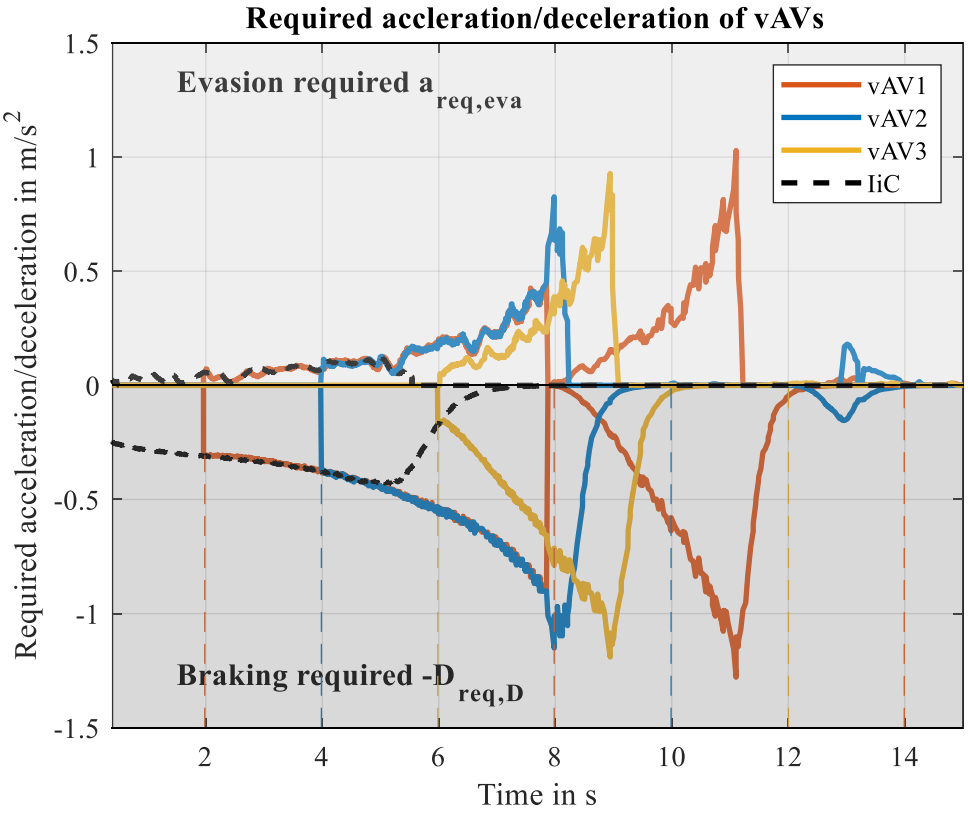

Figure 5-10: The required longitudinal decelerations below the zero line and the required lateral acceleration for evasion above the zero line of three vAV instances in a scenario with a motion prediction error.

As is obvious in Figure 5-10. both the $a_{\mathrm{req,eva}}$ and the $D_{\mathrm{req,D}}$ are quite low. Even though they increase for a while before their respective resets, their maximum values are still lower than 1.5 m/s^2. This is because the vAV instances always know the preceding object, and can thus make decisions in time. As a result, this critical scenario cannot be identified when overserving only the $a_{\mathrm{req,eva}}$ and the $D_{\mathrm{req,D}}$. However, the vAV instances could collide with the adjacent object if the time to change the lane is approximately identical to the time that the adjacent object catches the vAV instances. This condition is quantified by equation (3.21). Consequently, the vAV instances have to steer back to the previous lane to avoid collision with the adjacent object. Meanwhile, they have to brake simultaneously due to the preceding slow object.

With respect to the variables $v_{\mathrm{diff},y}$, d_y and $t_{\mathrm{tc},y}$, they are essential for the calculation of $a_{\mathrm{req,ste}}$. How these variables are changed in this case are described in appendix A.4. Based on these variables, the $a_{\mathrm{req,ste}}$ is obtained in this scenario.

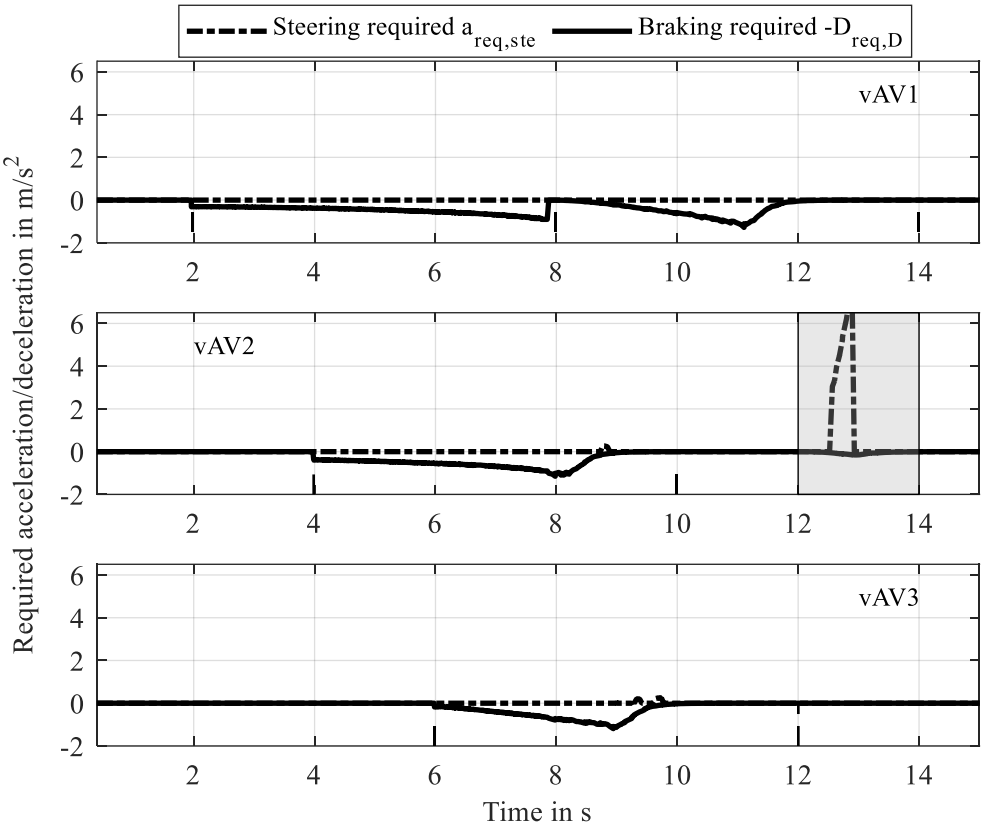

Figure 5-11: The required decelerations below the zero line, the required acceleration for steering above the zero line of vAV instances in the scenario with a motion prediction error.

The required lateral accelerations for steering $a_{\mathrm{req,ste}}$ of vAV instances are shown in Figure 5-11. As is obvious in this figure, the $a_{\mathrm{req,ste}}$ values of the vAV1 and vAV3 are low in this period, since the time difference Δt is so large that they will not collide with the adjacent object. The $D_{\mathrm{req,D}}$ of all vAV instances are low, which has been discussed in Figure 5-10. Nevertheless, the maximum $a_{\mathrm{req,ste}}$ of vAV2 is relative large, which means that it will collide with the adjacent object if it keeps changing the lane. Therefore, the $a_{\mathrm{req,ste}}$ and the $D_{\mathrm{req,D}}$ should be added in vector in the gray area according to the equation (3.23). The vAV2 should brake and steer to the previous lane simultaneously in order to avoid falling into a critical situation. In this case, the maximum criticality of the vAV2 is thus 6.28 m/s^2, which already exceeds the accepted acceleration.

The scenario indicates that the proposed criticality index C_{a} can be utilized to assess the safety of AVs in the lateral direction as well. Combining with results from case 1, the C_{a} is capable of evaluating the safety both in the longitudinal and lateral direction. Thus, it is quite suitable to apply it as a trigger for the VAAFO approach. Additionally, both cases demonstrate that the coverage of critical scenarios is enlarged by multiple vAV instances.

Case 3: A crash scenario during the operation of a driving automation system in the real world

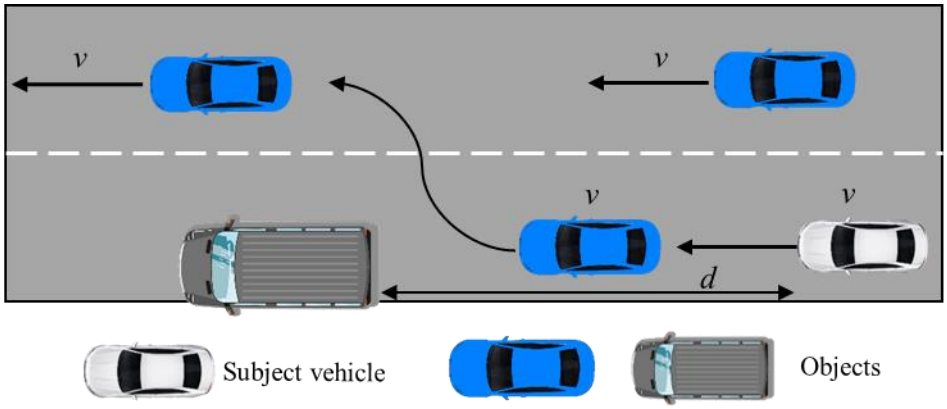

Figure 5-12: A study case of a real traffic accident to demonstrate the performance of the VAAFO approach.

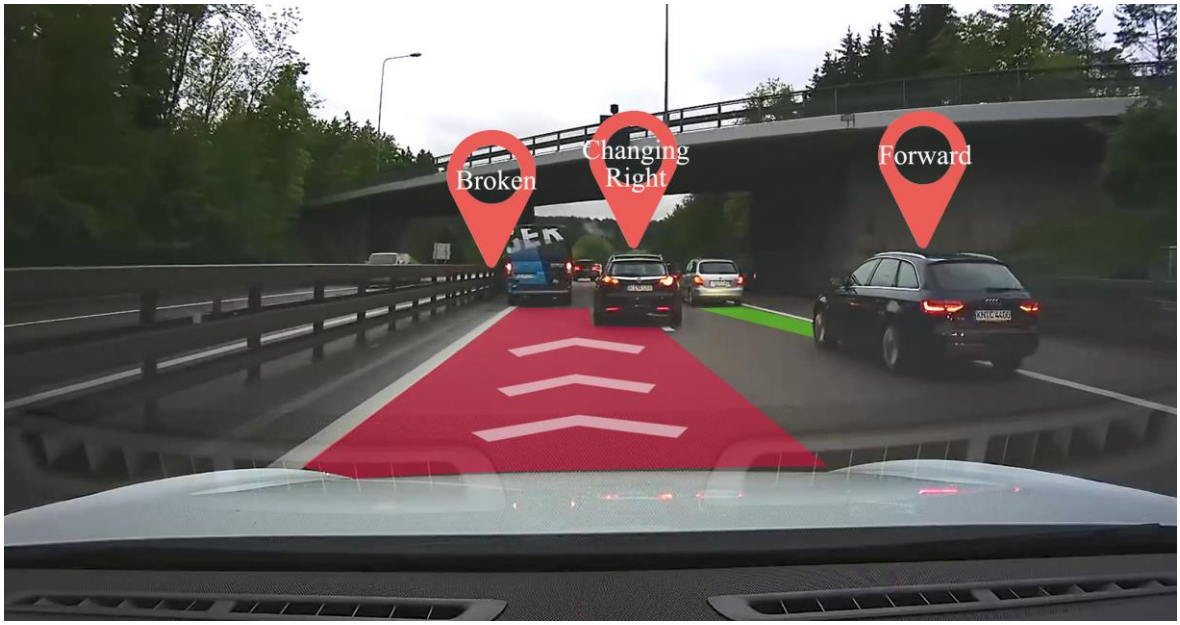

Figure 5-13: A snapshot of the critical scenario results from a level 2 AV. Own illustration according to the video from Thomann[206].

As mentioned in the Table 5-2, crash scenarios during the operation of a driving automation system in the real world are also an important source to generate test scenarios. If an AV is updated, it is worth to test it again in the scenarios in which the previous version has an unsafe behavior. Compared to the case 1 and case 2, the case 3 describes a real traffic accident caused by a level 2 AV. This real traffic accident is the well-known accident from a Tesla Model S on autopilot, which collides with a broken down van. Figure 5-12 describes this accident in detail. The broken down van (an obstacle) is still. Consequently, the preceding object of the subject vehicle cuts into the adjacent lane. As a result, a little space is left for the subject vehicle to react. Since the data of this accident is not free available, several

[206] Thomann, C.: Tesla Model S adaptive cruise control crashes into Van (2016).

key parameters have to be assumed. It is assumed that the moving objects and the subject vehicle have the same speed v. The distance between the subject vehicle and the van is d when the preceding object finishes cutting out. By defining the v as 20 m/s and d as 30 m, the scenario is concreted and can be simulated in CarMaker. Figure 5-13 shows an actual scene of the critical scenario, in which the preceding vehicle is changing the lane.

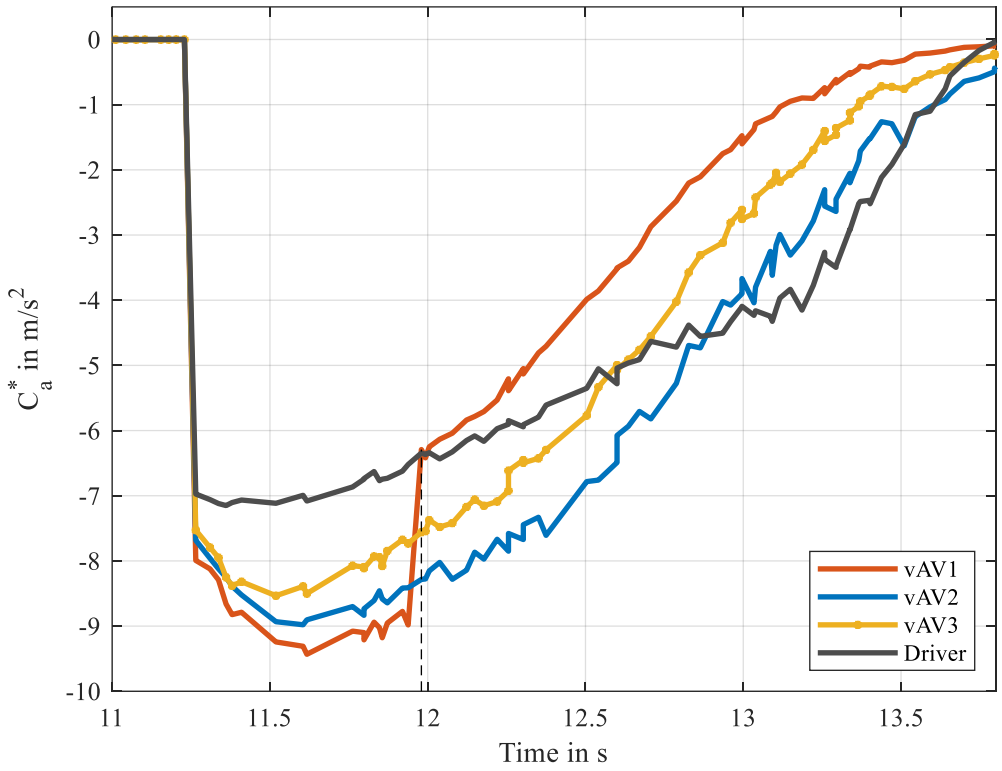

Figure 5-14: The calculated criticality indexes of the three vAV instances in the simulation case 3.

Since the working principle of the proposed criticality index C_a has been demonstrated in case 1 and case 2, only the final calculated criticality index C_a is shown, and the intermediate calculation process of C_a is ignored in case 3. Moreover, C_a^* is used instead of C_a, so that the optimal maneuver could be recognized by its sign. The results are illustrated in Figure 5-14. Initially, the C_a^* values of the three vAV instances are zero, since their velocities are identical to the velocity of the preceding object. When the preceding object leaves the current lane, large negative C_a^* values are found in all vAV instances. The deceleration maneuver is more favorably than the evasion maneuver in this scenario as the lane changing maneuver is impossible due to the occupation of the adjacent lane. Due to the relative high speed and short distance, the large required deceleration the vAV instances as well as the IiC are shown. The vAV1 is reset at 12 s so that it has the same value of C_a^* as the IiC (black line) at that time step. Afterwards, it has a smaller C_a than that of the IiC, since it brakes stronger. The maximum C_a of the vAV1 has achieved 9.3 m/s^2, which indicates that the situation is rather critical. Therefore, if such situation occurs, it can be discovered by the VAAFO approach. In this

case, specific parameters are assigned to the objects. Nevertheless, the parameters can be changed easily to generate more similar test scenarios.

5.3 Summary

In this chapter, two different simulation platforms are presented and introduced. Ideal sensor models from CarMaker are selected, and the corresponding fusion strategy of sensors is described and implemented. The necessary interfaces between the two different platforms are defined. The tracked objects are then transmitted into ROS and fused. As a result, a co-simulation platform is established. In the developed co-simulation platform, it is possible to demonstrate and verify the VAAFO approach preliminarily. A rule-based behavior planner and a MPC-based trajectory planner are developed to establish a driving automation system for the vAV instances. The necessary technical steps and the implemented algorithms are presented. Since it is impossible to simulate traffic flow due to the limitation of the simulation platform, several representative scenarios are chosen. They are derived from the top-down method, a real traffic accident of human drivers and a real traffic accident of a level 2 AV, respectively. Based on the results from the three studied cases, the performance of the trigger is demonstrated. The characteristic of the VAAFO approach is illustrated. It can be inferred that the coverage of critical scenarios are enlarged by multiple vAV instances. The defined criticality index can be utilized in both the longitudinal and the lateral direction of AVs. Since the generated scenarios are limited and artificial, more tests should be performed to further prove the performance of the VAAFO approach. The implementation of the VAAFO approach in a real test vehicle is introduced in the next chapter. Finally, the actual performance of the VAAFO concept in reality is addressed.

6 Verification in Reality

Since limited scenarios are generated in the simulation, a general conclusion about the performance of the VAAFO approach would be difficult to draw. Additionally, the proposed approach is not aimed to be applied in the simulation rather in reality, since one of the motivations is that AVs can be tested under real conditions silently. Therefore, the final application of the VAAFO approach must be in a real vehicle. Moreover, the results from the reality would be more instructive and conclusive. As a result, it is essential to implement the proposed approach in a real vehicle and test it on public roads. Due to the real traffic flow on public roads, the performance can be further revealed. The test vehicle and the sensors are first introduced. The sensor fusion strategy is presented briefly. In order to evaluate the triggers, one another criticality metric is calculated and compared with the defined criticality index. The uncertainties in the perceived environment are reduced, so that the errors in the environmental representation can be determined. Afterwards, the coverage degree of the approach is analyzed according to the discovered errors. The limitations of the application of the approach is also discussed. Finally, the application scope of the VAAFO approach can be derived.

6.1 Test Components Design

6.1.1 Test Platform

The test platform of the VAAFO approach is a S450 Mercedes-Benz that comes from the Automated Driving Darmstadt for Students (aDDa) project[207]. The sensor setup is shown in Figure 6-1:

- A continental ARS 408 long-range radar is in the front of the vehicle with a range of approximately 200m.
- A Velodyne 32-layers lidar is on the roof of the vehicle with a rotation frequency of 10 Hz.
- An automotive dynamic motion analyzer (ADMA) from GeneSys with real-time kinematic (RTK) is installed in the trunk of the vehicle and enables localization with centimeter accuracy. Meanwhile, velocity, acceleration, yaw angle, etc. can also be obtained by this equipment.
- A stereo camera and a mono camera from IDS are located under the windshield.

[207] aDDa: Automated Driving Darmstadt for Students (2021).

There are in total of two PCs in the trunk. One PC with dual CPU and GTX 1080Ti GPU is responsible for the perception. The planning runs on the other PC with a configuration of dual CPU. Since the planner needs a surrounding environment to make reasonable decisions, the lidar, which provides a 360 field of view, is essential. However, the objects that can be tracked by the lidar is limited by the available point clouds. Less point clouds exist at higher range. Thus, the actual effective detection range from lidar is narrowed. Furthermore, the accuracy of the velocity estimated by the lidar tracking has a low confidence, while the radial velocity can be measured directly by the radar using Doppler-Effect. However, the angular resolution of the radar is typically very low. Thus, the lidar and radar are fused in order to provide a satisfying result. The fusion of radar and lidar has been studied by many researchers[208,209]. Due to their respective advantages, this combination of sensors has generated some interest. As the development of an ADS is not the focus, localization is directly realized by the ADMA-RTK. The images from the cameras are taken as references in the post-processing phase.

Figure 6-1: Illustration of the sensor set-up and the test vehicle.

6.1.2 Map Creation

The map as a very important part for AD is essential for trajectory planning. A coarse map such as OpenStreetMap (OSM)[210] represents the roads as an imaginary center line. Some attributes are added to the center line in order to include more information about the roads,

[208] Göhring, D. et al.: Radar/lidar sensor fusion for car-following on highways (2011).

[209] Hajri, H.; Rahal, M.-C.: Lidar and radar high-level fusion for obstacle detection and tracking (2018).

[210] Haklay, M.; Weber, P.: Openstreetmap: User-generated street maps (2008).

e.g. the width of the road. This kind of description of a road is appropriate for navigation. But for localization, it is far below the required accuracy. In addition, the position of each lane of a road is implicitly defined, which could be very inaccurate. The inaccurate lane information poses a great challenge for the local trajectory planning. Furthermore, the complexity of OSM increases in an intersection since no clear center line is available. The OpenDRIVE describes a road in similar schema and is mainly for simulation. Consequently, Poggenhans et al.[211] propose the Lanelet2 framework to describe High Definition (HD) maps. The HD map defines different traffic elements explicitly, including the road topology network, the lanes and the traffic signs. By using a HD map, the localization of an AV with high precision can be addressed regardless of the GPS signal. Additionally, certain objects that are beyond the range of on-board sensors can be obtained, e.g., the position of a traffic light around a corner is known beforehand. Moreover, some traffic regulations can be obtained from the HD map, e.g., it is clear on a HD map which lane is only reserved for a turn and which lane is only drivable for specific traffic participants. Therefore, a HD map provides a lot of useful information for AVs. The Lanelet2 format is intended for designing AD functions especially for planning. For instance, Poggenhans et al.[212] utilize an example of global planning to demonstrate the Lanelet2 map framework. Another example using the Lanelet2 for planning comes from Narula et al.[213]

The creation of a HD map can be generally divided into three steps.[214] The first step is data acquisition. By using various sensors such as RTK-GNSS, an inertial measurement unit (IMU), cameras and lidars, the environment can be captured. The second step is data processing. The collected data is processed to extract the HD map features, including but not limited to traffic signs, road topology. The third step is the database management, which handles with the map management and access. With respect to the HD map, a motorway section is selected to demonstrate of the VAAFO approach. In order to create the map of the section, the important features of the motorway are first studied, e.g. the lane markings. Typically, the lane markings are highly retro-reflective paintings, which are clearly visible from the point clouds. This special characteristics can then be applied to identify and extract lane markings[215,216]. The second way to extract lane markings is image processing algorithms. If a camera and a lidar are extrinsically calibrated, it is even possible to use both sensors to obtain the position of lane markings. In this dissertation, the lane marking is extracted by a camera system and an ADMA-RTK. As aforementioned, the ADMA-RTK can achieve centimeter-level accuracy, i.e., the position of the test vehicle can be obtained accurately. From

[211] Poggenhans, F. et al.: Lanelet2: A high-definition map framework for the automated driving (2018).

[212] Poggenhans, F.; Janosovits, J.: Pathfinding and Routing in the Lanelet2 Map Framework (2020).

[213] Narula, K. et al.: Two-Level Hierarchical Planning in a Known Semi-Structured Environment (2020).

[214] Jo, K. et al.: Simultaneous localization and map change update for the high definition map (2018).

[215] Jaakkola, A. et al.: Retrieval algorithms for road surface modelling using laser-based mapping (2008).

[216] Kumar, P. et al.: Automated road markings extraction from mobile laser scanning data (2014).

the camera system, the left and right lateral distances from the lane markings to the center of the test vehicle can be acquired. As a result, the positions of the lane markings are known. Since the calculated positions of the lane markings are discrete, and there are even some outliners or missing points, it is essential to further process the data points of the lane markings.

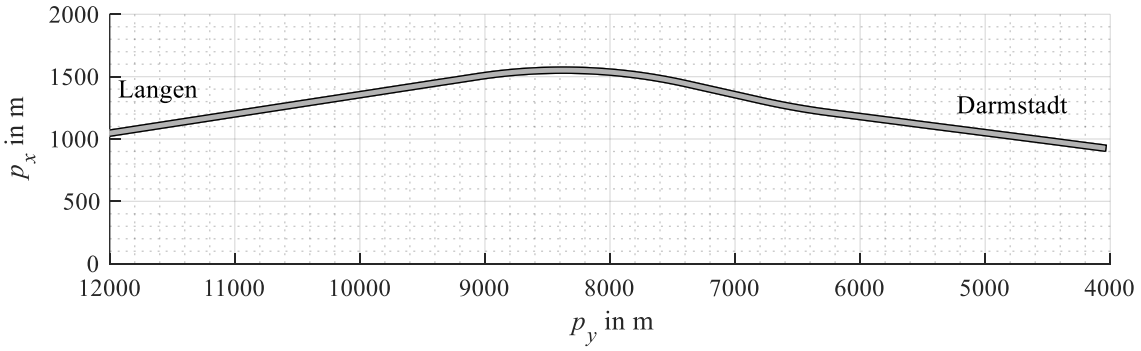

Figure 6-2: A section of a motorway from Darmstadt to Langen to test the approach both in simulation and in reality.

Instead of the commonly used clothoid model to model a road, the B-spline curve is applied. The B-spline curve has the advantages of changing the position of a control point without globally affecting the shape of the entire curve.[217] Loose and Franke[218] show that the B-spline curve outperforms the clothoid model on rural roads and in construction sites. By applying the B-spline, the lane markings can be thus obtained. With respect to the selection of the motorway section, the motorway A5 from Darmstadt to Langen is chosen. The motorway section is about 10 km long and has four lanes in each direction. The shape of this section is shown in Figure 6-2. The coordinate origin of the map is in the proving ground of Technical University of Darmstadt (TUDa). This section is a very busy way to Frankfurt. Moreover, different kinds of traffic objects e.g., trucks, motorcycles, and cars with a quite varied velocity from 80-200 km/h are available on this section. Since there is no intersection on this motorway section, and the road network is rather simple, the Lanelet2 format is not very necessary. A simple data format is developed, and a corresponding parser is implemented to load the map into ROS for the trajectory planning.

[217] Xu, H. et al.: A fast and stable lane detection method based on B-spline curve (2009).

[218] Loose, H.; Franke, U.: B-spline-based road model for 3d lane recognition (2010).

6.2 Sensor Fusion

The sensor-up has been presented in subchapter 6.1.1. The radar and lidar are selected as the perception sensors for the vAV instances. Generally, the sensor fusion strategy can be divided into three categories[219,220]:

- Low-level fusion; little processed sensor data is fused together. Thus, less information is lost. Nevertheless, the accuracy of the extrinsic calibration affects the fused results a lot. The sensors should also be highly synchronized to ensure a successful association.
- Middle-level fusion; the features in the sensor data are extracted and then fused. Therefore, the features are sensor specific. As a result, a general architecture is difficult to achieve if the number and the types of sensors increase.
- High-level fusion; Objects are tracked by each sensor independently and fused afterwards. However, the fusion can be a tough problem since different sensors have different capabilities and reliability. Due to its modularity and encapsulation of sensor data, various applications can be found.

Since the capabilities of radar and lidar can be distinguished easily, the high-level fusion is chosen. In addition, the radar is encapsulated in the test vehicle, and there is no access to the unprocessed data. Instead, its tracking results are provided directly, which include object class, object ID, relative distance, relative speed and relative acceleration. Therefore, the development of a tracking algorithm for the lidar becomes the focus for the high-level sensor fusion.

6.2.1 Lidar Tracking

Typically, the multi-object tracking process can be described by "tracking by detection" as illustrated in Figure 6-3. In the detection part, the ground is removed by segmentation of the point clouds. The point clouds, which belong possibly to a same object, are clustered. Subsequently, the pose of a segmented object is estimated either by model-based[221] or feature-based methods[222]. In addition to the analytical solution, the machine-learning based methods are studied recently. For instance, PointPillars[223] is a very popular method for lidar detection. The results show that it outperforms the state of the art significantly. Additionally, the class of an object can also be obtained. The detection process provides the estimated pose of an

[219] Aeberhard, M.; Kaempchen, N.: High-level sensor data fusion architecture for vehicle perception (2011).

[220] Banerjee, K. et al.: Online Camera LiDAR Fusion and Object Detection on Hybrid Data (2018).

[221] Morris, D. D. et al.: A view-dependent adaptive matched filter for ladar-based vehicle tracking (2017).

[222] Mertz, C. et al.: Moving object detection with laser scanners (2013).

[223] Lang, A. H. et al.: Pointpillars: Fast encoders for object detection from point clouds (2019).

object only for one time step. In order to track the objects continuously and estimate other variables such as velocity, a Kalman filter (KF) is usually applied in the tracking process. First, the state of an object is predicted based on a dynamic model, which could be constant velocity (CV), constant acceleration (CA), constant turn rate and velocity (CTRV) or constant turn rate and acceleration (CTRA). Based on sensor data, the predicted state of the object is then updated if the predicted results and measured results are associated successfully. As a result, the objects are tracked, and the next cycle begins. Schubert et al.[224] find that the dynamic model affects the tracking performance significantly. More sophisticated models provide better results than a simple one. However, this is not always true in different cases. Therefore, the interacting multiple model (IMM)[225] is motivated, which weights the estimated states of the filters considering a set of dynamic models. In the case of a non-linear dynamic model, the extended Kalman filter (EKF) and unscented Kalman filter (UKF) are utilized.

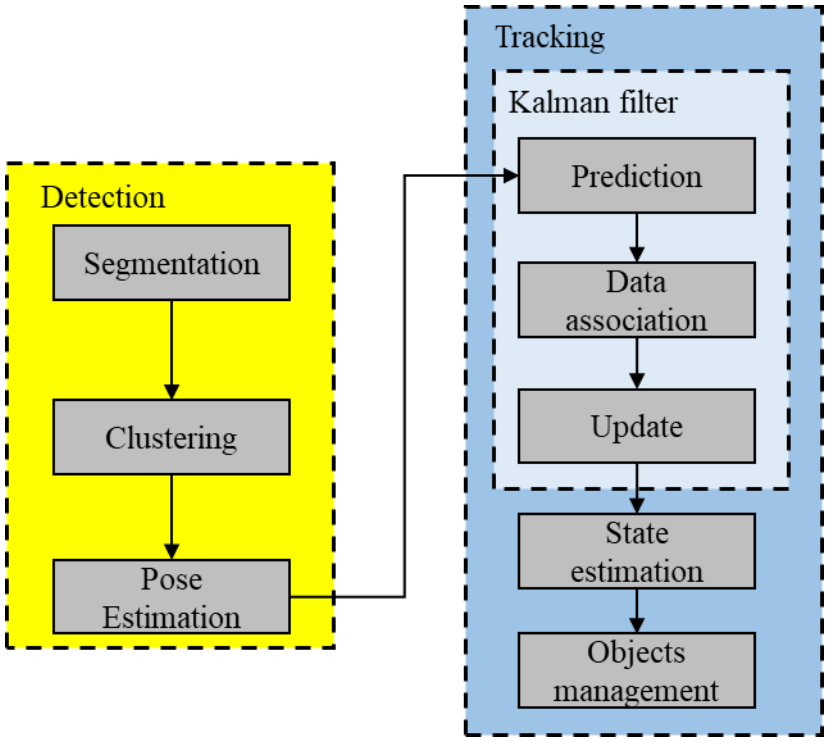

Figure 6-3: The tracking process of a lidar.

In this dissertation, the PointPillars method and an analytical solution from Rachman[226] are combined. Even though the Pointpillars provide better detection results than the analytical solution, the model in PointPillars is trained solely using the front cameras of the test vehicle. Thus, an analytical solution is applied to detect backward objects. Subsequently, a UKF with

[224] Schubert, R. et al.: Comparison and evaluation of advanced motion models for vehicle tracking (2008).

[225] Mazor, E. et al.: Interacting multiple model methods in target tracking: a survey (1998).

[226] Rachman, A.: 3D-LIDAR multi object tracking for autonomous driving (2017).

IMM is utilized for the tracking. Regarding the tracking algorithm, the code from Autoware[227] is taken as the basis. As a result, the obtained state of a tracked object is described as

$$x = ({}_{S}p_x,\ {}_{S}p_y,\ {}_{S}v_x,\ {}_{S}v_y, \psi, l, w) \tag{6.1}$$

${}_{S}p_x$ and ${}_{S}p_y$ represent the position, which is obtained by updating the predicted position using the Kalmann gain. The measured position is the average of the coordinates of clustered point clouds. This method to acquire the measured position of an object could bring some uncertainties if the distribution of the clustered point clouds changes, e.g. during a turning. However, the uncertainties are small when the motorway scenario is the focus, since occlusion and turning occurs more often in urban scenarios. ${}_{S}v_x$ and ${}_{S}v_y$ denote velocity, ψ is the yaw angle of an object, l and w are the length and width of an object, respectively.

6.2.2 Radar and Lidar Fusion

As aforementioned, the high-level fusion strategy is chosen to fuse the radar and the lidar. The extrinsic calibration between them is an essential step to realize the spatial alignment. The temporal alignment assures that the states of an object tracked by two sensors, whose time steps are approximately the same, are fused. These two kinds of alignments are easier to handle than the low-level fusion due to the already filtered kinematic information of an object. Since the implemented radar and lidar have different FoVs, objects that are tracked only by the lidar, e.g. the objects behind the subject vehicle, are handed over directly to the global object management. Similarly, objects tracked only by the radar are also directly given to the global object management. Only the objects in the overlapping FoV of lidar and radar are fused. Since the state of a tracked object by the radar is different from the state of a tracked object by the lidar, only the common state variables are fused. With respect to the fusion, the Bayesian approach[228] is applied, which takes data uncertainties into account. The detailed process of the fusion can be found in appendix A.5. In the object management, each tracked object is assigned with a unique identification number, so that the objects can be identified uniquely throughout their life when they go through the FoVs of different sensors.

6.2.3 SuT Architecture

In subchapter 5.1, the behavior planner and the trajectory planner are introduced. The tracking algorithm and the sensor fusion strategy are presented in this chapter. For the localization, the ADMA-RTK equipment is used. As a result, the entire architecture of the SuT is illustrated in Figure 6-4. In particular, the information from the created map is utilized to

[227] Kato, S. et al.: Autoware on board: Enabling autonomous vehicles with embedded systems (2018).

[228] Abdulhafiz, W. A.; Khamis, A.: Bayesian approach to multisensor data fusion (2013).

increase the tracking performance. The tracking and localization results are given to the behavior planner. The decision with minimum cost are then handed over to the MPC trajectory planner. Based on the VAAFO approach, there are in total of three planners. However, they use the same tracking results and the same map. By using the established SuT, the test of the VAAFO approach in reality can be carried out.

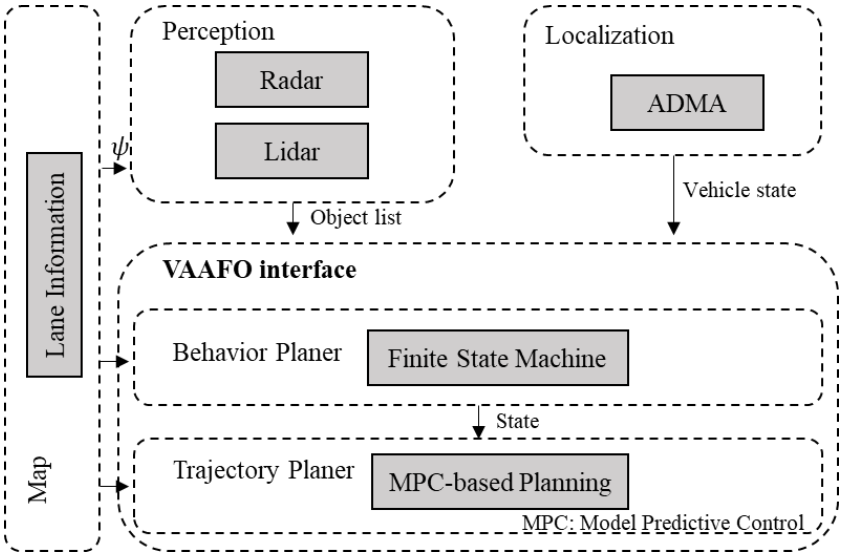

Figure 6-4: The architecture of the SuT.

6.3 Implementation

During the execution of the experiment, several human-machine interfaces are developed in order to observe the system status. In addition to the camera images as shown in Figure 6-5, the trajectories of the IiC and the vAV instances are also observed during the driving, as illustrated in Figure 6-6. The red box denotes the IiC, while the three yellow boxes represent the three vAV instances. The tracked objects are illustrated by blue boxes. The blue lines are the lane markings of the motorways, which is the created map as described in 6.1.2. The planned trajectories of the vAVs are described by green lines. During the verification of the VAAFO approach in the real world, a human driver is the IiC. Additionally, the calculated criticality index C_a of the IiC and vAVs are examined to decide whether the scenario should be saved. Subsequently, the identified scenarios are converted to the OpenSCENARIO format. Due to the great benefits of the VAAFO approach, the developed but unrefined ADS can be directly tested on public roads. Even if there are three planners required by the VAAFO approach, the approach runs fluently on the available hardware as the perception is not duplicated.

Since the primary goal is to evaluate the proposed approach and optimize the defined threshold of the proposed criticality index if necessary, the developed ring buffer is deactivated in order to record the necessary data online all the time, including the object list, trajectory of each vAV instance, etc. The recorded data lasts for several minutes with an average driving speed of 100 km/h on the motorway. Importantly, the ring buffer is not deactivated during a

normal operation of the VAAFO approach. With respect to the validation of the functionality of the ring buffer, it can be done in the post-processing phase with the recorded data. After the test drive, the data is available and analyzed in the following subchapters.

Figure 6-5: The camera images from a wide angle camera (left) and a stereo camera (right).

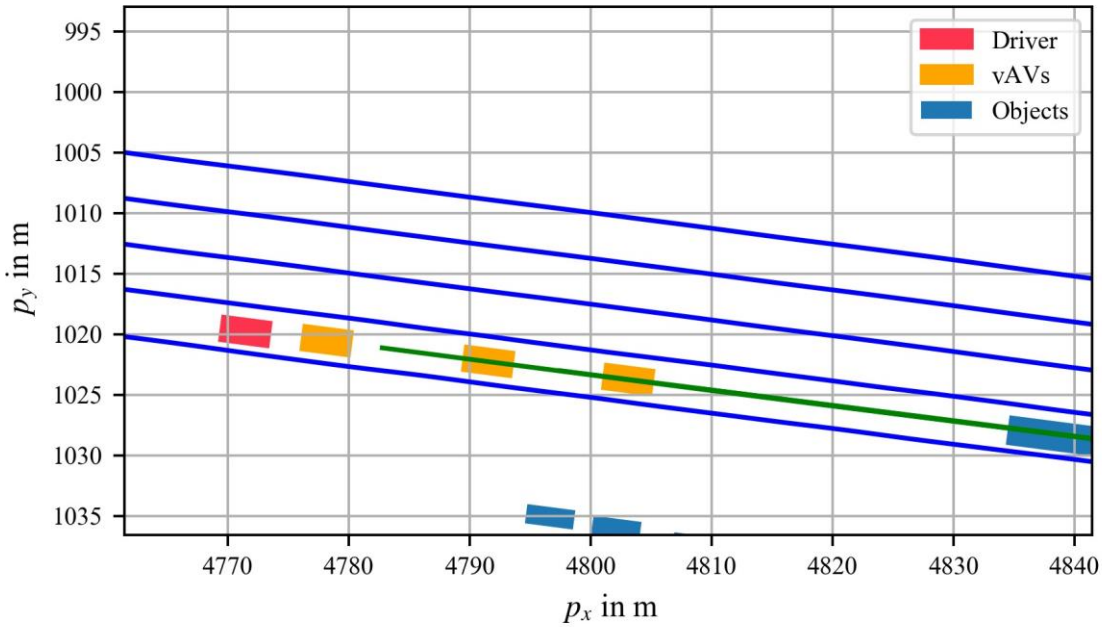

Figure 6-6: The observation of the trajectories of the IiC and vAV instances during the driving.

6.3.1 Triggers Demonstration

In the subchapter 3.3, four triggers in equation (3.13) - (3.16) are defined. It is necessary to show how these triggers change during the running of the VAAFO approach in reality. A scenario with a truck, whose state is estimated falsely, is taken as an example to show the four triggers. The Figure 6-7 illustrates an example during the driving. As is obvious in the figure, an incorrect state is estimated for the preceding truck. The state with a wrong orientation is then given to the decision module. Since the Frenet coordinate system is applied to describe the position of each object, it is easy to determine in which lane an object locates. As a result, the behavior planer considers the truck as a static object in the same lane as the

vAV instances, since there is no velocity in the driving direction even if the absolute estimated velocity is correct. Hence, the vAV instances have to decelerate or evade. During the observed period, the truck has a wrong estimated orientation for three times. In the remaining time, the truck is always tracked correctly as shown in Figure 6-8.

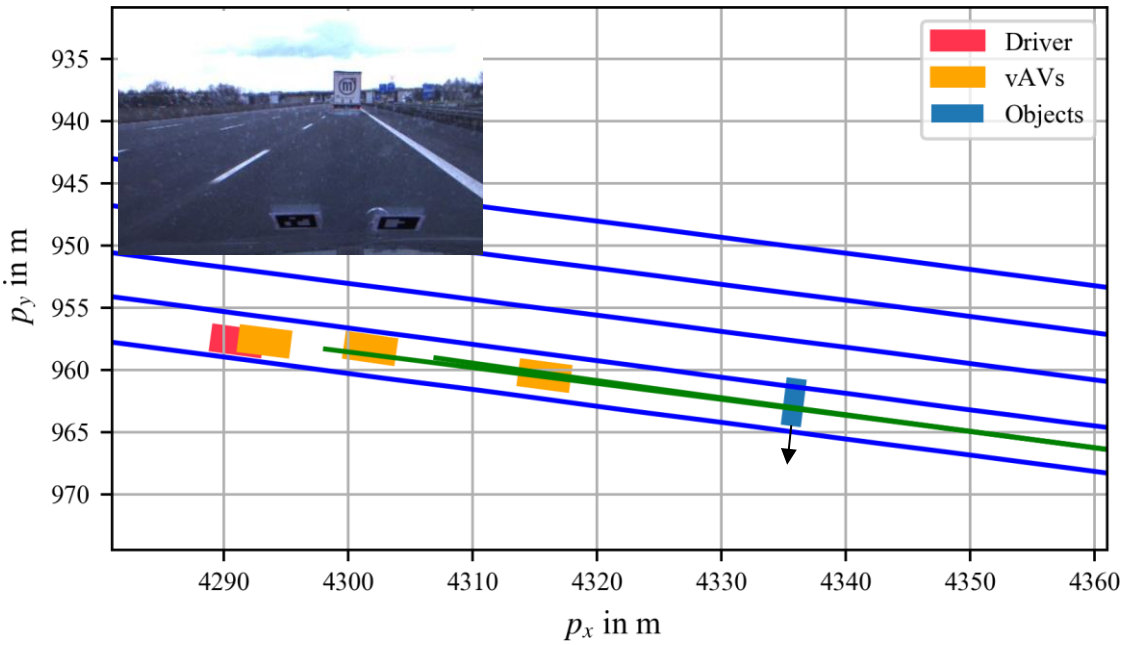

Figure 6-7: An example of an incorrect estimated dimension and orientation of the preceding truck.

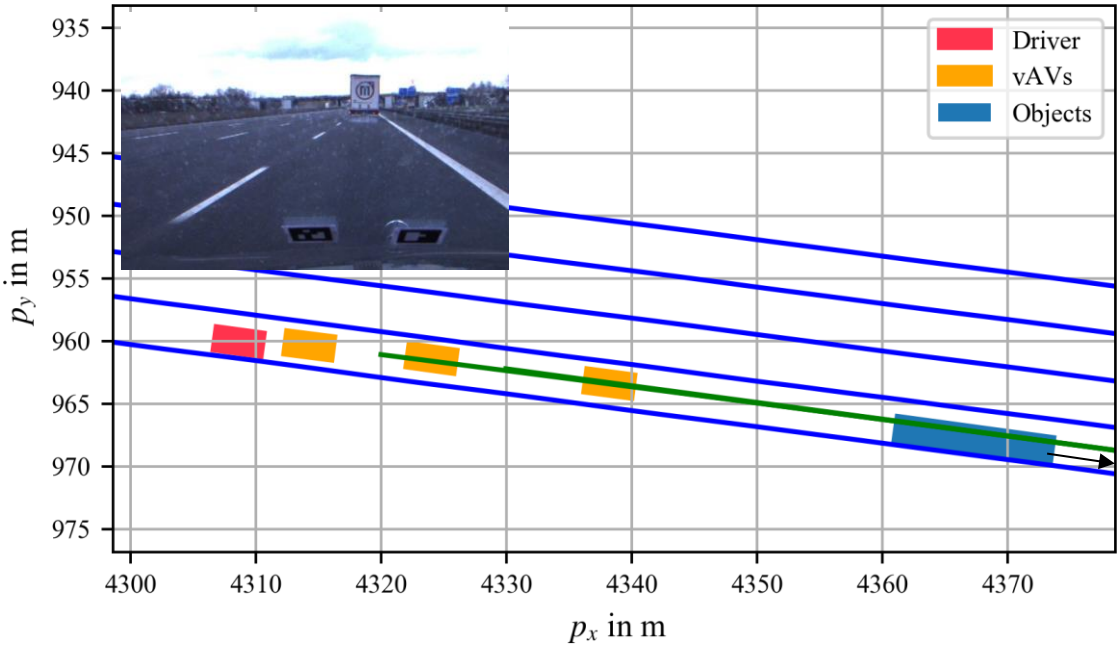

Figure 6-8: An example of a correct estimation of the state of the preceding truck.

Since the working principle of the criticality index C_a has been introduced elaborately in chapter 5, only the final calculated results of C_a are presented. Figure 6-9 shows the changing of the triggers in equation (3.15) and (3.16) during the observed period. By observing

the tracking results, there are in total of three times that the truck has an incorrect estimated orientation in this period. Correspondingly, three jumps of C_a are shown in Figure 6-9. In the observed period, the evasion maneuver is preferred to braking. In particular, each jump is reflected by different vAV instances, i.e., the perception errors can be discovered by different vAV instances. Even if one or two vAV instances miss the opportunity to find errors due to the different states result from the birth cycle parameter, the errors could still be found by other instances. Thus, the coverage of critical situations is enlarged by using three instances.

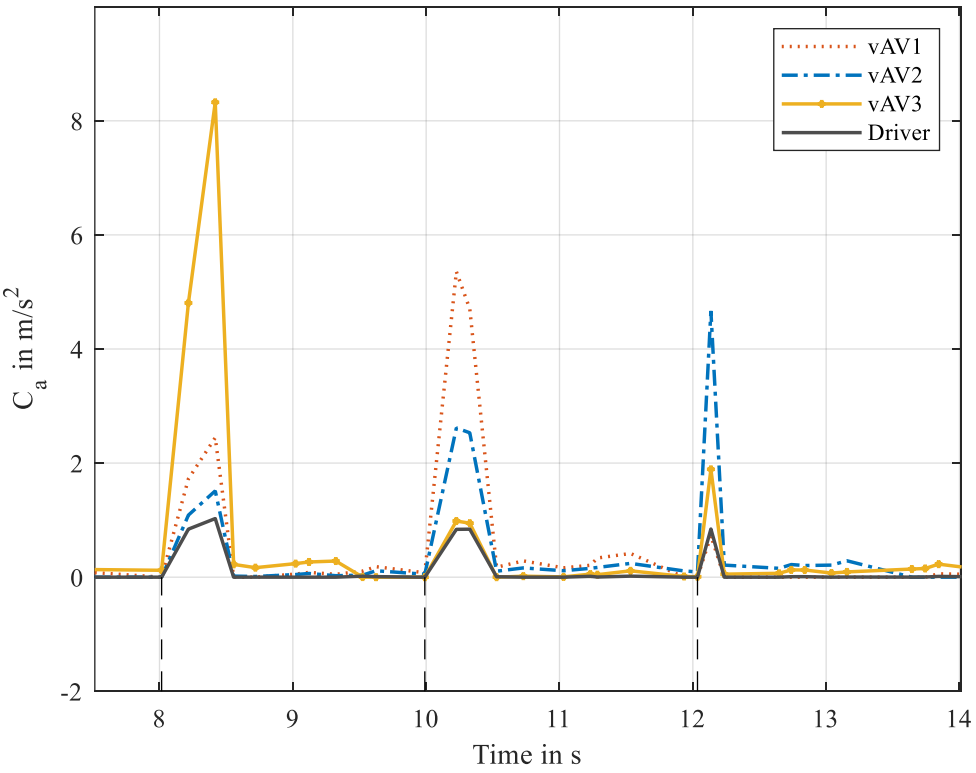

Figure 6-9: The criticality indexes of the three vAV instances during the observed period.

With respect to the triggers in equation (3.13) and (3.14), the Figure 6-10 is utilized to show the change in the criticality index. As is obvious in this figure, large ΔC_a are exhibited at the time steps, which correspond with the time steps of the jumps of C_a. Nevertheless, it does not indicate that the C_a and the ΔC_a have the same performance in identifying the critical situations, and thus one of them is redundant. Conversely, they should work together since they have different strengths in different situations, e.g., the C_a would be low in the case of a FP object, especially if the FP object exists for several time steps, since the vAV instances could react to it and take corresponding actions. Thus, the trigger may not be activated by C_a but by the ΔC_a, since C_a changes sharply when the FP object disappears suddenly. Even for a same critical scenario, which both C_a and ΔC_a have detected, could be missed by one of them due to their predefined thresholds, i.e., the calculated C_a or ΔC_a does not exceed its

own threshold. The possibility to save critical scenarios that both C_a and ΔC_a are used corporately is increased, since different thresholds for C_a and ΔC_a can be defined. More discussion about their differences can be found in the subchapter 3.3.3.

Based on the above analysis, it can be found that the triggers could be activated approximately simultaneously in a scenario when overseeing the time period from 8 s – 13 s. Therefore, a special ring buffer is necessary in order to save the same critical scenario for only once, e.g., the activation of other triggers is ignored for a specified period if one trigger is already activated. The designed ring buffer in the subchapter 3.4 has met exactly this requirement. The triggers are ignored for 6 s if one trigger has been activated. The data in the ring buffer is saved when the time length of the data is fulfilled. From the analysis of the results, it can prove that the ring buffer is reasonable designed.

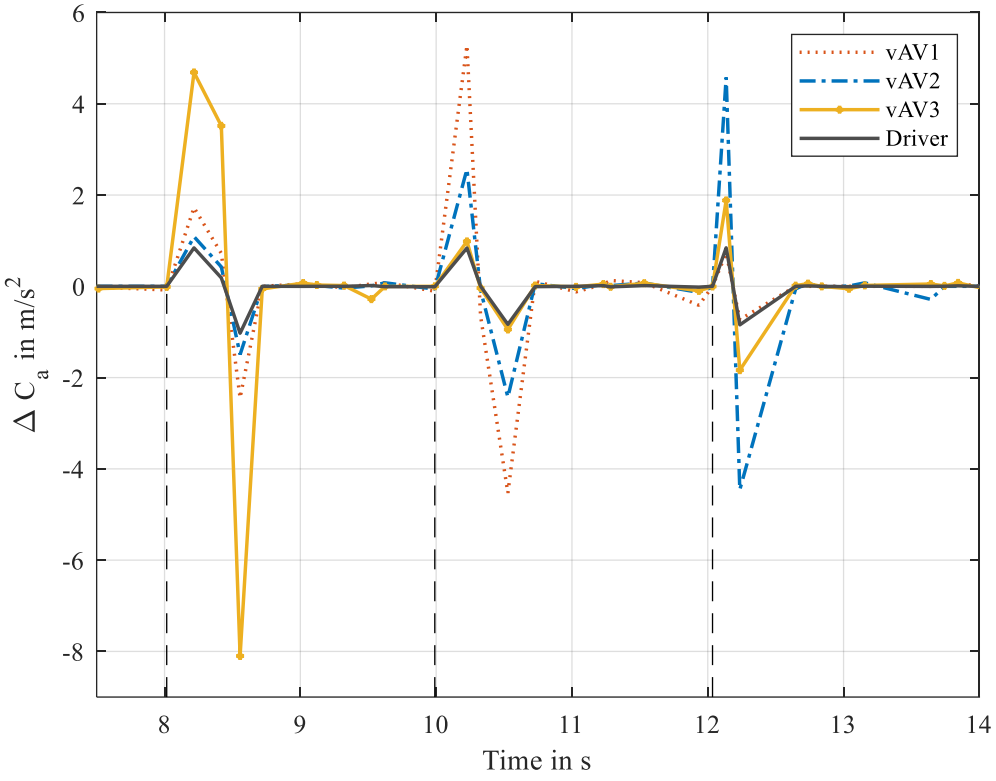

Figure 6-10: The changes in the criticality indexes of the three vAV instances.

6.4 Uncertainties Reduction

In the simulation, critical scenarios are established intentionally. However, it is unclear whether a scenario is actually critical or not when verifying of the approach in reality. In order to evaluate the performance of the triggers, the comparison with one another existing criticality metric would be helpful. Additionally, the uncertainties in the environmental representation should be eliminated, so that the sources of error can be distinguished, i.e.,

whether an error comes from the perception or from the planning could be determined. Consequently, the coverage degree of the VAAFO approach can be derived if the defined criticality index C_a is used. Notably, any other types of trigger, such as a machine-learning based trigger, can be applied in the VAAFO framework as well. For instance, an image with specific features can be identified by a trigger, which is trained beforehand and implemented in this framework afterwards. Therefore, the trigger could be replaced according to the demand, i.e., the trigger has great influences on the coverage of the VAAFO approach.

6.4.1 Labeling

To reduce of uncertainties in the environmental representation, the labeling method is selected. By labeling the point clouds, the ground truth can be obtained. The position, the orientation and the dimension of an object can be labeled manually at each time step, which is rather time consuming with 10 Hz from the lidar. Consequently, an interpolation is performed to accelerate the labeling. During the annotation, the Region of Interest (RoI) of several key frames have to be labeled manually. The cuboid RoIs between the previous labeled frames are estimated by interpolating the labeled RoI across the time interval. The interpolated frames can be corrected manually if necessary. In particular, the retrospective post-processing is used to obtain a more accurate dimension. The dimension of an object is determined when more point clouds of an object are available, since more point clouds are better to estimate the dimension. By applying this method to other objects through the entire recorded data, the position, orientation and dimension of all objects are obtained. However, the velocity cannot be acquired by the labeling, but is essential to calculate one another criticality metric such as TTC. Even though the radar can provide a very accurate velocity information, it does not completely cover the surrounding of the subject vehicle. Consequently, a differentiation method is applied to supplement the ground truth. With respect to the differentiation, a Savitzky-Golay filter with polynomial 3 and window length of 11 is used.

The estimated velocity by the differentiation and the velocity from the radar are compared in Figure 6-11. The dotted light gray line denotes the derivation of the position of a labeled object, which is selected randomly. Without filtering, the velocity varies very strongly and cannot be used directly. The filtered velocity and the velocity from the radar are illustrated with the solid black line and the dark gray line with star, respectively. As is obvious in Figure 6-11(a), the filtered velocity of the object coincides with the velocity from the radar very well. It proves that the filtered velocity has a very high accuracy with a maximum deviation of 1 m/s compared to the radar measured velocity, as illustrated in Figure 6-11(b). The high accuracy of the filtered velocity is further proved when comparing it with the velocity from the lidar tracking, since the lidar cannot measure velocity directly, but the velocity is estimated by tracking. Due to the high accuracy, the velocity estimated by filtering the derivative of the labeled position is finally applied to each object. Consequently, the velocities of the labeled objects are obtained.

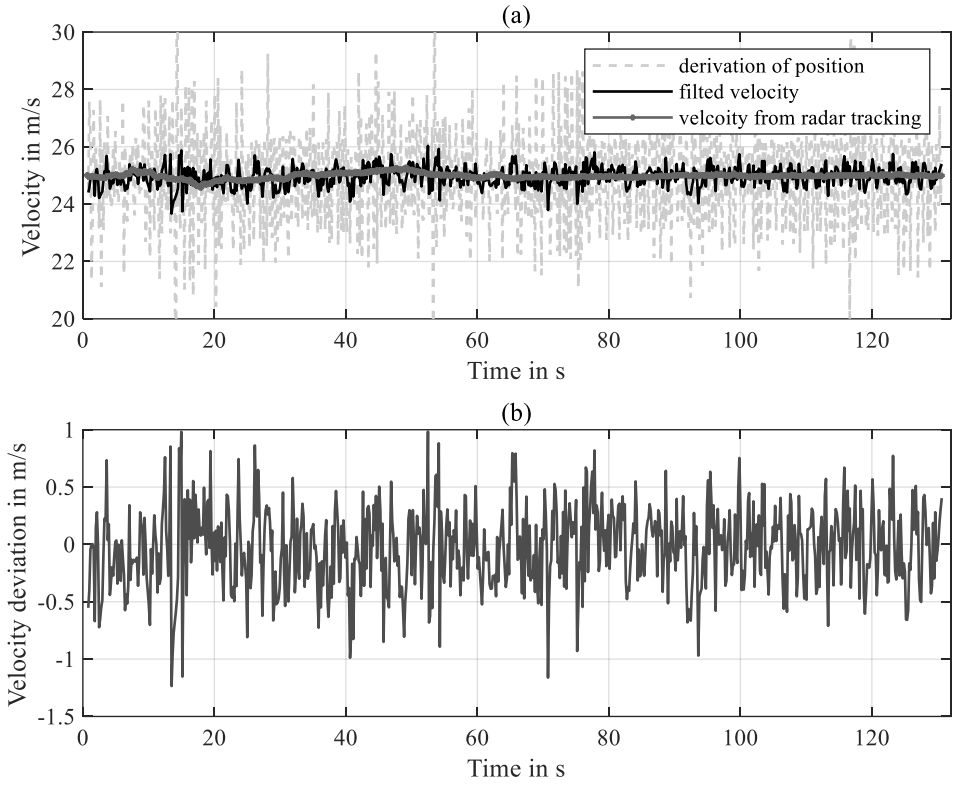

Figure 6-11: (a) Comparison of the velocities of an object from different approaches. (b) Velocity deviations between the filtered velocity and the velocity from the radar tracking.

Additionally, each object is assigned a unique ID during the labeling. The labeling process is illustrated in Figure 6-12. By observing the point clouds, a bounding box is created for each object. Different classes are marked with different colors. In the figure, the green denotes passenger cars, while the purple represents trucks. It is worth to mention that the dimension of a truck in Figure 6-12 is incorrect due to too few point clouds. However, a well estimated dimension of this truck is acquired by using the retrospective post-processing. The Figure 6-13 shows the corresponding labeled objects with known position, orientation and dimension. The velocity obtained by the Savitzky-Golay filter is drawn above each labeled object. As a result, all objects distributed on the four lanes from Darmstadt to Langen are accessible in the entire recorded data. This acquired information is then utilized for the calculation of the one another criticality metric.

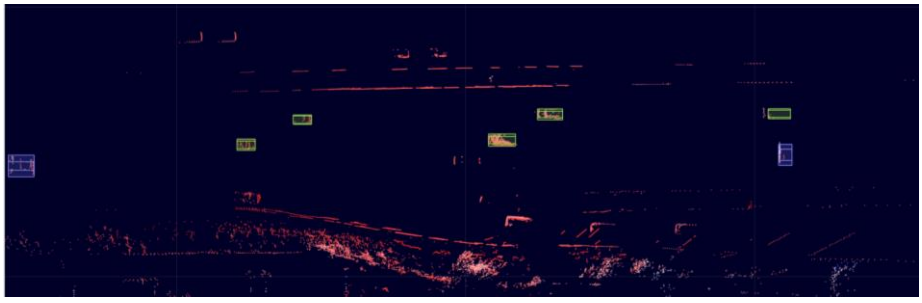

Figure 6-12: An example to illustrate the labeling process of the point clouds.

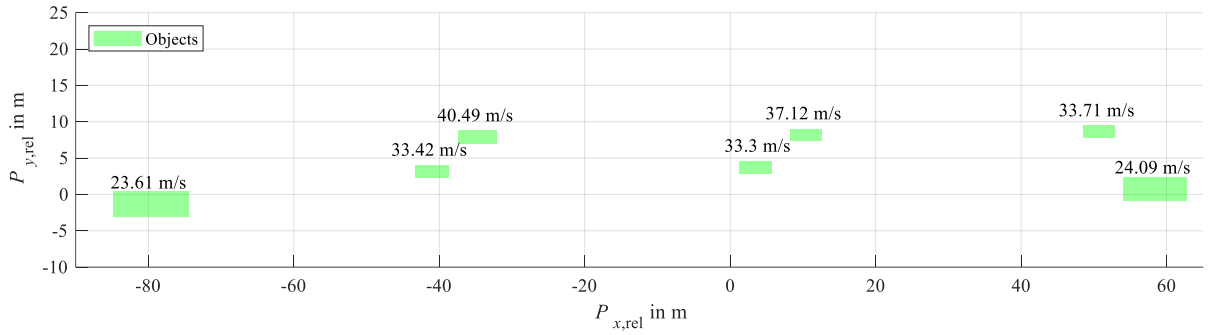

Figure 6-13: The labeled results of the objects at one time step.

6.5 Results Analysis

There are mainly two goals in the data analysis. The first goal is to analyze how the criticality index C_a changes online. The second goal is to compare the C_a with one another existing criticality metric. In the studied cases, TTC is selected as mentioned in subchapter 4.2.2. In that subchapter, four terms to classify the scenarios are defined to express explicitly the performance of C_a. They are FP scenarios, FN scenarios, TP scenarios and TN scenarios, respectively. Since the four terms are utilized frequently in this chapter, their definitions are explained again.

- A TP scenario; a critical scenario is identified by C_a as well.
- A FP scenario; an actual uncritical scenario is falsely rated as critical by C_a.
- A FN scenario; a critical scenario is missed by C_a.
- A TN scenario; an uncritical scenario is also not triggered by C_a.

In the subchapter 6.3.1, the four triggers are demonstrated during the driving. Since all the four triggers use the same criticality index, the new criticality index is the focus and analyzed in detail in this subchapter. In addition, inverse TTC (iTTC) is utilized instead of TTC, since TTC reaches infinite when the relative velocity $v_{\mathrm{diff},x}$ is zero. d_x is the relative distance in the driving direction. The iTTC is expressed by

$$it_{\mathrm{tc}} = \frac{v_{\mathrm{diff},x}}{d_x} \tag{6.2}$$

6.5.1 Evaluation of the Criticality Index

In the recorded data, the states of the vAV instances and IiC at each time step are available. In the post-processing phase, their decisions can be assessed again by iTTC in the ground truth environment in order to determine whether their decisions are safe in the driving direction. The results can then be used to assess the criticality index C_a, i.e., if an unsafe decision is found, it should also be discovered by C_a if the new criticality index works. The calculated

iTTC values of the IiC and vAV instances are illustrated in Figure 6-14. The interval between two vertical dotted lines represents the lifetime of an instance. As is obvious in the figure, the iTTC of the IiC is rather low during the driving, since the driver is defensive and keeps a large time gap with the preceding vehicle. As a result, the iTTC values of the vAV instances decrease by each reset. The $it_{\mathrm{tc,max}}$ values of all vAV instances are lower than 0.5 s^{-1}. It infers that the decisions of the vAV instances are highly likely safe in the longitudinal direction, since no perception errors exist in the ground truth environment. However, small increases in the iTTC values of the vAV instances can be found. The reason is that the vAV instances accelerate and try to achieve the predefined cruised speed after a reset, i.e., the vAV instances have not yet entered the adaptive cruise mode and the preceding object is first not considered. If the transition condition to the adaptive cruise mode is met, the preceding object affects the decisions of the vAV instances. As a result, the lane changing or the deceleration maneuver is motivated. Therefore, the iTTC value increases from a reset and then decreases if the lifetime is not yet over. In contrast, if the lane change mode is activated, the iTTC values increase further until a vAV enters the adjacent lane. Generally, the vAV instances behave a little more dynamically than the human driver.

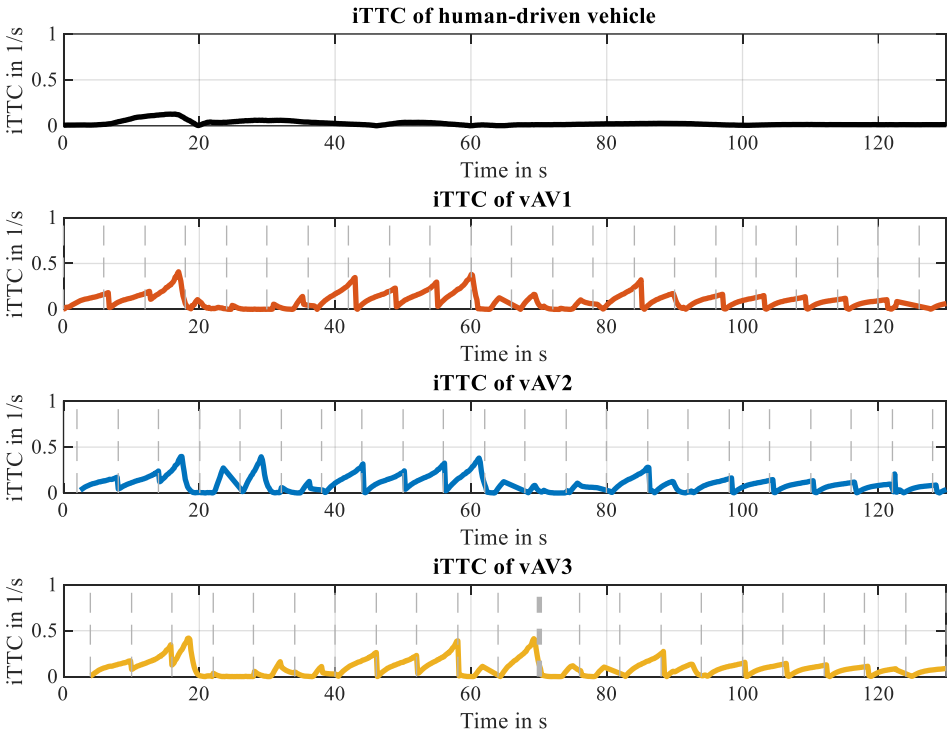

Figure 6-14: The calculated iTTC values of the IiC and vAV instances in the labeled environment.

Different from the iTTC, which is calculated offline in the labeled environment, the C_a is calculated online. The results of C_a are shown in Figure 6-15. C_a^* is used in this figure under consideration of the sign. As is obvious in this figure, there are several jumps of C_a^* during the driving. Notably, the IiC and the vAV instances have jumps simultaneously at several

time steps, which are depicted by gray areas. This indicates that there are perception errors since the IiC and the vAV instances utilize the same environmental representation to calculate their C_a^* values online, i.e., a FP object could result in large C_a^* values of the IiC and vAVs simultaneously, since the same state of the object is applied to calculate the C_a^* of the IiC and vAVs. Based on this characteristics, the reason of some jumps of C_a^* can be classified as the uncertainties in the perception. The scenarios, in which not all instances have jumps, should be further studied. These jumps are caused by the uncertainties in the perception or the unsafe lateral decisions, since the longitudinal decisions of vAV instances are uncritical based on the results of iTTC, and the proposed C_a is able to theoretically also identify the unsafe lateral decisions. The unsafe lateral decisions could be, for example, a vAV changes the lane without considering the rear left object.

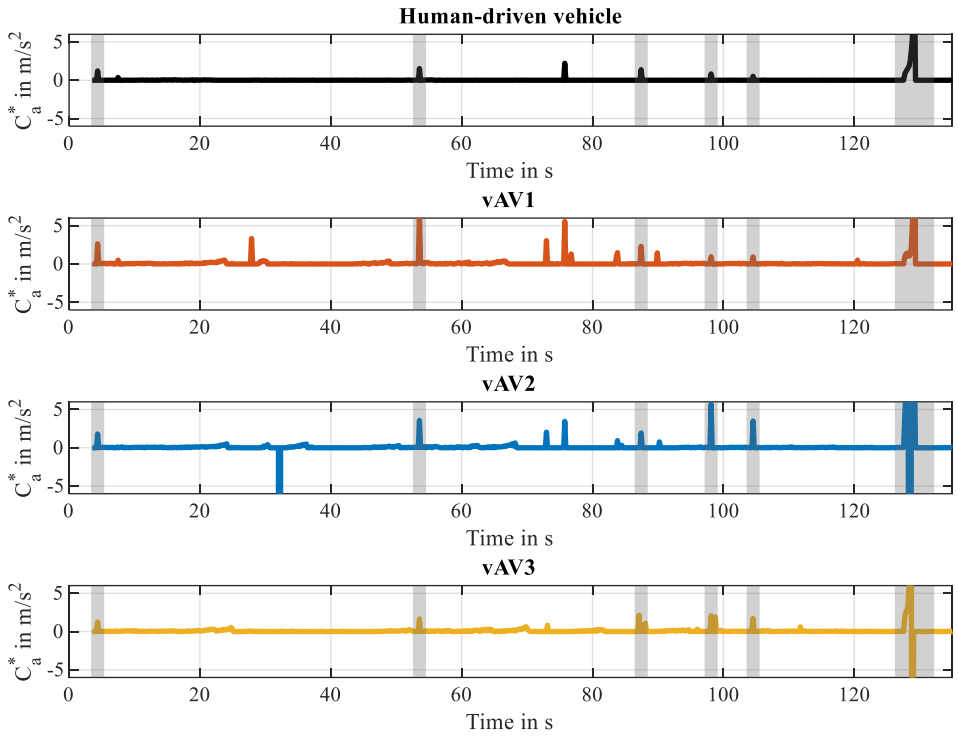

Figure 6-15: The criticality indexes of the IiC and vAV instances in the field operation. Gray areas denote that the IiC and vAV instances have jumps simultaneously.

The jumps of C_a^*, which cannot be explained intuitively, are further analyzed by a close look of the perception results and camera images. The results are summarized in Table 6-1. The scenarios, in which the absolute values of C_a^* are lower than 3 m/s^2, are not taken into account in the table, since they represent probably the normal maneuvers of vAV instances during the driving. The threshold of C_a cannot be too low. Otherwise, many FP scenarios are triggered to save, i.e., the scenarios are uncritical but saved by mistake. In addition, ± 20 m/s^2 is defined as the limit of C_a^* for a better illustration, since values larger than that have nearly

the same meaning of a rather critical situation. If more than one vAV have jumps of C_a^* simultaneously, the maximum absolute value among them is selected because it is sufficient to activate the trigger only once for the same scenario.

As can be seen in Table 6-1, those jumps are actually caused by perception errors. Due to the birth cycle parameter, vAV instances have different decisions and thus have different states. As a result, only some of the instances have discovered these scenarios with perception errors when observing their C_a values, i.e., critical scenarios can be discovered by different vAV instances. For example, only the vAV2 has a large C_a value at time step 32.16 s in Figure 6-15, other vAV instances have missed this critical situation. In other words, the coverage of critical scenarios is enlarged by using multiple instances. One or two vAV instances have low C_a in a critical scenario, the remaining vAV instances may have large C_a. As a result, the critical situation could still be discovered. In addition, vAV instances have different optimal maneuvers to avoid or mitigate a collision in different situations, e.g., the vAV2 has a large negative C_a^* at time step 32.16 s, which infers that a braking maneuver is better than an evasion in this situation, since the vAV is too close to a FP object.

Table 6-1: The analysis of the scenarios in which not all instances have simultaneous jumps of the criticality index.

Time (s)	**Extreme value of C_a^* (m/s^2)**	**Subject vehicle**	**Reason**
27.88	3.33	vAV1	A static FP object
32.16	-20	vAV2	A static FP object
72.96	3.05	vAV1	A static FP object

Additionally, it is necessary to calculate the C_a values of the IiC, since it can be used to identify the perception errors. In the recorded data, if the IiC and vAVs have jumps of C_a simultaneously, a perception error can be concluded, since other objects behave safely and the same environmental representation is used to calculate C_a of IiC and vAV instances. However, it is not difficult to image that the vAV instances may decelerate or change the lane in the case of a FP object, while the IiC keeps driving. Consequently, they do not have a jump of C_a simultaneously, and the vAV instances would miss this perception error but the IiC catches it. Therefore, it is also meaningful to online evaluate the safety of the IiC using the criticality index C_a.

Additionally, it demonstrates that the special designed ring buffer is appropriate, since a critical scenario can be discovered by more than one instances within a very short time period, e.g. the critical situation around 129 s. With the help of the designed ring buffer, this critical scenario is saved only once, so that the duplicate saving of the scenario could be avoided. Last but not least, the threshold of C_a should be carefully designed. Even if the situations are proved to have perception errors with a maximum C_a of around 3 m/s^2, those errors are probably irrelevant for the vAV, e.g., a FP object is far away from a vAV. With a lower threshold,

some uncritical scenarios are saved, which are actually useless for the verification and validation of AD. Those low C_a values could result from, e.g. a normal braking or an irrelevant error in the scenarios. More data would be helpful to find a better threshold.

6.5.2 Evaluation of the Criticality Index against iTTC

The above analysis demonstrates the online performance of the proposed criticality index C_a. Several conclusions are made based on the recorded data. However, it is unclear whether the C_a is actually better for the application of the VAAFO approach compared to other criticality metrics. Therefore, it is necessary to evaluate its performance against other criticality metrics. With respect to the comparison object, iTTC is chosen. The reasons to determine the thresholds for maximum iTTC are discussed in subchapter 4.2.2.

- A situation is not critical, when the maximum iTTC value is lower than 1 s^{-1}.
- A situation is critical, when the maximum iTTC value is larger than 5 s^{-1}, as discussed in subchapter 4.2.2.
- It is unclear whether a situation is critical or not when the maximum iTTC value is between 1 s^{-1} and 5 s^{-1}, since different people may have different opinions if the value of the maximum iTTC value falls into this range.

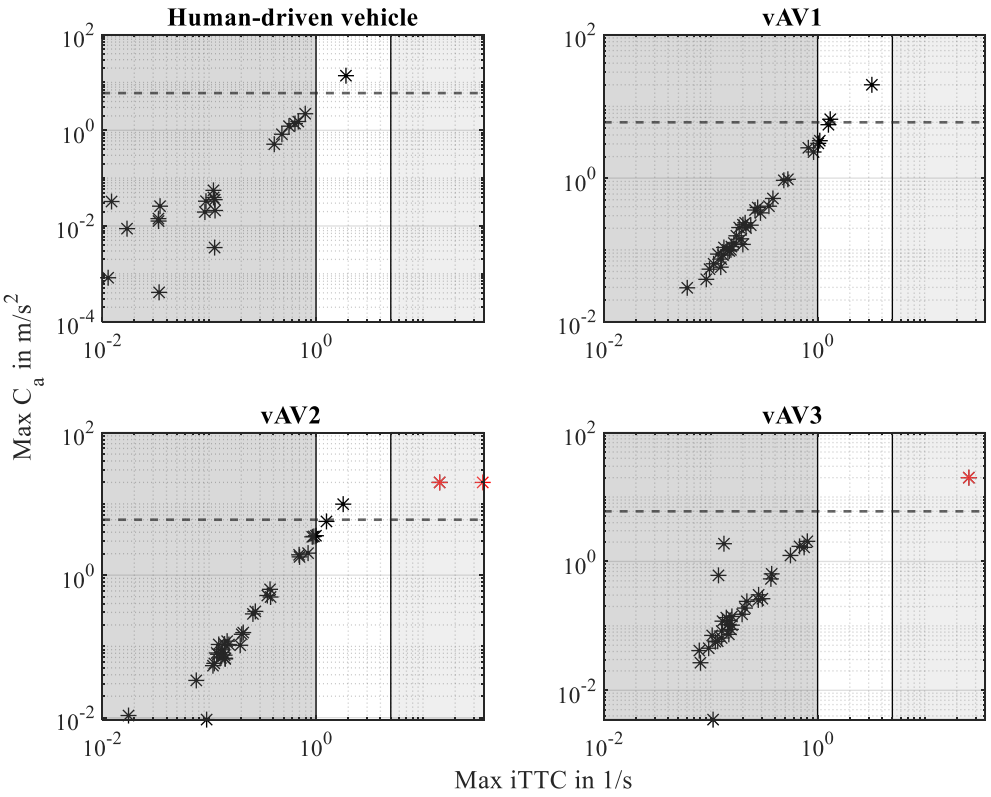

Figure 6-16: The maximum criticality index against the maximum iTTC of the four instances under the same scenarios in the recorded data.

Different from the subchapter 6.5.1, the iTTC is calculated online in this time. In order to compare the C_a with the iTTC, the maximum C_a and the maximum iTTC of the four instances (three vAV instances plus IiC) under a same scenario are calculated. The calculated results in all scenarios in the recorded data are illustrated in Figure 6-16. The horizontal axis denotes the maximum iTTC values of an instance in the scenarios of the recorded data, while the vertical axis represents the corresponding maximum C_a. 6 m/s^2 is drawn with horizontal dotted line in the figure. Three different areas are defined according to the thresholds of the maximum iTTC. The negative extreme values of C_a^* are illustrated with red points.

As is obvious in Figure 6-16, Large maximum C_a of vAV2 and vAV3 corresponds with large maximum iTTC apparently. It infers that a scenario, which is assessed as critical by maximum iTTC, is also categorized as critical by C_a. For example, the maximum iTTC of vAV2 reaches 36.17 s^{-1} in a scenario. In the same scenario, an impossible required deceleration is also shown. It infers that this scenario is truly rather critical and discovered by both criticality metrics. By a close look at the perception results, a sudden appeared FP object is the reason. The C_a value of the vAV2 at the time step 32.16 s in Figure 6-15 has reflected this perception error as well. Meanwhile, no scenarios, which have large maximum iTTC values, have low maximum C_a values. Consequently, the TP scenarios are identified successfully, while no FN scenarios exist. Additionally, it is apparent that the maximum C_a values are in line with maximum iTTC values in small value areas as well, e.g., the maximum iTTC of most scenarios are smaller than 1 s^{-1}, which indicates that those scenarios are likely uncritical. The maximum C_a in those scenarios are also small and distributed within the horizontal dotted lines. Therefore, TN scenarios are classified correctly by C_a.

Table 6-2: Analysis of the outliers that belong to the unknown area of the maximum iTTC.

Time (s)	Max C_a (m/s^2)	Max iTTC (s^{-1})	Subject vehicle	Reason
27.88	3.33	1.05	vAV1	A static FP object
53.55	6.62	1.31	vAV1	A static FP object
75.76	5.56	1.26	vAV1	A static FP object
98.13	5.67	1.25	vAV2	A static FP object
129.22	20	3.22	vAV2	A static FP object

However, there are some outliers, as shown in Figure 6-16, whose maximum iTTC values fall into the unknown area, i.e., it is difficult to judge whether they are actually critical or not according to their maximum iTTC values. Such outliers can be found obviously in vAV1 and vAV2. Some of them have even very large C_a but small maximum iTTC, e.g., the maximum C_a of vAV2 has reached the defined limit at time step 129.22 s, while the maximum iTTC is 3.22 s^{-1}. Hence, the question should be answered whether these scenarios in which the outliers appear, are FP scenarios or TP scenarios. To figure out the reasons, the recorded data are elaborately analyzed. The reasons of those outliers are presented in Table 6-2. From this table, it can be concluded that C_a can identify perception errors better than the iTTC,

since those outliers with large maximum C_a but low maximum iTTC are actually caused by perception errors, i.e., C_a is more sensitive to the perception errors. Each error is reflected by a jump of C_a. It demonstrates that the defined trigger C_a is more suitable for the safety evaluation of AVs online. Additionally, it indicates that the perception of the SuT should be improved due to too many FP objects.

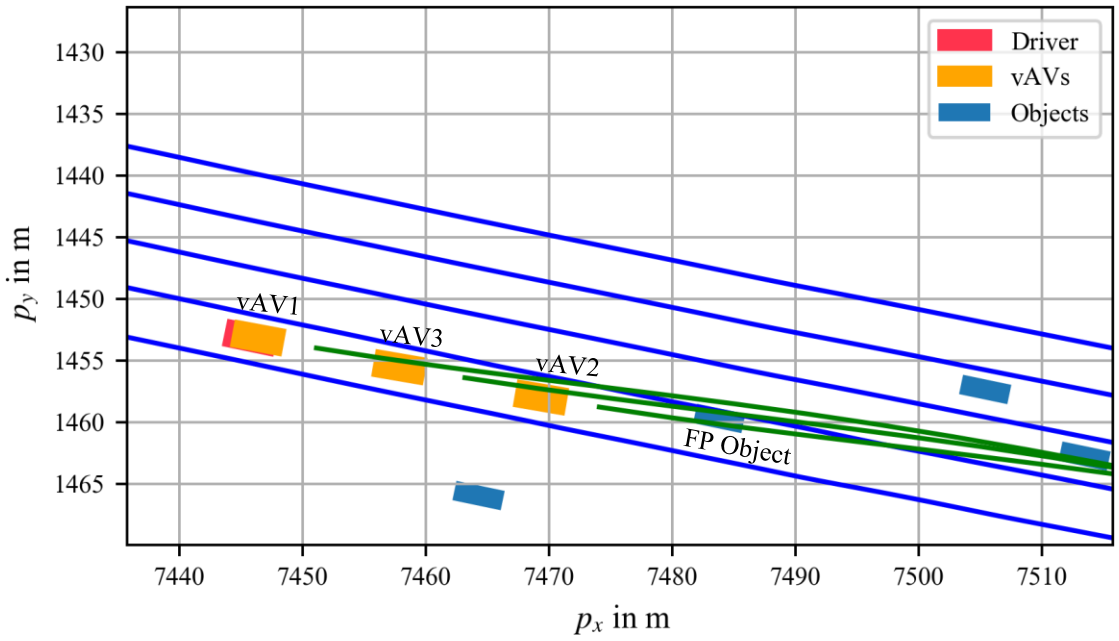

Figure 6-17: A scenario with a FP object during the driving.

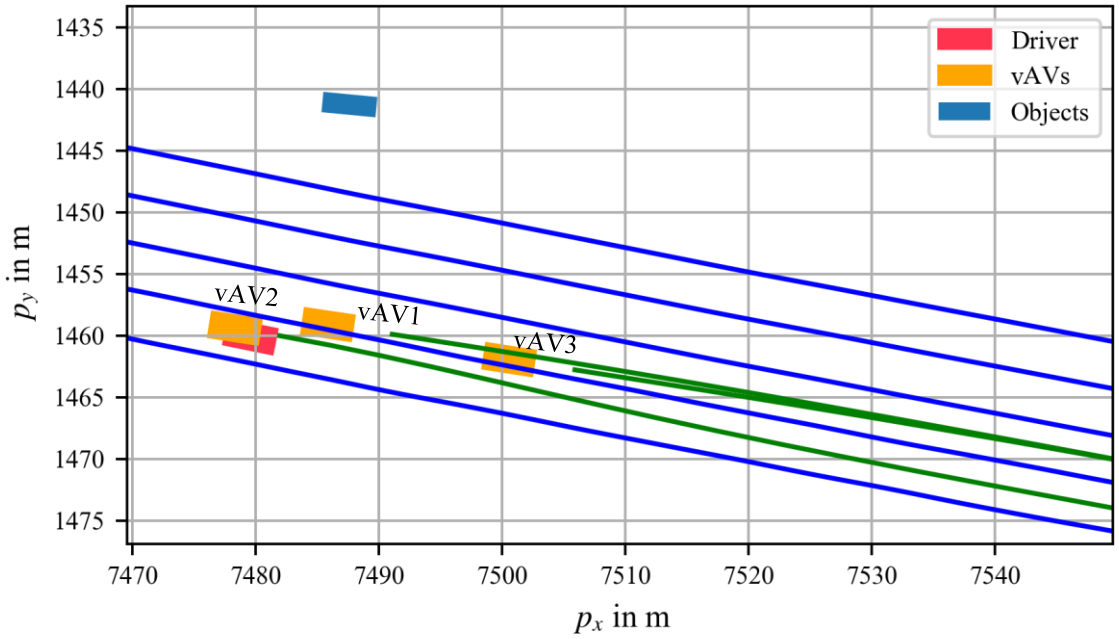

Figure 6-18: A snapshot of the scenario in which a FP object disappears.

Figure 6-17 illustrates one example of the outliers, which describes a FP object in a scenario. Due to the front FP object that locates in the same lane as the vAVs, the vAVs receive lane

change mode from the behavior planner. Thus, the lane changing trajectories are planned in the current situation, as denoted by the green lines. This scenario with a FP object occurs at time step 129.22 s and is first discovered by the vAV2. After a while, the FP object disappears as illustrated in Figure 6-18. The criticality index C_a and the iTTC in this scenario are analyzed in detail to investigate their common characteristics and the special aspects of the C_a. Subsequently, it is possible to derive the advantages of C_a compared to iTTC, and obtain more knowledge about the application of C_a.

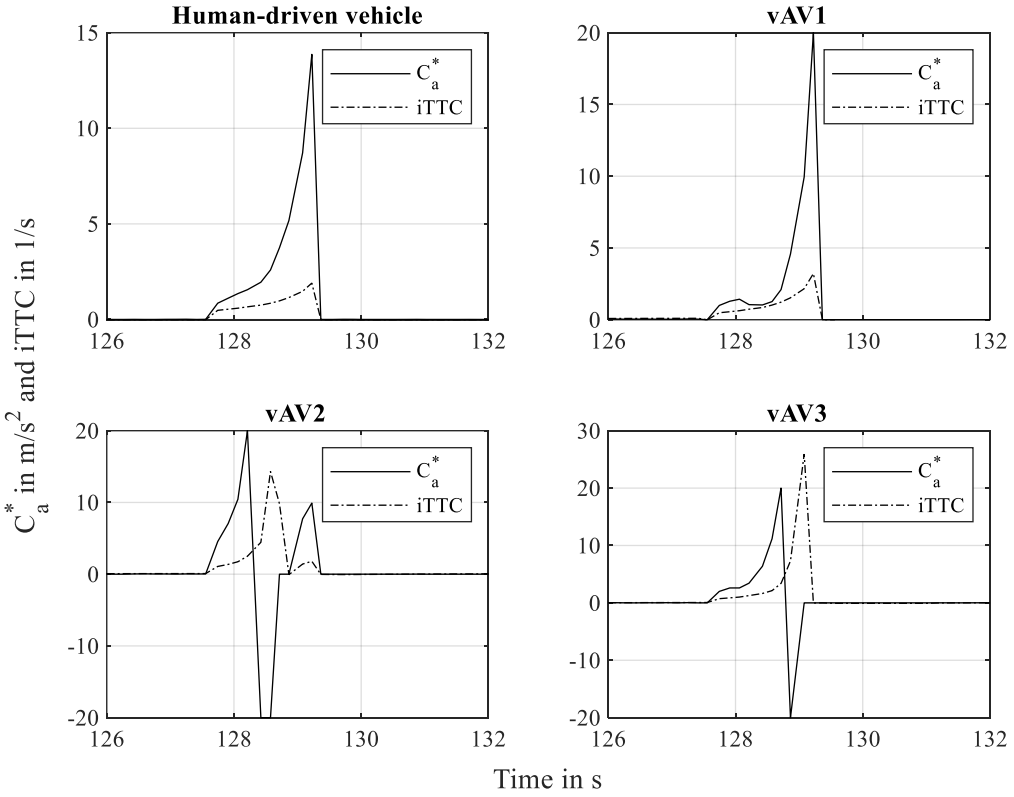

Figure 6-19: Analysis of the criticality index and iTTC at time step around 129 s to illustrate the characteristic of the proposed criticality index.

The maximum C_a and maximum iTTC of a scenario are reached simultaneously in most cases. Nevertheless, when the C_a and iTTC from time step 126 s to 132 s are studied in detail, the time offsets between the peak values of C_a and iTTC are obvious in vAV2 and vAV3, as illustrated in Figure 6-19. Therefore, it should be discussed when the peak values of C_a and iTTC arrive at the same time step and when their peak values have a time offset. If the preceding object does not accelerate or decelerate, e.g. a static FP object, thus the equation (3.17) and (3.18) can be simplified as

$$D_{\mathrm{req,D}}(t) = \frac{v_{\mathrm{diff},x}^2(t)}{2d_x(t)} \tag{6.3}$$

$$a_{\mathrm{req,eva}}(t) = 2\left|y_{\mathrm{eva}}(t)/t_{\mathrm{tc,e}}^2(t)\right| \tag{6.4}$$

With $D_{\mathrm{obj}} = 0$ and $v_y = 0$ if a vAV is not ready to change the lane.

With respect to the $t_{\mathrm{tc,e}}(t)$, it is the enhanced TTC and the deceleration of the preceding object is taken into account. In order to compare the $a_{\mathrm{req,eva}}(t)$ with the $D_{\mathrm{req,D}}(t)$, the enhanced TTC and TTC are first discussed. The equation (3.20) can be reformulated as

$$\frac{t_{\mathrm{tc,e}}^2(t)D_{\mathrm{rel}}(t)}{v_{\mathrm{diff},x}(t)} + 2t_{\mathrm{tc,e}}(t) = \frac{2d_x(t)}{v_{\mathrm{diff},x}(t)} \tag{6.5}$$

With $D_{\mathrm{rel}} \neq 0$ and $v_{\mathrm{diff},x} \neq 0$. The right side of the equation (6.5) represent two times of $t_{\mathrm{tc}}(t) = d_x(t)/v_{\mathrm{diff},x}(t)$. Negative values of TTC are ignored. Therefore, the following four conditions decide the numerical relationship between the enhanced TTC $t_{\mathrm{tc,e}}$ and TTC t_{tc}.

$$t_{\mathrm{tc,e}}(t) < t_{\mathrm{tc}}(t), \text{ if } D_{\mathrm{rel}} \text{ and } v_{\mathrm{diff},x} \text{ have the same sign.} \tag{6.6}$$

$$t_{\mathrm{tc,e}}(t) > t_{\mathrm{tc}}(t), \text{ if } D_{\mathrm{rel}} \text{ and } v_{\mathrm{diff},x} \text{ have the different signs.} \tag{6.7}$$

$$t_{\mathrm{tc,e}}(t) = t_{\mathrm{tc}}(t), \text{ if } D_{\mathrm{rel}} = 0 \tag{6.8}$$

If a vAV has not yet began to decelerate, i.e. $D_{\mathrm{rel}} = 0$, thus the equation (6.4) can be rewritten as

$$a_{\mathrm{req,eva}}(t) = 2|y_{\mathrm{eva}}(t)|v_{\mathrm{diff},x}^2(t)/d_x^2(t) \tag{6.9}$$

Comparing the equation (6.3) and (6.9), it can be found that

$$\text{If } d_x(t) \geq 4|y_{\mathrm{eva}}(t)|, \text{ then } D_{\mathrm{req,D}} \geq a_{\mathrm{req,eva}}, \text{ otherwise } D_{\mathrm{req,D}} < a_{\mathrm{req,eva}} \tag{6.10}$$

Conversely, if the vAV decelerates stronger than the preceding object ($D_{\mathrm{rel}}(t) < 0$) and $v_{\mathrm{diff},x}(t) > 0$, the enhanced TTC $t_{\mathrm{tc,e}}(t)$ is thus larger than $t_{\mathrm{tc}}(t)$. Thus,

$$a_{\mathrm{req,eva}}(t) \leq \frac{2|y_{\mathrm{eva}}(t)|v_{\mathrm{diff},x}^2(t)}{d_x^2(t)} = 4|y_{\mathrm{eva}}(t)|\frac{D_{\mathrm{req,D}}(t)}{d_x(t)} \tag{6.11}$$

Therefore, if $d_x(t) \geq 4|y_{\mathrm{eva}}(t)|$, $a_{\mathrm{req,eva}}(t)$ is still lower than the value of $D_{\mathrm{req,D}}(t)$. Finally, it can be concluded that an evasion maneuver is always a better choice compared to the braking maneuver as long as the $d_x(t) \geq 4|y_{\mathrm{eva}}(t)|$ and $D_{\mathrm{rel}} \leq 0$. Thus, the C_a^* is always positive at the beginning with respect to a FP object, since the C_a^* equals to $a_{\mathrm{req,eva}}$ according to the equation (3.23). The following two situations are discussed to explain why the C_a^* reaches its peak earlier than iTTC and why the C_a^* is negative at some time steps.

Situation one: $d_x(t) \geq 4|y_{\mathrm{eva}}(t)|$ and $D_{\mathrm{rel}} = 0$. Thus, the $t_{\mathrm{tc,e}}(t)$ equals to $t_{\mathrm{tc}}(t)$. As a result, when the iTTC reaches its peak, the enhanced TTC reaches its peak as well. According to equation (6.4), the $a_{\mathrm{req,eva}}$ depends only on the enhanced TTC, since the y_{eva} will not change if the vAV does not prepare to change the lane. Thus, it will reach the maximum value at the same time as the iTTC. Hence, it can be seen in Figure 6-19 that the C_a^* and iTTC of the IiC and vAV1 reach their peaks simultaneously.

Situation two: when the vAVs approach further the FP object, the evasion maneuver is still preferred. Therefore, the vAV2 and vAV3 have initial positive C_a^*. Afterwards, the FP object is too close to the vAV instances, thus $d_x \geq 4|y_{\mathrm{eva}}|$ is no longer fulfilled. The $a_{\mathrm{req,eva}}$ is so

large that the braking maneuver is chosen. As a result, the better maneuver changes suddenly from evasion to braking according to the equation (6.10) since negative C_a^* can been seen in vAV2 and vAV3. Additionally, a small time offset can be found in vAV2 and vAV3 when comparing the positive maximum value of C_a^* with the positive maximum value of iTTC. This is because the equation (6.4) takes the relative deceleration into account, while the iTTC considers no relative deceleration rather only the relative velocity. Due to an integral relationship, the deceleration-based criticality index could identify a critical situation earlier. Due to a reset of vAV2, it has then a second small peak at the same time step as the IiC.

Based on the above analyzed results, some special characteristics of the C_a are obtained. It can be conclude that the C_a is superior to the maximum iTTC in identifying the errors in AVs. The maximum iTTC becomes large when a scenario is already rather critical, while the C_a can reflect the criticality of a situation earlier. Even though they could reach the peak values simultaneously at some situations, the C_a has apparent large value. For example, the maximum value of iTTC of vAV1 in Figure 6-19 is about 3.2 s^{-1}, which will be regarded as uncritical if the threshold 5 s^{-1} is taken. However, the maximum value of C_a has already reached 20 m/s^2, and the situation is classified as critical if a threshold 6 m/s^2 is applied. Some critical situations are even missed by the maximum iTTC. Therefore, the maximum iTTC is not appropriate for identifying critical scenarios online. In contrast, the C_a is capable of discovering more perception errors. Each FP object can be reflected by C_a. However, some perception errors are found with small values of C_a. In order to not save any uncritical scenarios, the threshold should not be too low. More data would bring benefit to determine a better threshold. In addition, the evasion maneuver is always a prior choice if the vAV is far away from the preceding object. When the relative distance is small, the braking maneuver is better. Furthermore, the C_a of all four instances are all rather large within a very short time interval, as can be seen in Figure 6-19, which infers that the designed ring buffer with an ignoring period of the triggers is rather reasonable.

6.6 Summary

In this chapter, the basic required components for the implementation of the VAAFO approach in reality are first presented. The test platform is introduced and the location of each sensor is illustrated. A long range radar and a 32-layer lidar are utilized for the perception. An ADMA-RTK is used for the localization. The lidar tracking algorithm is introduced and implemented. Afterwards, the radar and lidar are fused by the Bayesian approach based on a high-level fusion architecture. The map as an essential part for the trajectory planning is created by cameras and the ADMA. The B-spline curve is used to fit the collected discrete points due to some missing points and outliers. Finally, the map is obtained and stored as an OpenDRIVE format. Additionally, the map is loaded into the ROS platform for the trajectory planning. Then, the entire SuT for the vAV instances is introduced. Finally, the VAAFO approach is teste online, and the data is collected during the driving from Darmstadt to Langen.

To determine the sources of the error, the uncertainties in the perception are reduced to evaluate the decisions of the vAV instances again by one another criticality metric. Several possible approaches to reduce the uncertainties are presented and compared. The labeling approach is finally selected, since it provides the most accurate results. With respect to the evaluation of the triggers, the online calculated criticality index C_a is analyzed. Its performance is further demonstrated against the iTTC. Finally, several conclusions are obtained. The coverage of critical scenarios is enlarged by using multiple vAV instances. The calculation of the C_a of the IiC is helpful to determine the source of errors. In addition, the C_a can identify errors of AVs better than the maximum iTTC. Based on these derived conclusions, the coverage degree of the VAAFO approach is discussed in the next chapter.

7 Coverage Analysis and Discussion

The technical details of the VAAFO approach are presented in the above chapters. Since the aim of the VAAFO approach is to support the safety validation of AD, it is necessary to discuss to what extent it can help address the current challenge of validating the safety of AD. In order to answer this question, three aspects are first analyzed. The first aspect is to study which part of an ADS can be tested and validated by the VAAFO approach. Only by figuring out this point, the application scope will be less ambiguous. The second aspect is to determine whether the approach is applicable to test all five levels of AVs. The third aspect deals with on the application timing of the VAAFO approach. The coverage can then be determined when the analysis of these three aspects are conducted.

7.1 Coverage Analysis

Aspect 1: which part of an ADS can be tested in the VAAFO framework?

Normally, an ADS consists of sense, plan and act. The act is not included based on the working principle of the approach. According to the simulation results, the plan module of an ADS can be tested, since there is no perception error in the simulation. The different simulation cases prove that the safety of a planning module in both longitudinal and lateral direction can be evaluated by the proposed criticality index. According to the test results in reality, the perception errors can also be identified. Moreover, the proposed criticality index can identify critical situations earlier than the maximum iTTC. Thus, it is more suitable for the online application. Additionally, it is more sensitive to errors. Therefore, both the perception and the plan modules of an ADS can be evaluated online by the criticality index. With the help of the framework, the probability of evaluating an ADS in different situations is increased. Each instance has different states and may have different decisions under the same scenario. Thus, different actions of an ADS are assessed simultaneously, and a more intensive testing compared to the conventional real-world testing is performed. Since the defined triggers focus on the decision level of an ADS, the perception and decision cannot be separately evaluated. An error from the perception could also result in an unsafe decision. Therefore, further analysis is required in order to determine the reasons.

In addition, the SuT can be replaced by a FuT in the proposed framework if the test of a function is the task. By changing the triggers accordingly, a certain function can be evaluated silently in the real world. As a result, much real-world data regarding this function can be obtained. For instance, a motion prediction algorithm can be tested online by comparing the predicted trajectory with the actual trajectory of an object. A distance deviation-based trigger would be useful to evaluate the performance of the motion prediction algorithm. Another

example could be a machine learning-based algorithm for the image recognition. The estimated class can be compared with the true class of an object, while the true class of an object can be obtained by online labeling. Thus, a judgment can be made whether the algorithm can recognize such object correctly. If a wrong estimation occurs, the data could be saved and utilized to train the algorithm again. Consequently, the machine learning-based algorithm could be improved gradually.

Therefore, it depends on what should be tested. With respect to the function level, a ground truth is required to determine whether the FuT has the correct output. However, it may be difficult to obtain a ground truth at the system level. Thus, the criticality metrics would be an appropriate choice to evaluate the system. The proposed framework can be utilized to test both the perception and decision modules. Additionally, the machine learning-based algorithms, which cannot be interpreted and are therefore difficult to approve, can also be tested safely online.

Aspect 2: Which level of driving automation system can be tested using the VAAFO approach?

The level 2 driving automation system has been released into the market, and the corresponding test process for such level has been defined. The test and validation of ADS (at least level 3) is a challenge currently as discussed in chapter 1. Therefore, the question to be discussed is whether an ADS can be tested using the VAAFO approach. Nowadays, a vehicle equipped with a level 2 driving automation system is not infrequently. With respect to a level 2 driving automation system, a driver performs the remaining dynamic driving task (DDT) that cannot be performed by the driving automation system. Thus, the IiC in this case is a driver assisted by a level 2 driving automation system. A level 3 driving automation system can be implemented in the vehicle and tested silently if the on-board hardware supports for the operation of an ADS. Consequently, it can be proved whether the level 3 driving automation system can successfully monitor the operation design domain (ODD) limits or a system failure, and then issue a timely request to a driver. According to the announcement from Tesla, all Tesla cars are standard equipped with autopilot hardware since 2016.[229] The autopilot is deactivated if a customer does not purchase it. By using the already available hardware, the VAAFO approach provides the possibility to test an ADS in the real world without intervening the normal driving of the IiC. As a result, much more experience about the performance of the ADS in the real world could be gained. The ADS can be tested and improved gradually based on the collected real data.

If the IiC is a level 3 driving automation system, a level 4 driving automation system can be tested in the VAAFO framework. Since a driver has to overtake the vehicle completely if a DDT performance-relevant system failure occurs, it is rather meaningful to see whether the level 4 driving automation system can achieve a minimal risk condition by itself if it keeps going without the takeover of the driver. When it tries to achieve the minimal risk condition,

[229] The Tesla Team: All Tesla Cars Being Produced Now Have Full Self-Driving Hardware (2021).

how it would do. These two questions could be answered with the help of the VAAFO approach, since the multiple vAV instances in the virtual world can continue to make decisions under the real conditions after a driver takes over the real vehicle. Thus, the decision results can be obtained, which are rather valuable for developing a level 4 driving automation system, since it has to handle such DDT performance-relevant system failure by itself. Similarly, a level 5 driving automation system can be tested when the IiC is a level 4 driving automation system. With respect to a level 4 driving automation system, it is limited in an ODD, while there is no such restriction for a level 5 driving automation system. In the VAAFO framework, the ODD does not have to be defined and monitored, since no additional risk is brought when a level 4 driving automation system is out of the ODD. Due to the principle of silent testing, the level 5 driving automation system is tested in the virtual world and can thus be tested outside of an ODD. Thus, the ODD can be gradually extended and there is no ODD any more at the end.

Aspect 3: When is the right time to apply the VAAFO approach?

In the development phase, an unrefined ADS or a porotype can be tested safely in the real world, as the developed ADS in this dissertation to demonstrate the VAAFO approach. The collected data in the real world would be more valuable to improve an ADS than the simulation results. In the implementation phase, an updated or upgraded version can be tested in parallel. As a result, when any part of an ADS is modified, including but not limited to hardware or software updates, the comparison with the current engaged version can be observed directly. Whether the updated or upgraded version outperforms the engaged version can thus be determined. Since it is possible to apply the VAAFO approach in each customer vehicle, it is not difficult to image that many benefits can be brought. For example, the test process is accelerated compared to the conventional real-world testing, since a safety driver is no longer necessary. The new relevant scenarios especially those previously unknown scenarios could be found, since different drivers experience different drive situations daily, so that the remaining unknown scenarios would be less and less with accumulated travel distances. As a result, the surprise indicated by Winner et al.[230] can be gradually discovered, and the test catalog for safety certification of AVs can be supplemented. The inclusion of known critical scenarios in the test catalog makes the test catalog increase steadily, but the surprise per distance decreases, as shown in Figure 7-1. Subsequently, the remaining risk can be estimated bases on certain critical assumptions. If the remaining risk is higher than an acceptable level, the VAAFO approach would be an effective way to reduce the remaining risk, since the required test kilometers is rather large in order to discover a surprise.

In summary, an ADS that includes perception and planning can be tested and validated based on the VAAFO approach, regardless of which level of driving automation system the IiC is.

[230] Winner, H. et al.: Validation and Introduction of Automated Driving (2018), p. 191.

Additionally, the VAAFO approach can play a major role in both the development and implementation phase. Moreover, the surprises can be found by the accumulated travel distances to reduce the remaining risk.

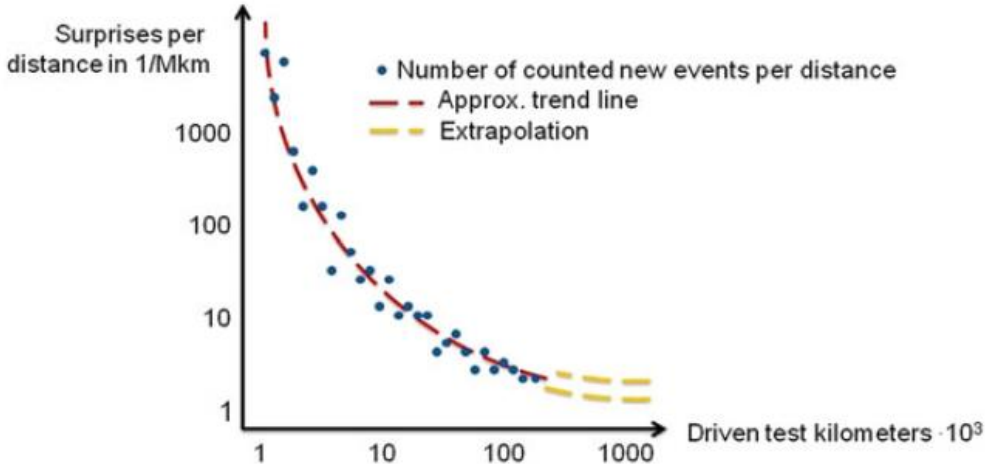

Figure 7-1: The number of surprises per distance covered.[230]

Note: Reprinted by permission from [Springer Nature Customer Service Centre GmbH]: [Springer] [Automotive Systems Engineering II] [Validation and Introduction of Automated Driving, Hermann Winner, Walther Wachenfeld, Phillip Junietz] [Copyright] (2018)

7.2 Limitations

Despite the many advantages of the VAAFO approach, there are some shortcomings or limitations that cannot be overlooked, which are discussed below.

Limitation 1: An ADS cannot be tested in the action space that the IiC will not reach.

Since the vAV instances do not exist in the real world, the interaction between the vAV instances and the traffic participants is unidirectional, i.e., the vAV instances can react to the traffic participants, but the traffic participants do not react to the vAV instances. Thus, an open-loop problem exists in the virtual world. A complete elimination of such problem is impossible based on the current framework. Even though the behavior of the traffic participants behind a vAV can be simulated to close the loop, the meaning of the silent testing technique will lost to some extent, since an ADS is no longer tested in a real environmental representation. In the VAAFO approach, the open-loop problem is mitigated with the help of the short lifetime parameter, and only matters when a vAV has a considerable position deviation from the IiC, as discussed in subchapter 3.6. However, the next reset will be conducted soon if such a large position deviation occurs. As a result, the vAV can continue to be tested after a reset if it has the same action space as the IiC. Therefore, the open-loop itself is not a big problem. However, if a vAV has an action space that the IiC does not have, i.e., they have different reachable kinematic ranges. For instance, an ADS is designed in a very conservative way and always keeps a large time gap to a preceding vehicle. As a result, the vAV would be always behind the IiC, which would make the safety assessment of the vAV

unreliable in this case due to the permanent negative influences from the open-loop. Therefore, the safety validation in the scenarios where the kinematics of a vAV are outside the range of the kinematics of an IiC should be performed using other approaches. The VAAFO approach is applicable in the scenarios where a vAV and an IiC have an overlapping action space. To mitigate this limitation, there are two possibilities. If an IiC is a human driver, the action space of IiC is enlarged when applying the approach in a fleet, since human drivers have different driving styles to some extent. If an IiC is a human driver assisted by a driving automation system, the overlapping action space is also enlarged as the action space of a driver is combined with that of a driving automation system. Another possible way is to limit the action space of an ADS that is out of the action space of an IiC. As a result, the overlapped action space can occur more frequently. This way is at least useful in the development phase to test certain functions of an ADS.

Limitation 2: A new vAV instance is born without historical memory

The historical memory, which denotes the information in the past, may be very crucial for some modules of an ADS. For instance, the long short-term memory (LSTM) is a very popular approach for motion prediction of tracked objects. In the LSTM, the historical information of an object is essential in order to provide an accurate prediction. Luckily, the motion prediction belongs to the perception level, which will not be reset in the VAAFO approach. However, some planners may need the historical information as well. The Figure 7-2 shows an example. The subject vehicle wants to cut in the main road, while many traffic objects are driving on the main road. As a result, the subject vehicle must wait for an appropriate chance to cut in. With respect to a finite state machine (FSM)-based behavior planner, the subject vehicle will stuck in a state and has no chance to change to other states. However, with a more intelligent behavior planner, the parameters could be adjusted accordingly so that the subject vehicle would drive onto the main road. Regarding the parameters adjustment, the historical memory is essential since it is the basis for the optimization.

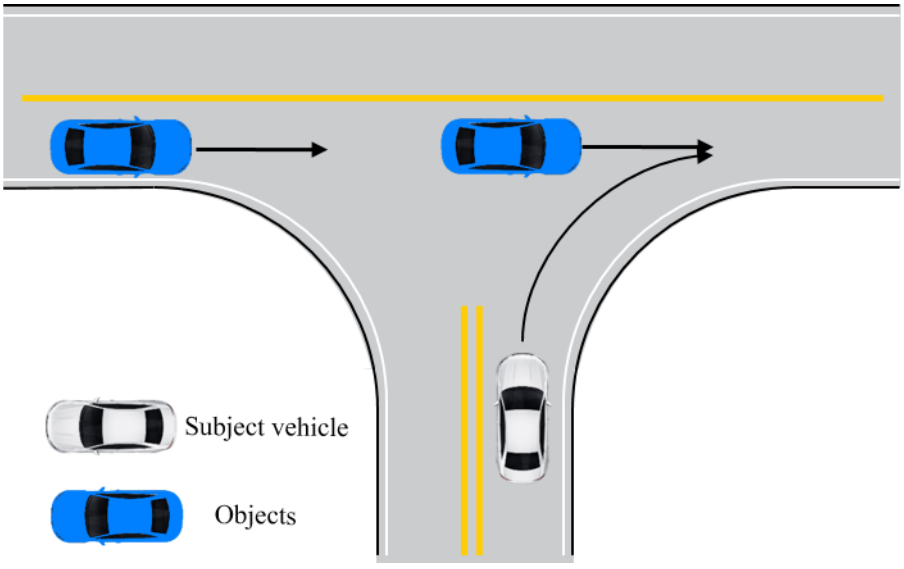

Figure 7-2: An example to illustrate the essential of the historical memory.

Limitation 3: not all errors can be identified by the proposed criticality index

Since the information of the surrounding objects are required to calculate the proposed criticality index, some other types of errors cannot be identified. For example, the subject vehicle stops at the wrong stop line due to the inaccuracy of the map. Another example could be the cross of a red traffic light at an intersection without traffic participants. As a result, the subject vehicle violates the traffic rules. In these scenarios, there is no interaction with the surrounding moveable objects. Thus, the identification of such errors is impossible by the proposed criticality index. Even if the triggers can be adapted according to the FuT in the VAAFO framework, the triggers for some kinds of errors are rather difficult to design. The aforementioned two examples belong exactly to this category.

7.3 Application Scope

Considering the coverage analysis and the limitations, the application scope of the VAAFO approach can be derived. Generally, the current proposed framework can be utilized to test the perception and decision modules of an ADS. Thus, if the software is not well designed, i.e., unsafe decisions emerge even in some simple scenarios, such errors in the software can be discovered by the approach. Additionally, the VAAFO approach is the only currently available approach for online detection of FP-prone scenarios by observing the criticality index of IiC and vAV instances. Furthermore, a level higher driving automation system than the engaged version can always be tested under real conditions without any additional risks. However, it requires that the IiC and the SuT have an overlapping action space, and the decision module does not rely on the historical memory based on the current framework. In addition, the trigger can be adjusted easily according to the demand. Other approaches should be studied to identify the errors that cannot easily be formulized as triggers.

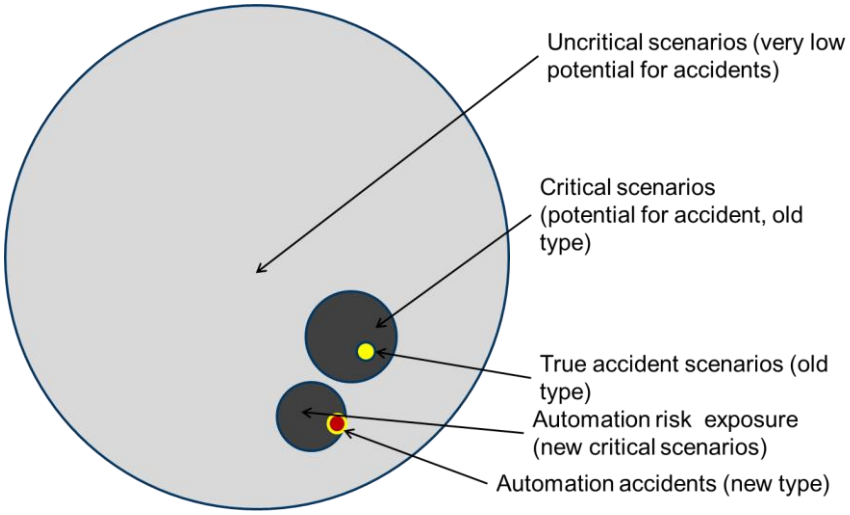

Figure 7-3: The “dark matter” problem of scenarios[232a]. (Hermann Winner, Walther Wachenfeld, Phillip Junietz, 2016), reprinted with permission

With respect to the role of the VAAFO approach for the safety verification and validation of AD, it can be considered as an extension of the real-world testing. The ODD for testing AD is extended and the safety driver is replaced by a normal driver. In addition, it can be regarded as an augmented reality of the simulation-based approach, since the environmental representation comes from the reality. No modelling of the environment is necessary. The scenario-based testing would be a promising approach for the verification and validation of AD.[231] However, the source of the scenarios is a problem. Winner et al.[232b] describe the source of the scenarios as a dark matter problem, since only the standard scenarios and the reported accident scenarios of AVs are known, as the red cycle illustrated in Figure 7-3. Other types of critical scenarios for AVs and their frequency stay in the dark area. Even though the real-world testing is a possible way to figure out the dark matter problem, its application is limited due to the slow testing process. Some unknown scenarios still exist.

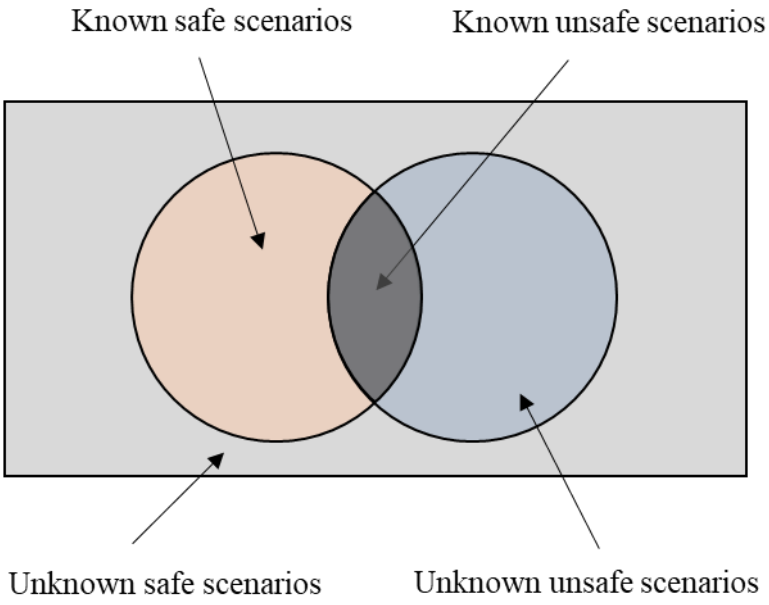

Figure 7-4: The relationship between known safe, known unsafe, unknown safe and unknown unsafe scenarios.

The dark matter can be further divided into unknown safe scenarios and unknown unsafe scenarios, as shown in Figure 7-4. Some of the unknown unsafe scenarios are already discovered by the current real-world testing or proving ground testing, and turned into know unsafe scenarios. Based on the known unsafe scenarios and the known safe scenarios, the generation and variation of scenarios for the scenario-based testing can be performed, i.e., prior knowledge is essential for the creation of scenarios when using the scenario-based testing. Therefore, the discovery of unknown unsafe scenarios serves as a very important source for the scenario-based testing. The unknown safe scenarios are of little interest, since an AV

[231] Neurohr, C. et al.: Fundamental considerations around scenario-based testing for automated driving (2020).

[232] Winner, H. et al.: (How) Can safety of automated driving be validated? (2016).a: -; b: p. 15.

could handle with the scenarios safely even the scenarios are unknown. In contrast, the unknown unsafe scenarios have a top priority. They include scenarios that have not been accounted for and scenarios that have not been identified.[233] They are the key scenarios that should be found and minimized. At this point, the VAAFO approach can contribute to find these unknown unsafe scenarios, since a lot of data can be obtained based on its principle. Therefore, the VAAFO framework can serve as an approach to find the relevant scenarios. Then, the scenario-based approach can be applied to generate more general and similar relevant scenarios. In the author's view, this combination is a promising way toward a safe AV.

The application of the VAAFO approach in collision avoidance systems (CASs) is worth to mention as well. Such system does not belong to the SAE levels of automation but is an essential part. The data of such system is usually available when an accident happens. If the driver or the CAS brakes sufficiently, no data would be obtained. The VAAFO approach provides a new way to acquire the data of such system without facing a real accident.

7.4 Summary

In this chapter, the potential contributions of the VAAFO approach for the safety verification and validation of AD is discussed. Its coverage is first analyzed. Principally, the approach is suitable for different levels of driving automation systems, and can be utilized to test the perception and decision modules. Then, the current existing limitations of the approach are presented. Based on the limitations and coverage analysis, the final application scope of the approach is derived. The approach can be combined with the scenario-based testing. The unknown unsafe scenarios could be minimized by the approach. The discovered scenarios can then be utilized as basic scenarios for generating more relevant scenarios. As a result, AVs can be improved and should be able to handle more scenarios. So, their functional boundaries will be gradually extended. Additionally, the approach is applicable to the systems of an AV with high test risks. The valuable data of those systems can be obtained without suffering from any additional risks in the VAAFO framework. Based on the derived application scope, the contribution of the VAAFO approach becomes clear, which could ease the current challenge of releasing AVs. With respect to the presented limitations, some possible methods to reduce or even eliminate them are introduced in the outlook and can be further studied to expand the application scope of the VAAFO approach.

[233] Hejase, M. et al.: A Validation Methodology for the Minimization of Unknown Unknowns (2020).

8 Conclusion and Outlook

8.1 Conclusion

The VAAFO approach as a new method for the safety verification and validation of AD is studied elaborately in this dissertation. The framework is established and the work flow is presented. Importantly, the VAAFO approach with all its essential components has been developed and implemented for the first time, and thus a first proof-of-concept of the silent testing with multiple instances has taken place. During the development of the VAAFO approach, some conclusions are drawn:

Firstly, a valid environmental representation to test vAV instances in the virtual world can be generated by a coordinate transformation and the two key parameters. With respect to the coordinate transformation, two different approaches for estimating the yaw acceleration are presented and compared. The real tests are carried out to validate the transformed results. Compared to the ground truth, it demonstrates that by predicting the data points for a half window length provides a better to estimate the yaw acceleration. In addition, the results show that the transformation process is correct. In addition to the coordinate transformation, the two key parameters are studied. They are the lifetime of one vAV instance and the birth cycle between the births of two time-adjacent vAV instances. Since both parameters can be either dynamic or constant, four combinations are discussed and compared. The analysis infers that the combination with constant lifetime and constant birth cycle outperforms the other combinations. Additionally, three vAV instances are derived by analyzing the limits of the lifetime parameter. The number of instances is supposed to cover critical scenarios at all times and ensure a valid environmental representation. As a result, vAV instances can be tested in the virtual world during the driving of an IiC in the real world.

Secondly, the proposed new criticality index is able to evaluate the safety of vAV instances online. In order to verify and validate the criticality index, simulation is executed. The possible ways to derive test scenarios are summarized, which could guide the derivation of test scenarios for testing other functions. The simulation results prove that the proposed criticality index is capable of assessing the safety of AVs in both the longitudinal and lateral directions. A critical scenario can be reflected successfully by the proposed criticality index. The test results of the implementation of the VAAFO approach in a real test vehicle on public roads further proves the conclusions derived from the simulation. The coverage of critical scenarios are enlarged by using multiple vAV instances. Additionally, the proposed criticality index is more sensitive to errors, and can identify critical situations earlier than the maximum TTC. Both the simulation and real test results indicate that the developed criticality index is quite appropriate to evaluate the safety of AVs online. Moreover, the results show that a

special designed ring buffer is essential in order to avoid saving a critical scenario for multiple times.

Thirdly, a scalable framework with standard interfaces for the VAAFO approach is established. Each necessary component is introduced. The entire architecture to connect different components is described and modular designed. As a result, the perception or the decision module can be replaced conveniently if a different version of FuT or the SuT should be tested. The interfaces between different components are defined. The defined triggers focus on the evaluation of the decision module, if the other modules of an AV are the focus of test, the triggers can be changed accordingly. Additionally, the proposed criticality index can be complemented by other existing criticality metrics to make a more comprehensive evaluation.

Fourthly, an ADS except motion control can be tested in the framework. According to real tests results, the errors from the perception and the decision modules can be detected by the proposed criticality index. By observing some phenomenon, whether an error comes from the perception or the decision can be even determined. With respect to the levels of driving automation system, a level higher than the current engaged level of driving automation system can always be tested in parallel in the development phase, since the test process is safe and the restriction in the virtual world is relaxed. In the implementation phase, an updated or the upgraded version can run silently during the driving. As a result, whether the update or the upgraded version outperforms the current version is obvious. Therefore, the VAAFO approach is capable of verifying and validating an ADS, which is at least level 3. Considering the existing limitations of the current VAAFO framework, the application scope of the approach is derived. Since it is possible to implement the approach in each customer vehicle with necessary hardware, the area of the unknown unsafe scenarios can be reduced. Through accumulated travel distances from the customer vehicles in daily driving operation, the macroscopic evaluation of AVs could even be concluded. Meanwhile, the unknown unsafe scenarios could be reduced gradually. The discovered previous unknown unsafe scenarios can then be utilized as scenario sources for the scenario-based testing. By using the collected valuable data by the VAAFO approach, the results of the scenario-based approach would be more informative and conclusive.

The current existing approaches, which include mainly the real-world testing, the simulation-based testing and the scenario-based testing, are shown to have some disadvantages a greater or less extent. Thus, the combination of different approaches is necessary. Through the analysis of the application scope of the VAAFO approach, it proves that it is possible to combine the VAAFO approach with other existing approaches. Critical scenarios can be found online by the VAAFO approach, which can then be varied to generate more relevant scenario for the scenario-based testing. In addition, the VAAFO approach opens a new way in the field of safety validation of AD and provide a new solution. Since there is currently no satisfying approach, the new technique could contribute to the safety verification and validation of AD to some extent. The basic knowledge and experience about this approach are gained by the development of the essential technical theory and the necessary fundamentals. Based on the

gained knowledge and experience, the approach can be applied when appropriate. Finally, its role in the entire family of safety validation of AD is determined.

8.2 Outlook

During the implementation of the approach, several simplifications are made. For example, only the tracked objects are transformed into the virtual world. Even though the objects are the most significant information for the decision module, there are still some other information in the environment that may also be relevant for the decision module. However, as along as the perceived information is based on the vehicle coordinate system, the same transformation process as described in subchapter 3.1 is still applicable. The occupancy grid map is useful, for instance, if the HD map is not available. Since the occupancy grid map is already based on an earth-fixed coordinate system, it can be directly projected in the virtual world. In the current VAAFO framework, which variables should be saved is little studied when the ring buffer is activated. However, the VAAFO user or organization can decide the variables to be saved by themselves with the help of the developed data recording interface. In this dissertation, the variables that are essential for the description of the OpenSCENARIO format are saved. However, other variables such as the point clouds, raw image may be useful as well for the verification of certain functions. A study about what data is useful for the safety verification and validation of AVs may be meaningful.

In the subchapter 7.2, three limitations are presented. With respect to the first limitation, a certain requirement for a vAV is posed. The VAAFO approach is applicable in the scenarios where a vAV have an overlapping action space with an IiC. This limitation cannot be completely solved due to the open-loop problem, but can be mitigated by either increasing the action space of an IiC or decreasing the action space of a vAV that lies outside the overlap area. Generally, every approach has its pros and cons. The VAAFO approach is no exception. However, each approach should leverage its strengths. The combination of different approaches would be a better solution to solve a complex problem. Regarding to the second limitation, a new vAV instance is initialized without historical memory in the current VAAFO framework. If a decision module needs the historical memory, this could be solved by initializing one or more vAV instances with historical memory. About the last limitation, some errors cannot be recognized by the criticality metrics, such as the violation of traffic rules but without resulting in a critical situation. This could be solved, for example, by concretizing and formalizing the traffic rules. The formalized rules can then be taken into account for the design of an ADS. Some researches[234,235,236] about formalization of the traffic

[234] Vanholme, B. et al.: Highly automated driving on highways based on legal safety (2012).

[235] Rizaldi, A.; Althoff, M.: Formalising traffic rules for accountability of autonomous vehicles (2015).

[236] Esterle, K. et al.: Formalizing traffic rules for machine interpretability (2020).

rules for the development of a legal safety functions are studied. However, not all traffic rules are easy to concretize, and the formalization itself should be validated as well. Furthermore, translating traffic rules into testable criteria would be also a possible way to address the last limitation. By using the derived criteria, it is possible to determine whether the decision of an ADS complies with the traffic rules. Both ways could help to solve the last limitation. Nevertheless, a lot of work remained with respect to this point.

A Appendix

A.1 Theory of the Yaw Acceleration Estimation

In the Savitzky-Golay filter, the jth smoothed data point Z_j is obtained by the measured data point z_{j+i} weighted by the convolution coefficients $C_{\text{onvl},i}$ and. l is the window length. n is the total number of data points. i is the ith point in the window length.

$$Z_j = \sum_{i=\frac{1-l}{2}}^{\frac{l-1}{2}} C_{\text{onvl},i}\, z_{j+i}, \quad \frac{l-1}{2} < j \leq n - \frac{l-1}{2} \tag{A.1}$$

The coefficients can be further obtained by the vandermonde matrix $\mathbf{J}$.

$$\mathbf{C_{onvl}} = (\mathbf{J^T J})^{-1}\mathbf{J^T} \tag{A.2}$$

Therefore, the $\mathbf{J}$ should be first acquired in order to obtain the smoothed data points. With respect to the method 1, since the filtered value at the latest time step is regarded as the smoothed value, no data points in the future are available, as shown in the left image of Figure A-1, the matrix $\mathbf{J}$ for a cubic polynomial can be expressed as:

$$\mathbf{J} = (\mathbf{E}, \mathbf{z}, \mathbf{z^2}, \mathbf{z^3}) \tag{A.3}$$

Where $\mathbf{z} = [1-l\,, 2-l\,, \cdots, 16-l\,, 0]^{\mathrm{T}}$ using a window length of 17. Only data points in the past are used to smooth the data point at the latest time step. The principles of the two methods are illustrated in Figure A-1. The black data points in the blue area are historical data, while the red data points in the brown area are estimated. t_{cur} represents the current time step.

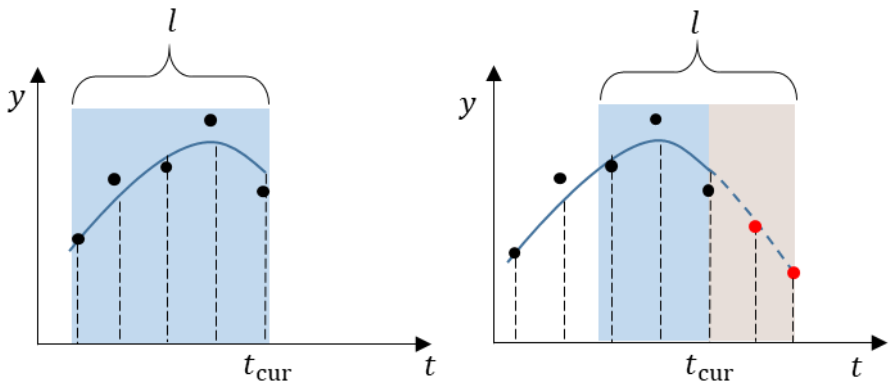

Figure A-1: left image: the illustration of the method 1; right image: the illustration of the method 2.

With respect the method 2, a cubic polynomial as expressed in (A.4) is first applied to fit the data points in a window length, as shown in the right image of Figure A-1.

$$Z = \sum_{k=0}^{3} b_k z^k \tag{A.4}$$

b denotes the coefficient of the kth order. Based on the time interval of two time steps, a period in the future covering a half window length of data points can be calculated. Using the cubic polynomial, the yaw rate in this period is estimated. The estimated data points are added to the last data points of the measurements. As a result, the middle of the window locates exactly at the latest time step. The extended data points are filtered by the Savitzky-Golay filter and the first derivative is then obtained.

A.2 Behavior Planner

Figure A-2 shows the defined modes for the behavior planer. S1-S13 are the switch conditions between different behaviors.

Each behavior is assigned with an initial cost. c_{stop} denotes the cost of the stop mode. c_{adap} is the cost of adaptive cruise mode. $c_{\text{chg,rt}}$ represents the cost of lane change right mode. $c_{\text{chg,lt}}$ denotes the cost of lane change left mode. c_{cruise} is the cost of cruise mode. The initial cost ranking between the different behaviors is

$$c_{\text{stop}} > c_{\text{adap}} > c_{\text{chg,rt}} > c_{\text{chg,lt}} > c_{\text{cruise}} \tag{A.5}$$

Table A-1: Different designed criteria and the corresponding descriptions

Nr.	Criterion	Description
Cond1	$d_x < d_{x,\text{s}}$	The clearance to a front vehicle d_x is less than a safe distance $d_{x,\text{s}}$
Cond2	$t_{\text{tc},x} < t_{\text{tc,crit}}$	The TTC value $t_{\text{tc},x}$ is less than a threshold $t_{\text{tc,crit}}$
Cond3	$d_{x,\text{fl}} < d_{x,\text{s}}$	The clearance to the front left vehicle $d_{\text{rel,lf}}$ is less than a safe distance $d_{x,\text{s}}$
Cond4	$d_{x,\text{rl}} < d_{x,\text{s}}$	The clearance to the rear left vehicle $d_{\text{rel,lr}}$ is less than a safe distance $d_{x,\text{s}}$
Cond5	$d_{x,\text{fr}} < d_{x,\text{s}}$	The clearance to the front right vehicle $d_{\text{rel,rf}}$ is less than a safe distance $d_{x,\text{s}}$
Cond6	$d_{x,\text{rr}} < d_{x,\text{s}}$	The clearance to the rear right vehicle $d_{\text{rel,rr}}$ is less than a safe distance $d_{x,\text{s}}$
Cond7	$l_{\text{ane,sub}} = l_{\text{ane,b}}$	The subject vehicle is located in the boundary lane
Cond8	$v_{x,\text{sub}} < v_{x,\text{l}}$	The velocity of the subject vehicle $v_{x,\text{sub}}$ is lower than a threshold $v_{x,\text{l}}$
Cond9	$v_{x,\text{obj}} < v_{x,\text{l}}$	The velocity of the preceding vehicle$v_{x,\text{obj}}$ is lower than a threshold $v_{x,\text{l}}$

The behavior with the minimum cost is the chosen behavior that is given to the trajectory planner. Based on the cost ranking, the cruise mode is first preferred at each update cycle.

When the cost of behavior will be increased to the collision cost depends on the defined criteria, as shown in Table A-1. The collision cost has the highest value.

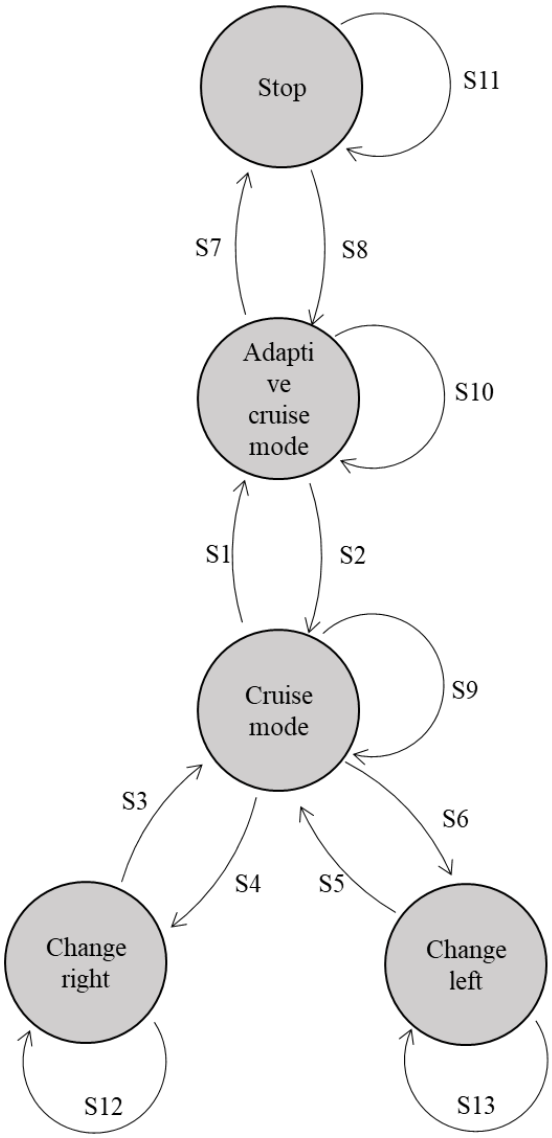

Figure A-2: The designed finite state machine for motorway scenarios.

Table A-2: The criteria to change the cost of a behavior.

Cost change	**Combination of criteria**
$c_{\text{cruise}} = c_{\text{coll}}$	Cond1 || Cond2
$c_{\text{chg,lt}} = c_{\text{coll}}$	Cond1 || Cond2 || Cond3 || Cond4 || Cond7
$c_{\text{chg,rt}} = c_{\text{coll}}$	Cond1 || Cond2 || Cond5 || Cond6 || Cond7
$c_{\text{stop}} < 0$	Cond1 and Cond8 and Cond9

The different switch conditions S1-S13 are implicitly expressed, since the behavior planner is considered as an optimization problem. If the defined criteria are met, the cost of the behavior itself is changed. As a result, a new cost ranking is generated. The behavior with minimum cost and has a transition with the current behavior is selected. It is worth to mention that the thresholds in Table A-1 should be calibrated for different modes, e.g., the $d_{x,\text{s}}$ in Cond1 for a stop mode could be different from that of a cruise mode. Table A-2 shows the

cost change of each behavior if certain criteria are met. c_{coll} denotes the collision cost, which is highest among other costs, i.e., if the cost of behavior will increase if it is unsafe. A negative value is assigned to the cost of stop mode if stop mode is the optimal maneuver.

A.3 Trajectory Planner

In this part, the constraints used in the MPC trajectory planner are presented elaborately. The constraints should be designed carefully in order to obtain reasonable solutions.

Acceleration constraints

The acceleration limits $\text{cstr}_{n,\text{a}} \in C_{\text{str},n}$ (the constraint set) can be written as:

$$\text{cstr}_{n,\text{a}} = [0\ 0\ 0\ 0\ \ {}_{\text{E}}a_{x,n}\ \ {}_{\text{E}}a_{y,n}] \tag{A.6}$$

The acceleration on the earth-fixed coordinate system can be further described as

$$\begin{bmatrix} {}_{\text{E}}a_{x,n} \\ {}_{\text{E}}a_{y,n} \end{bmatrix} = \begin{bmatrix} \cos(\psi) & -\sin(\psi) \\ \sin(\psi) & \cos(\psi) \end{bmatrix} \begin{bmatrix} {}_{\text{V}}a_{y,\max}\cos(2\pi i/k_{\text{ac}}) \\ {}_{\text{V}}a_{x,\max}\sin(2\pi i/k_{\text{ac}}) \end{bmatrix} \tag{A.7}$$

k_{ac} is the number of sides of the inscribed polygons in the acceleration ellipse and i is one of the side, i.e. $i \in [1, k_{\text{ac}}]$.

The yaw angle ψ of the vehicle can be determined from the velocity as follows

$$\psi = \text{atan2}\left({}_{\text{E}}v_{y,n},\ {}_{\text{E}}v_{x,n}\right) \tag{A.8}$$

The longitudinal maximum acceleration or maximum deceleration is expressed by

$${}_{\text{V}}a_{x,\max} = \begin{cases} D_{\max}, & \text{if } i \in [\frac{1}{4}k_{\text{ac}}, \frac{3}{4}k_{\text{ac}}] \\ \min\left(\mu g, \dfrac{EP_{\max}}{{}_{\text{V}}v_{x,n} \cdot m}\right), & \text{otherwise} \end{cases} \tag{A.9}$$

In equation (A.9), if the vehicle decelerates, the available maximum deceleration for braking $D_{\max}$ is utilized. Otherwise, the longitudinal acceleration is limited by the friction coefficient μ multiplies by the earth's gravity g and the maximum propulsion power $EP_{\max}$ that the vehicle has. The available longitudinal acceleration decreases with the increasing velocity when the propulsion power is constant. m is the mass of the vehicle.

The lower bound of acceleration is not limited. The upper limit of the acceleration is defined as

$$x_{\text{u},n,\text{acc}} = {}_{\text{V}}a_{x,\max} \cdot {}_{\text{V}}a_{y,\max} \cdot h \tag{A.10}$$

The apothem length h is extra multiplied by the maximum longitudinal and lateral accelerations to ensure the acceleration is inside the acceleration ellipse and defined as

$$h = \cos(\pi / k_{\mathrm{ac}}) \tag{A.11}$$

Speed Constraints

If the behavior gives the trajectory planner the command of the adaptive cruise mode or the cruise mode, the speed is constrained in order to achieve the goal speed. The speed constraint is defined as

$$\mathrm{cstr}_{n,\mathrm{vel}} = [0\ 0\ {}_{\mathrm{E}}e_{x,n,v}\ {}_{\mathrm{E}}e_{y,n,v}\ 0\ 0] \tag{A.12}$$

The unit vector of the velocity on the earth-fixed coordinate system can be further described as:

$${}_{\mathrm{E}}e_{x,n,v} = \cos(\psi_{\mathrm{ref}}),\ {}_{\mathrm{E}}e_{y,n,v} = \sin(\psi_{\mathrm{ref}}) \tag{A.13}$$

ψ_{ref} means the angle of two adjacent points on the reference line. Thus, the bounds on the speed are

$$x_{\mathrm{u},n,\mathrm{v}} = v_{\max}, x_{\mathrm{l},n,\mathrm{v}} = -v_{\max} \tag{A.14}$$

$v_{\max}$ is defined by the behavior planner.

Spatial constraints

Since the reference line is determined by the behavior planner, the trajectory planner should follow this reference line to minimize the cross-track errors. The spatial constraint can be formulized as

$$\mathrm{cstr}_{\mathrm{spatial}} = [e_x\ e_y\ 0\ 0\ 0\ 0] \tag{A.15}$$

$$e_x = -\sin(\psi_{\mathrm{ref}}), e_y = \cos(\psi_{\mathrm{ref}}) \tag{A.16}$$

$$e_{\mathrm{spatial}} = [e_x \quad e_y] \tag{A.17}$$

e_x and e_y are normalized components of the points along the reference line. They define the directional vector e_{spatial}, which is utilized to determine the lower and upper spatial constrains. The upper spatial constraint $x_{\mathrm{u,spatial}}$ and lower spatial constraint $x_{\mathrm{l,spatial}}$ are expressed by

$$x_{\mathrm{u,spatial}} = e_{\mathrm{spatial}} \cdot \begin{bmatrix} {}_{\mathrm{V}}p_{x,\mathrm{u}} \\ {}_{\mathrm{V}}p_{y,\mathrm{u}} \end{bmatrix} \tag{A.18}$$

$$x_{\mathrm{l,spatial}} = e_{\mathrm{spatial}} \cdot \begin{bmatrix} {}_{\mathrm{V}}p_{x,\mathrm{l}} \\ {}_{\mathrm{V}}p_{y,\mathrm{l}} \end{bmatrix} \tag{A.19}$$

$$\begin{bmatrix} {}_{\mathrm{V}}p_{x,\mathrm{u}} \\ {}_{\mathrm{V}}p_{y,\mathrm{u}} \end{bmatrix} = \begin{bmatrix} {}_{\mathrm{E}}p_{x,i} \\ {}_{\mathrm{E}}p_{y,i} \end{bmatrix} - \begin{bmatrix} {}_{\mathrm{E}}p_{x,\mathrm{sub}} \\ {}_{\mathrm{E}}p_{y,\mathrm{sub}} \end{bmatrix} + \begin{bmatrix} e_x \\ e_y \end{bmatrix} \tag{A.20}$$

$$\begin{bmatrix} {}_{\mathrm{V}}p_{x,\mathrm{l}} \\ {}_{\mathrm{V}}p_{y,\mathrm{l}} \end{bmatrix} = \begin{bmatrix} {}_{\mathrm{E}}p_{x,i} \\ {}_{\mathrm{E}}p_{y,i} \end{bmatrix} - \begin{bmatrix} {}_{\mathrm{E}}p_{x,\mathrm{sub}} \\ {}_{\mathrm{E}}p_{y,\mathrm{sub}} \end{bmatrix} - \begin{bmatrix} e_x \\ e_y \end{bmatrix} \tag{A.21}$$

${}_{\mathrm{E}}p_{x,i}$ and ${}_{\mathrm{E}}p_{y,i}$ are the ith point on a reference line. ${}_{\mathrm{E}}p_{x,\mathrm{sub}}$ and ${}_{\mathrm{E}}p_{y,\mathrm{sub}}$ denote the position of the subject vehicle. Through the spatial constraint, the subject vehicle will follow the reference line. If the behavior planner decides to enter lane change mode, the reference line is updated to the middle line of the intended lane.

Parameter list

The values of the important parameters for the trajectory planner are shown in Table A-3.

Table A-3: The values of the important parameters for the trajectory planning.

Parameter	Value	description
$\eth t$	0.2 s	The time interval between two time steps
N	40	The total number of time steps
k_{ac}	9	The number of acceleration constraints
$D_{\max}$	10 m/s^2	The maximum deceleration
${}_{\mathrm{V}}a_{y,\max}$	10 m/s^2	The maximum lateral acceleration
$EP_{\max}$	266 kW	The maximum engine power
μ	1.0	The friction coefficient between road and tire
m	1500 kg	The vehicle mass

A.4 Variables in Case 2

The lateral relative clearance d_y, the lateral relative velocity $v_{\mathrm{diff},y}$ and the longitudinal TTC value between the subject vehicle and the adjacent vehicle $t_{\mathrm{tc},x}$ in case 2 in chapter 5.2 are shown in Figure A-3. The d_y and $v_{\mathrm{diff},y}$ values of vAV1 and vAV3 keep almost constant except vAV2, which changes the lane. Thus, positive $v_{\mathrm{diff},y}$ values of vAV2 can be seen between 12 s and 13 s. The d_y decreases accordingly. The $t_{\mathrm{tc},x}$ is at the beginning very large. When the adjacent vehicle approaches the subject vehicle, the $t_{\mathrm{tc},x}$ decreases until they meet each other but in different lanes.

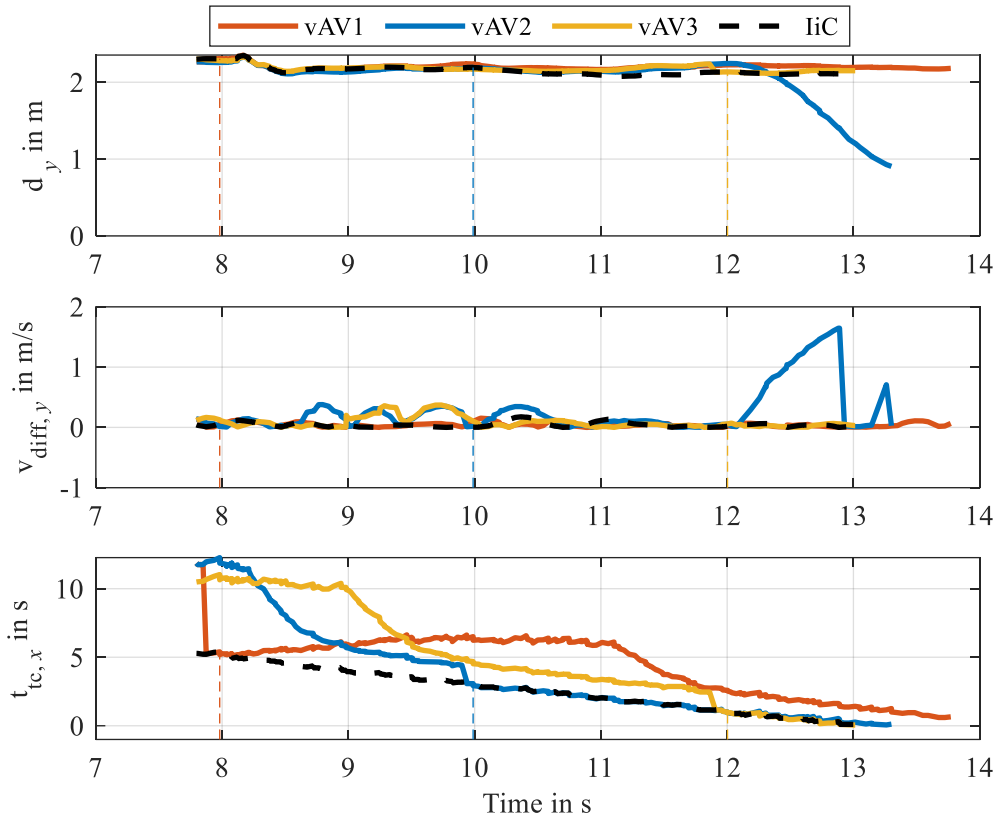

Figure A-3: The change in three important variables in case 2. The reset time steps are represented by vertical dotted lines with corresponding colors of vAV instances.

A.5 Sensor Fusion

The Bayes' theorem defines the posterior probability distribution of the state x_k given the measurements $Z_k = \{z_1, \cdots, z_k\}$ at time k as

$$p(x_k|Z_k) = \frac{p(z_k|x_k)p(x_k|Z_{k-1})}{p(Z_k|Z_{k-1})} \tag{A.22}$$

Since the denominator in equation (A.22) relies only on the measurements, the estimated state can be achieved by pursuing the maximum value of the numerator. This process is defined as the maximum a posterior (MAP) estimation, and is expressed by[237]

$$\hat{x}_{\mathrm{MAP}} = \max(p(x_k|Z_k)) \propto p(z_k|x_k)p(x_k|Z_{k-1}) \tag{A.23}$$

Actually, the probability distribution is sensor specific. However, the Gaussian distribution is frequently utilized to represent this probability distribution considering the sensor uncertainties and is given by the following equation

[237] Kumar, M. et al.: An approach for inconsistency detection in data fusion from multiple sensors (2006).

$$p(Z = z_k|X = x) = \frac{1}{\sigma_k\sqrt{2\pi}} e^{\frac{-(x-z_k)^2}{2\sigma_k^2}} \tag{A.24}$$

If the probability distribution of two sensor models are assumed to be Gaussian distribution, the fused MAP from the equation (A.23) is given by

$$\hat{x}_{\mathrm{MAP}} = \max\left(\frac{1}{2\sigma_1\sigma_2\pi} e^{\left\{\frac{-(x-z_1)^2}{2\sigma_1^2}+\frac{-(x-z_2)^2}{2\sigma_2^2}\right\}}\right) \tag{A.25}$$

σ_1 and σ_2 are the standard deviation of the two sensors. The equation (A.25) can be further rewritten as

$$\hat{x}_{\mathrm{MAP}} = \frac{\sigma_2^2}{\sigma_1^2+\sigma_2^2} z_1 + \frac{\sigma_1^2}{\sigma_1^2+\sigma_2^2} z_2 \tag{A.26}$$

The posterior joint probability distribution of two Gaussian distributions is a Gaussian distribution as well with a mean value $\hat{x}_{\mathrm{MAP}}$ and standard deviation σ

$$\sigma^2 = \frac{1}{\sigma_1^{-2}+\sigma_2^{-2}} \tag{A.27}$$

In the practical implementation, the equation (A.26) and (A.27) can be expressed by[238]

$$\hat{x} = \frac{P_2}{P_1+P_2}\hat{x}_1 + \frac{P_1}{P_1+P_2}\hat{x}_2 \tag{A.28}$$

$$P = \frac{1}{P_1^{-1}+P_2^{-1}} \tag{A.29}$$

$\hat{x}_1$ and $\hat{x}_2$ are the tracking results from two sensors. P_1 and P_2 are the corresponding covariances. Therefore, the smaller the covariance is, the higher the weight of the tracking results for that sensor.

[238] Chong, C.-Y. et al.: Architectures and algorithms for track association and fusion (2000).

List of References

Abdulhafiz, W. A.; Khamis, A.: Bayesian approach to multisensor data fusion (2013)
Abdulhafiz, Waleed A.; Khamis, Alaa: Bayesian approach to multisensor data fusion with Pre-and Post-Filtering, in: 2013 10th IEEE International Conference on Networking, Sensing and Control (ICNSC), 2013

aDDa: Automated Driving Darmstadt for Students (2021)
aDDa: Automated Driving Darmstadt for Students; https://www.tu-darmstadt.de/adda/adda/index.en.jsp, 2021, Access 19.05.2021

Aeberhard, M.; Kaempchen, N.: High-level sensor data fusion architecture for vehicle perception (2011)
Aeberhard, Michael; Kaempchen, Nico: High-level sensor data fusion architecture for vehicle surround environment perception, in: Proc. 8th Int. Workshop Intell. Transp, 2011

Akagi, Y. et al.: A risk-index based sampling method to generate scenarios for automated vehicle (2019)
Akagi, Yasuhiro; Kato, Ryosuke; Kitajima, Sou; Antona-Makoshi, Jacobo; Uchida, Nobuyuki: A risk-index based sampling method to generate scenarios for the evaluation of automated driving vehicle safety, in: 2019 IEEE Intelligent Transportation Systems Conference (ITSC), 2019

Allen, B. L. et al.: Analysis of traffic conflicts and collisions (1978)
Allen, Brian L.; Shin, B. T.; Cooper, Peter J.: Analysis of traffic conflicts and collisions, 1978

Alrifaee, B.; Maczijewski, J.: Real-time Trajectory optimization using Sequential Linearization (2018)
Alrifaee, Bassam; Maczijewski, Janis: Real-time Trajectory optimization for Autonomous Vehicle Racing using Sequential Linearization, in: 2018 IEEE Intelligent Vehicles Symposium (IV), 2018

Althoff, M.; Lutz, S.: Automatic generation of safety-critical test scenarios for collision avoidance (2018)
Althoff, Matthias; Lutz, Sebastian: Automatic generation of safety-critical test scenarios for collision avoidance of road vehicles, in: 2018 IEEE Intelligent Vehicles Symposium (IV), 2018

Amersbach, C.; Winner, H.: Functional Decomposition (2017)
Amersbach, Christian; Winner, Hermann: Functional Decomposition, in: 8. Tagung Fahrerassistenz, München, 2017

Amersbach, C.; Winner, H.: Defining Required and Feasible Test Coverage for Validation of HAV (2019)
Amersbach, Christian; Winner, Hermann: Defining Required and Feasible Test Coverage for Scenario-Based Validation of Highly Automated Vehicles*, in: 2019 IEEE Intelligent Transportation Systems Conference (ITSC), 2019

Amersbach, C.; Winner, H.: A contribution to overcome the parameter space explosion (2019)
Amersbach, Christian; Winner, Hermann: Functional decomposition—A contribution to overcome the parameter space explosion during validation of highly automated driving, in: Traffic Injury Prevention sup1, Issues 20, S52-S57, 2019

Amersbach, C. T.: Diss., Functional Decomposition Approach (2020)
Amersbach, Christian T.: Functional Decomposition Approach-Reducing the Safety Validation Effort for Highly Automated Driving, Dissertation TU Darmstadt, Darmstadt, 2020

Aparow, V. R. et al.: A Comprehensive Simulation Platform for Testing Autonomous Vehicles (2019)
Aparow, Vimal R.; Choudary, Apratim; Kulandaivelu, Giridharan; Webster, Thomas; Dauwels, Justin; Boer, Niels de: A Comprehensive Simulation Platform for Testing Autonomous Vehicles in 3D Virtual Environment, in: 2019 IEEE 5th International Conference on Mechatronics System and Robots (ICMSR), 2019

Archer, J.: Traffic conflict technique: Historical to current state-of-the-art (2001)
Archer, Jeffery: Traffic conflict technique: Historical to current state-of-the-art, in: Stockholm, Sweden: Kungl Tekniska Högskolan, 2001

Archer, J.: Methods for the assessment and prediction of traffic safety at urban intersections (2004)
Archer, Jeffery: Methods for the assessment and prediction of traffic safety at urban intersections and their application in micro-simulation modelling, in: Royal institute of technology, 2004

Arief, H. A. et al.: SAnE: Smart Annotation and Evaluation Tools for Point Cloud Data (2020)
Arief, Hasan A.; Arief, Mansur; Zhang, Guilin; Liu, Zuxin; Bhat, Manoj; Indahl, Ulf G.; Tveite, Håvard; Zhao, Ding: SAnE: Smart Annotation and Evaluation Tools for Point Cloud Data, in: IEEE Access, Issues 8, pp. 131848–131858, 2020

ASAM: OpenDRIVE (2021)
ASAM: OpenDRIVE; https://www.asam.net/standards/detail/opendrive/, 2021, Access 10.05.2021

ASAM: OpenSCENARIO (2021)
ASAM: OpenSCENARIO; https://www.asam.net/standards/detail/openscenario/, 2021, Access 10.05.2021

Åsljung, D. et al.: Comparing collision threat measures for verification of autonomous vehicles (2016)
Åsljung, Daniel; Nilsson, Jonas; Fredriksson, Jonas: Comparing collision threat measures for verification of autonomous vehicles using extreme value theory, in: IFAC-PapersOnLine (15), Issues 49, pp. 57–62, 2016

Åsljung, D. et al.: Using extreme value theory for vehicle level safety validation and implications (2017)
Åsljung, Daniel; Nilsson, Jonas; Fredriksson, Jonas: Using extreme value theory for vehicle level safety validation and implications for autonomous vehicles, in: IEEE Transactions on intelligent vehicles (4), Issues 2, pp. 288–297, 2017

Bagschik, G. et al.: Ontology based scene creation for the development of automated vehicles (2018)
Bagschik, Gerrit; Menzel, Till; Maurer, Markus: Ontology based scene creation for the development of automated vehicles, in: 2018 IEEE Intelligent Vehicles Symposium (IV), 2018

Baidu: Apollo-Homepage (2021)
Baidu: Apollo-Homepage; https://apollo.auto/, 2021, Access 15.03.2021

Banerjee, K. et al.: Online Camera LiDAR Fusion and Object Detection on Hybrid Data (2018)
Banerjee, Koyel; Notz, Dominik; Windelen, Johannes; Gavarraju, Sumanth; He, Mingkang: Online Camera LiDAR Fusion and Object Detection on Hybrid Data for Autonomous Driving, in: 2018 IEEE Intelligent Vehicles Symposium (IV), 2018

Bars, C.-R. C.: American Association of State Highway and Transportation Officials (2000)
Bars, Corrosion-Resistant C. D.: American Association of State Highway and Transportation Officials, in: Specification M254-77, Washington, DC, 2000

Batsch, F. et al.: Performance boundary identification using Gaussian process classification (2019)
Batsch, Felix; Daneshkhah, Alireza; Cheah, Madeline; Kanarachos, Stratis; Baxendale, Anthony: Performance boundary identification for the evaluation of automated vehicles using Gaussian process classification, in: 2019 IEEE Intelligent Transportation Systems Conference (ITSC), 2019

Batsch, F. et al.: A taxonomy of validation strategies to ensure safety of automated vehicles (2020)
Batsch, Felix; Kanarachos, Stratis; Cheah, Madeline; Ponticelli, Roberto; Blundell, Mike: A taxonomy of validation strategies to ensure the safe operation of highly automated vehicles, in: Journal of Intelligent Transportation Systems (0), Issues 0, pp. 1–20, 2020

Behrisch, M. et al.: SUMO - simulation of urban mobility: an overview (2011)
Behrisch, Michael; Bieker, Laura; Erdmann, Jakob; Krajzewicz, Daniel: SUMO - simulation of urban mobility: an overview, in: Proceedings of SIMUL 2011, The Third International Conference on Advances in System Simulation, 2011

Bock, J. et al.: Data basis for scenario-based validation of HAD on highways (2018)
Bock, Julian; Krajewski, R.; Eckstein, L.; Klimke, J.; Sauerbier, J.; Zlocki, A.: Data basis for scenario-based validation of HAD on highways, in: 27th Aachen colloquium automobile and engine technology, 2018

Bock, J. et al.: The ind dataset: A drone dataset of road user trajectories at german intersections (2019)
Bock, Julian; Krajewski, Robert; Moers, Tobias; Runde, Steffen; Vater, Lennart; Eckstein, Lutz: The ind dataset: A drone dataset of naturalistic road user trajectories at german intersections, in: 2020 IEEE Intelligent Vehicles Symposium (IV), 2019

Bolte, J. A. et al.: Towards corner case detection for autonomous driving (2019)
Bolte, Jan A.; Bar, Andreas; Lipinski, Daniel; Fingscheidt, Tim: Towards corner case detection for autonomous driving, in: 2019 IEEE Intelligent Vehicles Symposium (IV), 2019

Brannstrom, M. et al.: A situation and threat assessment for a rear-end collision avoidance system (2008)
Brannstrom, Mattias; Sjoberg, Jonas; Coelingh, Erik: A situation and threat assessment algorithm for a rear-end collision avoidance system, in: 2008 IEEE Intelligent Vehicles Symposium, 2008

Brechtel, S. et al.: Probabilistic MDP-behavior planning for cars (2011)
Brechtel, Sebastian; Gindele, Tobias; Dillmann, Rüdiger: Probabilistic MDP-behavior planning for cars, in: 2011 14th International IEEE Conference on Intelligent Transportation Systems (ITSC), 2011

Brechtel, S. et al.: Probabilistic decision-making under uncertainty using continuous POMDPs (2014)
Brechtel, Sebastian; Gindele, Tobias; Dillmann, Rüdiger: Probabilistic decision-making under uncertainty for autonomous driving using continuous POMDPs, in: 17th international IEEE conference on intelligent transportation systems (ITSC), 2014

Breitenstein, J. et al.: Corner Cases for Visual Perception in Automated Driving (2021)
Breitenstein, Jasmin; Termöhlen, Jan-Aike; Lipinski, Daniel; Fingscheidt, Tim: Corner Cases for Visual Perception in Automated Driving: Some Guidance on Detection Approaches, in: arXiv preprint arXiv:2102.05897, 2021

Brezak, M.; Petrović, I.: Real-time approximation of clothoids with bounded error for path planning (2013)
Brezak, Mišel; Petrović, Ivan: Real-time approximation of clothoids with bounded error for path planning applications, in: IEEE Transactions on Robotics (2), Issues 30, pp. 507–515, 2013

Broadhurst, A. et al.: Monte Carlo road safety reasoning (2005)
Broadhurst, Adrian; Baker, Simon; Kanade, Takeo: Monte Carlo road safety reasoning, in: IEEE Proceedings. Intelligent Vehicles Symposium, 2005, 2005

Buerkle, C. et al.: Towards Online Environment Model Verification (2020)
Buerkle, Cotnelius; Oboril, Fabian; Scholl, Kay-Ulrich: Towards Online Environment Model Verification, in: 2020 IEEE 23rd International Conference on Intelligent Transportation Systems (ITSC), 2020

Chartrand, R.: Numerical differentiation of noisy, nonsmooth data (2011)
Chartrand, Rick: Numerical differentiation of noisy, nonsmooth data, in: International Scholarly Research Notices, Issues 2011, 2011

Chong, C.-Y. et al.: Architectures and algorithms for track association and fusion (2000)
Chong, Chee-Yee; Mori, Shozo; Barker, William H.; Chang, Kuo-Chu: Architectures and algorithms for track association and fusion, in: IEEE Aerospace and Electronic Systems Magazine (1), Issues 15, pp. 5–13, 2000

Claussmann, L. et al.: A Review of Motion Planning for Highway Autonomous Driving (2020)
Claussmann, Laurène; Revilloud, Marc; Gruyer, Dominique; Glaser, Sébastien: A Review of Motion Planning for Highway Autonomous Driving, in: IEEE Transactions on Intelligent Transportation Systems (5), Issues 21, pp. 1826–1848, 2020

Colwell, I. et al.: A safety concept based on runtime restriction of the operational design domain (2018)
Colwell, Ian; Phan, Buu; Saleem, Shahwar; Salay, Rick; Czarnecki, Krzysztof: An automated vehicle safety concept based on runtime restriction of the operational design domain, in: 2018 IEEE Intelligent Vehicles Symposium (IV), 2018

Concas, F. et al.: Validation Frameworks for Self-Driving Vehicles: A Survey (2021)
Concas, Francesco; Nurminen, Jukka K.; Mikkonen, Tommi; Tarkoma, Sasu: Validation Frameworks for Self-Driving Vehicles: A Survey, in: Smart Cities: A Data Analytics Perspective, Springer, 2021

Cordts, M. et al.: The cityscapes dataset for semantic urban scene understanding (2016)
Cordts, Marius; Omran, Mohamed; Ramos, Sebastian; Rehfeld, Timo; Enzweiler, Markus; Benenson, Rodrigo; Franke, Uwe; Roth, Stefan; Schiele, Bernt: The cityscapes dataset for semantic urban scene understanding, in: Proceedings of the IEEE conference on computer vision and pattern recognition, 2016

Corso, A. et al.: Adaptive stress testing with reward augmentation for autonomous vehicle validatio (2019)
Corso, Anthony; Du, Peter; Driggs-Campbell, Katherine; Kochenderfer, Mykel J.: Adaptive stress testing with reward augmentation for autonomous vehicle validatio, in: 2019 IEEE Intelligent Transportation Systems Conference (ITSC), 2019

Cunto, F.; Saccomanno, F. F.: Calibration and validation of simulated vehicle safety performance (2008)
Cunto, Flávio; Saccomanno, Frank F.: Calibration and validation of simulated vehicle safety performance at signalized intersections, in: Accident Analysis & Prevention (3), Issues 40, pp. 1171–1179, 2008

Czarnecki, K.: Operational Design Domain for Automated Driving Systems (2018)
Czarnecki, Krysztof: Operational Design Domain for Automated Driving Systems: Taxonomy of Basic Terms, in: Waterloo Intelligent Systems Engineering (WISE) Lab, University of Waterloo, Canada, 2018

Das, S.; Maurya, A. K.: Defining Time-to-Collision Thresholds in Non-Lane-Based Environments (2019)
Das, Sanhita; Maurya, Akhilesh K.: Defining Time-to-Collision Thresholds by the Type of Lead Vehicle in Non-Lane-Based Traffic Environments, in: IEEE Transactions on Intelligent Transportation Systems (12), Issues 21, pp. 4972–4982, 2019

Dietmayer, K.: Prädiktion von maschineller Wahrnehmungsleistung (2015)
Dietmayer, Klaus: Prädiktion von maschineller Wahrnehmungsleistung beim automatisierten Fahren, in: Maurer, Markus; Gerdes, J. C.; Lenz, Barbara; Winner, Hermann (Eds.): Autonomes Fahren, Springer Berlin Heidelberg, Berlin, Heidelberg, 2015

Dietmayer, K. et al.: Repräsentation fusionierter Umfelddaten (2015)
Dietmayer, Klaus; Nuß, Dominik; Reuter, Stephan: Repräsentation fusionierter Umfelddaten, in: Winner, Hermann; Hakuli, Stephan; Lotz, Felix; Singer, Christina (Eds.): Handbuch Fahrerassistenzsysteme, Springer Fachmedien Wiesbaden, Wiesbaden, 2015

Dietmayer, K.: Predicting of Machine Perception for Automated Driving (2016)
Dietmayer, Klaus: Predicting of Machine Perception for Automated Driving, in: Maurer, Markus; Gerdes, J. C.; Lenz, Barbara; Winner, Hermann (Eds.): Autonomous Driving, Springer Berlin Heidelberg, Berlin, Heidelberg, 2016

Dijkstra, E. W.; others: A note on two problems in connexion with graphs (1959)
Dijkstra, Edsger W.; others: A note on two problems in connexion with graphs, in: Numerische mathematik (1), Issues1, pp. 269–271, 1959

Dobberstein, J. et al.: The openPASS-an approach to safety impact assessment via simulation (2017)
Dobberstein, Jan; Bakker, Joerg; Wang, Lei; Vogt, Timo; Düring, Michael; Stark, Lukas; Gainey, Jason; Prahl, Alexander; Mueller, Ralph; Blondelle, Gaël: The Eclipse Working Group openPASS-an open source approach to safety impact assessment via simulation, in: Proc. 25th ESV Conference, 2017

Domhardt, K.: Retrospektive Korrektur von Objektexistenzfehlern (2016)
Domhardt, Kai: Retrospektive Korrektur von Objektexistenzfehlern in der Umfelderfassung, Bachelorthesis No.: 1279/16., 2016

Dosovitskiy, A. et al.: CARLA: An open urban driving simulator (2017)
Dosovitskiy, Alexey; Ros, German; Codevilla, Felipe; Lopez, Antonio; Koltun, Vladlen: CARLA: An open urban driving simulator, in: Conference on robot learning, 2017

Engel, S. et al.: Car2pedestrian positioning: Methods for improving gps positioning (2013)
Engel, Sebastian; Kratzsch, Claudia; David, Klaus; Warkow, Dominik; Holzknecht, Marco: Car2pedestrian positioning: Methods for improving gps positioning in radio-based vru protection systems, in: 6. Tagung Fahrerassistenzsysteme, 2013

Erdogan, A. et al.: Real-world maneuver extraction for validation: A comparative study (2019)
Erdogan, Ahmetcan; Ugranli, Burak; Adali, Erkan; Sentas, Ali; Mungan, Eren; Kaplan, Emre; Leitner, Andrea: Real-world maneuver extraction for autonomous vehicle validation: A comparative study, in: 2019 IEEE Intelligent Vehicles Symposium (IV), 2019

Esterle, K. et al.: Formalizing traffic rules for machine interpretability (2020)
Esterle, Klemens; Gressenbuch, Luis; Knoll, Alois: Formalizing traffic rules for machine interpretability, in: arXiv preprint arXiv:2007.00330, 2020

Fayazi, S. A.; Vahidi, A.: Vehicle-in-the-loop verification of a smart city intersection control scheme (2017)
Fayazi, S. A.; Vahidi, Ardalan: Vehicle-in-the-loop (VIL) verification of a smart city intersection control scheme for autonomous vehicles, in: 2017 IEEE Conference on Control Technology and Applications (CCTA), 2017

Feng, S. et al.: Testing scenario library generation for connected and automated vehicles (2020)
Feng, Shuo; Feng, Yiheng; Sun, Haowei; Bao, Shan; Zhang, Yi; Liu, Henry X.: Testing scenario library generation for connected and automated vehicles, part II: Case studies, in: IEEE Transactions on Intelligent Transportation Systems, 2020

Frison, G.; Diehl, M.: HPIPM: a quadratic programming framework for model predictive control (2020)
Frison, Gianluca; Diehl, Moritz: HPIPM: a high-performance quadratic programming framework for model predictive control, in: arXiv preprint arXiv:2003.02547, 2020

Gassmann, B. et al.: Towards standardization of av safety: a library for responsibility sensitive safety (2019)
Gassmann, Bernd; Oboril, Fabian; Buerkle, Cornelius; Liu, Shuang; Yan, Shoumeng; Elli, Maria S.; Alvarez, Ignacio; Aerrabotu, Naveen; Jaber, Suhel; van Beek, Peter; others: Towards standardization of av safety: C++ library for responsibility sensitive safety, in: 2019 IEEE Intelligent Vehicles Symposium (IV), 2019

Geiger, A. et al.: Vision meets robotics (2013)
Geiger, Andreas; Lenz, Philip; Stiller, Christoph; Urtasun, Raquel: Vision meets robotics, in: The International Journal of Robotics Research (11), Issues 32, pp. 1231–1237, 2013

Gelbal, Ş. Y. et al.: Hardware-in-the-loop simulator for developing automated driving algorithms (2017)
Gelbal, Şükrü Y.; Tamilarasan, Santhosh; Cantaş, Mustafa R.; Güvenç, Levent; Aksun-Güvenç, Bilin: A connected and autonomous vehicle hardware-in-the-loop simulator for developing automated driving algorithms, in: 2017 IEEE International Conference on Systems, Man, and Cybernetics (SMC), 2017

Gelder, E. de**; Paardekooper, J.-P.: Assessment of automated driving systems using real-life scenarios (2017)**
Gelder, Erwin de; Paardekooper, Jan-Pieter: Assessment of automated driving systems using real-life scenarios, in: 2017 IEEE Intelligent Vehicles Symposium (IV), 2017

German Aerospace Center: PEGASUS-Project (2019)
German Aerospace Center: PEGASUS-Project; https://www.pegasusprojekt.de/en/home, 2019, Access 22.03.2021

Geyer, S. et al.: Concept and development of a unified ontology for test and use-case catalogues (2013)
Geyer, Sebastian; Baltzer, Marcel; Franz, Benjamin; Hakuli, Stephan; Kauer, Michaela; Kienle, Martin; Meier, Sonja; Weißgerber, Thomas; Bengler, Klaus; Bruder, Ralph; others: Concept and development of a unified ontology for generating test and use-case catalogues for assisted and automated vehicle guidance, in: IET Intelligent Transport Systems (3), Issues 8, pp. 183–189, 2013

Göhring, D. et al.: Radar/lidar sensor fusion for car-following on highways (2011)
Göhring, Daniel; Wang, Miao; Schnürmacher, Michael; Ganjineh, Tinosch: Radar/lidar sensor fusion for car-following on highways, in: The 5th International Conference on Automation, Robotics and Applications, 2011

Grindal, M. et al.: Combination testing strategies: a survey (2005)
Grindal, Mats; Offutt, Jeff; Andler, Sten F.: Combination testing strategies: a survey, in: Software Testing, Verification and Reliability (3), Issues 15, pp. 167–199, 2005

Guarino, N. et al.: What Is an Ontology? (2009)
Guarino, Nicola; Oberle, Daniel; Staab, Steffen: What Is an Ontology?, in: Staab, Steffen; Studer, Rudi (Eds.): Handbook on Ontologies, Springer Berlin Heidelberg, Berlin, Heidelberg, 2009

Guido, G. et al.: Comparing safety performance measures obtained from video capture data (2011)
Guido, Giuseppe; Saccomanno, Frank; Vitale, Alessandro; Astarita, Vittorio; Festa, Demetrio: Comparing safety performance measures obtained from video capture data, in: Journal of transportation engineering (7), Issues 137, pp. 481–491, 2011

Gyllenhammar, M. et al.: Towards an operational design domain that supports safety argumentation (2020)
Gyllenhammar, Magnus; Johansson, Rolf; Warg, Fredrik; Chen, DeJiu; Heyn, Hans-Martin; Sanfridson, Martin; Söderberg, Jan; Thorsén, Anders; Ursing, Stig: Towards an operational design domain that supports the safety argumentation of an automated driving system, in: 10th European Congress on Embedded Real Time Systems (ERTS 2020), 2020

Hajri, H.; Rahal, M.-C.: Lidar and radar high-level fusion for obstacle detection and tracking (2018)
Hajri, Hatem; Rahal, Mohamed-Cherif: Real time lidar and radar high-level fusion for obstacle detection and tracking with evaluation on a ground truth, in: arXiv preprint arXiv:1807.11264, 2018

Haklay, M.; Weber, P.: Openstreetmap: User-generated street maps (2008)
Haklay, Mordechai; Weber, Patrick: Openstreetmap: User-generated street maps, in: IEEE Pervasive computing (4), Issues 7, pp. 12–18, 2008

Hallerbach, S. et al.: Simulation-based identification of critical scenarios for automated vehicles (2018)
Hallerbach, Sven; Xia, Yiqun; Eberle, Ulrich; Koester, Frank: Simulation-based identification of critical scenarios for cooperative and automated vehicles, in: SAE International Journal of Connected and Automated Vehicles 2018-01-1066, Issues1, pp. 93–106, 2018

Hart, P. E. et al.: A formal basis for the heuristic determination of minimum cost paths (1968)
Hart, Peter E.; Nilsson, Nils J.; Raphael, Bertram: A formal basis for the heuristic determination of minimum cost paths, in: IEEE transactions on Systems Science and Cybernetics (2), Issues 4, pp. 100–107, 1968

Hartjen, L. et al.: Classification of driving maneuvers in urban traffic for parametrization of scenarios (2019)
Hartjen, Lukas; Philipp, Robin; Schuldt, Fabian; Friedrich, Bernhard; Howar, Falk: Classification of driving maneuvers in urban traffic for parametrization of test scenarios, in: 9. Tagung Automatisiertes Fahren, 2019

Hayward, J. C.: Near miss determination through use of a scale of danger (1972)
Hayward, John C.: Near miss determination through use of a scale of danger, in: Pennsylvania State University University Park, 1972

Heinrich, S.: Flash memory in the emerging age of autonomy (2017)
Heinrich, Stephan: Flash memory in the emerging age of autonomy, in: Flash Memory Summit, 2017

Hejase, M. et al.: A Validation Methodology for the Minimization of Unknown Unknowns (2020)
Hejase, Mohammad; Barbier, Mathieu; Ozguner, Umit; Ibanez-Guzman, Javier; Acarman, Tankut: A Validation Methodology for the Minimization of Unknown Unknowns in Autonomous Vehicle Systems, in: 2020 IEEE Intelligent Vehicles Symposium (IV), pp. 114–119, 2020

Hillenbrand, J. et al.: A multilevel collision mitigation approach (2006)
Hillenbrand, Jrg; Spieker, Andreas M.; Kroschel, Kristian: A multilevel collision mitigation approach—Its situation assessment, decision making, and performance tradeoffs, in: IEEE Transactions on Intelligent Transportation Systems (4), Issues 7, pp. 528–540, 2006

Hoel, C.-J. et al.: Combining Planning and Deep Reinforcement Learning in Decision Making (2020)
Hoel, Carl-Johan; Driggs-Campbell, Katherine; Wolff, Krister; Laine, Leo; Kochenderfer, Mykel J.: Combining Planning and Deep Reinforcement Learning in Tactical Decision Making for Autonomous Driving, in: IEEE Transactions on intelligent vehicles (2), Issues 5, pp. 294–305, 2020

Holder, M. et al.: Measurements revealing challenges in radar sensor modeling for virtual validation (2018)
Holder, Martin; Rosenberger, Philipp; Winner, Hermann; D'hondt, Thomas; Makkapati, Vamsi P.; Maier, Michael; Schreiber, Helmut; Magosi, Zoltan; Slavik, Zora; Bringmann, Oliver; others: Measurements revealing challenges in radar sensor modeling for virtual validation of autonomous driving, in: 2018 21st International Conference on Intelligent Transportation Systems (ITSC), 2018

Horváth, M. T. et al.: The Scenario-in-the-Loop (SciL) automotive simulation concept (2019)
Horváth, Márton T.; Tettamanti, Tamás; Varga, Balázs; Szalay, Zsolt: The Scenario-in-the-Loop (SciL) automotive simulation concept and its realisation principles for traffic control, in: Proceedings of the 8th Symposium of the European Association for Research in Transportation, Budapest, Hungray, 2019

Huber, B. et al.: Evaluation of Traffic Situations based on Multidimensional Criticality Analysis (2020)
Huber, Bernd; Herzog, Steffen; Sippl, Christoph; German, Reinhard; Djanatliev, Anatoli: Evaluation of Virtual Traffic Situations for Testing Automated Driving Functions based on Multidimensional Criticality Analysis, in: 2020 IEEE 23rd International Conference on Intelligent Transportation Systems (ITSC), 2020

IPG Automotive GmbH: CarMaker (2020)
IPG Automotive GmbH: CarMaker; https://ipg-automotive.com/de/produkte-services/simulation-software/carmaker/, 2020, Access 21.03.2021

ISO, I. S.; PAS, A. W.: 21448: Road vehicles—Safety of the intended functionality (2019)
ISO, I. S.; PAS, A. W.: 21448: Road vehicles—Safety of the intended functionality, in: Publicly Available Specification, 2019

ISO: ISO 26262: Road Vehicles—Functional Safety—Part 1: Vocabulary (2011)
ISO: ISO 26262: Road Vehicles—Functional Safety—Part 1: Vocabulary, 2011

ISO: ISO/TR 4804: Road Vehicles – Safety and security for automated driving systems (2020)
ISO: ISO/TR 4804: Road Vehicles – Safety and security for automated driving systems – Design, verification and validation methods, 2020

Jaakkola, A. et al.: Retrieval algorithms for road surface modelling using laser-based mapping (2008)
Jaakkola, Anttoni; Hyyppä, Juha; Hyyppä, Hannu; Kukko, Antero: Retrieval algorithms for road surface modelling using laser-based mobile mapping, in: Sensors (9), Issues 8, pp. 5238–5249, 2008

Jansson, J.: Diss., Collision Avoidance Theory (2005)
Jansson, Jonas: Collision Avoidance Theory: With application to automotive collision mitigation
Linköping University Electronic Press, 2005

Jiang, H.; Lu, F.: A Story Different from Tesla Driving the Chinese Automobile Industry (2018)
Jiang, Hong; Lu, Feng: To Be Friends, Not Competitors: A Story Different from Tesla Driving the Chinese Automobile Industry, in: Management and Organization Review (3), Issues 14, pp. 491–499, 2018

Jo, K. et al.: Simultaneous localization and map change update for the high definition map (2018)
Jo, Kichun; Kim, Chansoo; Sunwoo, Myoungho: Simultaneous localization and map change update for the high definition map-based autonomous driving car, in: Sensors (9), Issues 18, p. 3145, 2018

Jordan Golson: Tesla's new Autopilot will run in 'shadow mode' (2016)
Jordan Golson: Tesla's new Autopilot will run in 'shadow mode' to prove that it's safer than human driving; https://www.theverge.com/2016/10/19/13341194/tesla-autopilot-shadow-mode-autonomous-regulations, 2016

Junietz, P. et al.: Metric for the Safety Validation using Model Predictive Trajectory Optimization (2018)
Junietz, Philipp; Bonakdar, Farid; Klamann, Björn; Winner, Hermann: Criticality Metric for the Safety Validation of Automated Driving using Model Predictive Trajectory Optimization, in: 2018 21st International Conference on Intelligent Transportation Systems (ITSC), 2018

Junietz, P. et al.: Evaluation of Different Approaches to Address Safety Validation (2018)
Junietz, Philipp; Wachenfeld, Walther; Klonecki, Kamil; Winner, Hermann: Evaluation of Different Approaches to Address Safety Validation of Automated Driving, in: 2018 21st International Conference on Intelligent Transportation Systems (ITSC), 2018

Junietz, P. et al.: Gaining Knowledge on Automated Driving's Safety—The Risk-Free VAAFO Tool (2019)
Junietz, Philipp; Wachenfeld, Walther; Schönemann, Valerij; Domhardt, Kai; Tribelhorn, Wadim; Winner, Hermann: Gaining Knowledge on Automated Driving's Safety—The Risk-Free VAAFO Tool, in: Waschl, Harald; Kolmanovsky, Ilya; Willems, Frank (Eds.): Control Strategies for Advanced Driver Assistance Systems and Autonomous Driving Functions, Lecture Notes in Control and Information Sciences Nr. 476, Springer International Publishing, Cham, 2019

Junietz, P. M.: Diss., Microscopic and Macroscopic Risk Metrics (2019)
Junietz, Philipp M.: Microscopic and Macroscopic Risk Metrics for the Safety Validation of Automated Driving, Dissertation TU Darmstadt, Darmstadt, 2019

Kalra, N.; Paddock, S. M.: Driving to safety (2016)
Kalra, Nidhi; Paddock, Susan M.: Driving to safety, in: Transportation Research Part A: Policy and Practice, Issues 94, pp. 182–193, 2016

Kang, Y. et al.: Test your self-driving algorithm: An overview of publicly available driving datasets (2019)
Kang, Yue; Yin, Hang; Berger, Christian: Test your self-driving algorithm: An overview of publicly available driving datasets and virtual testing environments, in: IEEE Transactions on intelligent vehicles (2), Issues 4, pp. 171–185, 2019

Karaman, S.; Frazzoli, E.: Optimal motion planning using incremental sampling-based methods (2010)
Karaman, Sertac; Frazzoli, Emilio: Optimal kinodynamic motion planning using incremental sampling-based methods, in: 49th IEEE conference on decision and control (CDC), 2010

Karpathy, A.: System and Method for obtaining training data (2020)
Karpathy, Andrej.: System and Method for obtaining training data, Patent U.S. Patent WO/2020/056331, 2020

Karunakaran, D. et al.: Efficient statistical validation with edge cases to evaluate Automated Vehicles (2020)
Karunakaran, Dhanoop; Worrall, Stewart; Nebot, Eduardo: Efficient statistical validation with edge cases to evaluate Highly Automated Vehicles, in: 2020 IEEE 23rd International Conference on Intelligent Transportation Systems (ITSC), 2020

Kato, S. et al.: Autoware on board: Enabling autonomous vehicles with embedded systems (2018)
Kato, Shinpei; Tokunaga, Shota; Maruyama, Yuya; Maeda, Seiya; Hirabayashi, Manato; Kitsukawa, Yuki; Monrroy, Abraham; Ando, Tomohito; Fujii, Yusuke; Azumi, Takuya: Autoware on board: Enabling autonomous vehicles with embedded systems, in: 2018 ACM/IEEE 9th International Conference on Cyber-Physical Systems (ICCPS), 2018

Kim, W. et al.: Vehicle Path Prediction Using Yaw Acceleration for Adaptive Cruise Control (2018)
Kim, W.; Kang, C. M.; Son, Y. S.; Lee, S.; Chung, C. C.: Vehicle Path Prediction Using Yaw Acceleration for Adaptive Cruise Control, in: IEEE Transactions on Intelligent Transportation Systems (12), Issues 19, pp. 3818–3829, 2018

Klischat, M.; Althoff, M.: Generating critical test scenarios with evolutionary algorithms (2019)
Klischat, Moritz; Althoff, Matthias: Generating critical test scenarios for automated vehicles with evolutionary algorithms, in: 2019 IEEE Intelligent Vehicles Symposium (IV), 2019

Knabe, E.: Environment Simulator Minimalistic (esmini) (2021)
Knabe, Emil: Environment Simulator Minimalistic (esmini); https://github.com/esmini/esmini, 2021, Access 10.05.2021

Koenig, A. et al.: Bridging the gap between open loop tests and statistical validation (2017)
Koenig, Alexander; Gutbrod, Michael; Hohmann, Sören; Ludwig, Julian: Bridging the gap between open loop tests and statistical validation for highly automated driving, in: SAE International Journal of Transportation Safety 2017-01-1403, Issues 5, pp. 81–87, 2017

Koenig, A. et al.: Overview of HAD validation and passive HAD as a concept (2018)
Koenig, Alexander; Witzlsperger, Kathrin; Leutwiler, Florin; Hohmann, Sören: Overview of HAD validation and passive HAD as a concept for validating highly automated cars, in: at - Automatisierungstechnik (2), Issues 66, pp. 132–145, 2018

Koopman, P. et al.: A safety standard approach for fully autonomous vehicles (2019)
Koopman, Philip; Ferrell, Uma; Fratrik, Frank; Wagner, Michael: A safety standard approach for fully autonomous vehicles, in: International Conference on Computer Safety, Reliability, and Security, 2019

Koopman, P. et al.: Autonomous vehicles meet the physical world (2019)
Koopman, Philip; Osyk, Beth; Weast, Jack: Autonomous vehicles meet the physical world: RSS, variability, uncertainty, and proving safety, in: International Conference on Computer Safety, Reliability, and Security, 2019

Koopman, P.; Wagner, M.: Challenges in Autonomous Vehicle Testing and Validation (2016)
Koopman, Philip; Wagner, Michael: Challenges in Autonomous Vehicle Testing and Validation, in: SAE International Journal of Transportation Safety (1), Issues 4, pp. 15–24, 2016

Koopman, P.; Wagner, M.: Toward a Framework for Highly Automated Vehicle Safety Validation (2018)
Koopman, Philip; Wagner, Michael: Toward a Framework for Highly Automated Vehicle Safety Validation, in: , SAE Technical Paper Series, SAE International400 Commonwealth Drive, Warrendale, PA, United States, 2018

Krajewski, R. et al.: Data-driven maneuver modeling for safety validation of automated vehicles (2018)
Krajewski, Robert; Moers, Tobias; Nerger, Dominik; Eckstein, Lutz: Data-driven maneuver modeling using generative adversarial networks and variational autoencoders for safety validation of highly automated vehicles, in: 2018 21st International Conference on Intelligent Transportation Systems (ITSC), 2018

Krajewski, R. et al.: The highd dataset (2018)
Krajewski, Robert; Bock, Julian; Kloeker, Laurent; Eckstein, Lutz: The highd dataset, in: 2018 21st International Conference on Intelligent Transportation Systems (ITSC), 2018

Krajewski, R. et al.: The round dataset: A dataset of road user trajectories at roundabouts (2020)
Krajewski, Robert; Moers, Tobias; Bock, Julian; Vater, Lennart; Eckstein, Lutz: The round dataset: A drone dataset of road user trajectories at roundabouts in germany, in: 2020 IEEE 23rd International Conference on Intelligent Transportation Systems (ITSC), 2020

Kumar, G. A. et al.: LiDAR and camera fusion approach for object distance estimation (2020)
Kumar, G. A.; Lee, Jin H.; Hwang, Jongrak; Park, Jaehyeong; Youn, Sung H.; Kwon, Soon: LiDAR and camera fusion approach for object distance estimation in self-driving vehicles, in: Symmetry (2), Issues 12, p. 324, 2020

Kumar, M. et al.: An approach for inconsistency detection in data fusion from multiple sensors (2006)
Kumar, Manish; Garg, Devendra P.; Zachery, Randy A.: A generalized approach for inconsistency detection in data fusion from multiple sensors, in: 2006 American Control Conference, 2006

Kumar, P. et al.: Automated road markings extraction from mobile laser scanning data (2014)
Kumar, Pankaj; McElhinney, Conor P.; Lewis, Paul; McCarthy, Timothy: Automated road markings extraction from mobile laser scanning data, in: International Journal of Applied Earth Observation and Geoinformation, Issues 32, pp. 125–137, 2014

Lambert, F.: Tesla's fleet has accumulated even more than 1.2 billion miles in 'shadow mode' (2018)
Lambert, Fred: Tesla's fleet has accumulated over 1.2 billion miles on Autopilot and even more in 'shadow mode', report says; https://electrek.co/2018/07/17/tesla-autopilot-miles-shadow-mode-report/, 2018, Access 31.10.2018

Lang, A. H. et al.: Pointpillars: Fast encoders for object detection from point clouds (2019)
Lang, Alex H.; Vora, Sourabh; Caesar, Holger; Zhou, Lubing; Yang, Jiong; Beijbom, Oscar: Pointpillars: Fast encoders for object detection from point clouds, in: Proceedings of the IEEE/CVF Conference on Computer Vision and Pattern Recognition, 2019

Langner, J. et al.: Estimating the uniqueness of test scenarios derived from real-world-driving-data (2018)
Langner, Jacob; Bach, Johannes; Ries, Lennart; Otten, Stefan; Holzäpfel, Marc; Sax, Eric: Estimating the uniqueness of test scenarios derived from recorded real-world-driving-data using autoencoders, in: 2018 IEEE Intelligent Vehicles Symposium (IV), 2018

LaValle, S. M.: Rapidly-exploring random trees: A new tool for path planning (1998)
LaValle, Steven M.: Rapidly-exploring random trees: A new tool for path planning, Ames, IA, USA, 1998

Leitner, A.: ENABLE-S3: Project Introduction (2020)
Leitner, Andrea: ENABLE-S3: Project Introduction, in: Validation and Verification of Automated Systems, Springer, 2020

Liu, S. et al.: Computer Architectures for Autonomous Driving (2017)
Liu, Shaoshan; Tang, Jie; Zhang, Zhe; Gaudiot, Jean-Luc: Computer Architectures for Autonomous Driving, in: Computer (8), Issues 50, pp. 18–25, 2017

Loose, H.; Franke, U.: B-spline-based road model for 3d lane recognition (2010)
Loose, Heidi; Franke, Uwe: B-spline-based road model for 3d lane recognition, in: 13th International IEEE Conference on Intelligent Transportation Systems, 2010

Lyft: Data - Lyft (2019)
Lyft: Data - Lyft; https://self-driving.lyft.com/level5/data/, 2019, Access 26.03.2021

Lyft: Lyft-Homepage (2021)
Lyft: Lyft-Homepage; https://self-driving.lyft.com/, 2021, Access 15.03.2021

Mahmud, S. S. et al.: Application of proximal surrogate indicators for safety evaluation (2017)
Mahmud, S. S.; Ferreira, Luis; Hoque, Md S.; Tavassoli, Ahmad: Application of proximal surrogate indicators for safety evaluation: A review of recent developments and research needs, in: IATSS research (4), Issues 41, pp. 153–163, 2017

Maurer, M. et al.: Autonomous Driving (2016)
Maurer, Markus; Gerdes, J. C.; Lenz, Barbara; Winner, Hermann (Eds.) Autonomous Driving, Springer Berlin Heidelberg, Berlin, Heidelberg, 2016

Mazor, E. et al.: Interacting multiple model methods in target tracking: a survey (1998)
Mazor, Efim; Averbuch, Amir; Bar-Shalom, Yakov; Dayan, Joshua: Interacting multiple model methods in target tracking: a survey, in: IEEE Transactions on aerospace and electronic systems (1), Issues 34, pp. 103–123, 1998

Menzel, T. et al.: Scenarios for development, test and validation (2018)
Menzel, Till; Bagschik, Gerrit; Maurer, Markus: Scenarios for development, test and validation of automated vehicles, in: 2018 IEEE Intelligent Vehicles Symposium (IV), 2018

Mertz, C. et al.: Moving object detection with laser scanners (2013)
Mertz, Christoph; Navarro-Serment, Luis E.; MacLachlan, Robert; Rybski, Paul; Steinfeld, Aaron; Suppe, Arne; Urmson, Christopher; Vandapel, Nicolas; Hebert, Martial; Thorpe, Chuck; others: Moving object detection with laser scanners, in: Journal of Field Robotics (1), Issues 30, pp. 17–43, 2013

Minderhoud, M. M.; Bovy, P. H.: Extended time-to-collision measures for safety assessment (2001)
Minderhoud, Michiel M.; Bovy, Piet H. L.: Extended time-to-collision measures for road traffic safety assessment, in: Accident Analysis & Prevention (1), Issues 33, pp. 89–97, 2001

Mobileye: Responsibility-Sensitive Safety (RSS) A Model for Safe Autonomous Driving (2021)
Mobileye: Responsibility-Sensitive Safety (RSS) A Model for Safe Autonomous Driving; https://www.mobileye.com/responsibility-sensitive-safety/, 2021, Access 19.06.2021

Morris, D. D. et al.: A view-dependent adaptive matched filter for ladar-based vehicle tracking (2017)
Morris, Daniel D.; Hoffman, Regis; Haley, Paul: A view-dependent adaptive matched filter for ladar-based vehicle tracking, in: arXiv preprint arXiv:1709.08518, 2017

Mullins, G. E. et al.: Adaptive generation of challenging scenarios for testing of autonomous vehicles (2018)
Mullins, Galen E.; Stankiewicz, Paul G.; Hawthorne, R. C.; Gupta, Satyandra K.: Adaptive generation of challenging scenarios for testing and evaluation of autonomous vehicles, in: Journal of Systems and Software, Issues 137, pp. 197–215, 2018

Nadimi, N. et al.: Calibration and validation of a new time-based surrogate safety measure (2016)
Nadimi, Navid; Behbahani, Hamid; Shahbazi, HamidReza: Calibration and validation of a new time-based surrogate safety measure using fuzzy inference system, in: Journal of Traffic and Transportation Engineering (English Edition) (1), Issues 3, pp. 51–58, 2016

Nalic, D. et al.: Development of a co-simulation framework for systematic generation of scenarios (2019)
Nalic, Demin; Eichberger, Arno; Hanzl, Georg; Fellendorf, Martin; Rogic, Branko: Development of a co-simulation framework for systematic generation of scenarios for testing and validation of automated driving systems, in: 2019 IEEE Intelligent Transportation Systems Conference (ITSC), 2019

Nalic, D. et al.: Stress Testing Method for Scenario-Based Testing of Automated Driving Systems (2020)
Nalic, Demin; Li, Hexuan; Eichberger, Arno; Wellershaus, Christoph; Pandurevic, Aleksa; Rogic, Branko: Stress Testing Method for Scenario-Based Testing of Automated Driving Systems, in: IEEE Access, 2020

Narula, K. et al.: Two-Level Hierarchical Planning in a Known Semi-Structured Environment (2020)
Narula, Karan; Worrall, Stewart; Nebot, Eduardo: Two-Level Hierarchical Planning in a Known Semi-Structured Environment, in: 2020 IEEE 23rd International Conference on Intelligent Transportation Systems (ITSC), 2020

Németh, H. et al.: Proving Ground Test Scenarios in Mixed Virtual and Real Environment (2019)
Németh, Huba; Háry, András; Szalay, Zsolt; Tihanyi, Viktor; Tóth, Bálint: Proving Ground Test Scenarios in Mixed Virtual and Real Environment for Highly Automated Driving, in: Proff, Heike (Ed.): Mobilität in Zeiten der Veränderung, Springer Fachmedien Wiesbaden, Wiesbaden, 2019

Neumann-Cosel, K. von**: Virtual Test Drive: Simulation umfeldbasierter Fahrzeugfunktionen (2014)**
Neumann-Cosel, Kilian von: Virtual Test Drive: Simulation umfeldbasierter Fahrzeugfunktionen, Dissertation TU München, München, 2014

Neurohr, C. et al.: Fundamental considerations around scenario-based testing for automated driving (2020)
Neurohr, Christian; Westhofen, Lukas; Henning, Tabea; Graaff, Thies de; Möhlmann, Eike; Böde, Eckard: Fundamental considerations around scenario-based testing for automated driving, in: 2020 IEEE Intelligent Vehicles Symposium (IV), 2020

Nuss, D. et al.: Using grid maps to reduce the number of false positive measurements (2012)
Nuss, Dominik; Reuter, Stephan; Konrad, Marcus; Munz, Michael; Dietmayer, Klaus: Using grid maps to reduce the number of false positive measurements in advanced driver assistance systems, in: Intelligent Transportation Systems (ITSC), 2012 15th International IEEE Conference on, 2012

Okamura, M. et al.: Impact evaluation of a driving support system on traffic flow (2011)
Okamura, Makoto; Fukuda, Atsushi; Morita, Hirohisa; Suzuki, Hironori; Nakazawa, Masatoshi: Impact evaluation of a driving support system on traffic flow by microscopic traffic simulation, in: Advances in Transportation Studies Special Issue 2011, 2011

Olszewski, P. et al.: Review of current study methods for VRU safety. Part 1 - Main report (2016)
Olszewski, Piotr; Osińska, Beata; Szagała, Piotr; Włodarek, Paweł; Niesen, Sandra; Kidholm Osmann Madsen, Tanja; van Haperen, Wouter; Johnsson, Carl; Laureshyn, Aliaksei; Varhelyi, Andras; others: Review of current study methods for VRU safety. Part 1 - Main report, in: , 2016

Pek, C. et al.: An online verification framework for motion planning of self-driving vehicles (2019)
Pek, Christian; Koschi, Markus; Althoff, Matthias: An online verification framework for motion planning of self-driving vehicles with safety guarantees, in: AAET-Automatisiertes und vernetztes Fahren, 2019

Pek, C. et al.: Using online verification to prevent autonomous vehicles from causing accidents (2020)
Pek, Christian; Manzinger, Stefanie; Koschi, Markus; Althoff, Matthias: Using online verification to prevent autonomous vehicles from causing accidents, in: Nature Machine Intelligence (9), Issues 2, pp. 518–528, 2020

Pek, C.; Althoff, M.: Fail-Safe Motion Planning for Online Verification of Autonomous Vehicles (2020)
Pek, Christian; Althoff, Matthias: Fail-Safe Motion Planning for Online Verification of Autonomous Vehicles Using Convex Optimization, in: IEEE Transactions on Robotics, 2020

Petrov, P.; Nashashibi, F.: Modeling and nonlinear adaptive control for overtaking (2014)
Petrov, Plamen; Nashashibi, Fawzi: Modeling and nonlinear adaptive control for autonomous vehicle overtaking, in: IEEE Transactions on Intelligent Transportation Systems (4), Issues 15, pp. 1643–1656, 2014

Piazzi, A. et al.: Quintic G/sup 2/-splines for iterative steering of vision-based autonomous vehicles (2002)
Piazzi, Aurelio; Lo Bianco, C. G.; Bertozzi, Massimo; Fascioli, Alessandra; Broggi, Alberto: Quintic G/sup 2/-splines for the iterative steering of vision-based autonomous vehicles, in: IEEE Transactions on Intelligent Transportation Systems (1), Issues 3, pp. 27–36, 2002

Poggenhans, F. et al.: Lanelet2: A high-definition map framework for the automated driving (2018)
Poggenhans, Fabian; Pauls, Jan-Hendrik; Janosovits, Johannes; Orf, Stefan; Naumann, Maximilian; Kuhnt, Florian; Mayr, Matthias: Lanelet2: A high-definition map framework for the future of automated driving, in: 2018 21st International Conference on Intelligent Transportation Systems (ITSC), 2018

Poggenhans, F.; Janosovits, J.: Pathfinding and Routing in the Lanelet2 Map Framework (2020)
Poggenhans, Fabian; Janosovits, Johannes: Pathfinding and Routing for Automated Driving in the Lanelet2 Map Framework, in: 2020 IEEE 23rd International Conference on Intelligent Transportation Systems (ITSC), 2020

Ponn, T. et al.: An Optimization-based Method to Identify Relevant Scenarios (2019)
Ponn, Thomas; Gnandt, Christian; Diermeyer, Frank: An Optimization-based Method to Identify Relevant Scenarios for Type Approval of Automated Vehicles, in: Proceedings of the ESV—International Technical Conference on the Enhanced Safety of Vehicles, Eindhoven, The Netherlands, 2019

Ponn, T. et al.: Systematic Analysis of the Sensor Coverage of Automated Vehicles (2019)
Ponn, Thomas; Müller, Fabian; Diermeyer, Frank: Systematic analysis of the sensor coverage of automated vehicles using phenomenological sensor models, in: 2019 IEEE Intelligent Vehicles Symposium (IV), 2019

PTV, AG: PTV Vissim 10 user manual (2018)
PTV, AG: PTV Vissim 10 user manual, in: PTV AG: Karlsruhe, Germany, 2018

Rachman, A.: 3D-LIDAR multi object tracking for autonomous driving (2017)
Rachman, A.S.Abdul: 3D-LIDAR multi object tracking for autonomous driving: multi-target detection and tracking under urban road uncertainties
M. Sc. Thesis, Delft University of Technology, 2017

Rastelli, J. P. et al.: Dynamic trajectory generation using continuous-curvature algorithms (2014)
Rastelli, Joshue P.; Lattarulo, Ray; Nashashibi, Fawzi: Dynamic trajectory generation using continuous-curvature algorithms for door to door assistance vehicles, in: 2014 IEEE Intelligent Vehicles Symposium Proceedings, 2014

Rauch, A. et al.: Car2x-based perception in a high-level fusion architecture for perception systems (2012)
Rauch, Andreas; Klanner, Felix; Rasshofer, Ralph; Dietmayer, Klaus: Car2x-based perception in a high-level fusion architecture for cooperative perception systems, in: 2012 IEEE Intelligent Vehicles Symposium, 2012

Riedmaier, S. et al.: Survey on Scenario-Based Safety Assessment of Automated Vehicles (2020)
Riedmaier, S.; Ponn, T.; Ludwig, D.; Schick, B.; Diermeyer, F.: Survey on Scenario-Based Safety Assessment of Automated Vehicles, in: IEEE Access, Issues 8, pp. 87456–87477, 2020

Rizaldi, A.; Althoff, M.: Formalising traffic rules for accountability of autonomous vehicles (2015)
Rizaldi, Albert; Althoff, Matthias: Formalising traffic rules for accountability of autonomous vehicles, in: 2015 IEEE 18th international conference on intelligent transportation systems, 2015

Rong, G. et al.: Lgsvl simulator: A high fidelity simulator for autonomous driving (2020)
Rong, Guodong; Shin, Byung H.; Tabatabaee, Hadi; Lu, Qiang; Lemke, Steve; Možeiko, Mnš; Boise, Eric; Uhm, Geehoon; Gerow, Mark; Mehta, Shalin; others: Lgsvl simulator: A high fidelity simulator for autonomous driving, in: 2020 IEEE 23rd International Conference on Intelligent Transportation Systems (ITSC), 2020

Rosenberger, P. et al.: Benchmarking and Functional Decomposition of Lidar Sensor Models (2019)
Rosenberger, Philipp; Holder, Martin; Huch, Sebastian; Winner, Hermann; Fleck, Tobias; Zofka, Marc R.; Zöllner, J. M.; D'hondt, Thomas; Wassermann, Benjamin: Benchmarking and Functional Decomposition of Automotive Lidar Sensor Models, in: 2019 IEEE Intelligent Vehicles Symposium (IV), 2019

Russell, B. C. et al.: LabelMe: a database and web-based tool for image annotation (2008)
Russell, Bryan C.; Torralba, Antonio; Murphy, Kevin P.; Freeman, William T.: LabelMe: a database and web-based tool for image annotation, in: International journal of computer vision 1-3, Issues 77, pp. 157–173, 2008

SAE J2944: Operational Definitions of Driving Performance Measures and Statistics (2015)
SAE J2944: Operational Definitions of Driving Performance Measures and Statistics, 2015

SAE J3016: Taxonomy and Definitions for Terms Related to Automation Systems (2021)
SAE J3016: Taxonomy and Definitions for Terms Related to Driving Automation Systems for On-Road Motor Vehicles; https://doi.org/10.4271/J3016_202104, 2021

Särkkä, S.: Unscented Rauch‐Tung‐Striebel Smoother (2008)
Särkkä, Simo: Unscented Rauch‐Tung‐Striebel Smoother, in: IEEE Transactions on Automatic Control (3), Issues 53, pp. 845‐849, 2008

Schafer, R. W.: What is a Savitzky-Golay filter?[lecture notes] (2011)
Schafer, Ronald W.: What is a Savitzky-Golay filter?[lecture notes], in: IEEE Signal processing magazine (4), Issues 28, pp. 111–117, 2011

Scholtes, M. et al.: 6-Layer Model of Urban Traffic and Environment (2020)
Scholtes, Maike; Westhofen, Lukas; Turner, Lara R.; Lotto, Katrin; Schuldes, Michael; Weber, Hendrik; Wagener, Nicolas; Neurohr, Christian; Bollmann, Martin; Körtke, Franziska; others: 6-Layer Model for a Structured Description and Categorization of Urban Traffic and Environment, in: arXiv preprint arXiv:2012.06319, 2020

Schubert, R. et al.: Comparison and evaluation of advanced motion models for vehicle tracking (2008)
Schubert, Robin; Richter, Eric; Wanielik, Gerd: Comparison and evaluation of advanced motion models for vehicle tracking, in: 2008 11th international conference on information fusion, 2008

Schuldt, F. et al.: Effiziente systematische Testgenerierung in virtuellen Umgebungen (2013)
Schuldt, Fabian; Saust, Falko; Lichte, Bernd; Maurer, Markus; Scholz, Stephan: Effiziente systematische Testgenerierung für Fahrerassistenzsysteme in virtuellen Umgebungen, in: Automatisierungssysteme, Assistenzsysteme und Eingebettete Systeme Für Transportmittel, 2013

Shalev-Shwartz, S. et al.: On a formal model of safe and scalable self-driving cars (2017)
Shalev-Shwartz, Shai; Shammah, Shaked; Shashua, Amnon: On a formal model of safe and scalable self-driving cars, in: arXiv preprint arXiv:1708.06374, 2017

Shi, T. et al.: Driving Decision for Lane Change Behavior based on Deep Reinforcement Learning (2019)
Shi, Tianyu; Wang, Pin; Cheng, Xuxin; Chan, Ching-Yao; Huang, Ding: Driving Decision and Control for Automated Lane Change Behavior based on Deep Reinforcement Learning, in: 2019 IEEE Intelligent Transportation Systems Conference (ITSC), 2019

Sippl, C. et al.: Distributed real-time traffic simulation for autonomous vehicle testing (2018)
Sippl, Christoph; Schwab, Benedikt; Kielar, Peter; Djanatliev, Anatoli: Distributed real-time traffic simulation for autonomous vehicle testing in urban environments, in: 2018 21st International Conference on Intelligent Transportation Systems (ITSC), 2018

Stahl, T. et al.: Online Verification Concept for Autonomous Vehicles (2020)
Stahl, Tim; Eicher, Matthis; Betz, Johannes; Diermeyer, Frank: Online Verification Concept for Autonomous Vehicles - Illustrative Study for a Trajectory Planning Module, in: arXiv preprint arXiv:2005.07740, 2020

Sun, P. et al.: Scalability in perception for autonomous driving: Waymo open dataset (2020)
Sun, Pei; Kretzschmar, Henrik; Dotiwalla, Xerxes; Chouard, Aurelien; Patnaik, Vijaysai; Tsui, Paul; Guo, James; Zhou, Yin; Chai, Yuning; Caine, Benjamin; others: Scalability in perception for autonomous driving: Waymo open dataset, in: Proceedings of the IEEE/CVF Conference on Computer Vision and Pattern Recognition, 2020

Szalay, Z.: Next Generation X-in-the-Loop Validation Methodology for Automated Vehicle Systems (2021)
Szalay, Zsolt: Next Generation X-in-the-Loop Validation Methodology for Automated Vehicle Systems, in: IEEE Access, Issues 9, pp. 35616–35632, 2021

Tak, S. et al.: Development of a deceleration-based surrogate safety measure for rear-end collision (2015)
Tak, Sehyun; Kim, Sunghoon; Yeo, Hwasoo: Development of a deceleration-based surrogate safety measure for rear-end collision risk, in: IEEE Transactions on Intelligent Transportation Systems (5), Issues 16, pp. 2435–2445, 2015

Takács, Á. et al.: Assessment and standardization of autonomous vehicles (2018)
Takács, Árpád; Drexler, Dániel A.; Galambos, Péter; Rudas, Imre J.; Haidegger, Tamás: Assessment and standardization of autonomous vehicles, in: 2018 IEEE 22nd International Conference on Intelligent Engineering Systems (INES), 2018

Templeton, B.: Tesla's "Shadow" Testing Offers A Useful Advantage (2019)
Templeton, Brad: Tesla's "Shadow" Testing Offers A Useful Advantage On The Biggest Problem In Robocars; https://www.forbes.com/sites/bradtempleton/2019/04/29/teslas-shadow-testing-offers-a-useful-advantage-on-the-biggest-problem-in-robocars/?sh=6fa4d1413c06, 2019, Access 13.04.2021

Tesla: What is Shadow Mode Tesla Autonomy (2019)
Tesla: What is Shadow Mode Tesla Autonomy; https://www.youtube.com/watch?v=SAceTxSelTI, 2019, Access 13.04.2021

The Tesla Team: All Tesla Cars Being Produced Now Have Full Self-Driving Hardware (2021)
The Tesla Team: All Tesla Cars Being Produced Now Have Full Self-Driving Hardware; www.tesla.com, 2021, Access 13.02.2021

Thomann, C.: Tesla Model S adaptive cruise control crashes into Van (2016)
Thomann, Chris: Tesla Model S adaptive cruise control crashes into Van; https://www.youtube.com/watch?v=qQkx-4pFjus, 2016, Access 02.11.2021

Tribelhorn, W.: Konzeptionierung und Implementation einer „Silent Testing"-Methode (2018)
Tribelhorn, Wadim: Konzeptionierung und prototypische Implementation einer „Silent Testing"-Methode zur automatisierten Bewertung der Fahrstreifenmarkierungserkennung für automatisierte Fahrzeuge, Masterthesis No.: 703/18, 2018

Tuncali, C. E. et al.: Simulation-based adversarial test generation with machine learning components (2018)
Tuncali, Cumhur E.; Fainekos, Georgios; Ito, Hisahiro; Kapinski, James: Simulation-based adversarial test generation for autonomous vehicles with machine learning components, in: 2018 IEEE Intelligent Vehicles Symposium (IV), 2018

Tuncali, C. E.; Fainekos, G.: Rapidly-exploring random trees for testing automated vehicles (2019)
Tuncali, Cumhur E.; Fainekos, Georgios: Rapidly-exploring random trees for testing automated vehicles, in: 2019 IEEE Intelligent Transportation Systems Conference (ITSC), 2019

Ulbrich, S. et al.: Defining and Substantiating the Terms Scene, Situation, and Scenario (2015)
Ulbrich, Simon; Menzel, Till; Reschka, Andreas; Schuldt, Fabian; Maurer, Markus: Defining and Substantiating the Terms Scene, Situation, and Scenario for Automated Driving, in: 2015 IEEE 18th International Conference on Intelligent Transportation Systems - (ITSC 2015), 2015

Utesch, F. et al.: Towards behaviour based testing to understand the black box of autonomous cars (2020)
Utesch, Fabian; Brandies, Alexander; Fouopi, Paulin P.; Schießl, Caroline: Towards behaviour based testing to understand the black box of autonomous cars, in: European Transport Research Review (1), Issues 12, pp. 1–11, 2020

van der Horst, R.; Hogema, J.: Time-to-collision and collision avoidance systems (1993)
van der Horst, Richard; Hogema, Jeroen: Time-to-collision and collision avoidance systems, in: , 1993

Vanholme, B. et al.: Highly automated driving on highways based on legal safety (2012)
Vanholme, Benoit; Gruyer, Dominique; Lusetti, Benoit; Glaser, Sebastien; Mammar, Said: Highly automated driving on highways based on legal safety, in: IEEE Transactions on Intelligent Transportation Systems (1), Issues 14, pp. 333–347, 2012

Wachenfeld, W. et al.: The worst-time-to-collision metric for situation identification (2016)
Wachenfeld, Walther; Junietz, Philipp; Wenzel, Raphael; Winner, Hermann: The worst-time-to-collision metric for situation identification, in: Intelligent Vehicles Symposium (IV), 2016 IEEE, 2016

Wachenfeld, W.; Winner, H.: The new role of road testing for the safety validation
Wachenfeld, Walther; Winner, Hermann: The new role of road testing for the safety validation of automated vehicles, in: Watzenig, Daniel; Horn, Martin. (Eds.): Automated Driving, Springer, 2017

Wachenfeld, W.; Winner, H.: Virtual Assessment of Automation in Field Operation (2015)
Wachenfeld, Walther; Winner, Hermann: Virtual Assessment of Automation in Field Operation A New Runtime Validation Method, in: 10. Workshop Fahrerassistenz-systeme, 2015

Wachenfeld, W.; Winner, H.: The Release of Autonomous Vehicles (2016)
Wachenfeld, Walther; Winner, Hermann: The Release of Autonomous Vehicles, in: Maurer, Markus; Gerdes, J. C.; Lenz, Barbara; Winner, Hermann (Eds.): Autonomous Driving, Springer Berlin Heidelberg, Berlin, Heidelberg, 2016

Wächter, A.; Biegler, L. T.: An interior-point filter line-search algorithm for nonlinear programming (2006)
Wächter, Andreas; Biegler, Lorenz T.: On the implementation of an interior-point filter line-search algorithm for large-scale nonlinear programming, in: Mathematical programming (1), Issues 106, pp. 25–57, 2006

Walden, D. D. et al.: A guide for system life cycle processes and activities (2015)
Walden, David D.; Roedler, Garry J.; Forsberg, Kevin; Hamelin, R. D.; Shortell, Thomas M.: Systems engineering handbook: A guide for system life cycle processes and activities, John Wiley & Sons, 2015

Wang, B. et al.: LATTE: point cloud annotation via sensor fusion, one-click annotation and tracking (2019)
Wang, Bernie; Wu, Virginia; Wu, Bichen; Keutzer, Kurt: LATTE: accelerating lidar point cloud annotation via sensor fusion, one-click annotation, and tracking, in: 2019 IEEE Intelligent Transportation Systems Conference (ITSC), 2019

Wang, C. et al.: Reduction of Uncertainties for Safety Assessment of Automation (2020)
Wang, Cheng; Xiong, Fanglei; Winner, Hermann: Reduction of Uncertainties for Safety Assessment of Automated Driving under Parallel Simulations, in: IEEE Transactions on intelligent vehicles, 2020

Wang, C.; Winner, H.: Validation Automated Driving and Identification of Critical Scenarios (2019)
Wang, Cheng; Winner, Hermann: Overcoming Challenges of Validation Automated Driving and Identification of Critical Scenarios, in: 2019 IEEE Intelligent Transportation Systems Conference (ITSC), 2019

Waymo: On the Road to Fully Self-Driving: Waymo Safety Report (2017)
Waymo: On the Road to Fully Self-Driving: Waymo Safety Report; https://goo.gl/7HUiew, 2017

Waymo: Waymo Safety Report (2020)
Waymo: Waymo Safety Report; https://waymo.com/safety/, 2020

Waymo LLC: Waymo-Homepage (2021)
Waymo LLC: Waymo-Homepage; https://waymo.com/, 2021, Access 15.03.2021

Weber, N. et al.: A simulation-based, statistical approach for the derivation of concrete scenarios (2020)
Weber, Nico; Frerichs, Dirk; Eberle, Ulrich: A simulation-based, statistical approach for the derivation of concrete scenarios for the release of highly automated driving functions, in: AmE 2020-Automotive meets Electronics; 11th GMM-Symposium, 2020

Werling, M. et al.: Optimal trajectory generation for dynamic street scenarios in a Frenét Frame (2010)
Werling, Moritz; Ziegler, Julius; Kammel, Sören; Thrun, Sebastian: Optimal trajectory generation for dynamic street scenarios in a Frenét Frame, in: IEEE International Conference on Robotics and Automation (ICRA), 2010, Anchorage, AK, IEEE, Piscataway, NJ, 2010

Wikipedia: Online (2021)
Wikipedia: Online; https://de.wikipedia.org/w/index.php?oldid=209581826, 2021, Access 16.03.2021

Wikipedia: Model predictive control - Wikipedia (2021)
Wikipedia: Model predictive control - Wikipedia; https://en.wikipedia.org/w/index.php?oldid=1015488533, 2021, Access 16.05.2021

Wikipedia: Top-down and bottom-up design - Wikipedia (2021)
Wikipedia: Top-down and bottom-up design - Wikipedia; https://en.wikipedia.org/w/index.php?oldid=1010273232, 2021, Access 16.05.2021

Winner, H.: Device for providing signals in a motor vehicle (2006)
Winner, Hermann: Device for providing signals in a motor vehicle, Patent U.S. Patent 7,138,909, 2006

Winner, H. et al.: Maße für den Sicherheitsgewinn von Fahrerassistenzsystemen (2013)
Winner, Hermann; Geyer, Sebastian; Sefati, Mohsen: Maße für den Sicherheitsgewinn von Fahrerassistenzsystemen, in: Maßstäbe des sicheren Fahrens, Issues 6, 2013

Winner, H.: Grundlagen von Frontkollisionsschutzsystemen (2015)
Winner, Hermann: Grundlagen von Frontkollisionsschutzsystemen, in: Winner, Hermann; Hakuli, Stephan; Lotz, Felix; Singer, Christina (Eds.): Handbuch Fahrerassistenzsysteme: Grundlagen, Komponenten und Systeme für aktive Sicherheit und Komfort, Springer Fachmedien Wiesbaden, Wiesbaden, 2015

Winner, H. et al.: (How) Can safety of automated driving be validated? (2016)
Winner, Hermann; Wachenfeld, Walther; Junietz, Philipp: (How) Can safety of automated driving be validated?, in: 7. Grazer Symposium Virtuelles Fahrzeug, 2016

Winner, H. et al.: Validation and Introduction of Automated Driving (2018)
Winner, Hermann; Wachenfeld, Walther; Junietz, Phillip: Validation and Introduction of Automated Driving, in: Winner, Hermann; Prokop, Günther; Maurer, Markus (Eds.): Automotive Systems Engineering II, Springer International Publishing, Cham, 2018

Winner, H.; Wachenfeld, W.: Absicherung automatischen fahrens (2013)
Winner, Hermann; Wachenfeld, Walther: Absicherung automatischen fahrens, in: 6. FAS-Tagung München, Munich, Issues 9, 2013

Xu, H. et al.: A fast and stable lane detection method based on B-spline curve (2009)
Xu, Huarong; Wang, Xiaodong; Huang, Hongwu; Wu, Keshou; Fang, Qiu: A fast and stable lane detection method based on B-spline curve, in: 2009 IEEE 10th International Conference on Computer-Aided Industrial Design & Conceptual Design, 2009

Zhang, M. et al.: A finite state machine based controller and its stochastic optimization (2017)
Zhang, Mengxuan; Li, Nan; Girard, Anouck; Kolmanovsky, Ilya: A finite state machine based automated driving controller and its stochastic optimization, in: Dynamic Systems and Control Conference, 2017

Zhang, S. et al.: Accelerated evaluation of autonomous vehicles in the lane change scenario (2018)
Zhang, Songan; Peng, Huei; Zhao, Ding; Tseng, H. E.: Accelerated evaluation of autonomous vehicles in the lane change scenario based on subset simulation technique, in: 2018 21st International Conference on Intelligent Transportation Systems (ITSC), 2018

Zhao, D. et al.: Accelerated evaluation of automated vehicles in car-following maneuvers (2017)
Zhao, Ding; Huang, Xianan; Peng, Huei; Lam, Henry; LeBlanc, David J.: Accelerated evaluation of automated vehicles in car-following maneuvers, in: IEEE Transactions on Intelligent Transportation Systems (3), Issues 19, pp. 733–744, 2017

Zhou, J.; Re, L. d.: Reduced Complexity Safety Testing for ADAS & ADF (2017)
Zhou, Jinwei; Re, Luigi d.: Reduced Complexity Safety Testing for ADAS & ADF, in: IFAC-PapersOnLine (1), Issues 50, pp. 5985–5990, 2017

Own Publications

Wang, C.; Winner, H.: Overcoming Challenges of Validation Automated Driving and Identification of Critical Scenarios, in: 2019 IEEE Intelligent Transportation Systems Conference (ITSC), 2019

Wang, C.; Xiong, F. l.; Winner, H.: Reduction of Uncertainties for Safety Assessment of Automated Driving under Parallel Simulations, in: IEEE Transactions on intelligent vehicles, 2020

Wang, C.; Storms, K.; Winner, H.: Online Safety Assessment of Automated vehicles Using Silent Testing, in: IEEE Transactions on intelligent transportation system, 2021

Supervised Theses

Sokolovski, Stanislav: Retrospektive Korrektur der Existenzunsicherheiten und Zustandsunsicherheiten in der Sensordatenfusion zur Bewertung der Automation, Masterthesis No.:700/18

Du, Ruixin: Simulation des Verhaltens der Automation und Erkennung der potenziellen kritischen Szenarien, Masterthesis No.:704/18

Li, Haiyu: Entwicklung und Implementierung eines Folgemodells für VAAFO, Bachelorthesis No.:1330/18

Lu, Jianbo: Entwicklung und Implementierung einer Strategie von Fahrstreifenwechsel zur Simulation des Verhaltens der Verkehrsteilnehmer, Masterthesis No.:731/18

Xiong, Fanglei: Entwickelung und Implementierung des JIPDA Trackers zur Reduzierung von FP/FN Objekten, Masterthesis No.:727/18

Xing, Xiajie: Entwicklung einer Methode zur Reduzierung der Existenzunsicherheiten in der Objektliste, Masterthesis No.:732/18

Guo, Fengwei: Entwicklung einer Trajektorienplanung zur Unterstützung der Verhaltenssimulation der Verkehrsteilnehmer, Masterthesis No.:728/18

Kang, Jian: Entwicklung eines Algorithmus zur Fusion der Daten von Radar und Lidar, Masterthesis No.:767/19

Pang, Zhichao: Entwicklung einer Methode zur Speicherung und Visualisierung der von VAAFO identifizierten kritischen Szenarien, Masterthesis No.:776/20

Li, Xu: Entwicklung und Implementierung eines Algorithmus für Prädiktion des Zustands der verfolgten Objekte, Masterthesis No.:785/20